12-2016

Repurposing non-antimicrobial drugs to treat multi-drug resistant bacterial and fungal infections

Shankar Thangamani
Purdue University

Graduate School Form
30 Updated 12/26/2015

PURDUE UNIVERSITY
GRADUATE SCHOOL
Thesis/Dissertation Acceptance

This is to certify that the thesis/dissertation prepared

By Shankar Thangamani

Entitled

REPURPOSING NON-ANTIMICROBIAL DRUGS TO TREAT MULTI-DRUG RESISTANT BACTERIAL AND FUNGAL INFECTIONS

For the degree of Doctor of Philosophy

Is approved by the final examining committee:

Dr. Mohamed Seleem
Co-chair

Dr. Kenitra Hammac
Co-chair

Dr. Cynthia Stauffacher

Dr. Suresh Mittal

To the best of my knowledge and as understood by the student in the Thesis/Dissertation Agreement, Publication Delay, and Certification Disclaimer (Graduate School Form 32), this thesis/dissertation adheres to the provisions of Purdue University's "Policy of Integrity in Research" and the use of copyright material.

Approved by Major Professor(s): Dr. Mohamed Seleem and Dr. Kenitra Hammac

Approved by: Dr. Suresh Mittal 8/22/2016

Head of the Departmental Graduate Program Date

REPURPOSING NON-ANTIMICROBIAL DRUGS TO TREAT MULTI-DRUG RESISTANT BACTERIAL AND FUNGAL INFECTIONS

A Dissertation

Submitted to the Faculty

of

Purdue University

by

Shankar Thangamani

In Partial Fulfillment of the

Requirements for the Degree

of

Doctor of Philosophy

December 2016

Purdue University

West Lafayette, Indiana

ACKNOWLEDGEMENTS

Firstly, I am grateful to the almighty for providing me this wonderful opportunity, good health, wellbeing and strength that were necessary to complete my studies.

I like to express my sincere gratitude and appreciation to my major advisors Dr. Mohamed Seleem and Dr. Kenitra Hammac for their guidance and support during the graduate training. I thank Dr. Seleem for his confidence in me to work on multiple projects and his encouragement in all aspects to complete this work. He always been accessible to discuss data or personal matters. He encouraged and supported me to improve my presentation skills. Knowledge that I have acquired from his discussions will extend beyond the lab and into all aspects of my life. I also like to thank Dr. Hammac for her feedback and support in teaching and ADDL projects.

I would like to thank Dr. Ramesh Vemulapalli for his support and valuable suggestions throughout my PhD. Without him, I would not be able to complete my studies. I am also indebted to Dr. Chang Kim for providing me an opportunity to learn and improve my research skills. I would also like to thank my committee members Dr. Cynthia Stauffacher and Dr. Suresh Mittal for their valuable inputs and suggestions.

I also thank Dr. Puliyur .S. Mohakumar (The University of Georgia) and Dr. Ramesh Selvaraj (The Ohio State University) for inspiring me to pursue my graduate studies.

I thank all my past and current lab colleagues: Jeeho lee, Myunghoo Kim, Jeongho Park, Seika Hashimoto-Hill, Jinsam Chang, Jeongho Yoon, Bon-hee Gu, Benjamin Ulrich, Yaqing Qie, Neha Debral, Haroon Mohamed, Waleed Younis, Maha Ahmed, Mostafa, Mohamed Fathy, Ahmed Hassan, Hassan Elsayed, Youssef Ahmed for their support and fun times at Purdue.

I thank all my friends and parents for their love and continuous support. Finally, I thank my better half Madhu and my kid Megna for their love, patience, emotional support and sacrifices.

TABLE OF CONTENTS

Page

Page

LIST OF TABLES

LIST OF FIGURES

Figure Page

Figure Page

LIST OF ABBREVIATIONS

MIC Minimum inhibitory concentration

MBC Minimum bactericidal concentration

MFC Minimum fungicidal concentration

MRSA Methicillin-resistant *Staphylococcus aureus*

VRSA Vancomycin-resistant *Staphylococcus aureus*

VISA Vancomycin-intermediate resistant *Staphylococcus aureus*

VRE Vancomycin-resistant Enterococci

FdUrd 5-fluoro-2'-deoxyuridine

TSST-1 Toxic shock syndrome toxin

APCs Antigen-presenting cells

PVL Panton valentine leukocidin

IL-1β Interleukin 1beta

IL-6 Interleukin 6

TNFα Tumor necrosis factor α

MCP-1 Monocyte chemoattractant protein 1

SSTI Soft-tissue infections

PBNP Polymixin B nonapeptide

Trx Thioredoxin

mtDNA Mitochondrial DNA

FDA Food and Drug Administration

CFU Colony forming unit

NSAIDs Nonsteroidal anti-inflammatory drugs

LDL Low density lipoprotein

MOI Multiplicity of infection

OM	Outer membrane
MHB	Mueller-Hinton broth
MSA	Mannitol salt agar
TSA	Trypticase soy agar
TSB	Trypticase soy broth
MOA	Mechanism of action
CLSI	Clinical and Laboratory Standards Institute
COX2	Cyclooxygenase-2
HaCat	Human keratinocyte cells
Hla	α-hemolysin

ABSTRACT

Thangamani, Shankar. Ph.D., Purdue University, December 2016. Repurposing Non-Antimicrobial Drugs to Treat Multi-Drug Resistant Bacterial and Fungal Infections. Major Professors: Mohamed. N. Seleem and Kenitra Hammac.

Bacterial and fungal resistance to conventional antimicrobials is a burgeoning global health epidemic that necessitates urgent action. Even more alarming, the development of new antimicrobials to treat these multidrug-resistant pathogens has not kept pace with the rapid emergence of resistance to current antimicrobials. Antimicrobial drug development through the traditional *de novo* process is a risky venture given the significant financial and time investment required by researchers and limited success rate of translating these compounds to the clinical setting. This has led researchers to mine existing libraries of clinical molecules in order to repurpose old drugs for new applications (as antimicrobials). The main aim of this research endeavor was to screen and validate approved drug libraries and small molecules for their antimicrobial activity against multidrug-resistant bacterial and fungal pathogens, including *Staphylococcus aureus* and *Candida albicans*.

The present study identified four approved drugs (auranofin, ebselen, simvastatin and celecoxib) that exhibited potent antimicrobial activity against multidrug-resistant bacterial and fungal pathogens. Notably, auranofin, an FDA-approved anti-rheumatic drug possessed excellent antibacterial activity against *S. aureus* and was found to exert its effect

by inhibiting multiple biosynthetic pathways including DNA, protein and cell wall synthesis. Furthermore, auranofin was found to be efficacious in a mouse model of *S. aureus* systemic infection, as it significantly reduced the bacterial load in murine organs, including the spleen and liver. Ebselen, an organoselenium compound known to be clinically safe, exhibited potent anti-staphylococcal activity by inhibiting bacterial protein synthesis. Other approved drugs including simvastatin (anti-hyperlipedmic drug) and celecoxib (non-steroidal anti-inflammatory drug) also possessed anti-staphylococcal activity against various clinical isolates of *S. aureus.* Our study also revealed that three drugs (auranofin, ebselen and simvastatin) markedly reduced the production of major staphylococcal toxins including Panton-Valentine leucocidin (PVL) and α-hemolysin (Hla), thereby improving the treatment outcome against toxin-producing bacterial pathogens. Furthermore, all these drugs effectively reduced both the bacterial load and inflammatory cytokines in a mouse model of *S. aureus* skin infection.

In addition to their antibacterial activity, auranofin and ebselen were found to possess potent antifungal activity against two major pathogens, *Candida* and *Cryptococcus*; they exerted their antifungal effect through inhibition of mitochondrial proteins (auranofin) and glutathione synthesis (ebselen) respectively. Additionally, these two drugs proved superior to control antifungals, as they reduced the fungal load in a *Caenorhabditis elegans* animal model. Taken altogether, the potent *in vitro* and *in vivo* antimicrobial activity (against bacterial and (or) fungal pathogens) of auranofin, ebselen, simvastatin and celecoxib indicates these four drugs have considerable promise to be successfully repurposed for use as antimicrobial agents.

CHAPTER 1. DRUG REPURPOSING FOR THE DEVELOPMENT OF NOVEL ANTIMICROBIALS

(Thangamani S, Mohammad H, Younis W, Seleem MN. Drug repurposing for the treatment of staphylococcal infections. *Current Pharmaceutical Design*. 2015;21(16): 2089-100)

1.1 Introduction

Bacterial and fungal resistance to conventional antimicrobials is a burgeoning global health epidemic that necessitates urgent action. Reports by the Centers for Disease Control and Prevention in the United States and the European Centre for Disease Control and Prevention indicate more than two million individuals in the United States and nearly 400,000 individuals in Europe are stricken each year with infections caused by multidrug-resistant pathogens, including methicillin-resistant *Staphylococcus aureus* (MRSA), carbapenem-resistant *Klebsiella pneumoniae*, vancomycin-resistant *Enterococcus faecium* and fluconazole-resistant *Candida* [1,2]. Treatment of these infections are often expensive costing residents an estimated $55 billion in the United States and €1.5 billion in the European Union in total costs every year [1,2]. Furthermore, the issue of bacterial and fungal resistance to antimicrobials around the world appears to be getting worse with the emergence of pathogens exhibiting resistance to agents of last resort [3-5]. Even more

alarming, the development and approval of new antimicrobials capable of being used to treat infections caused by multidrug-resistant pathogens has not been able to keep pace with the rapid emergence of bacterial and fungal resistance to currently efficacious antimicrobials. Drug development of novel compounds is a time-consuming, costly, and high-risk venture given that few compounds successfully make it through stringent regulatory requirements to reach the marketplace. Collectively, this points to a critical need for the identification of novel strategies to develop antibiotics to deal with this challenging health issue. One strategy which warrants more attention as a unique method for identifying new antimicrobials is drug repurposing.

Drug repurposing, is a clever strategy to identify new applications ("off" targets) for drugs approved for other clinical diseases [6]. This strategy has been successful employed to unearth new potential treatment options for different diseases including cancer, amyotrophic lateral sclerosis (ALS), Alzheimer's disease, and malaria [7]. On average, 20-30 new drugs receive FDA-approval each year; of these, 30% are repurposed agents [8,9]. Thus this points to repurposing being a quicker strategy to stock the drug discovery pipeline, particularly for antibiotics and antifungals, compared to the traditional process of *de novo* synthesis of new compounds which can cost pharmaceutical companies $800 million to upwards of $1 billion in research and development expenditures and require 10-17 years to attain regulatory approval [10,11]. Repurposing existing approved drugs permits companies to bypass much of the preclinical work and early stage clinical trials required for new compounds (particularly toxicological and pharmacological analysis of drugs) thus cutting into the cost (by nearly 40%) associated with bringing a drug to the marketplace [10].

In addition to lower drug discovery-associated costs, repurposing approved drugs (particularly for identification of new antimicrobials) has several additional benefits. Given these drugs have already been tested in human patients, valuable information pertaining to pharmacokinetic and pharmacodynamics parameters are known [7]. This permits a better understanding of the overall pharmacology of the drug, potential routes of administration (i.e. systemic versus local applications), and establishing an appropriate dosing regimen for patients. Moreover, as the toxicity profile of these drugs in humans has been extensively studied, valuable information has already been obtained regarding potential adverse side effects present with using the drug at certain therapeutic doses. This information is important as it pertains to antimicrobials as the concentration where toxicity is observed with host tissues can be correlated with the minimum inhibitory concentration (MIC) values obtained in standard bacterial susceptibility assays to determine if drugs are viable candidates for repurposing as antimicrobials.

Interestingly, several antibiotics have been repurposed for other clinical indications. For example, the third-generation cephalosporin, ceftriaxone, was initially approved for use in treating bacterial infections, including community-acquired pneumonia and meningitis [12-14]. In bacteria, it interacts with penicillin-binding protein 2 to inhibit cell wall synthesis [15]. Surprisingly, when tested in a neurodegenerative mice model of ALS, ceftriaxone was found to reduce the loss of neurons and muscle strength by increasing expression of glutamate transporter GLT1 thus decreasing the concentration of the toxic neurochemical glutamate present near motor neurons [16]. This provided hope that this antibiotic could be repurposed as a novel treatment option for patients suffering from ALS. Unfortunately, a phase III clinical trial testing ceftriaxone in ALS patients was stopped

after it was suspected that the drug would not be able to help slow down progression of the disease or increase the rate of survival in affected patients [17]. A recent study found that ceftriaxone also possesses antitumor activity and may be an alternative chemotherapeutic agent for use in lung cancer patients [6]. In addition to ceftriaxone, the tetracycline antibiotic, minocycline, has been shown to slow down the emergence of ALS in mice and enhance patient survival in an ALS mouse model [18]. Another antibiotic, fosmidomycin, that targets isoprenoid synthesis in bacterial cells, has been shown to have excellent activity against the parasite *Plasmodium falciparum*, thus permitting investigation for use as a treatment for malaria [19]. Its mode of action in the malaria parasite involves inhibition of a key enzyme (1-deoxy-D-xylulose 5-phosphate reductoisomerase) in the non-mevalonate pathway [20]. Clinical trials performed with fosmidomycin in combination with a second antibiotic (clindamycin) in malaria-stricken patients have obtained promising results thus far, further supporting the repackaging of fosmidomycin for use as a new treatment option against malaria [20,21]. Furthermore, the antibiotic rapamycin (also known as sirolimus) was approved in 1999 by the FDA for use in patients to prevent organ transplant rejection; it was later found to have potential use in two other diseases - Autoimmune Lymphoproliferative Syndrome (ALPS) and the lung disease, lymphangioleiomyomatosis [22-24].

Though antibiotics have entered clinical trials to be repurposed for other clinical indications, to date, not a single drug has been successfully repurposed for use as an antibiotic, particularly for hard-to-treat infections caused by bacteria such as *S. aureus*. As stated earlier, there are several approved drugs for different ailments that have been successfully repurposed as anti-infective agents especially to treat parasitic and protozoal

diseases (Table 1.1). Hence, given the significant problem posed by pathogenic bacteria and fungi, more effort and attention needs to be focused on using drug repurposing as a tool to uncover new treatment options for infections especially caused by multi-drug resistant pathogens, such as *S. aureus*. The present review will delve into approved drugs which have demonstrated promise to be repurposed as agents for *S. aureus* infections, discuss alternative applications for drugs possessing antimicrobial activity, and address current limitations to expedite the discovery and development of approved drugs to be repurposed for use as antibiotics.

Table 1.1 List of drugs which have been repurposed as anti-infective agents

Drugs	Initial use	Repurposed use	References
Auranofin	Antirheumatic agent	Amoebiosis	[25]
Miltefosine	Skin metastases (breast cancer)	Vischeral leishmaniasis	[26,27]
Amphotericin B	Antifungal	Visceral leishmaniasis	[28]
Dapsone	Pulmonary tuberculosis	Malaria	[29-31]
Eflornithine	Antitumour agent/*P. carinii* infection in AIDS patients	Human African sleeping sickness	[32-36]
Doxycycline	Antibacterial	Malaria	[37]
Paromomycin	Antibiotic	Visceral and cutaneous leishmaniasis	[38-40]
Spiramycin	Antibacterial	Toxoplasmosis	[41]
Chloroquine	Malaria	Amebiasis and sarcoidosis	[42,43]
Atovaquone	Malaria	Toxoplasmosis and *P. carinii* pneumonia	[44-46]

1.2 Approved non-antimicrobial drugs with activity against *S. aureus*

Several studies have presented approved non-antibiotic drugs that possess antimicrobial activity, especially against *S. aureus*, indicating these drugs have potential alternative use for treatment of staphylococcal infections. However, the major hindrance for repurposing these drugs pertains to a lack of *in vivo* studies to confirm these drugs do possess antibacterial activity in an animal model. The primary criteria for *in vivo* systemic studies pertain to the availability of enough free drug in the plasma, when given at the tolerable dose, to ensure inhibition of bacterial growth. Hence considering the human plasma concentration of the approved non-antibiotic drugs, hereby we classify the antimicrobial activity of approved non-antibiotic drugs into two categories (a) drugs with activity in a clinical range that can be achieved systemically and (b) drugs with activity that cannot be achieved systemically (Table 1.2).

1.2.1 Drugs with activity in a clinical range that can be achieved systemically

Several of the approved drugs discussed below have antimicrobial activity (denoted as the minimum inhibitory concentration (MIC) or lowest concentration of drug capable of inhibiting bacterial growth) several folds lower than the plasma concentration of the drug in humans. Therefore these particular drugs might be potential candidates to consider for treatment of systemic staphylococcal infections.

Auranofin

Auranofin, a FDA-approved gold compound has been used for treating rheumatoid arthritis for almost 30 years [47,48]. However, its exact mechanism of action (MOA) in

treating rheumatoid arthritis still remains unclear [49,50]. Interestingly, independent of its anti-rheumatoid action, auranofin has also been shown to have anti-parasitic effects. For example, auranofin has been shown to be capable of killing *Schistosoma mansoni* at a concentration of 5 μM and is also active against bloodstream and procyclic stages of *Trypanosoma brucei* with a half-maximal inhibitory concentration, IC_{50}, of 0.5 μM [51,52]. It also inhibits the growth of the malaria parasite, *Plasmodium falciparum, in vitro* with an IC_{50} value of 142 nM [53-55]. Of particular interest, is the recent discovery of auranofin's efficacy in treatment of human amebiasis caused by *Entamoeba histolytica.* Auranofin exhibited anti-Entamoeba activity with a half-maximal effective concentration (EC_{50} = concentration of drug necessary to reduce the culture density to 50%) of 0.5 μM. The EC_{50} for *E. histolytica* was seven-fold lower than the clinically achievable blood concentration of the drug (3.5 μM). Even though auranofin is rapidly metabolized and 60% is bound to plasma proteins, it was found to be effective in two animal models of amebic colitis and amebic liver abscess [25,56]. Based on these studies, auranofin was granted orphan-drug status from the FDA for treatment of human amebiasis in 2012 [25].

With regards to auranofin's antibacterial activity, two recent studies have demonstrated that auranofin also possesses potent antimicrobial activity against *S. aureus* [57,58]. The *in vitro* MIC reported for this drug ranges from 0.125 to 0.5 mg/L [57,58]. More importantly, auranofin demonstrated bactericidal activity against several multidrug-resistant of *S. aureus* within an achievable clinical drug concentration in humans [25,57,58]. Based on these promising preliminary studies, and its recent approval by the FDA as an anti-amoebic drug, auranofin might be a potential agent to repurpose for the treatment of systemic and topical staphylococcal infections. However, future studies are needed to reveal its mechanism of

action against *S. aureus* and establish its antibacterial activity *in vivo* in different animal models of *S. aureus* infection.

Ebselen

Ebselen, an organoselenium compound also known as PZ51 or DR3305, has been widely investigated for its anti-inflammatory, anti-atherosclerotic and antioxidative properties [59-62]. This particular drug has a well-studied toxicology and pharmacology profile and is currently undergoing clinical trials as a treatment option for different ailments including arthritis, cardiovascular disease, stroke, atherosclerosis, and cancer [60,63-66]. In addition to being used as a treatment for multiple diseases, ebselen has also been shown to possess potent antimicrobial activity *in vitro* [67,68]. It has activity against yeast and *Escherichia coli* and works by interfering with proton-translocation and inhibiting the thioredoxin reducatse (TrxR) enzyme respectively [68,69]. Another interesting study has shown that it has potent antimicrobial activity against *S. aureus* with a MIC of 0.20 µg/ml [67]. This minimum inhibitory concentration is well within the plasma concentration (4-6µg/ml) which is attained after1 mg/kg bolus injection combined with 1 mg/kg per hour intravenous infusion in rats [70]. Surprisingly, this drug has not been investigated further as a treatment option for staphylococcal infections in spite of its excellent antibacterial activity in antimicrobial susceptibility assays.

Table 1.2 Approved drugs with activity against *S. aureus*

Drugs	Class/type	MICs (µg/ml)	References
5-fluoro-2'-deoxyuridine	antineoplastic	0.0007-0.002*	[71]
Auranofin	anti-rheumatoid	0.125-0.5*	[57,58]
Ebselen	organoselenium compound	0.2*	[67]
5-fluorouracil	antineoplastic	0.5 – 0.8	[72]
Mitomycin-C	antineoplastic	0.25	[73]
Mithramycin	antineoplastic	0.25	[73]
Disulfiram	alcohol deterrent	1.33	[74]
Triflupromazine	antipsychotic	2-5	[75]
Dactinomycin	antineoplastic	4	[73]
Oxymetazoline	Vasoconstrictor(decongestant)	5	[76]
Daunorubicin	antineoplastic	8	[73]
Doxorubicin	antineoplastic	16	[73]
Levocabastine	antihistamines	20	[76]
Emadastine	antihistamines	20	[76]
Dicyclomine	antispasmodic	25	[77]
Prochlorperazine	antipsychotic	20-25	[78]
Simvastatin	antihyperlipidemic	29-74	[79]
Celecoxib	NSAIDs	32	[80]
Tetrahydrozoline	vasoconstrictor (decongestant)	50	[81]
Methotrexate	antineoplastic	64 – 102	[72]
Tegaserol	narcotic and analgesic	80	[76]
Amitriptyline hydrochloride	antidepressant	100	[82]
Azelastine hydrochloride	antihistaminic	125- 250	[83]
Mitpranolol	antiarrhythmic, antiglucoma	140	[84]
Promethazine	neuroleptic and antihistaminic	125- 250	[83]
Butorphanole	narcotic and analgesic	180	[84]
Diclofenac	anti-inflammatory	200	[85]
Tropicamide	anticholinergic	200	[84]
Oxyfedrine	vasodilator	200-250	[86]
Aminopterin	antineoplastic	256	[73]
Fluvastatin	antihyperlipidemic	400	[76]
Ketamine	anesthetic	450	[76]
Proxymetacaine	anesthetic	500	[76]
Mequitazine	Antihistaminic and anticholinergic	625-125	[83]
Cyproheptadine hydrochloride	antihistaminic	625-125	[83]
Ibuprofen	NSAIDs	1250	[87]
Acetaminophen	NSAIDs	1250	[87]

Table 1.3 continued

Telmisartan	antihypertensive	2000	[76]
Perazine	antipsychotic	2000	[88]
Amlodipine	antihypertensive	3000	[81]
Docusate sodium	laxative	3000	[89]
Etodalac	NSAIDs	4000	[76]
Alverine	spasmolytic	4000	[76]
Fluvoxamine	thymoleptic	4000	[88]
Tolfenamic acid	NSAIDs	5000	[76]
Temozolomide	antineoplastic	5000	[76]
Acepromazine	antiemetic, sedative	5000	[81]
Riluzole	anticonvulsive, antiepileptic	5000	[88]
Tamoxifen	anti-neoplastic	6000	[88]
Solifenacin succinate	spasmolytic	7000	[89]
Perphenazine	antipsychotic	8000	[81]
Oxaprozin	NSAIDs	13000	[76]
Citalopram	antidepressant	13000	[89]
Zofenopril	ACE inhibitor	15000	[88]
Sertraline	antidepressant	16000	[90]
Chlorpromazine	antipsychotic	20000	[81]
Acebutolol	antihypertensive	23000	[81]
Clopidogrel	anticoagulant	24000	[89]

* MICs below the plasma concentration of the drug in humans

Considering its potent *in vitro* anti-staphylococcal activity, studies on the antibacterial MOA of ebselen and evaluating its *in vivo* activity against *S. aureus* could be useful for developing ebselen as an antibacterial agent to treat multidrug-resistant staphylococcal infections [67,68].

5-Flurouracil, 5-fluoro-2'-deoxyuridine, and mitomycin C

Antimetabolites such as 5-flurouracil, 5-fluoro-2'-deoxyuridine (FdUrd), and mitomycin C belong to a class of antineoplastic drugs which are used for treatment of various malignant diseases [91]. They primarily act by inhibiting DNA and RNA synthesis

[91]. In addition to their anticancer activity, these three drugs also exhibit potent antimicrobial activity below the concentration that can be achieved in human plasma [72]. For example, 5-fluorouracil has been shown to inhibit *S. aureus* at a concentration ranging from 0.5 – 8.0 µg/mL, *in vitro*; at this concentration, these drugs fall within the mean plasma concentrations of 13.4 and 8.3 µg/mL, which is attained after a single intravenous (250 mg) and oral dose (500 mg), respectively[72,92,93].

Similarly, FdUrd, an interchangeable metabolite of 5-fluro uracil is capable of inhibiting *S. aureus* growth at a MIC ranging from 0.0007-0.002 µg/ml, which is several hundred folds lower than the mean plasma concentration of 14.1 $\pm$ 2.7 µg/ml, which is attained after a continuous infusion of 1000 mg/m^2 per 24 hour dose of 5-flurouracil for 5 days [71,94,95]. In addition, 5-fluoro-2'-deoxyuridine is a pro-drug which needs the deoxyribonucleoside kinase (dNK) enzyme to exert its action; this enzyme is present in *S. aureus* [71,95].

Another anticancer drug, mitomycin C, when given at a dose of 60 mg/m^2 in humans has been shown to have a peak plasma concentration of 1.9 µg/ml. This drug inhibits *S. aureus* growth at a MIC of 0.06 - 0.25 µg/ml, which is well within the range capable of being reached in the plasma [72,93,96]. Hence, considering promising *in vitro* antibacterial studies conducted this far, these drugs warrant further evaluation as anti-staphylococcal drugs. Future studies would need to be conducted to test their *in vivo* antibacterial efficacy in different animal models.

1.2.2 Drugs with activity that cannot be achieved systemically

Most of the approved non-antimicrobial drugs that possess anti-staphylococcal activity have MIC values that are higher than their plasma concentration; thus, using these drugs for treatment of systemic infections might not be a viable option. However, they can be potentially used for topical application for treating staphylococcal skin infections. Community-associated methicillin-resistant *S. aureus* (CA-MRSA) strains have become a significant source of staphylococcal skin infections. In particular, the strain MRSA USA300 has emerged as one of the most highly prevalent isolates in United States responsible for skin and soft tissue infections [97,98]. Additionally, MRSA colonization in the skin and mucosa is considered an important risk factor for invasive infections [99]. Thus repurposing approved drugs, with high MIC values that cannot be achieved systemically, for use to treat MRSA skin infection and as decolonizing agents is a sensible approach which warrants further investigation. These drugs can be either used as single agents or can be combined with conventional antimicrobials to enhance the efficacy and extend the life span of traditional antimicrobials. Furthermore, several of these drugs have additional benefits that will permit their use as a topical antimicrobial agent. For example, the drugs simvastatin and celecoxib have been shown to inhibit the pro-inflammatory cytokines tumor necrosis factor-α (TNF-α) and IL-6 [100,101]. Controlling excess inflammation, particularly by limiting TNF-α and IL-6 production, in chronic wounds plays a beneficial role in wound healing [102-107]. Additionally, simvastatin has been shown to enhance wound healing and angiogenesis in diabetic mice [108]. Hence, taking into account the antimicrobial activities of these agents combined with their beneficial properties (such as anti-

inflammatory properties), further investigation is warranted to test these approved drugs in topical *S. aureus* infection animal models.

1.3 Novel uses of approved drugs

For the past few decades, the development of new antimicrobials has slowed down while the evolution of bacterial resistance has continued to rise; hence, there is an urgent need to identify alternative strategies to combat infections caused by multidrug-resistant *S. aureus* [109-111]. Emergent approaches that have drawn great interest recently include drugs with indirect antimicrobial activity which work by (i) targeting virulence factors and toxins (anti-virulence agents) [110,112,113], (ii) enhancing host immunity (immunomodulators) [111,114], and (iii) enhancing entrance of other antimicrobials into target cells by increasing the permeability of the outer membrane or by inhibiting efflux pumps (helper drugs) [115]. These novel approaches can be combined with traditional antibiotics to enhance the efficacy and extend the life span of antimicrobial drugs and to minimize the evolution of bacterial resistance to these agents. Here we provide several examples of FDA-approved non-antimicrobial drugs which do not have direct antimicrobial activity or have very high MIC *in vitro* that cannot be achieved clinically; though they cannot be used systemically, they have potential for use to disrupt bacterial pathogenesis or to modulate a host's immune response to combat staphylococcal infections.

1.3.1 Targeting virulence factors and toxins

Targeting staphylococcal virulence factors and toxins is an important strategy to disarm the pathogen in the host. The basic strategy involves inhibiting the mechanisms that

play a role in promoting *S. aureus* invasion, pathogenesis, and persistence [110,113]. Even though, *S. aureus* is not killed directly in this strategy, it greatly reduces the ability of bacteria to colonize the host [110].

Several FDA-approved drugs that do not possess direct antimicrobial activity *in vitro* have been shown to inhibit important virulence factors and toxins. For example, salicylic acid, the major metabolite of aspirin, inhibits the global regulators of virulence genes in *S. aureus* such as *sar*A and *agr* [116]. Repression of these two genes, at a clinical achievable dose, leads to the down regulation of various exotoxins and exoenzymes, such as fibronectin protein binding genes (*fnb*A and *fnb*B) and α-hemolysin (*hla*), which are responsible for *S. aureus* adhesion and host tissue cytolysis[116,117]. This may have the potential to be used as an adjunctive agent for the treatment of multidrug-resistant *S. aureus* infections [116].

Other drugs such as cisplatin and chloroquine are also known to protect infected hosts from the effects of bacterial toxins. Cisplatin is an anticancer drug that acts primarily by interacting with DNA to form DNA adducts, thereby leading to the activation of apoptosis [118]. In addition to this, cisplatin also protects macrophages from anthrax lethal toxin (LT) by inhibiting LT translocation into cells [119]. This protective effect has also been confirmed in murine models [119]. Similarly, chloroquine, a well-known anti-malarial drug, blocks the entry of anthrax toxins and increases animal survival in anthrax-toxin challenge.[120-122]. Future studies are needed to gain more insights into the molecular actions of these drugs with bacterial toxins. Additionally, it will be worthy to investigate the effect of these FDA-approved drugs on *S. aureus* toxin production, toxin interaction with host cells, and the host immune response.

1.3.2 Efflux pump inhibitors

Efflux mediated resistance towards antibiotics in *S. aureus* has been gaining more attention recently and is recognized as the first line of bacterial defense against antimicrobials [123]. Several efflux pumps in staphylococci are associated with resistance to various antimicrobials. Efflux pumps such as Tet (K) and Tet (L) contribute to tetracycline resistance, NorA, NorB, NorC, MepA and MdeA are associated with fluoroquinolone resistance, while Mef(A) and Msr(A) mediate resistance to macrolides [123,124].

FDA-approved drugs have been shown to inhibit important efflux pumps in *S. aureus.* For example, the phenothiazine group of drugs such as chlorpromazine, fluphenazine, prochlorperazine, and thioridazine, which are primarily used for the treatment of schizophrenia and other psychotic disorders, showed marked inhibitory activity against efflux pumps in *S. aureus* [125,126]. All four drugs have also been found to inhibit NorA-mediated efflux in *S. aureus* and enhance the activity of norfloxacin several fold [127]. Chlorpromazine and thioridazine have also been shown to reduce MRSA resistance to oxacillin [128]. Similarly, reserpine, an antipsychotic and antihypertensive drug, also inhibits an efflux pump in *S. aureus* that subsequently makes it susceptible to both oxacillin and norfloxacin [127,128]. Another antihypertensive drug, verampil, has also been shown to reduce fluoroquinolone-resistance in *S. aureus* [129,130].

Proton pump inhibitors, such as omeprazole and lansoprazole, which are used for the treatment of gastroesophageal efflux and dyspepsia in humans, have also been proven to be potent inhibitors of *S. aureus* efflux pumps [131]. These drugs greatly enhance the activity of fluoroquinolones such as levofloxacin, ciprofloxacin, and norfloxacin in strains of *S.*

aureus expressing NorA [131]. Therefore, therapeutic development of bacterial efflux pump inhibitors (in combination with antimicrobials to permit entry of the antimicrobial into the pathogen) is a useful strategy to consider as a treatment for *S. aureus* infections. However, a limitation of the non-antibiotic drugs discussed above is none possess activity at a concentration lower than those achievable in human serum [131]. Hence, future studies are needed to focus on making modifications to these drugs to enhance their activity against *S. aureus*. Additionally, screening of FDA-approved drug libraries can be done to identify more potent efflux pump inhibitors within the applicable clinical range in humans.

1.3.3 Immuno-modulatory drugs

S. aureus possesses diverse immune evading mechanisms to alter the host immune response in such a way that favors their invasion, survival, and replication in the host [132,133]. Hence, modulation of this complex host immune response to the pathogen is another reasonable approach to target these bacterial infections that has been widely investigated in recent years [111,114]. In general, pathogens develop strategies to become invisible to the host immune system and in turn the host fails to mount an effective immune response to clear the pathogen [132-134]. On the other hand, there are circumstances where pathogens, such as *S. aureus* and its virulence factors, are capable of hyper stimulating the host immune system, leading to the uncontrolled production of inflammatory markers and other mediators which result in tissue damage and septic shock [135,136]. This happens more often in acute infections such as in sepsis where the strong inflammatory response and cytokine storm that follows may lead to shock and death [137-139]. In addition, *S. aureus* is also known to secrete various exotoxins such as α-hemolysin, leukocidins and toxic shock syndrome

toxin (TSST-1) which can activate antigen-presenting cells (APCs) and T-cells leading to the induction of a strong inflammatory cascade reaction [135,136,140]. Superantigens such as TSST-1 and enterotoxins also bypass normal antigen processing by APCs and induce direct proliferation of T-cells, even at a picomolar concentration [140,141]. Hence, finding immunomodulatory agents that can be effectively combined with antibiotics may produce a better outcome in patients afflicted with a *S. aureus* infection. [142-145].

Non-antibiotic FDA-approved drugs with immuno-modulatory activity to treat bacterial infections have been investigated by various researchers. Even though some of these drugs have no direct antimicrobial activity *in vitro*, they have been shown to aid in achieving a better resolution of staphylococcal infections by reducing toxin production or by modulating host immune response to enhance bacterial clearance.

Statins

Statins are one of the major classes of FDA-approved lipid lowering drugs that act on HMG-CoA reductase; these drugs have been widely used to prevent cardiovascular disease in humans [146-148]. In addition to their role in cardiovascular disease, numerous functions of statins, independent of their lipid lowering property, have been studied recently [149]. The antibacterial activity of statins, particularly simvastatin, has been explored by several groups [150-157]. However, the high MIC value obtained for statins is a major concern with using statins directly as antimicrobial agents [158]; this has led to researchers searching for alternative uses for statins for treating bacterial infections.

Statins act at various cellular and molecular levels and regulate multiple anti-inflammatory actions, reduce oxidative stress, and inhibit leukocyte-endothelial

interactions and leukocyte migration. All these effect are beneficial in treating sepsis [159]. Furthermore, statins inhibit several different cytokines including TNF-α, IL-1β, IL-6, and IL-8, thereby lowering the inflammatory activity of neutrophils and macrophages and dampening the immune response involved in sepsis [159-165]. In addition to the extensive inflammatory response, the release of several mediators such as C-reactive protein also plays a major role in sepsis [166]. C-reactive protein promotes thrombus formation by enhancing endothelial cell–monocyte interaction, increases tissue factor expression, and activates the complement system leading ultimately to organ dysfunction and death [159,166,167]. However, statins greatly reduce the levels of C-reactive protein and its subsequent actions in sepsis [168-170]. Statins also inhibit leukocyte migration by reducing various adhesion molecules such as VLA4, P-selectin, CD11b, CD11a and CD18 [171-173]. In addition, a study demonstrated that simvastatin pre-treatment also reduces *S. aureus* α-toxin induced leukocyte rolling, adhesion, and transmigration [174]. Furthermore, the overall beneficial role of statins in *S. aureus* septicemia is supported by a retrospective and clinical study which demonstrated significant reduction in mortality among patients with statin therapy compared with patients not taking statins [158,175,176]. Hence, the promising evidence compiled thus far of statins in limiting the effects of sepsis make it worthwhile to investigate the exact molecular mechanism by which statins exhibit their action to propel them into clinical trials in the future, as a novel therapeutic approach for sepsis management.

Nicotinamide

Beyond the use of nicotinamide (vitamin B3) as a supplement, it inhibits inflammatory cytokines such as IL-1β, IL-6, IL-8, and TNF-α and is used for the treatment of inflammatory skin disorders such as atopic dermatitis and acne vulgaris [177,178]. In addition, nicotinamide, in combination with nafcillin, improved the survival outcome of staphylococcal septic shock in mice [179]. However, the exact molecular mechanism behind this immune modulation activity remains unclear. Another study showed nicotinamide enhanced *S. aureus* killing *in vivo* by modulating host factors [180]. Host factors, such as phagocytic ability of monocytes and macrophages, greatly influence bacterial clearance. In particular, a higher expression of anti-staphylococcal peptides such as lactoferrin (LTF) and cathelicidin in monocytes and macrophages greatly increases their phagocytic ability and bacterial killing [180-183]. However, the expression of antimicrobial peptides (LTF and cathelicidin) in phagocytic cells is regulated by CCAAT/enhancer-binding protein ε (C/EBPε), a myeloid-specific transcription factor [180-183]. Nicotinamide increases the activity of C/EBPε in neutrophils and enhances the killing of *S. aureus* up to 1000-fold *in vivo* [180]. Hence, by manipulating C/EBPε expression, the phagocytic ability of certain immune cells can be enhanced, which further increases their bactericidal activity. [180].

Additionally, nicotinamide also reduces staphylococcal enterotoxin (SEB)-induced responses [184]. Nicotinamide inhibits the SEB-induced T-cell proliferation and inflammatory cytokines such as IL-2 and IFN-γ, and protects mice from SEB-induced toxicity [184]. Thus, taken collectively, nicotinamide with potent immuno-modulatory activities via increased *S. aureus* killing and damping the SEB-induced inflammatory response should have therapeutic value for the treatment of staphylococcal infections.

Dexamethasone

Dexamethasone is a steroid drug with potent anti-inflammatory and immunosuppressive activity that has been used for the treatment of various systemic and localized skin diseases. Being a potent anti-inflammatory drug, it also inhibits staphylococcal enterotoxin (SEB)-induced inflammatory cytokines such as TNF-α, IFN-γ, IL-1α, IL-2, and IL-6 and protects mice from hypothermia and shock [185-188].

Rapamycin

Rapamycin, a FDA-approved immunosuppressive drug is used to prevent graft rejection in renal transplantation [189]; it has also been shown to have a protective effect in a SEB-induced septic shock mice model by inhibiting cytokines such as TNF-α, IFN-γ, IL-2, IL-6, and IL-1α. Additionally, it inhibits production of chemokines such as chemo attractant protein 1 (MCP-1) and macrophage inflammatory protein 1(MIP-1) in peripheral blood mononuclear cell PMBC [190,191]. When tested i*n vivo,* rapamycin protected all treated mice from lethal staphylococcal shock even when administrated 24 hours after SEB challenge [190,191].

Pentoxifylline

Pentoxifylline, a FDA-approved drug used for the treatment of intermittent claudication resulting from peripheral artery disease, has a protective role on SEB or TSST-1 induced lethal effects [192,193]. It suppresses T cell activation and inhibits the

cytokines TNF-α, IFN-γ, and IL-1α [192]. Furthermore, pentoxifylline prevents mice lethality in a SEB-induced shock model [192].

The examples described above demonstrate the great potential of FDA-approved non-antimicrobial immunomodulators to be combined with traditional antimicrobials to modulate the host immune response and can be further explored as a novel viable therapeutic strategy for the treatment of staphylococcal infections.

1.3.4 Anti-biofilm agents

Biofilm-forming *S. aureus* often cause serious complications leading to life-threatening infections [194]. Studies on staphylococcal biofilm present on indwelling medical devices such as catheters, implanted devices, and prosthetic heart valves have drawn great interest over the past few decades [194]. *S. aureus* biofilm-associated infections are challenging to treat with conventional antibiotics [194,195]. Hence, novel drugs and strategies are in immediate need to deal with biofilm infections [195]. Several FDA-approved non-antibiotic drugs have been shown to possess anti-biofilm activity. For example, nitazoxanide (NTZ), an anti-protozoal agent approved for the treatment of *Cryptosporidium parvum* and *Giardia intestinalis* infections in humans, is shown to have anti-biofilm activity [196]. Nitazoxanide exhibits anti-staphylococcal activity at a MIC ranging from 8 to 16 μg/ml. Additionally, at sub inhibitory concentrations (IC_{50} of 1 to 3 μg/mL), NTZ is shown to inhibit biofilm formation by *Staphylococcus epidermidis* [197].

Several FDA-approved drugs are known to disrupt adherent microbial biofilms. Examples include auranofin (anti-rheumatoid drug), benzbromarone (gout drug), pyrvinium pamoate (antihelminthic), yohimbine hydrochloride (mydriatic vasodilator),

and zotepine (antipsychotic) which have all been shown to be capable of inhibiting pre-formed microbial biofilms [198]. Further testing of these drugs against different staphylococcal biofilms, both alone and with conventional antimicrobials, should be considered as a new avenues to target multidrug-resistant staphylococcal infections and associated biofilms.

1.4 Identifying new antibiotic leads from approved drugs which can serve as novel antibiotics

From 2008-2012, only three new antibiotics received approval from the FDA [199]. Interestingly, in 2014, thus far the FDA has already approved three new antibiotics (dalvance, tedizolid phosphate, and oritavancin) indicating the agency is recognizing the urgent need for new antibiotics to treat difficult bacterial infections; all three approved drugs are indicated for use in treating acute bacterial skin and skin structure infections caused by pathogens such as MRSA [200,201]. These antibiotics are not new drug classes but rather modified derivatives of older antibiotics which interfere with the same biochemical pathways and molecular targets known for many years. For example, dalvance and oritavancin belong to the glycopeptide class of antibiotics (which interfere with bacterial cell wall synthesis) while tedizolid phosphate is an oxazolidinone which inhibits bacterial protein synthesis.

Though numerous new molecular/druggable targets inside bacteria have been identified in recent years, no compounds have been successfully developed (and received approval) that interact and bind to these targets. Given that only four new antibiotic classes have been identified in the past 40 years using the traditional drug discovery approach, new

techniques need to be considered to discover drugs capable of binding to these unique targets [202]. Drug repurposing presents a new method to screen for existing drugs that can interact with these critical targets inside pathogens. This could lead to the development of new antimicrobial classes which interact with different molecular targets compared to traditional antibiotics. Understanding which moiety on the drug interacts with the molecular target can also permit medicinal chemists to make rational modifications to the parent drug to construct analogues with enhanced binding affinity for the target (with the hope of improved antimicrobial activity), improved pharmacokinetic profile of the drug, and reduced toxicity to host tissues. Also this could permit the identification of new bacterial targets which have not been previously known.

1.5 Challenges for repurposing non-antibiotic drugs for *S. aureus*

Though repurposing approved drugs for use as antimicrobials is an exciting avenue for discovery of new potential treatments for bacterial infections, there are multiple obstacles hindering progress in identifying and developing these agents. One of the biggest challenges in the field of antibiotic drug discovery is the lack of interest by pharmaceutical companies and industry to invest resources in this area. The reality is that the vast majority of drugs currently available in the market were discovered by the pharmaceutical industry. In the United States alone, only 9% of new drugs discovered between the years of 1960 and 1969 came from government agencies, universities, and not-for-profit organizations [8]. This trend continued to hold true in latter parts of the 20th century as over 93% of new drugs approved in the United States, from 1990 to 1992, were procured from industry; government agencies and academic institutions each accounted for just over 3% of new

drugs in this time span [10]. Thus industry is a key cog in the identification and development of drugs which are capable of reaching the healthcare setting. However, given the low return on investment for antibiotics, companies, particularly Big Pharma, have moved away from developing new antibiotics. This can be illustrated with a simple example; from 2009-2012, Merck's leading medication for diabetes (Januvia) outsold its top-selling antibiotic (Invanz, a carbapenem antibiotic) by US$11 billion [203]. Moreover, a review of the top 100 best-selling drugs from April 2013 through March 2014 revealed treatments for chronic diseases such as rheumatoid arthritis (Humira, Enbrel, Remicade), depression (Cymbalta, Seroquel XR), asthma (Advair), high-cholesterol (Lipitor, Crestor, Zocor), multiple sclerosis (Copaxone, Tecfidera), Alzheimer's disease (Namenda), diabetes (Lantus Solostar, Januvia), AIDS (Atripla, Truvada, {Prezista), high blood pressure (Diovan, Metoprolol), and cancer (Rituxan, Avastin, Gleevec) generated the most sales for pharmaceutical companies; interestingly no antimicrobials were found on this list. Given the associated costs involved with drug discovery, the lack of sales generated by antibiotics (in comparison to drugs developed for chronic diseases such as asthma, diabetes, and high blood pressure), and stringent regulations required for new antibiotics to receive regulatory approval, this significantly reduces the incentive needed by companies to pursue developing novel antimicrobials [199]. This has led to several major companies, including Pfizer and Roche, to terminate their antibiotics research & development division; as of 2013, only four major pharmaceutical companies have active antimicrobial drug discovery programs [202,203]. This leaves government agencies, academic institutions, and small companies with the burden of filling this gap to generate new antimicrobials. While repurposing existing drugs is a mechanism for these institutions to curb costs associated

with the drug discovery process, most of these agencies lack the resources available to industry for drug discovery. Additionally, these organizations face a second major obstacle in the path to repurposing drugs as antimicrobials.

A second major challenge to repurposing approved drugs as antimicrobials pertains to the lack of accessibility to libraries containing clinical drug collections. As highlighted by Chong and Sullivan, no single collection of the nearly 10,000 known clinical drugs currently exists [7]. Instead these drugs are dispersed throughout several different collections or are not available to researchers (in part due to existing patents present for certain drugs). Among the publicly available compound collections include the National Institute of Neurological Disorders and Stroke (NINDS) collection of 1,040 compounds, the Prestwick Chemical Library in Washington, DC (containing more than 1,000 approved drugs), and the Johns Hopkins Clinical Compound Library (consisting of more than 1,500 compounds) [7]. Combined with other drug collections available for commercial purchase, this amounts to only 40% of the total known approved drugs and clinical molecules which are available for screening for antimicrobial activity [7]. However, redundancy and overlap between these different libraries presents an additional problem as a compound may be present in more than one collection making screening these compounds more difficult.

Obtaining access to the remaining 60% of clinical drugs, for screening for antimicrobial activity, is a significant impediment to identifying new clinical applications for these drugs. Moreover, it would be valuable to researchers if they can gain access to libraries of compound metabolites and drugs which entered phase II and III clinical trials but failed to receive approval for the initial clinical indication. Most drugs fail in phase II clinical trials because they prove ineffective in treating the disease they were initially

intended to be used for [11]. Though these compounds may not have succeeded in gaining approval for their initial clinical application, they may still have promise for alternative uses, for example as antibiotics for *S. aureus* infections. Gaining access to these compounds, clinical data generated for these compounds, and information pertaining to why they failed in clinical trials will permit researchers to rationally design potential solutions to overcome these issues in repurposing these compounds for other clinical applications. However, many of these clinical failures are often not made publicly accessible by pharmaceutical companies (for competitive and financial reasons); additionally given these companies often are focused on developing drugs for specific diseases, they may not have the resources (i.e. models to study infectious diseases in humans) or personnel to identify new applications for these failed compounds [11]. Establishing relationships and bridging the gap between industry (who would provide these compounds and clinical data garnered), academic research institutions (to screen these compound libraries for hits for antimicrobial activity), and government agencies (to assist with sponsoring clinical trials to test drugs to be repurposed as antimicrobials) is very important in order to find new applications for both approved drugs and compounds which have entered into late stage clinical trials but ultimately failed.

1.6 Conclusion

Development of new antimicrobials is very slow and there are not enough new antimicrobials in the drug pipeline to keep pace with the emergence of multidrug-resistant bacterial strains. Moreover, pharmaceutical companies lacking interest in antimicrobial drug discovery has contributed to the dearth of new and novel antibiotics. Therefore

alternative strategies are in urgent need to battle against multidrug-resistant infections such as those caused by *S. aureus*. Repurposing approved drugs presents an emerging approach with reduced cost, discovery time, and risk associated with antibiotic development. We presented several approved drugs that possess potent anti-staphylococcal activity *in vitro*; with further mechanistic and *in vivo* studies, these drugs might be a potential candidate drugs that can be considered for systemic and (or) topical applications. Independent of antimicrobial activity, some drugs also have the ability to interfere with *S. aureus* pathogenesis and modulate host immune response to enhance bacterial killing and clearance. This is an additional novel application of the approved drugs which warrants further exploration. With the promising activity and the past success in drug repurposing, repositioning existing drugs might form a potential alternative strategy to discover new antimicrobials and might drive interest of researchers both in academia and the pharmaceutical industry to invest more research resources in this area.

CHAPTER 2. DRUG REPURPOSING FOR BACTERIAL INFECTIONS

2.1 Antibacterial activity and mechanism of action of auranofin against multi-drug resistant bacterial pathogens

(Thangamani S, Mohammad H, Abushahba MF, Hamed MI, Sobreira TJ, Hedrick VE, Paul LN, Seleem MN. Antibacterial activity and mechanism of action of auranofin against multi-drug resistant bacterial pathogens. *Scientific Reports.* 2016 Mar 3;6:22571.)

2.1.1 Introduction

Bacterial resistance to antibiotics is a significant public health challenge, as infections caused by antibiotic-resistant bacteria claim the lives of nearly 23,000 people each year in the United States alone [204]. A single pathogen, methicillin-resistant *Staphylococcus aureus* (MRSA), is responsible for nearly half of these fatalities. MRSA has been linked to invasive diseases including pneumonia [205] and sepsis [206], that affect a diverse population of patients including individuals with a compromised immune system [207] such as young children [208]. While a powerful arsenal of antibiotics was once capable of treating *S. aureus*-based infections, clinical isolates of MRSA have emerged to numerous antibiotics, including agents of last resort such as vancomycin [4] and linezolid [209].

Most current antibiotics were discovered via the time-consuming and financially taxing process of *de novo* synthesis and screening of chemical compounds[210]. An alternative approach to unearthing new antibacterials that is garnering more recent attention is screening libraries of approved drugs (or drugs that made it to clinical trials but ultimately failed to receive regulatory approval) in order to identify candidates that can be repurposed as antimicrobials [210]. Recently, we assembled and screened 50% of the commercially available drugs (~ 2,200 drugs) and small molecules tested in human clinical trials [7,211](727-NIH Clinical Collections 1 and 2, 1,600-Pharmakon from Microsource, Approved Oncology Drugs Set-NIH, and few small libraries) and identified three drugs that exhibited potent antibacterial activity at a dose that is clinically achievable. One of these drug, auranofin is capable of inhibiting growth of clinically-pertinent isolates of MRSA at submicrogram/mL concentrations *in vitro*. Auranofin is an oral gold-containing drug initially approved by the U.S. Food and Drug Administration (FDA) for treatment of rheumatoid arthritis. In a study by Debnath *et al*, auranofin was found to exhibit potent anti-parasitic activity against *Entamoeba histolytica* providing evidence that this drug could be repurposed as an antimicrobial agent [25]. More recent studies have discovered this drug also possesses potent antibacterial activity including against important pathogens such as MRSA [25,212-215].

Building upon this seminal work, the goals of the present study were to further investigate the antibacterial mechanism of action of auranofin and to examine potential applications of auranofin as an antibacterial agent for systemic MRSA infections. We have identified that auranofin appears to target multiple biosynthetic pathways in *S. aureus*, including inhibition of cell wall, DNA, and protein synthesis; this latter property permits

auranofin to mitigate specific virulence factors including reducing the production of key toxins such as α-hemolysin and Panton-Valentine leucocidin, a fact previously unknown. Auranofin is less effective against Gram-negative pathogens in large part due to the presence of the outer membrane in these pathogens. Furthermore, *in vivo* studies demonstrate that auranofin is capable of treating invasive MRSA infections, thereby expanding the potential therapeutic applications of this drug for use as a novel antibacterial agent. The findings presented in this study provide strong evidence that auranofin can be repurposed as a novel antibacterial agent for treatment of invasive MRSA infections in humans.

2.1.2 Materials and Methods

Bacterial strains and reagents

Bacterial strains used in this study are presented in Tables 1 and 2. Mueller-Hinton broth (MHB) was purchased from Sigma-Aldrich while Trypticase soy broth (TSB), Trypticase soy agar (TSA), and mannitol salt agar (MSA) were purchased from Becton, Dickinson and Company (Cockeysville, MD). Auranofin (Enzo Life Sciences), vancomycin hydrochloride (Gold Biotechnology) and linezolid (Selleck Chemicals) were al purchased from commercial vendors.

Antibacterial assays

The broth microdilution method was employed to determine the MICs of all test agents (tested in triplicate) as per the Clinical and Laboratory Standards Institute (CLSI) guidelines [216]. Test agents were incubated with bacteria for 16 hours at 37°C prior to

determining the MIC. The MIC was classified as the lowest concentration of drug capable of inhibiting visible growth of bacteria by visual inspection.

Gram-negative bacteria outer membrane permeabilization assay

The MIC of auranofin and control antibiotics, in the presence of polymixin B nonapeptide (PMBN), against Gram-negative bacteria was measured as described in the antibacterial assay section above. A subinhibitory concentration of PMBN (10 μg/ml) was added to TSB to increase the outer membrane permeability and facilitate the entrance of auranofin, as described elsewhere [217,218].

Macromolecular synthesis assay

S. aureus ATCC 29213 was used for the macromolecular synthesis assay and the assay was carried out using auranofin and control antibiotics (ciprofloxacin, rifampicin, linezolid, vancomycin and cerulenin) as described elsewhere [211].

Proteomics analysis

Sample Preparation: An overnight culture of MRSA USA300 cells were treated with 10 × MIC of auranofin (1.25 μg/ml), linezolid (20 μg/ml) and vancomycin (10 μg/ml) for one hour at 37°C. Bacterial cells were centrifuged and sequence grade Lys-C/Trypsin (Promega) was used to enzymatically digest samples. Samples were reduced and alkylated prior to digestion. All trypsin digestions were carried out in a Barocycler NEP2320 (PBI) at 50°C under 20 kpsi for two hours. After digestion, samples were cleaned using MicroSpin C18 columns (Nest Group, Inc.) and the resulting pellets were re-suspended in

97% H_2O/3% ACN/0.1% FA. A small aliquot (5 µL) of sample was analyzed via nanoLC-MS/MS.

LC-MS/MS: Samples were run on an Eksigent 425 nanoLC system coupled to the Triple TOF 5600 plus [219]. The gradient was 120 min at 300 nl/min over the cHiPLC–nanoflex system. The trap column was a Nano cHiPLC 200 µm × 0.5 mm ChromXP C18-CL 3 µm 120 Å followed by the analytical column, the Nano cHiPLC 75 µm × 15 cm ChromXP C18-CL 3 µm 120 Å. The sample was injected into the Triple TOF 5600 plus through the Nanospray III source. Data acquisition was performed at 50 precursors at 50 min/scan.

Analysis: WIFF files from mass spectrometric analysis were processed using the MaxQuant computational proteomics platform version 1.5.2.8 [220]. The peak list generated was screened against the *Bos taurus* (41521 entries unreviewed) and *Staphylococcus aureus* (10972 entries reviewed) sequence from UNIPROT retrieved on 04/10/2015 and a common contaminants database. The following settings were used for MaxQuant: initial precursor and fragment mass tolerance set to 0.07 and 0.02 Da respectively, a minimum peptides length of seven amino acids, data was analyzed with 'Label-free quantification' (LFQ) checked and the 'Match between runs' interval set to 1 min, the FASTA databases were randomized and the protein FDR was set to 5%, enzyme trypsin permitted two missed cleavage and three modifications per peptide, fixed modifications were carbamidomethyl (C), variable modifications were set to Acetyl (Protein N-term) and Oxidation (M). The MaxQuant results used in-house script, and the average LFQ intensity values for the technical replicates were used for each sample. Both the *Bos taurus* and the common contaminant proteins were removed. Values were transformed [$\log_2(x)$] and the missing values were inputted using the average values of all samples. The heat maps and statistical

analyses were performed in the R environment (www.cran.r-project.org) and Qlucore OMICS explorer (version 3.0, Qlucore, Lund, Sweden). A one-way analysis of variance (ANOVA) was performed on the LFQ intensities and only proteins with $P < 0.05$ were selected for further analyses.

Growth curve of *E. coli* in the presence of auranofin

Wild-type and *trxB*/*gor* double mutant *E. coli* strains (wild-type: novablue (DE3)-K12, *trxB/gor* double mutant: Origami-2) were incubated with indicated concentration of auranofin in the presence and absence of PMBN (10 µg/ml) for 16 hours at 37°C. Bacterial growth was monitored using a spectrophotometer (OD = 600 nm).

Analysis of *S. aureus* toxin production by ELISA

The effect of auranofin and two control antibiotics (vancomycin and linezolid) on production of two key *S. aureus* toxins (α-hemolysin and Panton-Valentine leukocidin) was measured by ELISA as has been previously described [211].

Intracellular infection assay

J774A.1 murine macrophage-like cells were infected with MRSA USA300 for 30 min at a multiplicity of infection (MOI) ratio of 1:100. Infected cells were subsequently washed three times with DMEM medium containing 10 IU lysostaphin [221]. Auranofin (0.5 µg/ml), vancomycin (4 µg/ml) and linezolid (8 µg/ml), in triplicates, in complete DMEM medium containing 4 IU lysostaphin was then added. After 24 hours of incubation at 37°C (with 5% CO_2), the cells were washed three times with phosphate-buffered saline (PBS)

and lysed with 0.1% Triton X-100 (Sigma-Aldrich). Cell lysates were plated onto TSA plates and MRSA colony forming units (CFU) were counted after incubation of plates for 24 hours at 37°C.

Mice studies

Eight week old female BALB/c mice (Harlan Laboratories, Indianapolis, IN) were used in all mice studies. The animal care and all experiments were approved and performed in accordance with the guidelines approved by Purdue University Animal Care and Use Committee (PACUC). Eight-week old female BALB/c mice (n = 10 per group) were used and the study was carried out as described before [222]

Systemic - lethal infection : An overnight culture of MRSA USA300 cells were washed and re-suspended in PBS. Each mouse received an intraperitoneal (i.p.) injection (200 µl) containing the bacterial suspension (9×10^9 CFU). One hour after infection, mice were divided into four groups (ten mice per group). Mice were treated orally with auranofin (either 0.125 or 0.25 mg/kg), linezolid (25 mg/kg), or the vehicle alone (10% ethanol). Treatment was provided once daily for three days following infection. Mortality was monitored daily for five days and the moribund mice were euthanized humanely using CO_2 asphyxiation.

Systemic – non-lethal infection: The infection protocol was carried out as described above (systemic-lethal infection) with the following exceptions. Each mouse received an i.p. injection containing 2×10^7 CFU MRSA USA300. Mice were divided into three groups (five mice per group) and treated orally with auranofin (0.25 mg/kg), linezolid (25 mg/kg), or vehicle (10% ethanol) alone. Mice were treated once daily for two days. Twenty-four

hours after the last dose, mice were euthanized and their spleen and liver were excised, homogenized in TSB, plated onto MSA plates, and incubated at 37°C for 24 hours prior to counting MRSA CFU post-treatment.

Combination testing of auranofin with commercial antibiotics

Additive activity of auranofin with conventional antibiotics (ciprofloxacin, linezolid and gentamicin) was evaluated as described in a previous study[223,224]. Briefly, MRSA USA300 was incubated with auranofin, control antibiotics, or a combination of auranofin + a control antibiotic at different concentrations for 16 hours. Next, the optical density (at 600 nm) was measured using a spectrophotometer. Percent bacterial growth for each treatment regimen was calculated and presented.

Growth curve of *S. aureus* in the presence of auranofin

MRSA USA300 was incubated with indicated concentration of auranofin for 16 hours at 37°C and the percent bacterial growth was monitored using a spectrophotometer (OD = 600 nm).

Time kill assay

An overnight culture of MRSA USA300 was diluted to 6×10^5 CFU/mL and treated with 5 × MIC of auranofin, vancomycin or linezolid (in triplicate) in Mueller Hinton broth and incubated at 37°C. Samples were collected at indicated time points, serially diluted in PBS, and transferred to TSA plates. Plates were incubated at 37°C for 24 hours prior to counting MRSA colony forming units (CFU).

DNA intercalation assay

DNA intercalation assay was carried out using pUC 18 plasmid as described elsewhere [225]. Briefly, 250 ng of plasmid DNA was incubated with the indicated concentration of auranofin and doxorubicin in a total volume of 25 µl and the reaction mixtures were incubated for 30 min at 37°C. An electrophoretic assay was run using 1% agarose gel without ethidium bromide at 50 volts for 4 hours. The gel was stained with ethidium bromide and visualized for DNA mobility.

Cytotoxicity assay

In vitro toxicity assay was carried out in mouse macrophage (J774A.1) cells by MTS assay as described before [226]. Briefly, auranofin at a concentration ranging from 0 to 256 µg/ml was added to the cells. After 24 hours of incubation, the cytotoxicity effect of auranofin was measured by the addition of MTS assay reagent 3-(4,5-dimethylthiazol-2-yl)-5-(3-carboxymethoxyphenyl)-2-(4-sulfophenyl)-2H tetrazolium). Results are expressed as percent cell viability of auranofin-treated cells in comparison to cells treated with DMSO.

Statistical analyses

Statistical analyses were assessed using GraphPad Prism 6.0 (Graph Pad Software, La Jolla, CA). *P* values were calculated via the Student *t* test or Kaplan-Meier (log rank) survival test as indicated. *P* values of ≤ 0.05 were deemed significant.

2.1.3 Results

Auranofin is a potent inhibitor of multidrug-resistant Gram-positive bacteria

The antimicrobial activity of auranofin was assessed against a panel of clinical isolates of multidrug-resistant Gram-positive pathogens using the broth microdilution

Figure 2.1 Growth curve of MRSA USA300 in the presence of auranofin. Bacteria were incubated with indicated concentrations of auranofin and the growth was measured using a spectrophotometer

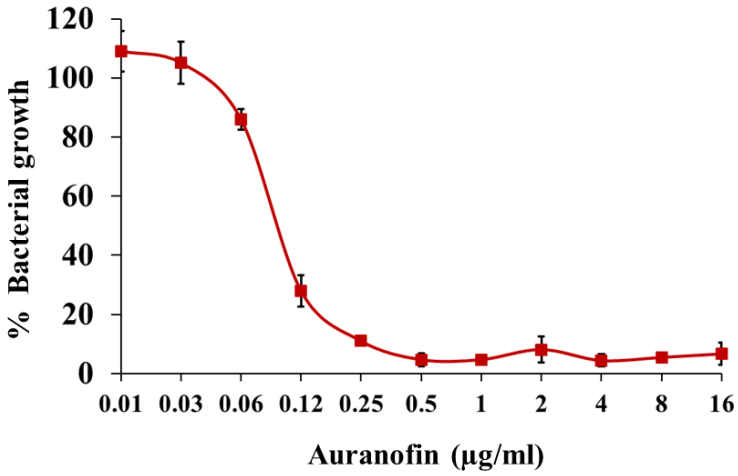

method (Table 2.1). Auranofin exhibited potent bactericidal activity against all tested bacteria including strains that are resistant to conventional antimicrobials such as methicillin and vancomycin. The minimum inhibitory concentration (MIC) of auranofin, required to inhibit growth of different MRSA strains, were found to be in the range of 0.0625 to 0.125 µg/ml (Table 2.1 and Figure 2.1).

Table 2.1 MICs of auranofin and control antibiotics against Gram-positive bacteria

Strain ID	Phenotypic Characteristics	Auranofin MIC (µg/ml)	Linezolid MIC (µg/ml)	Vancomycin MIC (µg/ml)
MRSA (USA100)	Resistant to ciprofloxacin, clindamycin, erythromycin	0.125	2	2
MRSA (USA200)	Resistant to clindamycin, methicillin	0.0625	2	1
MRSA (USA300)	erythromycin, gentamicin, Resistant to erythromycin, methicillin, tetracycline	0.125	2	1
MRSA (USA400)	Resistant to methicillin, tetracycline	0.0625	2	1
MRSA (USA700)	Resistant to erythromycin, methicillin	0.125	4	1
MRSA (USA800)	Resistant to methicillin	0.0625	4	1
MRSA (USA1000)	Resistant to erythromycin, methicillin	0.125	2	1
MRSA (USA1100)	Resistant to methicillin	0.125	2	1
E. faecalis ATCC49533	Resistant to streptomycin	0.125	2	1
E. faecalis ATCC7080	-	0.125	2	1
E. faecalis ATCC 51229 (VRE)	Resistant to Vancomycin. Sensitive to Teicoplanin	0.125	2	8
E. faecium E0120 (VRE)	Resistant to gentamicin and vancomycin	0.25	2	>128
E. faecium ATCC6569	-	0.125	2	1
S. pneumoniae 51916	Resistant to cephalosporins	0.25	1	1
S. pneumoniae 70677	Resistant to erythromycin, penicillin, and tetracycline	0.25	1	1
Streptococcus agalactiae MNZ938	Beta-hemolytic, Serogroup: Group B	0.0625	0.25	0.25
Streptococcus agalactiae MNZ 933	Beta-hemolytic, Serogroup: Group B	0.0625	0.25	0.5
Streptococcus agalactiae MNZ 929	Beta-hemolytic, Serogroup: Group B	0.0015	0.25	0.25

The antibacterial activity of auranofin against MRSA is superior (16-fold lower MIC for auranofin) to several commercial antibiotics including vancomycin (MIC of 1 µg/ml) and linezolid (MIC ranged from 2-4 µg/ml); the MIC values determined for auranofin against MRSA correlate with MIC values reported in previous published studies [212,214]. Auranofin retained its antibacterial activity against an array of MRSA strains exhibiting resistance to numerous antibiotic classes including glycopeptides, oxazolidones, tetracycline, β-lactams, macrolides, and aminoglycosides; these results indicate that cross-resistance between these

antibiotics and auranofin is unlikely to occur. The bactericidal activity of auranofin was confirmed via a standard time-kill assay (Figure 2.2); auranofin, at 5 × MIC, exhibited slow bactericidal activity (similar to vancomycin), completely eliminating MRSA USA300 cells within 48 hours.

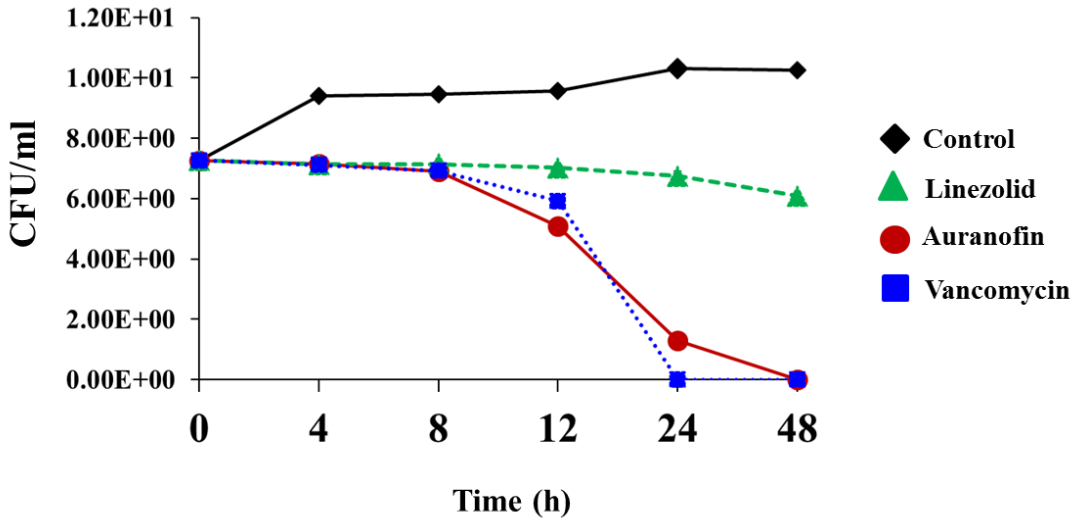

Figure 2.2 Time-kill assay for auranofin tested against *S. aureus*. Killing kinetics of auranofin and antibiotics (vancomycin and linezolid) at 5 × MIC against MRSA USA300 in MHB are displayed. The results are presented as mean ± SD (n = 3). Data without error bars indicate that the SD is too small to be seen.

Vancomycin required 24 hours to achieve the same effect, which is in agreement with previously published reports [227]. In addition to possessing anti-MRSA activity, auranofin also exhibited potent antibacterial activity against vancomycin-sensitive enterococcus and vancomycin-resistant enterococcus (VRE), *Streptococcus pneumoniae* and *Streptococcus agalactiae* with MIC values ranging from 0.0015 to 0.25 µg/ml (Table 2.1).

The outer membrane in Gram-negative bacteria negates auranofin's antibacterial activity

Confirmation of auranofin's potent antibacterial activity against multiple Gram-positive pathogens led us to analyze if auranofin exhibits broad-spectrum antibacterial activity by also inhibiting growth of important Gram-negative pathogens. Interestingly, auranofin alone did not show activity against Gram-negative bacteria which is in agreement with previous reports[212-214]. We sought to investigate if the presence of the outer membrane (OM) in Gram-negative bacteria contributed to the lack of antibacterial activity observed, by preventing auranofin from gaining entry into the bacterial cell (as has been observed with conventional antimicrobials such as erythromycin and fusidic acid) [217,218]. The inclusion of the permeabilizing agent polymixin B nonapeptide (PMBN), at a sub inhibitory concentration, in the culture broth resulted in auranofin exhibiting potent activity against all tested strains of Gram-negative pathogens including *Pseudomonas aeruginosa, Escherichia coli,* metallo-β-lactamase (NDM-1) and carbapenemase-resistant (KPC) *Klebsiella pneumoniae, Salmonella Typhimurium* and extremely drug-resistant (XDR) *Acinetobacter baumannii* with MICs ranging from 0.125 to 1 µg/ml (Table 2.2). In addition to this, a four-fold decrease in auranofin's MIC (from 32 to 8 µg/ml) was observed when the efflux pump AcrAB was deleted in *E. coli.* AcrAB has been shown to contribute to the antibiotic-resistant phenotype in multiple strains of *E. coli* and has been implicated in *E.coli* resistance to numerous antibiotics including ampicillin, rifampicin, and chloramphenicol [228]. Thus, in addition to the physical barrier imposed by the Gram-negative OM, the ability of auranofin to gain entry into Gram-negative bacteria to exhibit its antibacterial activity may be impeded by the presence of efflux pumps (such as AcrAB).

Table 2.2 MICs of auranofin and control antibiotics against Gram-negative bacteria

Bacteria	Minimum Inhibitory Concentration (MIC) (μg/ml)						
	PMBN	Auranofin		Erythromycin		Fusidic acid	
		PMBN		PMBN		PMBN	
		(-)	(+)	(-)	(+)	(-)	(+)
Acinetobacter baumannii ATCC BAA19606	>256	16	0.25	64	0.5	64	0.5
Acinetobacter baumannii ATCC BAA1605	>256	16	0.5	64	0.5	128	1
Acinetobacter baumannii ATCC BAA747	>256	16	0.25	64	1	128	0.5
Escherichia coli O157:H7 ATCC 700728	256	64	0.5	128	1	>256	16
Escherichia coli O157:H7 ATCC 35150	256	32	0.5	128	1	>256	16
Salmonella Typhimurium ATCC 700720	>256	128	1	256	2	>256	16
Klebsiella pneumoniae ATCC BAA 2146	>256	256	0.5	>256	128	>256	32
Klebsiella pneumoniae ATCC BAA 1705	>256	256	1	>256	64	>256	64
Pseudomonas aeruginosa ATCC 9721	>256	>256	0.25	>256	1	>256	1
Pseudomonas aeruginosa ATCC 27853	>256	256	0.125	256	1	>256	1
Pseudomonas aeruginosa ATCC BAA-1744	>256	>256	0.25	>256	1	>256	1
Pseudomonas aeruginosa ATCC 25619	>256	256	0.25	256	1	>256	1
Pseudomonas aeruginosa ATCC 35032	>256	>256	0.5	>256	1	>256	1
Pseudomonas aeruginosa ATCC 10145	>256	256	0.25	256	1	>256	2
Pseudomonas aeruginosa ATCC 15442	>256	>256	0.25	>256	2	>256	1
Escherichia coli 1411	>256	32	0.5	32	4	>256	4
Escherichia coli SM1411Δ *acrAB*	>256	8	0.5	0.03	<0.03	8	<0.03
Escherichia coli (Novablue (DE3)-K12)	256	16	0.5	16	0.5	>256	0.5
Escherichia coli (Origami-2) (*trxB/gor* mutant)	256	16	0.5	32	0.5	256	0.06

PMBN polymyxin B nonapeptide: (-) No PMBN was added to the media; (+) (10 μg/ml) of PMBN was added to the media

Auranofin inhibits multiple biosynthetic pathways in *S. aureus*

After confirming auranofin possesses potent antibacterial activity *in vitro*, particularly against drug-resistant strains of *S. aureus*, we next moved to determine the antibacterial mechanism of action of auranofin. A macromolecular synthesis assay was employed to initially investigate auranofin's antibacterial mechanism of action. The effect of auranofin on the incorporation of radiolabeled precursors into five major biosynthetic pathways of *S. aureus* was assessed. This assay revealed a clear dose-dependent inhibition of three pathways, indicating that auranofin might possess multiple targets (Figure 2.3). Auranofin, at a sub-inhibitory concentration, significantly inhibited cell wall and DNA synthesis. When tested at its MIC, auranofin was found to also inhibit protein synthesis. At higher concentrations (8 × MIC auranofin), partial inhibition of lipid synthesis was also observed. However, auranofin did not significantly inhibit RNA synthesis at any of the tested concentrations. The results from the macromolecular synthesis assay suggest that auranofin possesses a complex mode of action that involves inhibition of multiple biosynthetic pathways including cell wall, DNA, and protein synthesis.

Primary disruption of DNA synthesis in the macromolecular synthesis assay is often associated with DNA intercalators. However, when auranofin was examined for evidence of DNA intercalation, no effect on DNA migration was observed in relation to the untreated control. Unlike doxorubicin, auranofin, even at a concentration (1mg/ml) that is 8000-fold higher than the average MIC against MRSA, shows no evidence of a shift in plasmid DNA (Figure 2.4). These data suggest that the disruption of DNA synthesis by auranofin is not due to intercalation with DNA.

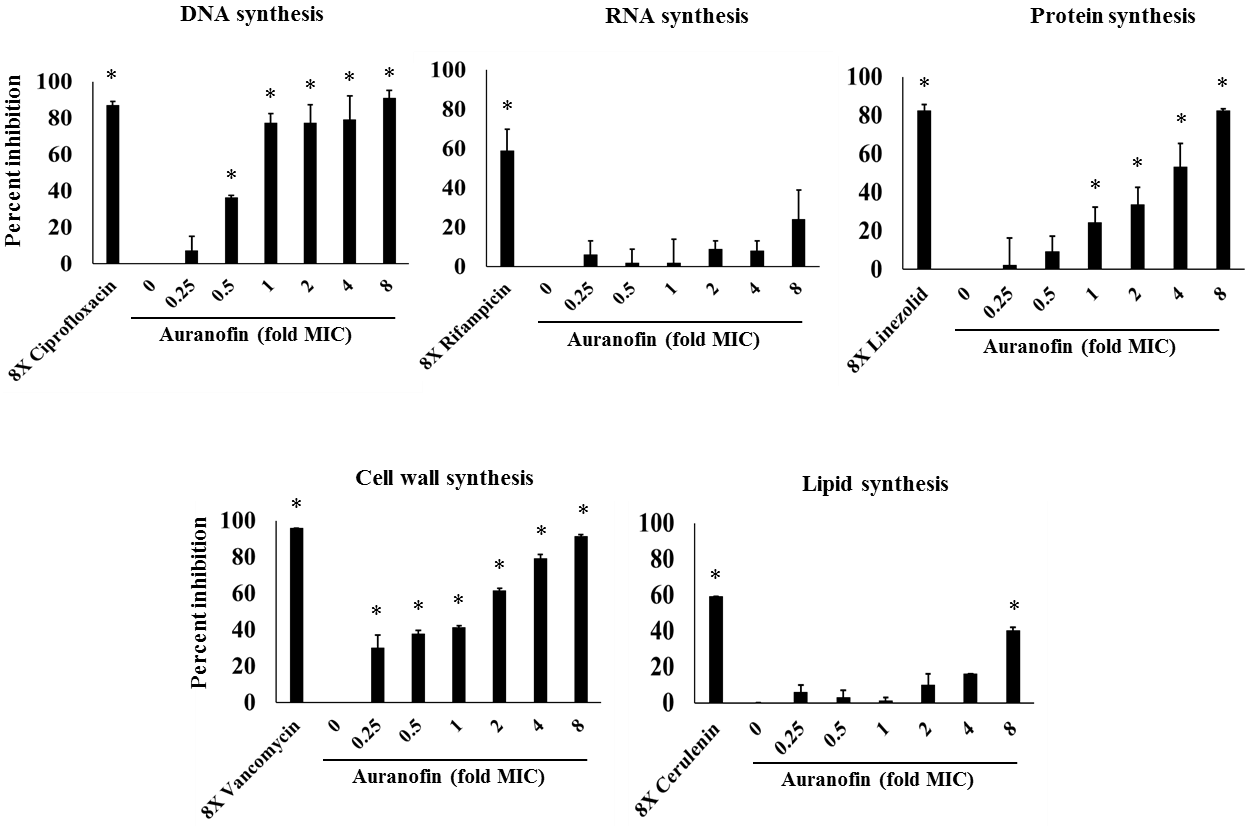

Figure 2.3 Antibacterial mechanism of action of auranofin examined via the macromolecular synthesis assay. Incorporation of radiolabeled precursors of DNA, RNA, protein, cell wall and lipid synthesis ([3H] thymidine, [3H] uridine, [3H] leucine, [14C] N-acetylglucosamine and [3H] glycerol, respectively) were quantified in *S. aureus* ATCC 29213 after treatment with 1 × and 8 × MIC of auranofin, and 8 × MIC of control antibiotics. Results are expressed as percent inhibition of each pathway based on the incorporation of radiolabeled precursors. Statistical analyses were done using the two-tailed Student's't' test. *P* values of (* ≤ 0.05) are considered as significant.

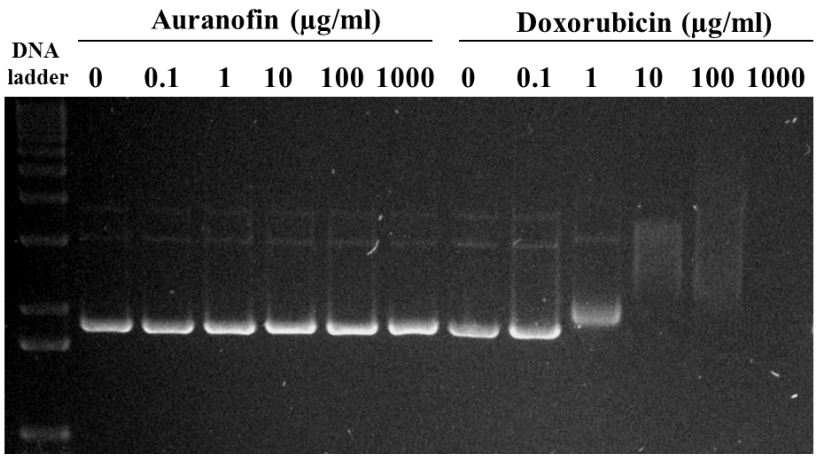

Figure 2.4 DNA mobility assay in the presence of auranofin and doxorubicin. pUC 18 plasmid was incubated with the indicated concentration of auranofin and doxorubicin for 30 min at 37°C. An electrophoretic assay was run using 1% agarose gel, stained with ethidium bromide and visualized for DNA mobility.

Auranofin treatment in *S. aureus* leads to downregulation of proteins in five major biosynthetic pathways

Proteomic profiling is a powerful tool that can be employed to investigate the response of bacteria to antibacterial compounds and assess the impact of such compounds on different cellular pathways [229-231]. Therefore, the alteration in the *S. aureus* proteome caused by auranofin was investigated and compared with linezolid and vancomycin in relation to an untreated control group. The proteomic analysis identified 530 proteins in all samples and found 222 of these proteins showed significant differential expression ($P \leq 0.05$). The PCA analysis demonstrated that the variance inside each group is very low with distinct classifications and the protein

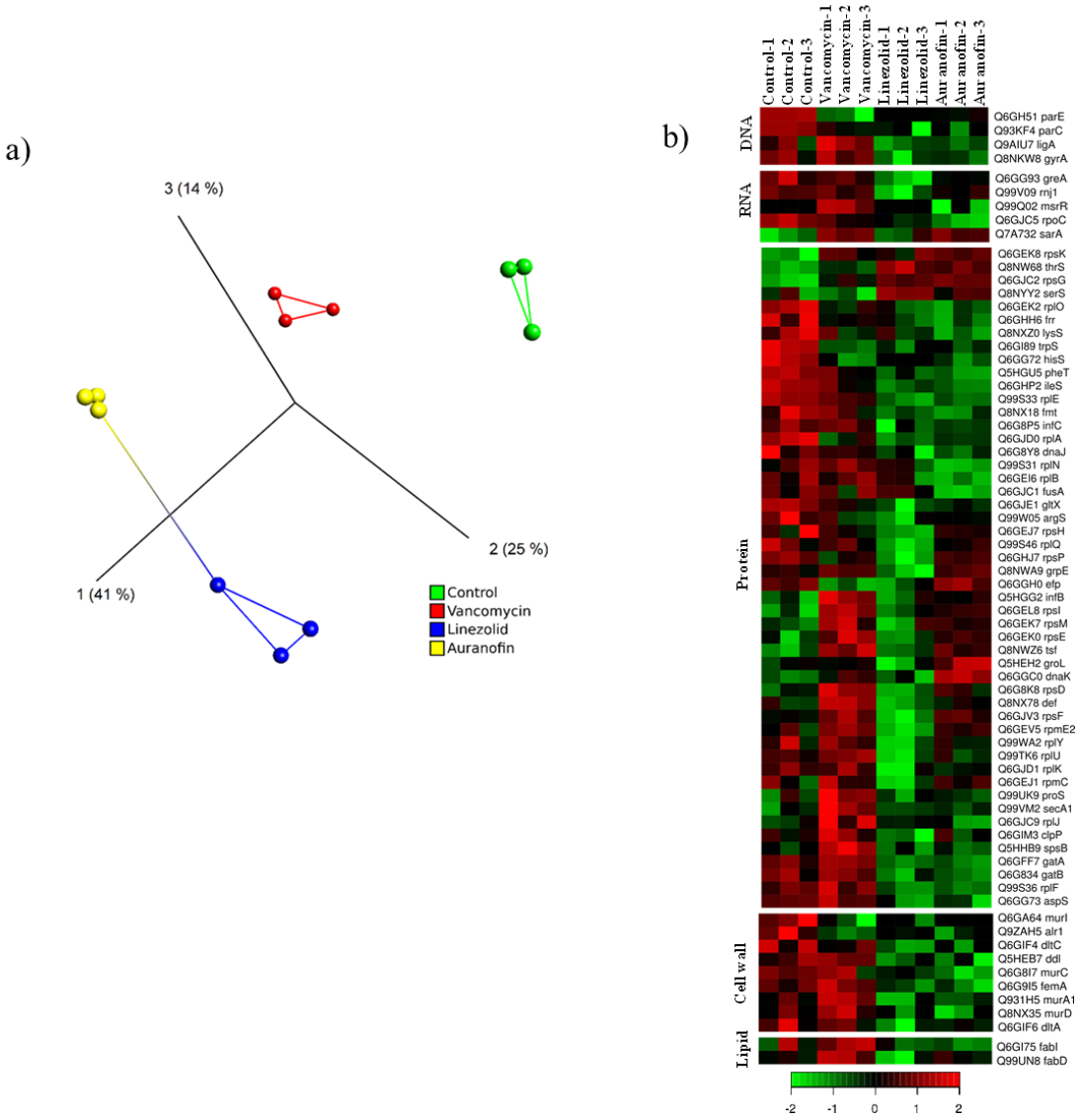

Figure 2.5 Auranofin treatment in *S. aureus* leads to downregulation of proteins in five major biosynthetic pathways. (a) The PCA analysis shown for auranofin, vancomycin, linezolid and control proteins quantified by proteomic analysis. The plot depicts the variance inside each group and the protein expression pattern of drug treated and control groups. (b) Heat map generated comparing auranofin-, vancomycin- and linezolid-treated cells to untreated control *S. aureus* cells is shown. Triplicate samples were used for each group. One-way analysis of variance (ANOVA) was used for statistical analysis and the proteins that were significantly differentially ($P \leq 0.05$) expressed were mapped. Red color indicates significantly increased ratios and green color represents significantly decreased ratios.

expression pattern of the auranofin-treated group resembles that of the linezolid-treated group more so than either the control or vancomycin-treated groups (Figure 2.5a). The proteins were separated into five groups based on molecular function (DNA, RNA, protein synthesis, cell wall and lipid synthesis) (Figure 2.5b). Similar to the protein synthesis inhibitor linezolid, treatment with auranofin leads to the down regulation of most of the proteins involved in all five major biosynthetic pathways. The average fold changes (log_2) of proteins between auranofin and the control group involved in each pathway was: -0.76 (DNA), -0.37 (RNA), -0.26 (protein), -0.76 (cell wall) and -0.18 (lipid). In the presence of auranofin, approximately 55% of the proteins were significantly differentially expressed as compared to the control group ($P \leq 0.05$). Of the 222 proteins that showed significant differential expression, only 20% of these proteins were upregulated in the auranofin-treated group compared to 40% of proteins that were upregulated in the control group ($P \leq 0.05$). These results suggest that auranofin treatment leads to significant down regulation of most of the proteins involved in all five major biosynthetic pathways, which contributes to the bactericidal effect of auranofin against *S. aureus*.

Thioredoxin reductase is not the sole target for auranofin in *S. aureus*

A recent investigation of auranofin as an antibacterial agent [213] reported that auranofin exerts its bactericidal activity by targeting thiol-redox homeostasis through direct inhibition of the thioredoxin reductase enzyme. The authors postulate that the glutathione system present in certain species of Gram-negative (and Gram-positive) bacteria limits their susceptibility to auranofin (as this system is functionally similar to the thioredoxin system and can maintain redox homeostasis inside the bacterial cell when the thioredoxin

reductase enzyme is inhibited). This led the authors to conclude that auranofin's primary antibacterial mechanism is through inhibition of thioredoxin reductase. While auranofin has been shown to inhibit thioredoxin reductase both in *S. aureus* and *M. tuberculosis*, we suspect that this enzyme is not the sole antibacterial target of auranofin for the reasons outlined below. First, we have confirmed that the lack of antibacterial activity of auranofin against Gram-negative bacteria (as presented in Table 2.2) is due to the permeability barrier conferred by the outer membrane (OM)

Figure 2.6 Growth curve of novablue (DE3)-K12 wild-type and *trxB/gor* Origami-2 double

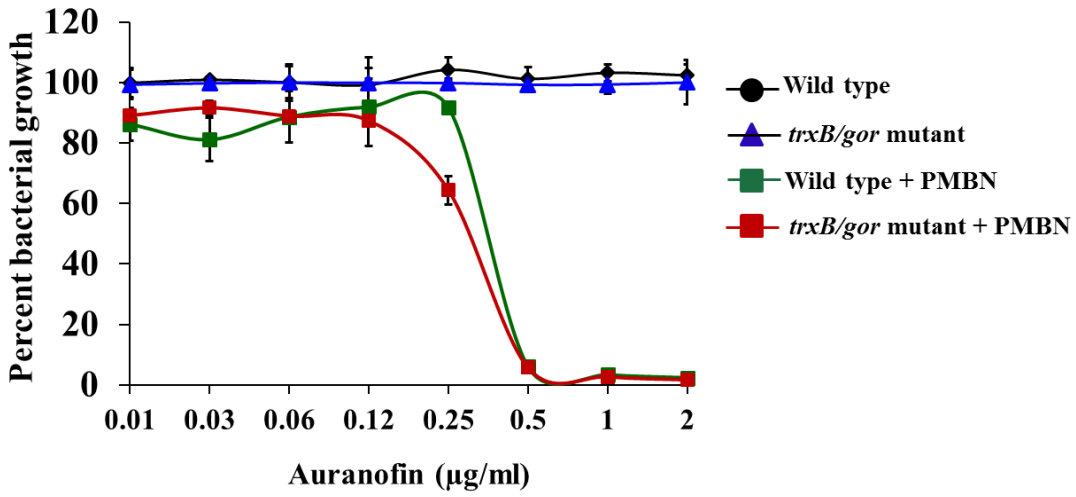

mutant *E. coli* strains in the presence of auranofin. *E. coli* strains were incubated with indicated concentrations of auranofin in the presence and absence of PMBN (10 µg/ml) and the growth was measured using a spectrophotometer.

and is not glutathione-mediated. Second, an *E. coli* double mutant strain (Origami-2) containing mutations to both the thioredoxin reductase (*trxB*), the purported target of auranofin, and glutathione reductase (*gor*), responsible for maintaining redox homeostasis in the absence of TrxB, genes exhibited identical antibacterial activity to the wild-type *E.*

coli strain (Novablue (DE3)-K12) (MIC = 16 µg/ml) (Table 2.2). However, there is a greater than 32-fold improvement in antibacterial activity of auranofin when combined with a subinhibitory concentration of PBNP (MIC = 0.5 µg/ml) (Table 2.2). This observation was further validated by assessing the growth of wild-type and the double mutant *E. coli* (Origami-2) strains in the presence of increasing concentrations of auranofin (with or without PBMN) (Figure 2.6). Once again, the viability of the Origami-2 double mutant was severely impacted by auranofin in the presence of a subinhibitory concentration of PBMN; however, in the absence of PBMN, the double mutant strain exhibited a similar growth pattern to the wild-type *E. coli* strain. This analysis, when combined with the macromolecular synthesis assay and proteomics results, supports the notion that thioredoxin reductase is not the sole target of auranofin in bacteria. Additionally, the outer membrane, and not the glutathione system alone, is responsible for limiting auranofin's antibacterial activity against Gram-negative bacteria.

Auranofin inhibits *S. aureus* toxin production

Confirmation that auranofin inhibits bacterial protein synthesis by macromolecular synthesis assay, led us to inquire whether this drug would be capable of suppressing the production of key virulence factors, such as toxins, produced by pathogens like MRSA. Antimicrobials capable of disrupting or suppressing bacterial protein synthesis, including agents like linezolid, are valuable and preferred options for treating patients impacted by toxin-mediated bacterial infections, such as toxic shock syndrome (TSS) and pneumonia caused by *S. aureus* [232-235]. For example, inhibition of protein synthesis and the subsequent suppression of toxin production is one of the advantages of linezolid's

mechanism of action over vancomycin [232-235]. Therefore to assess the capability of auranofin to dampen production of key *S.-aureus* toxins, ELISA was utilized to detect toxin production for MRSA USA300 treated with auranofin and two control antibiotics (vancomycin and linezolid). Auranofin significantly inhibited production of two major *S. aureus* toxins including Panton-Valentine leukocidin (PVL) and α-hemolysin (Hla) (Figure 2.7a). These results indicate that auranofin, similar to linezolid, possesses an advantage in the management of toxin-mediated staphylococcal infections due to its ability to suppress production of key staphylococcal toxins.

Auranofin effectively clears intracellular bacteria

As auranofin exhibited potent anti-MRSA activity against extracellular bacteria, we were curious to explore the ability of auranofin to eliminate MRSA harboring inside eukaryotic cells. MRSA is capable of entering multiple cell types, including macrophages, in mammalian tissues thus permitting it to evade host defenses and permitting an infection to persist for an extended time period [236]. Such infections are particularly challenging to treat given many antibiotics are unable to permeate cellular membranes to gain entry into these intracellular niches to kill MRSA [226,237-242]. One such example is the antibiotic vancomycin, which has a clinical failure rate of more than 40% in treating *S. aureus* pneumonia; failure is attributed in part to the inability of vancomycin to penetrate infected alveolar macrophages to kill MRSA [243].

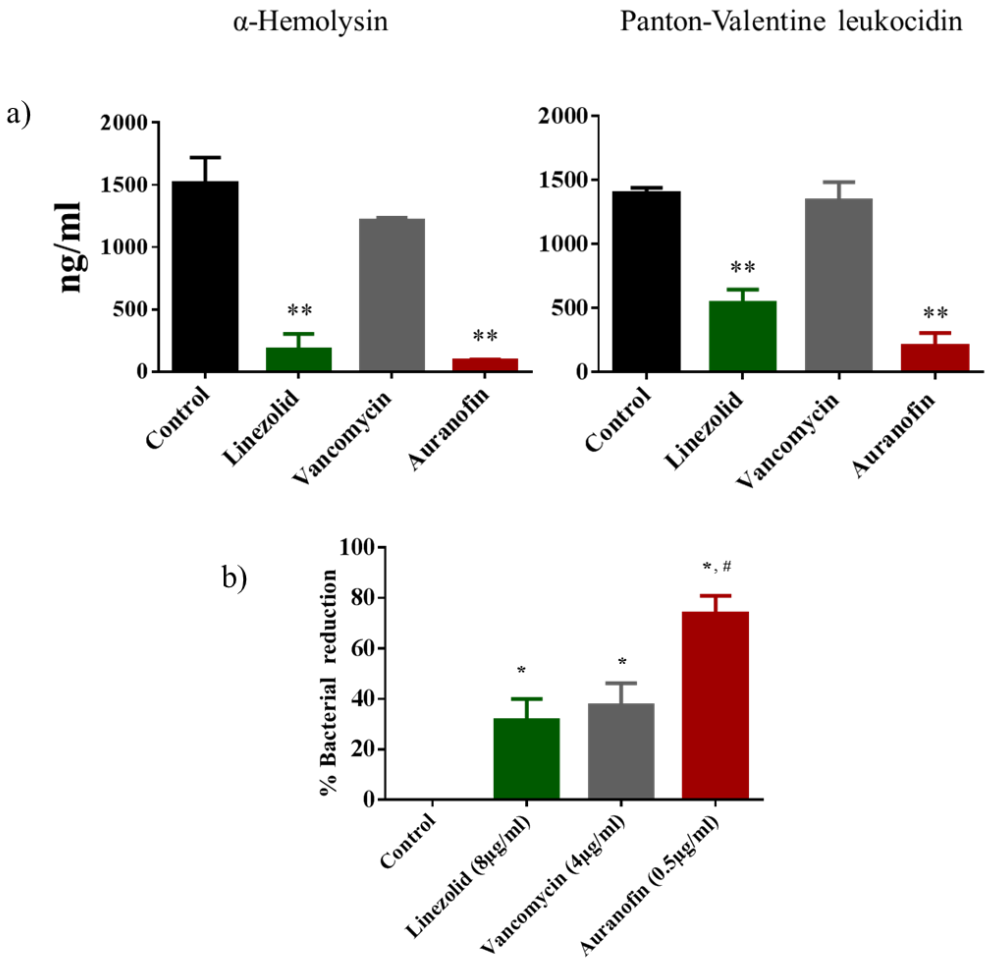

Figure 2.7 Auranofin inhibits MRSA toxin production and effectively clears intracellular bacteria. **(a)** Toxin production (ng/ml) in *S. aureus* MRSA USA300 after treatment with auranofin or control antibiotics (linezolid or vancomycin) for one hour (data corrected for organism burden). The results are presented as mean ± SD (n = 3). Statistical analysis was done by two-tailed Student's 't' test. Asterisks (**) indicate statistical significance in relation to the control (DMSO or water). *P* values of (** $P \leq 0.01$) are considered significant. **(b)** MRSA USA300 infected J774A.1 cells were treated with auranofin and control antibiotics (vancomycin or linezolid) for 24 hours and the percent bacterial reduction was calculated compared to untreated control groups. The results are given as mean ± SD (n = 3). Two-tailed Student's 't' test was employed and *P* values of (*, # ≤ 0.05) are deemed significant. Auranofin was compared to controls (*) and to antibiotics (#).

In order to investigate the efficacy of auranofin in clearing intracellular MRSA, this drug was tested against macrophage cells (J774.A1) infected with MRSA. At a non-toxic concentration of 0.5 µg/ml (Figure 2.9); auranofin effectively clears more than 60% of intracellular MRSA (Figure 2.7b). In contrast, conventional antibiotics such as linezolid (8 µg/ml) and vancomycin (4 µg/ml) are not able to reduce the bacterial burden inside infected macrophages by more than 30% (Figure 2.7b). Altogether the results suggest that auranofin is capable of eradicating MRSA harboring inside mammalian cells. These findings suggest that auranofin is a potential valuable treatment option for challenging infections/diseases (such as pneumonia) where MRSA reside inside host cells.

Auranofin rescues mice from MRSA septicemic infection

The efficacy of auranofin was evaluated in both a lethal and non-lethal systemic MRSA infection model. In the lethal septicemic study, mice were infected intraperitoneally with MRSA USA300. One hour post-infection, four groups of mice (n = 10 mice per group) were treated orally with auranofin at a clinical dose of 0.125 or 0.25 mg per kg, linezolid at a dose of 25 mg per kg, or the vehicle alone as a control. Mice were treated once daily for three days and monitored for a total of five days. Both auranofin and linezolid provided a significant protection from mortality (Figure 2.8a). The survival rate of infected mice improved dramatically when the dose of auranofin was increased. 80% of mice that received a higher dose of auranofin, (0.25 mg per kg) survived for five days. All mice in the group that received linezolid (25 mg per kg) survived for five days. These results suggest that the potent *in vitro* activity of auranofin

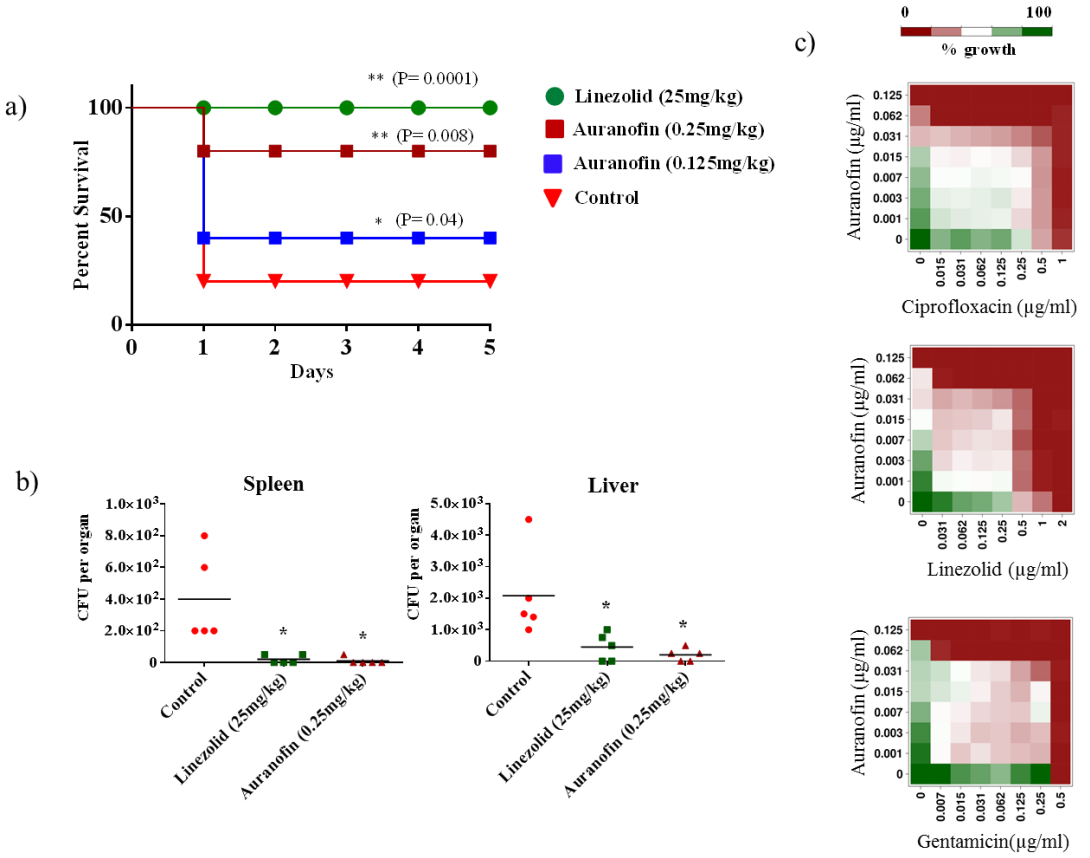

Figure 2.8 Auranofin is effective in a mouse model of MRSA septicemic infection. **(a)** Ten mice per group were infected (i.p) with lethal dose of MRSA USA300 and treated orally with auranofin (0.125 or 0.25 mg/kg), linezolid (25 mg/kg), or the vehicle alone for three days (one dose per day). Mice were monitored for five days and the percent survival was calculated. A log rank test was performed using 95% confidence intervals and the statistical significance was calculated in order to compare treated to control groups. *P* values of (* ≤ 0.05) (** $P \leq 0.01$) are considered as significant. **(b)** Five mice per group were infected (i.p) with non-lethal dose of MRSA USA300 and treated orally with auranofin (0.25 mg/kg), linezolid (25 mg/kg), or the vehicle alone for two days (one dose per day). 24 hours after the last treatment, mice were euthanized and their spleen and liver were excised and homogenized in TSB to count viable MRSA colonies. The number of CFU from each mouse is plotted as individual points. Statistical analysis was conducted using the two-tailed Student's 't' test and *P* values of (* ≤ 0.05) are considered as significant. **(c)** Auranofin in combination with systemic antimicrobials effectively inhibits the growth of *S. aureus*. Growth of MRSA USA300 was measured after incubating with auranofin, control antibiotics, or a combination of auranofin + a control antibiotic. The checkerboard assay was performed by diluting one drug along the ordinate and the second drug along the abscissa of a 96-well plate. Percent bacterial growth was measured using a spectrophotometer.

translates *in vivo* in protecting mice from septicemic MRSA infection. Next we moved to study the efficacy of auranofin in reducing the burden of MRSA in a non-lethal septicemic mouse model. Mice were infected with a non-lethal dose of MRSA USA300 and each group of mice received two oral doses of auranofin (0.25 mg per kg), linezolid (25 mg per kg) or the vehicle alone. As depicted in Figure 2.8b, auranofin and linezolid produced a significant reduction in mean bacterial load in murine organs including the spleen and liver. Both treatment with auranofin and treatment with linezolid reduced the mean bacterial load by more than 95% in the spleen (Figure 2.8b). However, in the liver, auranofin produced a 90% reduction in MRSA load whereas linezolid was only able to reduce the burden of MRSA by 70% (Figure 2.8b).

Combination therapy of auranofin with systemic antimicrobials

Utilizing a single agent to treat bacterial infections in the clinical setting appears to have become less effective with the rise of additional strains of multidrug-resistant *S. aureus* [244,245]. Combining two or more antibiotics together for the treatment of MRSA infections has been explored as an alternative strategy in the healthcare setting in order to improve the morbidity associated with these infections and to reduce the potential emergence of additional resistant strains [244,246,247]. Therefore, we investigated auranofin's ability to be used in combination with antimicrobials frequently used to treat systemic MRSA infections. When tested against a highly-prevalent strain of MRSA USA300, auranofin exhibited an additive effect in inhibiting bacterial growth when combined with the antibiotics ciprofloxacin, linezolid and gentamicin (average fractional inhibitory concentration, FIC index = 0.5 to 1) (Figure 2.8c). Thus the above results indicate auranofin

is a potential candidate for further investigation as a partner with conventional antimicrobials for the treatment of systemic staphylococcal infections.

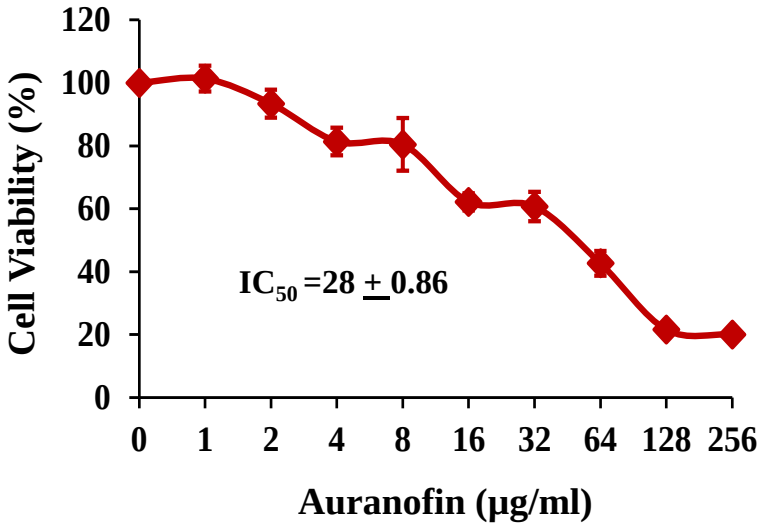

Figure 2.9 Cytotoxicity assay in murine macrophage-like cells (J774A.1) cells. J774A.1 cells were treated with different concentration of auranofin ranging from 0 to 256µg/ml. DMSO was used as a negative control. Cell viability was measured by MTS assay and IC_{50} of auranofin to cause cytotoxicity in J774A.1 cells was calculated.

2.1.4 Discussion

Methicillin-resistant *Staphylococcus aureus* infections continue to pose a significant challenge to healthcare providers in part due to the diminishing arsenal of effective antibiotics available to treat infected patients. The development of novel antibacterial treatments utilizing the traditional approach in drug discovery has not kept pace with the rapid emergence of bacterial resistance to conventional antibiotics. This has led researchers to explore alternative methods to discover new treatment options for

bacterial infections; one method that is less time-consuming and more financially viable is repurposing drugs (initially approved for other clinical indications) that possess potent antimicrobial activity. Auranofin is an example of a clinical drug that has been successfully repurposed recently for another indication. Initially approved as a treatment option for patients suffering from rheumatoid arthritis, auranofin was granted orphan-drug status from the FDA as an anti-parasitic agent intended for treatment of human amebiasis in 2012 [25]

The successful repurposing of auranofin as an anti-parasitic agent paved the way for researchers to explore other clinical applications for auranofin. Recent studies, including the present work, demonstrate that auranofin possesses potent antibacterial activity against important Gram-positive pathogens, including MRSA. One of the key structural features of auranofin is that it is an organogold compound; however unlike other gold compounds including sodium aurothiomalate and sodium aurothioglucose hydrate (MIC >16 µg/ml), auranofin exhibits potent antibacterial activity against an array of different Gram-positive bacteria (including *S. aureus, E. faecium, E. feacalis, S. pneumoniae and S. agalactiae*) with an average minimum inhibitory concentration (0.125 µg/ml) eighteen times lower than the achievable drug concentration in human plasma (2.37 µg/ml which is equivalent to a mean steady-state blood gold concentration of 3.5 µM)[25] This is in agreement with previous published studies [212,214]; however several of these reports have indicated that auranofin lacks antibacterial activity against Gram-negative bacteria. A recent study suggested that this lack of activity was due to the presence of the glutathione system in Gram-negative bacteria which helps to mediate resistance to auranofin in these pathogens [213]. However, when we assessed auranofin's antibacterial

activity against both wild-type and Origami-2 (*trxb*/*gor* double mutant) *E. coli* mutant strains, neither strain was susceptible to auranofin even at a concentration of 16 µg/ml [248]. This suggests an alternative mechanism may be responsible for the lack of activity observed with auranofin against Gram-negative bacteria.

Further investigation revealed that the presence of the outer membrane in Gram-negative bacteria is the main culprit responsible for the lack of antibacterial activity observed. When wild-type and Origami-2 *E. coli* strains were incubated with auranofin supplemented with a subinhibitory concentration of PMBN (to permeabilize the outer membrane), both strains showed similar sensitivity to auranofin with a MIC value of 0.5 µg/ml (Table 2.2). This observation was further validated by assessing the growth of wild-type and double mutant *E. coli* strains in the presence of increasing concentrations of auranofin (with or without PBMN). Once again, the viability of the Origami-2 double mutant was severely impacted by the presence of auranofin (in the presence of a subinhibitory concentration of PBMN); however, in the absence of PBMN, the double mutant strain exhibited a similar growth pattern to the wild-type *E. coli* strain. Thus the lack of direct antibacterial activity of auranofin observed against Gram-negative bacteria appears to be a byproduct of the barrier imposed by the outer membrane in addition to the presence of active efflux pumps more so than the presence of the glutathione system.

Confirmation of auranofin's potent antibacterial activity led us to next explore the potential mechanism of action (MOA) against *S. aureus*. Previous studies have found that auranofin inhibits *Clostridium difficile* and *Treponema denticola* growth through the disruption of selenium metabolism [249,250]. We hypothesized that the MOA of auranofin in *S. aureus* differs from the MOA in *C. difficile* and *T. denticola* due to the absence of

selenoproteins in *S. aureus* [251]. In order to examine this hypothesis, we tested the activity of auranofin on *S. aureus* cultures supplemented with selenium in the form of selenite or L-selenocysteine [249,250]. Unlike in *C. difficile* and *T. denticola,* our selenium supplementation did not reverse the inhibitory action of auranofin observed with *S. aureus* (data not shown). This clearly indicates that the MOA of auranofin differs between *S. aureus* and *C. difficile*. Next, we attempted to generate a *S. aureus* mutant that is resistant to auranofin. Determination of mutation frequencies for resistance to auranofin were carried out as described before [252]. No colonies resistant to auranofin at three-, five-, or ten-fold the MIC were detected which is in agreement with a previous report [213].

The inability to generate a resistant mutant to auranofin suggests this drug may have multiple targets or possess a nonspecific mode of action against *S. aureus* [253]. To assess this, a macromolecular synthesis assay was employed testing auranofin at different concentrations against *S. aureus*. Interestingly, at a subinhibitory concentration (0.5 × MIC), auranofin leads to significant reduction in both the cell wall and DNA biosynthetic pathways. At its MIC, auranofin also suppresses bacterial protein synthesis, indicating auranofin may in fact have a complex mode of action against *S. aureus*. Harbut *et al*'s recently reported auranofin exerts its antibacterial activity primarily by targeting thiol-redox homeostasis through direct inhibition of the thioredoxin reductase enzyme (TrxB in *Staphylococcus aureus* and TrxB2 in *Mycobacterium tuberculosis*). While inhibition of TrxB activity in *S. aureus* can lead to inhibition of DNA synthesis, it does not explain the inhibition of cell wall synthesis observed with auranofin. Taken altogether, our analysis indicates that the thioredoxin reductase enzyme most likely is not the sole target of auranofin in *S. aureus* and in Gram-negative bacteria; this is in agreement with a recent

report investigating auranofin's antibacterial activity against *Streptococcus pneumoniae* and *S. aureus* [215]. Further studies are needed to fully elucidate the exact antibacterial molecular target(s) of auranofin.

In the course of investigating auranofin's mode of action via macromolecular synthesis, we discovered that auranofin inhibits protein synthesis in *S. aureus*. This discovery led us to analyze whether auranofin's inhibitory activity against bacterial protein synthesis would lead to suppression in the production of key toxins in *S. aureus*. Our study revealed that auranofin is capable of inhibiting production of both Panton-Valentine leukocidin and α-hemolysin, two pore-forming cytotoxins that injure host immune cells and promote infection [254]. Thus, in addition to its direct –cidal effect on bacteria, auranofin may alleviate the morbidity associated with MRSA infections by limiting bacteria from generating harmful toxins.

We next moved to confirm auranofin's antibacterial ability *in vivo* using two murine MRSA systemic infection models (non-lethal and lethal). Both *in vivo* studies performed in mice confirmed auranofin retains its antibacterial activity *in vivo*. In addition to this, auranofin demonstrated the ability to eradicate intracellular MRSA present inside infected macrophage cells; this expands the potential application if auranofin for use in treatment of systemic MRSA infections. Furthermore, auranofin demonstrated additive activity when combined with antibiotics traditionally used to treat systemic MRSA infections which is in agreement with previous a study [213]. Thus, auranofin has potential use both as a single agent and as a combinatorial partner with conventional antibiotics to treat MRSA infections. This latter statement is important given the emergence of resistance to systemic antimicrobials currently used in the clinic; pairing these antibiotics with auranofin may

stymie the rate at which resistance to these antibiotics arises. Finally, because of increased interest in repurposing auranofin, a Phase II clinical trial seeking to determine the pharmacokinetic parameters and the safety of increased doses of auranofin are currently underway (ClinicalTrials.gov identifier: NCT01419691 and NCT02089048). This strongly supports the postulate that auranofin has considerable promise to be repurposed as an antibacterial agent for the treatment of systemic bacterial infections.

2.2 Repurposing auranofin for the treatment of cutaneous staphylococcal infections

(Thangamani S, Mohammad H, Abushahba MF, Hamed MI, Sobreira TJ, Hedrick VE, Paul LN, Seleem MN. Repurposing auranofin for the treatment of cutaneous staphylococcal infections. *International journal of antimicrobial agents and chemotherapy*. 2016 Jan 23; S0924-8579(16)00012-1)

2.2.1 Introduction

Staphylococcus aureus, is the most frequently isolated pathogen from human skin infections and is the leading cause of nosocomial wound infections [107,211,255,256]. Virulence factors and toxins (such as α-hemolysin and Panton-Valentine leukocidin) secreted by drug-resistant strains of *S. aureus* permit this pathogen to evade the host immune system, leading to recurring/chronic infection, prolonged inflammation, and delayed healing of infected wounds [107,256]. Furthermore, cutaneous staphylococcal skin infections can develop into invasive infections that ultimately result in septicemia [257,258]. Recently, skin infections

with biofilm-producing *staphylococci* have become an emerging clinical problem; treatment failure is occurring more frequently with topical drugs of choice including mupirocin and fusidic acid, indicating new treatment options are urgently needed [211,259,260]. The recent FDA approval of drugs such as tedizolid phosphate and dalbavancin to combat skin infections caused by Gram-positive pathogens [261,262] further highlights the pressing need for the identification of new antibacterials capable of treating cutaneous MRSA infections.

Most current antibiotics were discovered by screening libraries of chemical compounds in order to find new lead "hits" that could be subsequently modified to enhance potency physicochemical properties and mitigate toxicity [210]. However, this process is a risky venture given the significant financial and time investment required by researchers and limited success rate of translating these compounds to the clinical setting. An alternative approach to unearthing new antibacterials that has received more attention recently is evaluating the repository of approved drugs (or drugs that made it to clinical trials but failed to receive regulatory approval) in order to identify candidates that can be repurposed as antimicrobials [210]. Recently, we assembled and screened half of all commercially available drugs (~ 2,200 drugs) and small molecules used in human clinical trials [7,211] and identified three drugs (auranofin, ebselen and 5-fluoro-2'-deoxyuridine) that exhibited potent antibacterial activity against important clinical pathogens. One of these drugs, auranofin, was found to inhibit growth of clinical isolates of MRSA at submicrogram/mL concentrations *in vitro*.

Auranofin is an oral gold-containing drug initially approved for treatment of rheumatoid arthritis [263]. Recent studies have demonstrated that auranofin also possesses

potent anti-parasitic [263] and antibacterial activity [249,264], including against MRSA and *Streptococcus pneumoniae* [58,212,213,265]. Recent studies by Harbut *et al*. [213] and Aguinagalde *et al* [265] demonstrated that auranofin is efficacious in the treatment of invasive staphylococcal infections. However, the efficacy of auranofin for treatment of cutaneous MRSA infections remains unexplored.

Building upon these recent reports, the present study investigated the *in vitro* antibacterial and antibiofilm activities of auranofin against multidrug-resistant clinical isolates of *S. aureus* and tested the efficacy of auranofin in a mouse model of MRSA skin infection. In addition to this, our study aimed to examine the immune-modulatory activity of auranofin in MRSA infected skin lesions. The findings presented in this study lay the foundation for repurposing auranofin as a novel topical antibacterial agent for treatment of cutaneous MRSA infections in humans.

2.2.2 Materials and Methods

Bacterial strains and reagents

Bacterial strains used in this study are presented in Table 1. Auranofin (Enzo Life Sciences), mupirocin (AppliChem), clindamycin (Sigma-Aldrich), and fusidic acid (Sigma-Aldrich) were all purchased from commercial vendors. Mueller-Hinton broth (MHB) was purchased from Sigma-Aldrich while Trypticase soy broth (TSB), Trypticase soy agar (TSA), and mannitol salt agar (MSA) were purchased from Becton, Dickinson and Company (Cockeysville, MD).

Antibacterial assays

In order to examine auranofin's antibacterial activity against *S. aureus*, the broth microdilution method was utilized to determine the minimum inhibitory concentration (MIC) of each drug (tested in triplicate) following the guidelines outlined by the Clinical and Laboratory Standards Institute (CLSI). Each drug was incubated with the appropriate strain of *S. aureus* for 16 hours at 37°C before the MIC was confirmed. The MIC was classified as the lowest concentration of each test agent where bacterial growth was not visible.

Mice infection

Eight week old female BALB/c mice (Harlan Laboratories, Indianapolis, IN) were used in this study. All animal procedures were approved by the Purdue University Animal Care and Use Committee (PACUC) (protocol number: 1207000676). An *in vivo* murine MRSA skin infection study was conducted, as described elsewhere [211,266]. Briefly, mice (five mice per group) received an intradermal injection (40 µl) of MRSA USA300 containing 1.65×10^8 colony forming unit (CFU). Approximately two days later, an open wound/abscess formed at the site of injection. Five groups of mice were then treated topically with a suspension containing 2% fusidic acid, 2% mupirocin, or 0.5%, 1%, or 2% auranofin in petroleum jelly. Another two groups were treated orally with 25 mg/kg of either linezolid or clindamycin. The control group was treated with petroleum jelly (vehicle). Mice were treated twice daily for five days. 24 hours after the last dose was administered, mice were humanely euthanized via CO_2 asphyxiation. The region around the skin wound was slightly swabbed with 70% ethanol, and the wound (1 cm^2) was

precisely excised, homogenized, serially diluted in PBS, and then transferred to MSA plates. Plates were incubated at 37°C for 24 hours prior to counting MRSA CFU.

Detection of cytokines from MRSA murine skin infection experiment

Skin homogenates obtained from the murine skin infection experiment described above were centrifuged. The supernatant was collected and used to quantify the levels of inflammatory cytokines including tumor necrosis factor-α (TNF-α), interleukin-6 (IL-6), interleukin-1 beta (IL-1β), and monocyte chemo attractant protein-1 (MCP-1). Duo-set ELISA Kits (R&D Systems, Inc.) were used for cytokine detection using the manufacturer's protocol.

Combination testing of auranofin with commercial antibiotics

The additive activity of auranofin with conventional topical antibiotics (mupirocin, fusidic acid and retapamulin) was evaluated as described in a previous study [223,224]. Briefly, MRSA USA300 was incubated with auranofin, control antibiotics, or a combination of auranofin + a control antibiotic at different concentrations for 16 hours. Next, the optical density (at 600 nm) was measured using a spectrophotometer. The percent bacterial growth for each treatment regimen was calculated and presented.

Biofilm assay

Auranofin's ability to disrupt adherent staphylococcal biofilm was analyzed using the microtiter dish biofilm formation assay [204,211]. *S. aureus* (ATCC 6538) and *S. epidermidis* (ATCC 35984) were inoculated in TSB supplemented with 1% glucose and transferred to

all wells of a 96-well tissue-culture treated plate. Bacteria were incubated at 37°C for 24 hours to permit the formation of an adherent biofilm. The medium was removed and wells were carefully washed with PBS four times to remove planktonic bacteria. TSB was transferred to all wells of the 96-well plate prior to addition of auranofin and control antibiotics (linezolid and vancomycin). Drugs were added at the indicated concentrations and incubated again at 37°C for 24 hours. Afterward, plates were washed by submerging in tap water. The biofilms were stained with 0.1% (wt/vol) crystal violet for 30 min at room temperature before subsequently being washed four times with water. Plates were air dried for one hour prior to the addition of 95% ethanol to solubilize dye bound to the biofilm. The biofilm mass was quantified by measuring the optical density of wells (at 595 nm) using a micro plate reader (Bio-Tek Instruments Inc.). Data are presented as the average percent biofilm mass reduction of each test agent (tested in triplicate) in relation to untreated wells.

Effect of auranofin and conventional antibiotics on persister cells

The effect of auranofin and conventional antibiotics (linezolid, retapamulin and vancomycin) on *S. aureus* planktonic cells that demonstrated tolerance to ciprofloxacin (persister cells) was investigated as described in a previous report [267]. Briefly, an overnight culture of MRSA USA300 (1×10^{10} CFU) was incubated with ciprofloxacin (10 µg/ml) (80X MIC) at 37°C for six hours. Bacteria were then centrifuged and test agents (auranofin, linezolid, retapamulin, vancomycin, ciprofloxacin) were added at a concentration of 100 × MIC. MIC of retapamulin and ciprofloxacin against MRSA USA300 were 0.5 and 0.125 µg/ml respectively. Bacteria were incubated with test agents at 37°C for 48 hours. Samples

were collected after 0, 2, 4, 6, 24, and 48 hours, diluted in PBS, and transferred to TSA plates. Plates were incubated at 37°C for 24 hours before viable CFU for each treatment group was determined.

Toxicity assay

Human keratinocyte (HaCat) cells were seeded at a density of 40,000 cells per well in a 96-well tissue culture plate and the MTS assay was carried out. Auranofin at a concentration ranging from 0 to 16 µg/ml was added to appropriate wells and the cells were incubated for 24 hours. Finally, the cells were washed with PBS and the MTS assay reagent 3-(4,5-dimethylthiazol-2-yl)-5-(3-carboxymethoxyphenyl)-2-(4-sulfophenyl)-2H tetrazolium) was added. After four hours incubation at 37°C, the absorbance was measured at 490 nm using an ELISA microplate reader (Molecular Devices, Sunnyvale, CA, USA). Results are expressed as percent cell viability of auranofin-treated cells in comparison to cells treated with DMSO.

Statistical analyses

Statistical analyses were assessed using GraphPad Prism 6.0 (GraphPad Software, La Jolla, CA). *P* values were calculated using the Student's *t* test or Kaplan-Meier (log rank) survival test, as indicated. *P* values of ≤ 0.05 were deemed significant.

2.2.3 Results and Discussion

In vitro antibacterial activity of auranofin

The antimicrobial activity of auranofin was assessed against a panel of clinically-relevant strains of multidrug-resistant *Staphylococcus aureus* (Table 2.3). Auranofin

inhibited growth of all tested strains including those resistant to conventional antimicrobials such as methicillin and vancomycin. The minimum inhibitory concentration (MIC) of auranofin required to inhibit 50% (MIC_{50}) and 90% (MIC_{90}) of MRSA, VRSA and methicillin-sensitive *S. aureus* (MSSA) strains was found to be 0.0625 (MIC_{50}) and 0.125 µg/ml (MIC_{90}), respectively. With regards to vancomycin-intermediate *S. aureus* (VISA), the MIC_{90} value were found to be 0.125 µg/ml. The MIC values determined for auranofin correlate with results reported in other studies [212,214,265].

Table 2.3 Minimum Inhibitory Concentration (MIC) of auranofin and control antibiotics against *Staphylococcus aureus* and *S. epidermidis*

Strain type	Strain ID	Phenotypic properties	Auranofin (µg/ml)	Linezolid (µg/ml)	Vancomycin (µg/ml)
Methicillin-sensitive *S. aureus* (MSSA)	ATCC 6538	Quality control and biofilm-forming strain	0.0625	2	1
	RN4220		0.0625	2	1
	NRS72	Resistant to penicillin	0.125	2	1
	NRS77		0.0625	2	1
	NRS846		0.0625	2	1
	NRS860		0.125	2	1
Methicillin resistant *S. aureus* (MRSA)	USA300	Resistant to erythromycin, methicillin, and tetracycline	0.125	2	1
	NRS194	Resistant to methicillin	0.0625	2	1
	NRS108	Resistant to gentamicin	0.125	2	1
	NRS119 (Lin^r)	Resistant to linezolid	0.0625	>16	1
	ATCC 43300	Resistant to methicillin	0.0625	2	1
	ATCC BAA-44	Multidrug-resistant strain	0.0625	2	1
	NRS70	Resistant to erythromycin, clindamycin, and spectinomycin	0.0625	2	1
	NRS71	Resistant to tetracycline and methicillin	0.0625	2	1
	NRS100	Resistant to tetracycline and methicillin	0.0625	2	1
	NRS123	Resistant to tetracycline and methicillin	0.0625	2	2
	NRS107	Resistant to methicillin and mupirocin	0.0625	2	1
Vancomycin-intermediate *S. aureus* (VISA)	NRS1	Resistant to aminoglycosides and tetracycline; glycopeptide-intermediate *S. aureus*	0.0625	2	8
	NRS19	Glycopeptide-intermediate *S. aureus*	0.125	1	2
	NRS37	Glycopeptide-intermediate *S. aureus*	0.125	1	4

Table 2.3 continued

Vancomycin-resistant *S. aureus* (VRSA)	VRS1	Resistant to vancomycin	0.0625	1	>16
	VRS2	Resistant to vancomycin, erythromycin, and spectinomycin	0.0625	1	8
	VRS3a	Resistant to vancomycin	0.0625	2	>16
	VRS3b	Resistant to vancomycin	0.0625	2	>16
	VRS4	Resistant to vancomycin, erythromycin, and spectinomycin	0.0625	2	>16
	VRS5	Resistant to vancomycin	0.0625	2	>16
	VRS6	Resistant to vancomycin	0.125	2	>16
	VRS7	Resistant to vancomycin and β-lactams	0.0625	2	>16
	VRS8	Resistant to vancomycin	0.0625	2	>16
	VRS9	Resistant to vancomycin	0.0625	2	>16
	VRS10	Resistant to vancomycin	0.125	2	>16
	VRS11a	Resistant to vancomycin	0.0625	2	>16
	VRS11b	Resistant to vancomycin	0.0625	2	>16
	VRS12	Resistant to vancomycin	0.125	2	>16
	VRS13	Resistant to vancomycin	0.0625	2	>16
S. epidermidis	NRS101	Prototype biofilm producer; resistant to Methicillin and gentamicin	0.0625	2	1

Interestingly, auranofin (16-fold lower MIC) exhibited higher potent antibacterial activity against MSSA and MRSA compared to the antibiotics vancomycin (MIC of 1 μg/ml) and linezolid (MIC ranged from 2-4 μg/ml). Auranofin managed to retain its antibacterial activity against MRSA strains that are resistant to several antibiotic classes including glycopeptides, oxazolidones, tetracycline, β-lactams, macrolides, and aminoglycosides; this suggests that cross-resistance between these particular antibiotics and auranofin is unlikely to occur.

Auranofin is superior to conventional antibiotics in reducing the bacterial load in a mouse model of MRSA skin infection

Confirmation of auranofin's potent *in vitro* anti-MRSA activity, led us to next investigate the efficacy of this drug in treating MRSA skin infections. *S. aureus*, in

particular MRSA, is a leading cause of skin infections in humans globally; of particular concern is MRSA USA300 which has been linked to the majority of skin and soft tissue infections present in the United States [255]. To assess auranofin's potential use as a topical antimicrobial agent *in vivo*, mice were intradermally infected with MRSA USA300 and the efficacy of auranofin and control antimicrobials on MRSA load were investigated. . A significant reduction in the mean bacterial load was observed for each treatment condition when compared with the control group receiving the vehicle (petroleum jelly) alone ($P \leq 0.05$) (Figure 2.10). Mice treated with 2% auranofin produced the largest reduction in MRSA CFU (3.64±0.14 $\log_{10}$), followed by 2% fusidic acid (2.83±0.16 $\log_{10}$), 2% mupirocin (2.63±0.14 $\log_{10}$), 1% auranofin(2.51±0.11 $\log_{10}$), clindamycin (25 mg/kg) (1.90±0.24 $\log_{10}$), 0.5% auranofin (1.88±0.18 $\log_{10}$) and linezolid (25 mg/kg) (1.77±0.11 $\log_{10}$) (Figure 2.10).

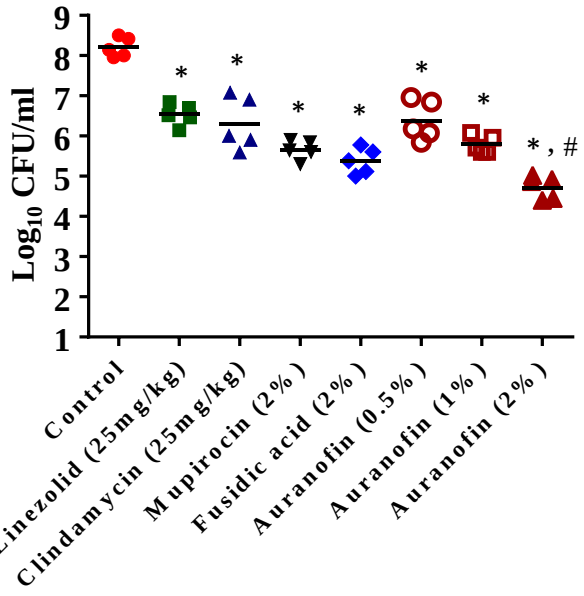

Figure 2.10 Efficacy of treatment of MRSA murine skin lesions with auranofin 0.5, 1, and 2%, linezolid and clindamycin (25 mg/kg), mupirocin (2%), fusidic acid (2%) and petroleum jelly (negative control) twice daily for five days were evaluated. Statistical analysis was calculated by the two-tailed Student's *t* test. *P* values of (*, # $P \leq 0.05$) are considered as significant. Auranofin was compared both to controls (*) and to antibiotics (#).

Topical application of auranofin (2%) produced a more significant reduction ($P \leq 0.05$) in the mean bacterial load when compared to treatment with drugs of choice including mupirocin (2%) and fusidic acid (2%). Thus auranofin shows promise for use as a topical antimicrobial and, in our study, is superior to conventional antimicrobials commonly used to treat MRSA skin infections.

Auranofin reduces inflammatory cytokines induced by MRSA skin infection

Exotoxins including α-hemolysin, leukocidins and toxic shock syndrome toxin (TSST-1) secreted by *S. aureus* during an infection induce a strong inflammatory cascade reaction [107,256]. This cascade is thought to play a greater role in the severity of *S. aureus* skin infections more than the size of the bacterial burden and can lead to an infection persisting for a longer time period [256]. Therefore, we investigated the immunomodulatory activity of auranofin in a topical application against MRSA skin infection. Supernatants collected from the wounds of mice infected with MRSA USA300 were used to detect the levels of inflammatory cytokines such as TNF-α, IL-6, IL-1β and MCP-1. Wounds treated with either a 1 or 2% ointment of auranofin significantly reduced all inflammatory cytokines tested (IL-6, IL-1β, TNF-α, and MCP-1) (Figure 2.11). Auranofin (at 0.5%) also significantly reduced IL-6 and TNF-α. Mice administered an oral dose of clindamycin reduced IL-1β and TNF-α, whereas oral treatment of mice with linezolid reduced only IL-1β. Thus it appears that auranofin has more potent anti-inflammatory activity, due to the reduction in the presence of several pro-inflammatory cytokines, compared to the conventional antimicrobials tested (linezolid, clindamycin, mupirocin and fusidic acid).

The results garnered from this study suggest auranofin's anti-inflammatory properties warrant further investigation in the treatment of chronic wounds caused by *S. aureus* [102,105,107].

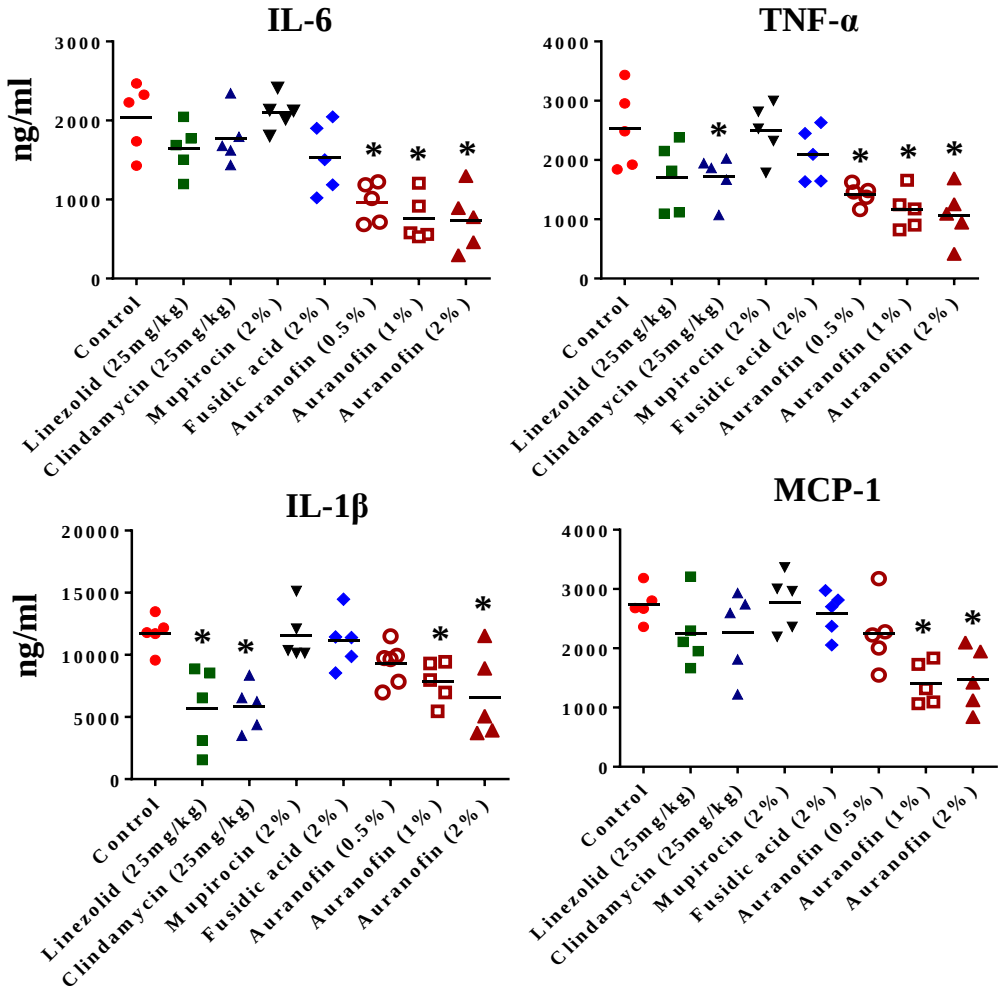

Figure 2.11 Effect of auranofin on inflammatory cytokines in MRSA skin lesions. Supernatants from skin homogenates were used for cytokine detection by ELISA. Statistical analysis was calculated by the two-tailed Student's *t* test. *P* values of (* $P \leq 0.05$) are classified as significant

Combinational therapy of auranofin with topical antimicrobials

With the rapid emergence of MRSA strains resistant to topical antimicrobials of choice, including to mupirocin and fusidic acid, combination therapy using multiple antibacterials is being explored [260,268,269]. Therefore, we assessed the activity of auranofin against MRSA USA300 in the presence of topical antimicrobials such as mupirocin, retapamulin and fusidic acid. Auranofin, in combination with all three tested topical antibiotics, exhibits additive activity (average fractional inhibitory concentration (FIC) index ranges from 0.5 to 1) in inhibiting MRSA growth (Figure 2.12). This suggests that auranofin can be potentially combined with traditional topical antimicrobials such as mupirocin, retapamulin and fusidic acid for the treatment of staphylococcal skin infections though further *in vivo* studies are needed to confirm this point.

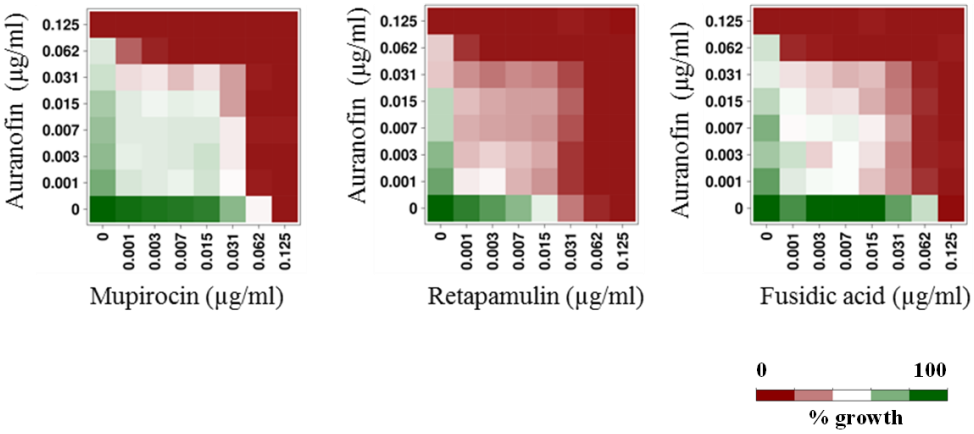

Figure 2.12 Auranofin in combination with three topical antimicrobials effectively inhibits the growth of *S. aureus*. Growth of MRSA USA300 was measured after incubating with auranofin, control antibiotics, or a combination of auranofin + a control antibiotic. The checkerboard assay was performed by diluting one drug along the ordinate and other drug along the abscissa of the 96-well plate. Percent bacterial growth was measured using a spectrophotometer.

Auranofin kills bacterial persister cells and reduces pre-formed biofilms

Treatment of bacterial infections with current antimicrobials are often challenging due to the inability of conventional antibiotics to target and disrupt adherent bacterial biofilms [270]. These problematic infections can become chronic when specialized dormant cells

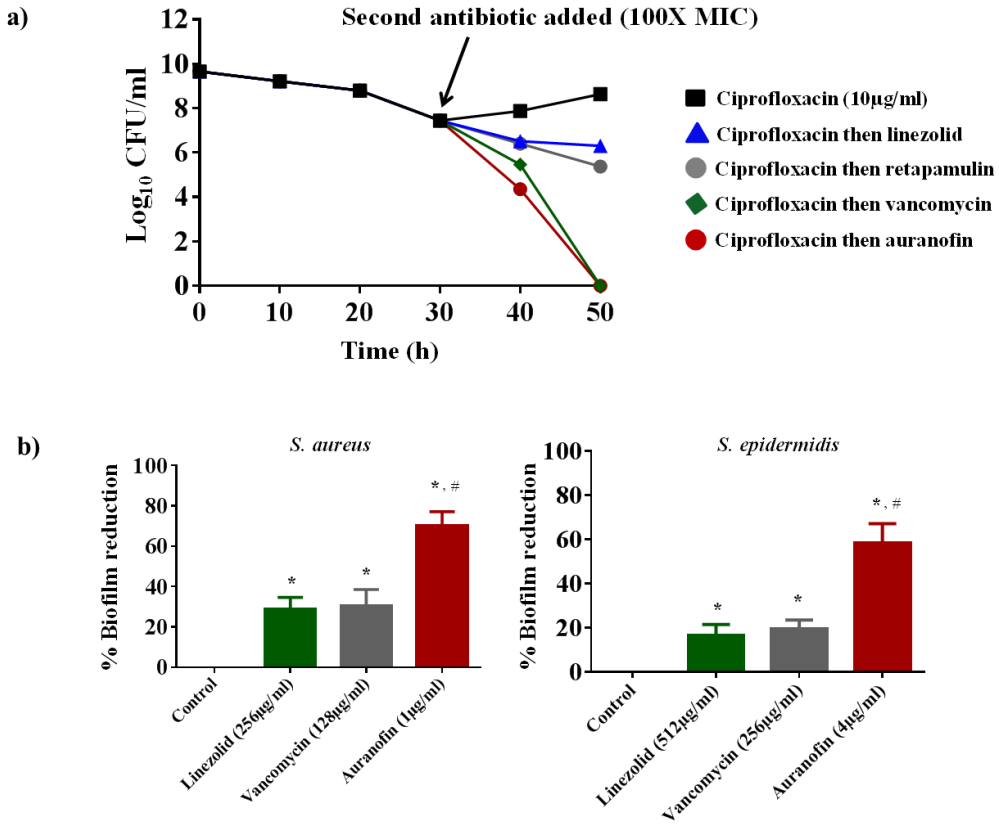

Figure 2.13 Auranofin effectively kills persister cells and reduces established biofilms of *S. aureus* and *S. epidermidis*. (A) Effect of auranofin and control antibiotics on ciprofloxacin tolerant MRSA USA300 were determined by time kill assay. (B) Effect of auranofin, vancomycin and linezolid on pre-formed Staphylococcus biofilms. The results are presented as means ± SD (n = 3). Statistical analysis was calculated using the two-tailed Student's *t* test. *P* values of (*, # $P \leq 0.05$) are deemed significant. Auranofin was compared both to controls (*) and to antibiotics (#).

called persisters (that are normally resistant to antibiotics), become encased within these biofilms thus protecting them from exposure to and eradication by antibiotics [267]. To assess the ability of auranofin to mitigate the impact of staphylococcal biofilms, we first investigated the effect of auranofin on persister cells. When treated with ciprofloxacin, MRSA USA300 (in exponential growth phase) produces a biphasic killing pattern that results in surviving persister cells (Figure 2.13a). The subsequent addition of conventional antimicrobials such as linezolid and retapamulin had minimal impact in reducing the number of persisters. However, treatment with auranofin resulted in complete eradication of persister cells after 48 hours, a result that is comparable to vancomycin (Figure 3.4a). Auranofin's ability to kill *S. aureus* persisters led us to next assess auranofin's impact on disrupting pre-formed staphylococcal biofilms. Auranofin, at 1 µg/ml, significantly reduced *S. aureus* biofilm mass by more than 60%; in contrast, even at high concentrations neither linezolid (256 µg/ml) nor vancomycin (128 µg/ml) were able to reduce biofilm mass by more than 30% (Figure 2.13b). Similarly, auranofin, at 4 µg/ml, was more effective at reducing *S. epidermidis* biofilm mass (60% reduction observed), compared to both linezolid (512 µg/ml) and vancomycin (256 µg/ml), which reduced biofilm mass by only 20% (Figure 2.13b). These results demonstrate that auranofin is capable of killing *S. aureus* persister cells and reducing adherent staphylococcal biofilms. This lays the foundation for further analysis using auranofin as a novel treatment option for both chronic and biofilm-related staphylococcal infections.

In vitro cytotoxicity study

Toxicity of auranofin to HaCaT cells was investigated using the MTS assay. Results indicate that the concentration of auranofin required to inhibit 50% (IC_{50}) of HaCaT cell growth is 6.38±0.29 µg/ml (Fig. 2.14). This value is nearly one hundred times larger than the MIC_{50} value for auranofin against MRSA. Additionally, auranofin is currently approved for long-term treatment of rheumatoid arthritis and patients have been taking the drug daily (6 mg/day) for more than five years, a much longer course of treatment than is traditionally prescribed for antibiotics (one to two weeks) [271]. Thus toxicity with auranofin should not be a significant impediment to repurposing this drug as a novel antibacterial agent for the treatment of cutaneous MRSA infections.

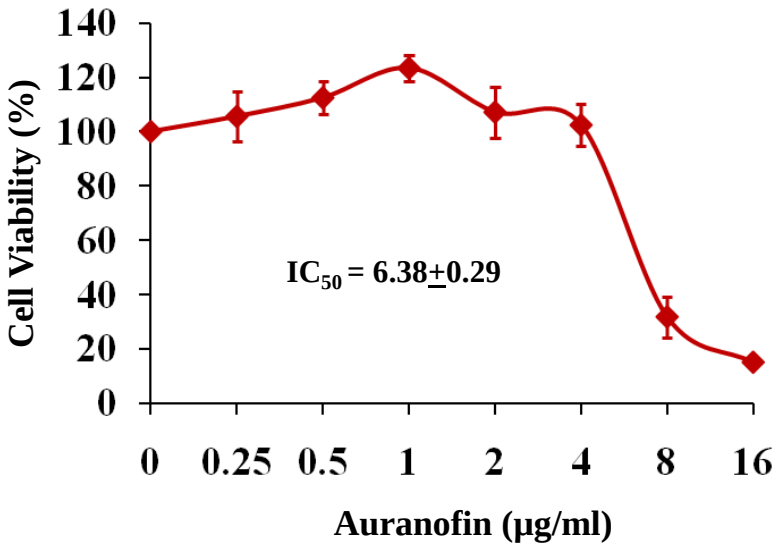

Figure 2.14 Cytotoxicity assay in human keratinocyte (HaCaT) cells. HaCaT cells treated with different concentration (0 to 16 µg/ml) of auranofin for 24 hours were assessed for cell viability by MTS assay. IC_{50} of auranofin (reducing viability of HaCaT cells by 50%) was calculated.

2.2.4 Conclusion

In summary, the present study demonstrates that auranofin, an antirheumatic drug, also possesses potent *in vitro* antistapylococcal activity against multidrug-resistant *S. aureus*. The *in vitro* results for auranofin were confirmed in a murine MRSA skin infection model that demonstrated that auranofin is superior to conventional antimicrobials (mupirocin and fusidic acid) in reducing the bacterial burden in infected wounds. In addition to decreasing the bacterial load, auranofin exhibits potent anti-inflammatory activity, reducing the presence of four key cytokines (IL-6, IL-1β, TNF-α, and MCP-1) known to increase the morbidity associated with skin infections. Furthermore, auranofin's ability to disrupt adherent staphylococcal biofilms and kill persister cells combined with its excellent safety profile, collectively support the notion that auranofin is a good candidate for repurposing as a topical antimicrobial for the treatment of staphylococcal skin infections.

2.3 Repurposing ebselen for the treatment of staphylococcal infections

(Thangamani S, Younis W, Seleem MN. Repurposing ebselen for treatment of multidrug-resistant staphylococcal infections. *Scientific Reports*. 2015, Jun 26;5:11596)

2.3.1 Introduction

In 2013, the Centers for Disease Control and Prevention (CDC) reported that more than 11,000 people died from a methicillin-resistant *Staphylococcus aureus* (MRSA)-related infection in the United States; this figure represents nearly half of all fatalities

caused by antibiotic-resistant bacteria. Apart from the high mortality rate, *S. aureus* is the most common pathogen associated with skin and soft tissue infections in humans[272-274] . Furthermore, *S. aureus* and its secreted toxins, and ability to form biofilm, are responsible for interfering with the wound-healing process and causing systemic complications in affected patients. In addition, the rising prevalence of multidrug-resistant *S. aureus* strains and the extensive use of drugs of choice increase the likelihood that more challenging–to-treat isolates will become a new scourge. Without a doubt, novel antimicrobials and novel approaches to developing them are urgently needed; however, new antimicrobials are becoming increasingly difficult to develop and are currently unable to keep pace with the emergence of resistant bacteria[109]. The concept of repurposing drugs to find new applications outside the scope of their original medical indication is recently gaining much attention and has resulted in successes in a number of disease areas[275,276]. Unlike *de novo* drug discovery, repurposing old drugs with known pharmacology and toxicology greatly reduces the time, cost, and risk associated with antibiotic innovation[277,278]. In an attempt to repurpose non-antibiotic drugs as antimicrobial agents, we screened National Institute of Health (NIH) Clinical Collection library against MRSA[275]. Ebselen (2-phenyl-1, 2-benzisoselenazol-3(2*H*)-one, PZ51), a selenium-containing compound, showed potent activity, in an applicable clinical range, against *S. aureus, which is in agreement with the previous finding*[67].

Previous studies reported that ebselen possesses anti- atherosclerotic, anti-inflammatory and antioxidative properties[59-62]. In addition, antimicrobial properties of ebselen has also been explored. It has been shown to inhibit yeast and *Escherichia coli in vitro*[67,68]. It interferes with proton-translocation function and ATPase activity in yeast,

while in *E. coli,* it inhibits the thioredoxin reducatse (TrxR) enzyme[69,68]. However, clinical applications and the underlying mechanism of action for its antibacterial activity against *S. aureus* still remain unclear[68].

Thus, the aim of our study is to assess the antibacterial action of ebselen and its spectrum of activity against clinical isolates of MRSA; to investigate its antimicrobial mechanism of action, anti-biofilm activity, and effect on toxin production in MRSA; and finally to validate its antimicrobial efficacy, anti-inflammatory properties, and potential clinical applications in MRSA infected animal model.

2.3.2 Materials and Methods

Bacterial strains and reagents

Staphylococcus strains used in this study are presented in Table 1. Mueller-Hinton broth (MHB) was purchased from Sigma-Aldrich. Trypticase soy broth (TSB), Trypticase soy agar (TSA), and Mannitol salt agar (MSA) were purchased from Becton, Dickinson (Cockeysville, MD). Ebselen was purchased from (Adipogen corp, San Diego), vancomycin hydrochloride (Gold Biotechnology), linezolid (Selleck Chemicals), mupirocin (applichem, NE), and chloramphenicol (Sigma-Aldrich).

Antibacterial assays

MICs of drugs and antibiotics were evaluated by broth micro dilution method in MHB according to the Clinical and Laboratory Standards Institute (CLSI)[216]. The MIC was interpreted as the lowest concentration of the drug that completely inhibited the visible growth of bacteria after incubating plates for at least 16hrs at 37°C. Each drug was tested

in triplicate in at least two independent experiments and the highest MIC value was reported.

Macromolecular synthesis assay

Macromolecular synthesis assay was carried out in *S. aureus* strain ATCC 29213. Briefly, 100 µl of *S. aureus* grown in TSB at exponential phase (OD600 = 0.2 to 0.3), was added to triplicate wells and different concentrations of ebselen and control antibiotics (ciprofloxacin, rifampicin, linezolid, vancomycin and cerulenin) was added. DMSO treated cells served as a negative control. Cells treated with drugs and DMSO were incubated at 37°C to allow the drug to act on bacterial cells. After 30 min incubation, radio labeled precursors for DNA, RNA, protein, cell wall and lipid synthesis such as [3H] thymidine (0.5µCi), [3H] uridine (0.5µCi), [3H] leucine (1.0 µCi), [14C] N-acetylglucosamine (0.4 µCi), [3H] glycerol (0.5 µCi), respectively, were added for each reaction. After 15 min, reactions of DNA and RNA synthesis were stopped using 12 µl of 5% trichloroacetic acid (TCA). Similarly, protein synthesis was stopped after 40 min using 12 µl of 5% TCA. Reaction wells containing cell wall and lipid synthesis were stopped after 40 min using 100 µl of 8% SDS and 375 µl of chloroform/methanol (1:2) respectively. Reactions (DNA, RNA and protein) were incubated on ice for 30 min and the TCA precipitated materials were collected on a 25 mm GF/1.2 µM PES 96 well filter plate. After washing five times with cold 5% TCA, the filters were dried and counted using a Packard Top Count microplate scintillation counter. For cell wall synthesis, reaction tubes were then heated at 95°C for 30 min, cooled, centrifuged, and spotted onto nitrocellulose membrane filters (0.8 µM). After washing three times with 0.1% SDS, the filters were rinsed two times with

deionized water, allowed to dry, and then counted using a Beckman LS3801liquid scintillation counter. For lipid synthesis, reactions tubes were centrifuged at 13,000 rpm in a microfuge for 10 min, and then 150 µl of the organic phase was transferred to a scintillation vial and allowed to dry for at least 1 hour. Samples were then counted using liquid scintillation counting. Based on the incorporation of radiolabeled precursors of DNA, RNA, protein, cell wall and lipid synthesis, results were expressed as percent inhibition of macromolecular synthesis pathways.

Measuring toxin production by ELISA

We tested the effect of ebselen on production of two important toxins Hla and PVL by ELISA as described before[279,280]. Briefly, Overnight grown MRSA USA300 bacterial culture was diluted approximately to 5×10^8 CFU/ml in TSB. 10X MICs of drugs and antibiotics were added and incubated in the shaking incubator at 37°C. After 1hr the bacterial culture was centrifuged and the supernatants were used for toxin detection.

ELISA plates (Nunc) were coated with 2 µg/ml of sheep anti-Hla IgG (Toxin technology) in 100 µl of coating buffer and left overnight at 4 °C. Plates were then washed 3 times with Tris-buffered saline (TBS) containing 0.05% tween 20 (wash buffer) and then blocking solution containing TBS with 2% bovine serum albumin was added. After 1hour incubation at 37°C, plates were washed 3 times with wash buffer. A total of 100 µL of bacterial supernatants were added and incubated the plates at 37°C for 2 hours. Purified Hla (Toxin technology) was used to generate a standard curve. Plates were again washed 3 times with wash buffer and 100 µL of sheep anti-Hla HRP conjugate at a dilution of 1:300 was added. After 1 hour of incubation at 37°C and final washing, 100 µL of 3, 3′, 5,

5′-tetramethylbenzidine substrate (Sigma-Aldrich) was added, and the reaction was stopped after 10 minutes with 100 μL of 0.2N H2S04. Plates were read on a spectrophotometer at optical density (OD) 450, and data were analyzed with SoftMax Pro (Molecular Devices). The nominal range of this assay was 0.1–6 μg /mL

For PVL Luk-S toxin, ELISA plates (Nunc) were coated as before with 2 μg /ml of mouse anti- PVL Luk-S monoclonal antibody (IBT Bioservices). Purified *S. aureus* LukS-PV (His-tag) (IBT Bioservices) was used to generate a standard curve. The experiment was carried as before except detection antibodies rabbit anti-PVL Luk-S (2 μg/ml) and rabbit IgG HRP conjugate (R&D Systems) at a dilution of 1:6000 was used. The concentrations of each toxin was compared as unadjusted concentrations (ng/ml) and corrected for organism inoculum for each treatment (ng/ml to $\log_{10}$ CFU/ml).

Biofilm assay

Biofilm assay was performed as described before[216]. Briefly, biofilm-forming clinical isolates of *S. aureus* (ATCC 6538) and *S. epidermidis* (ATCC 35984) were inoculated in 96-well flat-bottom cell culture plates (polystyrene) in TSB supplemented with 1% glucose at 37°C for 24 h. Then culture medium was removed, and wells were carefully washed with PBS four times to remove planktonic bacteria. Ebselen and antibiotics (linezolid, mupirocin and vancomycin) were added at different concentrations in TSB, and plates were incubated at 37°C for 24 h. The wells were rinsed by submerging the entire plate in a tub containing tap water. Biofilms were stained with 0.1% (wt/vol) crystal violet for 30 min. After staining, the dye was removed and the wells were washed four times with water. The plates were dried for 1 h and ethanol (95%) was added to solubilize the dye bound to the

biofilm. The OD of biofilm mass was measured at 595-nm absorbance by using a micro plate reader (Bio-Tek Instruments Inc.)

Cytotoxicity assay

Human keratinocyte (HaCat) cells were seeded at a density of 10,000 cells per well in a 96-well tissue culture plate (CytoOne, CC7682-7596) in DMEM media containing 10% fetal bovine serum (FBS) and incubated overnight at 37˚C. Then cells were treated with ebselen at different concentrations from 0 to 128 µg/ml for 24 hours. Treated cells were washed four times with PBS and the DMEM media containing MTS assay reagent, 3-(4,5-dimethylthiazol-2-yl)-5-(3carboxymethoxyphenyl)-2-(4-sulfophenyl)-2H-tetrazolium) (Promega, Madison, WI, USA) was added. After 4hrs of incubation at 37˚C, absorbance was measured using ELISA microplate reader (Molecular Devices, Sunnyvale, CA, USA). Percent cell viability of ebselen treated cells were calculated in relative to the untreated cells.

Mice infection

Eight weeks old female BALB/c mice were used for this study (Harlan Laboratories, Indianapolis, IN). All animal procedures were approved by Purdue University Animal Care and Use Committee (PACUC). The murine model of MRSA skin infection has been described before [266]. Mice were injected intradermally with 40 µl of MRSA USA300 (6.7×10^8) CFU per mouse. Forty-eight hours after infection and formation of open wound, the mice were divided into eight groups (n=5). Four groups were treated topically with either 0.5%, 1%, or 2% ebselen in petroleum jelly (ointment- skin protectant) or 1% ebselen

in lipoderm (dermal and transdermal delivery cream base). Two groups received the vehicles alone (petroleum jelly or lipoderm). One group was treated topically with 2% mupirocin in petroleum jelly and the last group was treated orally with linezolid (25 mg/kg). All groups were treated twice a day for 5 days. Twenty-four hours after the last treatment, the area around the wound was lightly swabbed with 70% ethanol and the wound was excised for bacterial counting on MSA after homogenization.

Cytokines detection

Skin homogenates were centrifuged and the supernatants were used to detect the cytokine level by ELISA. Tumor necrosis factor-α (TNF-α), interleukin-6 (IL-6), interleukin-1 beta (IL-1β), and monocyte chemo attractant protein-1(MCP-1) Duo-set ELISA Kits (R&D Systems, Inc.) were used for the quantification of cytokines The experiment was carried out as per the manufacture instructions [281].

Bliss model of synergism

Synergism was calculated using the Bliss Independence Model, which calculates a degree of synergy using the formula: $S = (f_{A0}/f_{00})(f_{0B}/f_{00})-(f_{AB}/f_{00})$, where f_{AB} refers to bacterial growth rate in the presence of the combined drugs at a concentration *A*, for one of the antibiotics, and *B* for the ebselen; f_{A0} and f_{0B} refer to the bacterial growth rates in the presence of antibiotics (or) ebselen at a concentration of *A* and *B*, respectively; f_{00} refers to the bacterial growth rate in the absence of drugs; and *S* corresponds to the degree of synergy, a parameter that determines a synergistic interaction for positive values and an antagonistic

interaction for negative ones. Growth rates at 12hr are determined and the degree of synergism was calculated as described before[282].

Statistical analyses

Statistical analyses were assessed by Graph Pad Prism 6.0 (Graph Pad Software, La Jolla, CA). *P* values were calculated by the two-tailed Student *t* test. *P* values of < 0.05 were considered as significant.

2.3.3 Results

Antibacterial activity of ebselen

The antimicrobial activity of ebselen was tested against a panel of clinical isolates of multi-drug resistant *S. aureus* (Table 2.4). Ebselen showed potent bactericidal activity against MRSA, vancomycin-resistant *S. aureus* (VRSA), linezolid-resistant *S. aureus*, mupirocin-resistant *S. aureus*, methicillin-resistant *S. epidermidis*, and multidrug-resistant strains with a minimum inhibitory concentration (MIC) ranging from 0.125 µg/ml to 0. 5 µg/ml (Table 2.4).

Table 2.4 MICs of ebselen and antibiotics against clinical isolates of *Staphylococcus* strains

Strain type	Strain ID	MICs (μg/ml)		
		Ebselen	Linezolid	Vancomycin
Methicillin resistant *S.*	USA100	0.125	2	2
aureus (MRSA)	USA200	0.125	2	1
	USA300	0.125	2	1
	USA400	0.5	2	1
	USA500	0.125	2	1
	USA700	0.125	4	1
	USA800	0.125	4	1
	USA1000	0.125	2	1
	USA1100	0.125	2	1
	ATCC 43300	0.125	2	1
	ATCC BAA-44	0.25	2	1
Linezolid-resistant *S. aureus*	NRS119	0.125	>16	1
Mupirocin-resistant *S. aureus*	NRS 107	0.125	2	1
Vancomycin-resistant *S.*	VRS1	0.25	1	>16
aureus (VRSA)	VRS2	0.25	1	8
	VRS3a	0.25	2	>16
	VRS3b	0.25	2	>16
	VRS4	0.125	2	>16
	VRS5	0.25	2	>16
	VRS6	0.25	2	>16
	VRS7	0.5	2	>16
	VRS8	0.125	2	>16
	VRS9	0.25	2	>16
	VRS10	0.25	2	>16
S. epidermidis	NRS101	0.5	2	2
S. aureus	ATCC 6538	0.125	2	1

Mechanism of action

Given the potent anti-staphylococcal activity of ebselen *in vitro*, we investigated its anti-staphylococcal mechanism of action by macromolecular synthesis assay. As shown in Figure 2.15, ebselen primarily inhibited protein synthesis at 1X the MIC. However, additional secondary effects were observed at a higher concentration (8X MIC). At higher concentration, ebselen inhibited DNA, RNA and lipid synthesis similar to control antibiotics such as ciprofloxacin, rifampicin and cerulenin respectively.

Ebselen inhibits MRSA toxin production

The effect of ebselen on production of important toxins such as Panton-Valentine leucocidin (PVL) and α-hemolysin (Hla) was tested by ELISA. The concentrations of each toxin were compared as unadjusted concentrations (ng/ml) and corrected for organism inoculum for each treatment (ng/ml to $\log_{10}$ colony-forming units, CFU/ml). Ebselen significantly suppressed toxin production in MRSA USA300 (Figure 2.16).

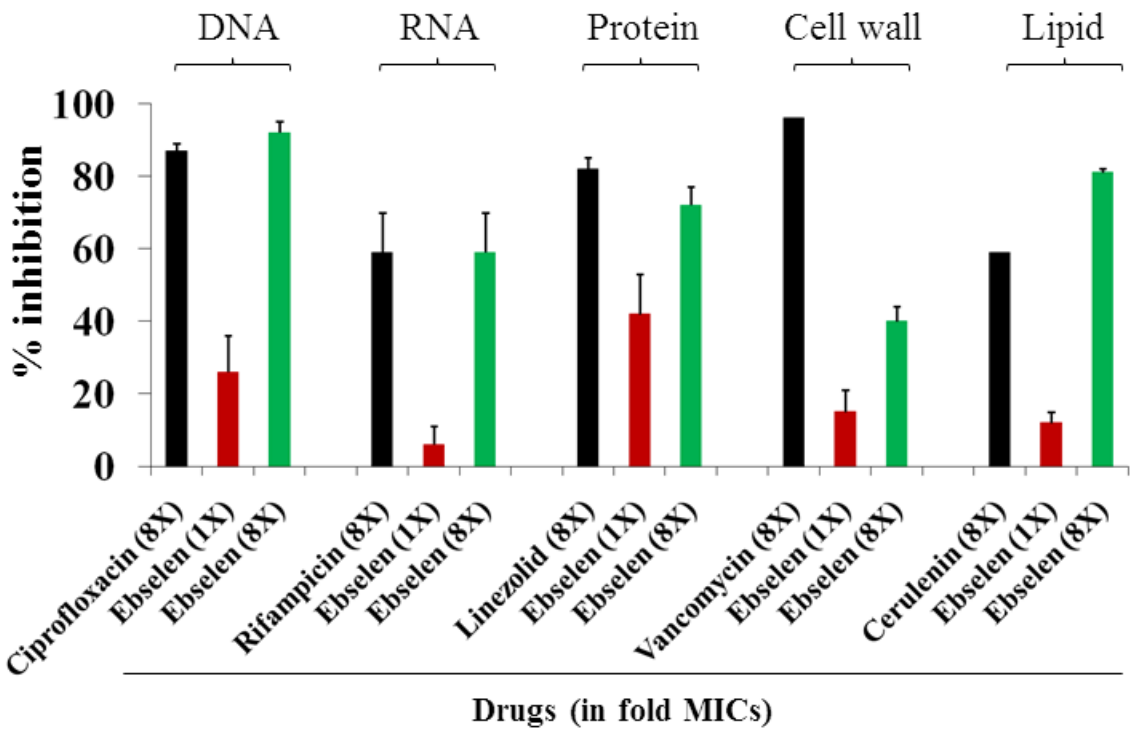

Figure 2.15 Macromolecular synthesis in the presence of ebselen. Incorporation of radiolabeled precursors of DNA, RNA, protein, cell wall and lipid synthesis ([3H] thymidine, [3H] uridine, [3H] leucine, [14C] N-acetylglucosamine and [3H] glycerol, respectively) were quantified in *S. aureus* ATCC 29213. Results were expressed as percent of inhibition calculated based on the incorporation of radiolabeled precursors.

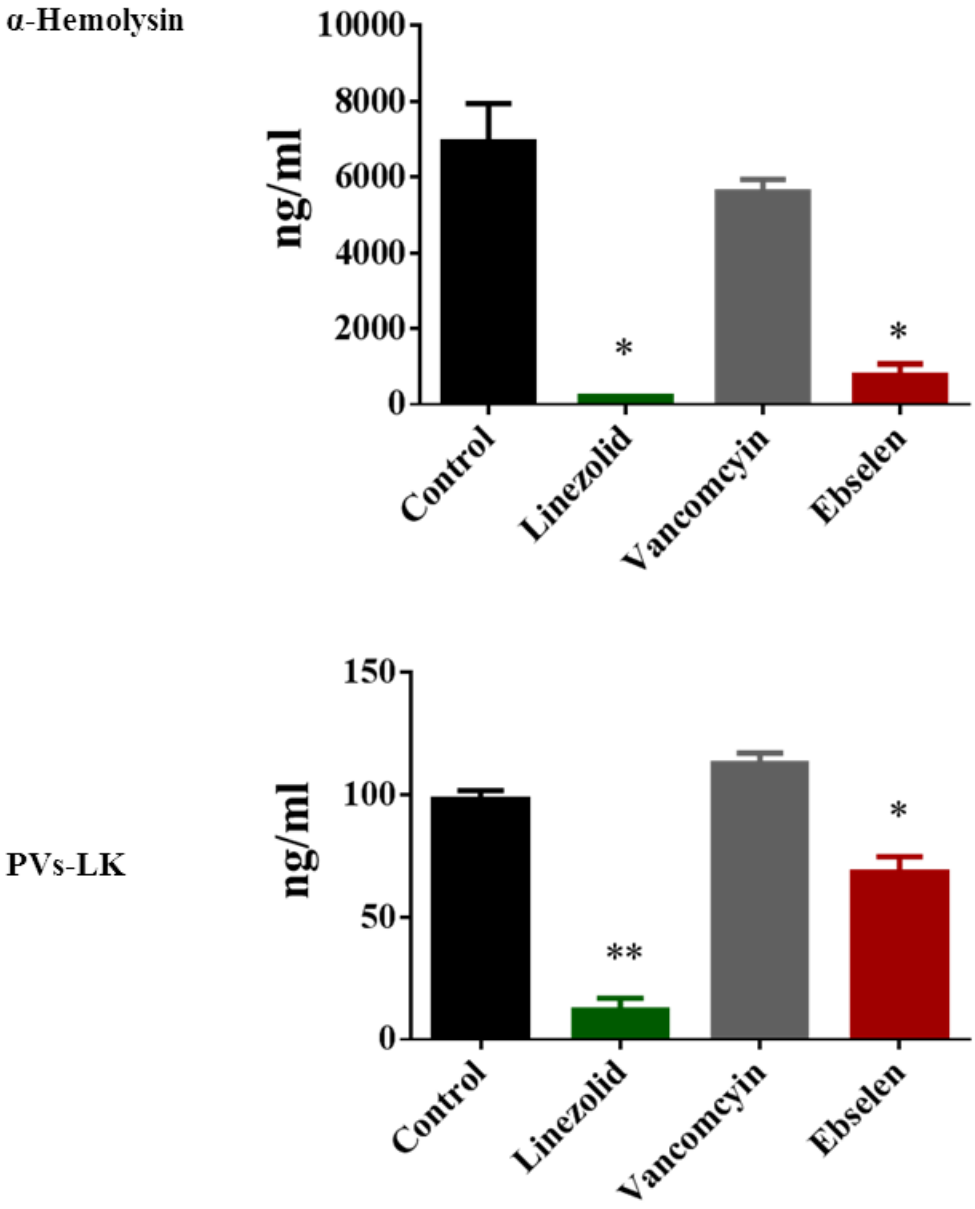

Figure 2.16 Effect of ebselen on toxin production. Toxin production (ng/ml) in *S. aureus* MRSA USA300 after antibiotic/drug exposure for 1 hour corrected for organism burden. The results are given as means ± SD (n = 3). ** indicate statistical significant different from control (DMSO or water). *P* values of (* $P \leq 0.05$) (** $P \leq 0.01$) are considered as significant.

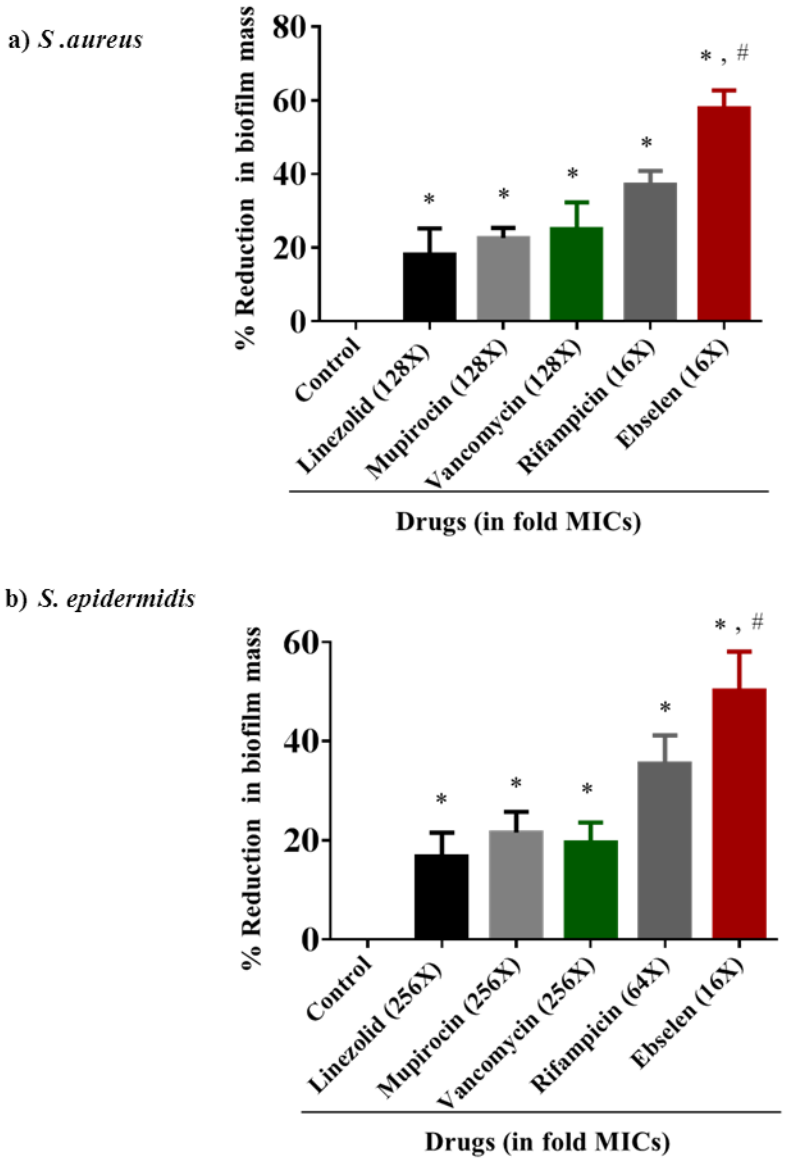

Figure 2.17 The effects of ebselen and antibiotics (linezolid, mupirocin, vancomycin and rifampicin) on established biofilms of *S. aureus* (a) or *S. epidermidis* (b). The established biofilms were treated with control antibiotics or ebselen and stained with crystal violet. Optical density of dissolved crystal violet was measured using a spectrophotometer. Values are the mean of triplicate samples with the standard deviation bars. *P* values of (*,#$P \leq$ 0.05) are considered as significant. Ebselen was compared to controls (*) and to antibiotics (#).

Activity against biofilms

Considering the excellent broad-spectrum activity of ebselen against the MRSA and VRSA strains, we also considered the possibility that ebselen would be active against established biofilm. Biofilm-forming strains of *S. aureus* and *S. epidermidis* were used and the biofilm mass was estimated after treatment with ebselen and control antibiotics. Ebselen was significantly superior in reducing adherent biofilms of both *S. aureus* and *S. epidermidis* when compared to conventional antibiotics (linezolid, mupirocin, vancomycin and rifampicin). Ebselen (2µg/ml) at 16X MIC significantly reduced the biofilm mass, approximately by 60%. Control antibiotics, such as linezolid (256µg/ml), mupirocin (16µg/ml) and vancomycin (128µg/ml) at 128X MIC were able to reduce the biofilm mass only by 20%. Rifampicin (0.5µg/ml) at 16X MIC reduced the biofilm mass by only 40% (Figure 2.17a).

Ebselen (8µg/ml) at (16X MIC), significantly reduced the strong biofilms of *S. epidermidis*, by more than 50%. However, linezolid (512µg/ml), mupirocin (32µg/ml) and vancomycin (256µg/ml) at 256X MIC reduced biofilm mass by only 20% and rifampicin (2µg/ml) at 64X MIC reduced biofilm mass by 40% (Figure 2.17b).

Cytotoxicity study

Safety of ebselen in mammalian cells was evaluated against human keratinocyte cells (HaCat) by MTS assay. Ebselen did not show toxicity up to 32 µg/ml. The results demonstrated that half maximal inhibitory concentration (IC_{50}) required by ebselen to inhibit 50% of HaCat cells was found to be 58.78 ± 0.64µg/ml (Figure 2.18).

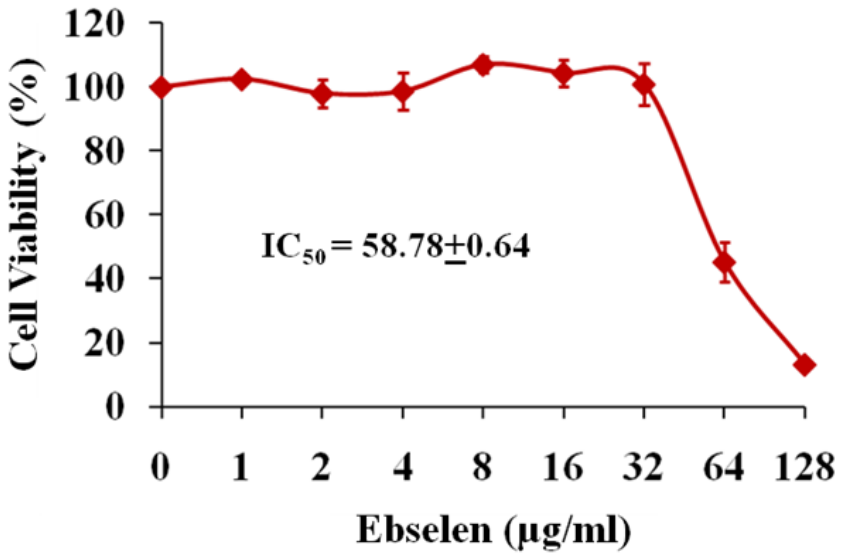

Figure 2.18 Cytotoxicity assay in human keratinocyte (HaCat) cells. HaCat cells were treated with different concentration of ebselen ranging from 0 to 128µg/ml. DMSO was used as a negative control. Cell viability was measured by MTS assay and IC_{50} of ebselen to cause cytotoxicity in HaCat cells was calculated.

The therapeutic efficacy of ebselen in a mouse model of MRSA skin infection

(i) Bacterial load

Five groups of mice were treated topically either with vehicle alone (petroleum jelly) or control antibiotic (2% mupirocin) or ebselen (0.5%, 1%, or 2%) twice a day for five days. One group of mice was treated with linezolid orally. As shown in Figure 2.19a, ebselen (1% and 2%) significantly reduced the mean bacterial counts compared with the control group ($P \leq 0.01$). The group treated with 2% mupirocin had the highest reduction

in CFU (2.28±0.25 log_{10}), followed by 2% ebselen (1.71±0.11 log_{10}), linezolid (25 mg/kg) (1.55±0.01 log_{10}), and 1% ebselen (1.02±0.17 log_{10}).

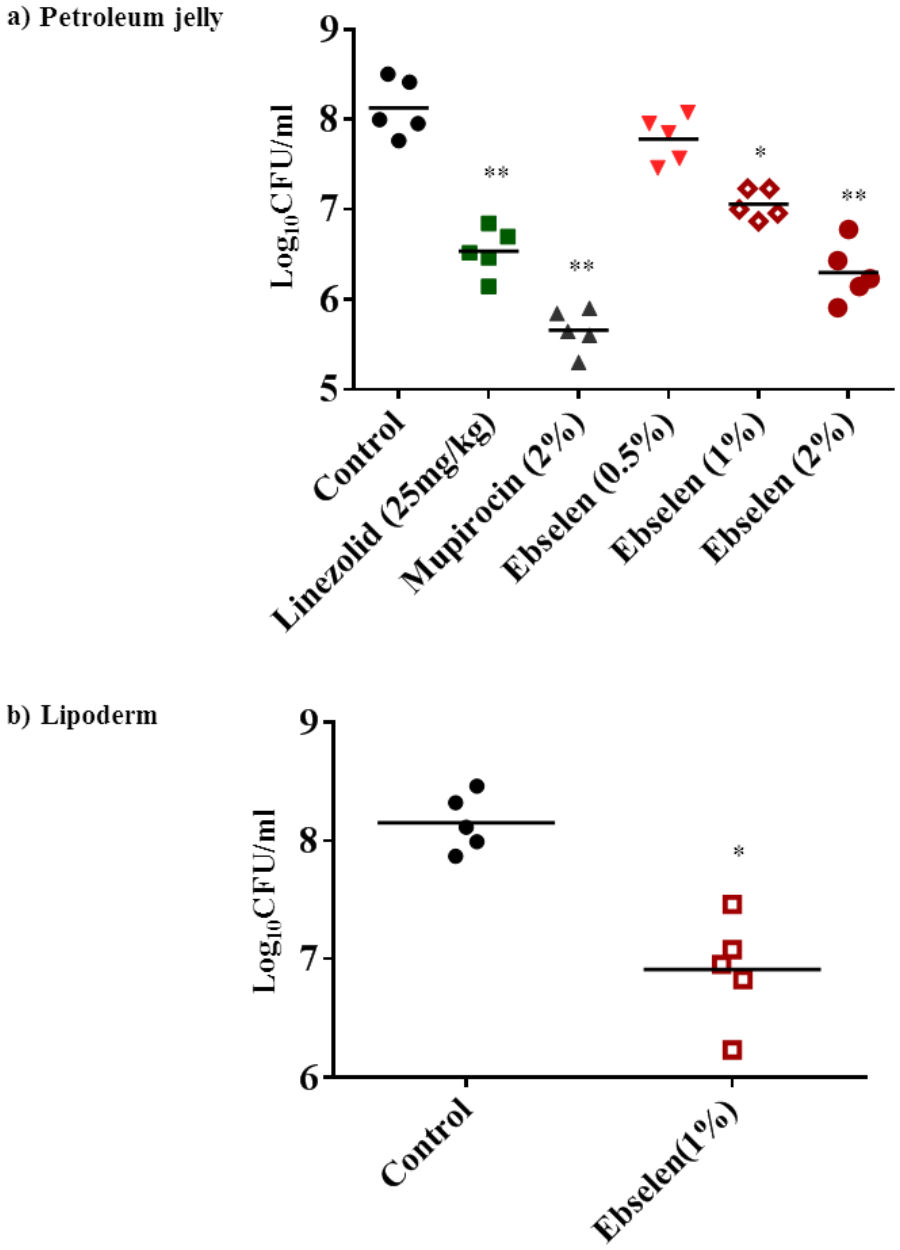

Figure 2.19 Efficacy of treatment of MRSA skin lesions with ebselen 0.5, 1, and 2%, linezolid (25 mg/kg), mupirocin (2%) and petroleum jelly (negative control) twice daily for 5 days (a). Treatment with ebselen 1% and lipoderm (negative control) twice daily for 5 days (b). Statistical analysis was calculated by the two-tailed Student *t* test. *P* values of (* $P \leq 0.05$) (** $P \leq 0.01$) are considered as significant. (#).

(ii) Effect of vehicle

In order to investigate the effect of the vehicle on the efficacy of ebselen in the treatment of MRSA skin infections, two groups of mice were treated topically either with vehicle alone (lipoderm base)[283] or ebselen 1% formulated in lipoderm base twice a day for five days. Ebselen 1% significantly reduced the mean bacterial counts by 1.37±0.20 $\log_{10}$ compared with the control group ($P \leq 0.01$) (Figure 2.19b). No significant difference was observed in reducing the mean bacterial count between the ebselen 1% formulated in petroleum jelly and lipoderm base (Figure 2.19a and 2.19b).

Effect of ebselen on inflammatory cytokines induced by MRSA skin infection

To study the immune-modulatory activities of ebselen in a topical application against MRSA skin infection, we used ELISA to measure the pro-inflammatory cytokines tumor necrosis factor-α (TNF-α), interleukin-6 (IL-6), interleukin-1 beta (IL-1β) and monocyte chemo attractant protein-1(MCP-1) in the infected wounds. As shown in Figure 2.20, ebselen 2% and 1% significantly reduced all tested pro-inflammatory cytokines, including IL-6, IL-1β, TNF-α, and MCP-1. However, ebselen at 0.5% significantly reduced IL-6 and MCP-1 only. Ebselen had considerably higher anti-inflammatory activity compared to antibiotics (linezolid and mupirocin).

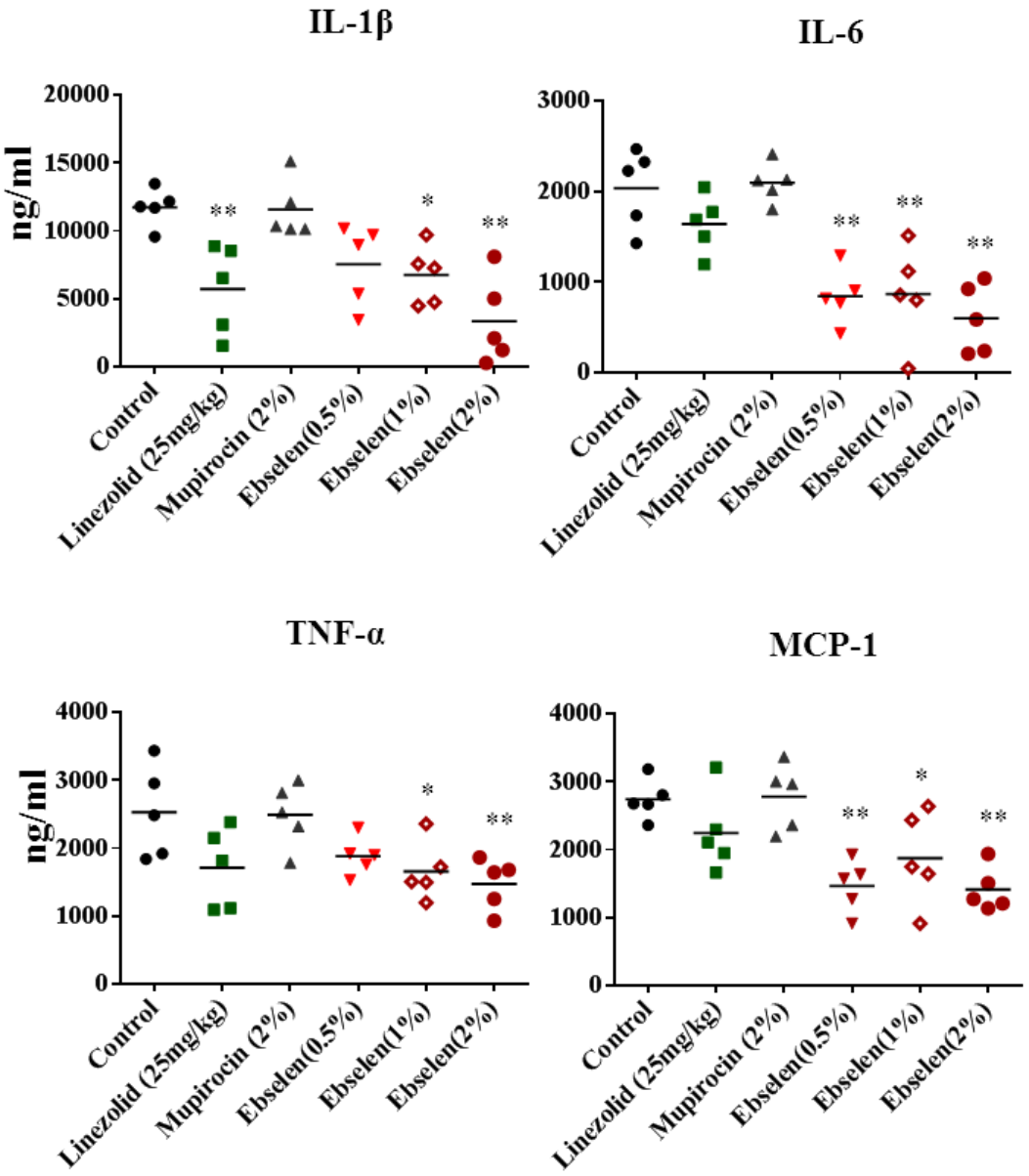

Figure 2.20 Effect of ebselen on cytokines production in MRSA skin lesions. Supernatants from skin homogenates were used for cytokine detection by ELISA. Each points represents single mice and each group has 5 mice. Statistical analysis was calculated by the two-tailed Student *t* test. *P* values of (* $P \leq 0.05$) (** $P \leq 0.01$) are considered as significant.

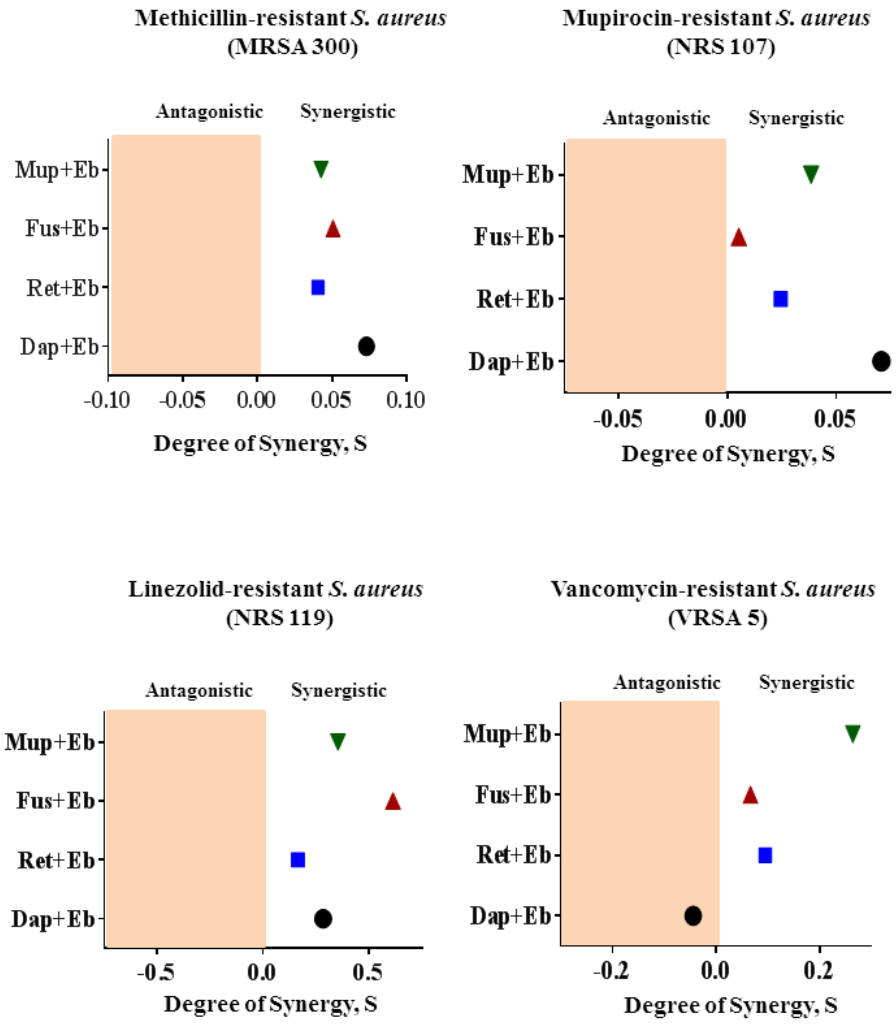

Figure 2.21 Synergistic activity of ebselen with topical antimicrobials. The Bliss Model for Synergy confirms a synergistic effect, between ebselen and topical antimicrobials (mupirocin, fusidic acid, retapamulin and daptomycin) against various resistant strains of *S. aureus*. Degree of synergy was quantified after 12h of treatment with ebselen (0.0312 µg/ml) in combination with sub-inhibitory concentrations of topical antimicrobials. (Circle) daptomycin + ebselen, (Square) retapamulin + ebselen, (Triangle) fusidic acid + ebselen and (Inverted triangle) mupirocin + ebselen.

Synergistic activity of ebselen with topical antimicrobials *in vitro*

The antimicrobial activity of ebselen in combination with topical antimicrobials (mupirocin, fusidic acid, retapamulin and daptomycin) was investigated *in vitro* by the Bliss model of synergism against four clinical isolates. With the exception of the VRSA5 strain and the antibiotic daptomycin, ebselen acted synergistically with all tested antibiotics against *S. aureus* clinical isolates (Figure 2.21).

2.3.4 Discussion

For the past few decades the rise of multi-drug resistant *S. aureus* has been an emerging issue in hospital and community settings[109,206]. More importantly, the management of *S. aureus* strains associated with skin infections is becoming a serious issue in community settings[284,285]. With the increasing incidence of multidrug-resistant *S. aureus* strains, there is a pressing need for new antimicrobials to circumvent this burgeoning problem. However, the discovery and development of new antimicrobials has been slowing since 1960. Even today, the global antibiotic market is still dominated by a few classes of antibiotics that were discovered half a century ago[109]. Moreover, pharmaceutical companies are not interested in investing in antibiotic research and development because of low return compared to other drugs being developed for chronic ailments[109,286,287]. As an alternative to the traditional *de novo* antibiotic development, repurposing non-antimicrobial drugs is a novel and less expensive way to speed up the drug-development process.

In an intensive search for antimicrobial activity among non-antibiotic drugs, we and others[67,68] identified ebselen as a potent antimicrobial agent against Gram-positive pathogens including MRSA. Ebselen, an organoselenium compound, is known to be clinically safe with a well-known pharmacology profile and it is currently undergoing clinical trials for the prevention and treatment of various disorders such as cardiovascular disease, arthritis, stroke, atherosclerosis, and cancer[60,63-66]. Ebselen showed potent bactericidal activity against multiple clinical isolates of MRSA, including MRSA USA100, USA200, USA500, USA1000, and USA1100, which are resistant to various antimicrobials, including penicillin, fluoroquinolone, macrolides, and aminoglycosides. It also showed potent activity against multidrug-resistant clinical isolates of *S. aureus* strains, including a linezolid-resistant strain (NRS119), vancomycin-resistant strains (VRSA1-VRSA10), and a mupirocin-resistant strain (NRS107). Moreover, ebselen demonstrated excellent activity against MRSA USA300, a community-associated strain responsible for outbreaks of staphylococcal skin and soft-tissue infections (SSTI) in the United States[288].

Although the antimicrobial activity of ebselen has been reported before[67,68], its mechanism of action in *S. aureus* and its *in vivo* efficacy have never been explored. Ebselen, in our study, inhibited protein synthesis in *S. aureus.* Inhibition of protein synthesis at a concentration equivalent to the MIC demonstrates that, protein synthesis is likely primary antibacterial mechanism of action of ebselen. In addition, secondary effects on DNA, RNA ,lipid synthesis and to a lesser extent on cell wall synthesis were also noticed at higher concentrations (8X MIC). It is possible that disruption of protein synthesis could lead to downstream inhibition of other pathways. This provides valuable insight into ebselen's potential target in *S. aureus*. However, further work is needed to identify the cellular target

of ebselen in *S. aureus*. For treatment of infections caused by toxin-producing pathogens such as *S. aureus,* inhibition of protein synthesis is an important consideration in the selection of antimicrobial agents[280]. Because antimicrobials that suppress translation in *S. aureus* markedly suppress the formation of toxins such as PVL and Hla , which will lead to better treatment outcomes[280,289-291]. In the light of our results, showing potent inhibition of bacterial protein synthesis, we tested the effect of ebselen on production of two important toxins in MRSA USA300 (Hla and PVL) by ELISA. Ebselen significantly suppressed toxin production after 1hour incubation with MRSA. Inhibition of protein synthesis and the subsequent inhibition of toxin production are great advantages of ebselen as an antimicrobial agent.

Bacterial biofilms, which serve to protect the bacteria and hinder penetration of antibacterial drugs, contribute significantly to the treatment failure of Staphylococcus infections[216]. Given the potent antibacterial activity of ebselen against planktonic multidrug-resistant strains, we also considered the possibility that ebselen would be active against established bacterial biofilms of *S. aureus* and *S. epidermidis* (a leading cause of hospital-acquired implant-based infections)[292]. Ebselen was superior in reducing adherent biofilms of both *S. aureus* and *S. epidermidis* when compared to conventional antibiotics (linezolid, mupirocin and vancomycin).

In view of our results demonstrating the potent antimicrobial and antibiofilm activities of ebselen *in vitro* against MRSA, we moved forward with an *in vivo* experiment in a mouse model of MRSA skin infection. Ebselen 1% and 2% in petroleum jelly significantly reduced the mean bacterial counts compared with the control group ($P \leq 0.01$).

The lipoderm base enhanced the antimicrobial activity of ebselen but the reduction in bacterial load was not significant from petroleum jelly vehicle.

Since the clinical severity of *S. aureus* skin infections is driven by the excess host pro-inflammatory cytokines rather than by bacterial burden[256,293], ebselen with its recognized immune-modulatory, anti-inflammatory, and antioxidant activities[59,294] should be superior to traditional antibiotics for treatment of skin infections[107,293]. In this study, topical treatment with ebselen 1 and 2% significantly reduced IL-1β, IL-6, TNF-α and MCP-1 which might benefit the healing of infected wounds[102-106]. Linezolid also inhibits IL-1β which is in line with previous findings[293,295]. Prolonged inflammation especially due to inflammatory cytokines such as IL-6, TNF-α, and MCP-1, greatly delays healing in chronic wounds[107]. Ebselen significantly ($P \leq 0.01$) inhibits all three cytokines (IL-6, TNF-α, and MCP-1), which should provide a favorable outcome in wound healing[107].

With the increasing incidence of MRSA strains resistant to topical drugs of choice, such as mupirocin and fusidic acid, combination therapies are being explored[259,260,268,269]. To investigate whether ebselen has the potential to act synergistically with topical antimicrobials against multidrug-resistant strains, the Bliss independence model was utilized[282]. Ebselen acted synergistically with topical antimicrobials against resistant strains of *S. aureus,* thus providing a strong platform to combine ebselen with topical antimicrobials in treating staphylococcal skin infections and reducing the likelihood of strains developing resistance to monotherapy.

2.4 Repurposing clinical molecule ebselen to combat drug resistant pathogens

(Thangamani S, Younis W, Seleem MN. Repurposing Clinical Molecule Ebselen to Combat Drug Resistant Pathogens. *PLoS One*. 2015 Jul 29;10(7):e0133877)

2.4.1 Introduction

Infections caused by Gram-positive drug-resistant pathogens are a leading cause of mortality. Three species—methicillin-resistant *Staphylococcus aureus* (MRSA), *Streptococcus pneumoniae* and vancomycin-resistant enterococcus (VRE)—are responsible annually for at least 84% of the antibiotic-resistant bacteria mortality in the United States alone [1]. Further exacerbating the issue of bacterial resistance is the slow rate of the development and approval of new antimicrobials. For almost 80 years, antimicrobials have been crucial allies in the treatment of bacterial infections caused by these pathogens. However, multidrug resistant strains have recently emerged that are resistant to almost all antimicrobials once deemed effective, including fluoroquinolones, macrolides, and β-lactams [296]. Collectively, this points to an urgent need for the discovery of new antimicrobials and novel strategies to develop them. One novel strategy that warrants more attention as a unique method for development of new antimicrobials is drug repurposing [276]. Our recent attempt to identify non-antibiotic drugs with potent antimicrobial activity, within an applicable clinical range, identified organoselenium compound ebselen (EB) as having potent antibacterial activities against Gram-positive pathogens [297]. EB is considered a clinically safe molecule but without proven use yet [275].

It has anti-oxidative, anti-inflammatory, and anti-atherosclerotic properties [59]. Additionally, EB has been shown to exhibit antimicrobial activity *in vitro* and *in vivo* [67,68,298,299]. EB exhibited antimicrobial activity by inhibition of thioredoxin reducatse (TrxR) enzyme of *Escherichia coli* and H^+-ATPase function and proton-translocation function in yeast [67-69]. However, the antibacterial mechanism of action of EB against Gram-positive bacteria remains unidentified [68].

The potent antimicrobial activity of EB against Gram-positive pathogens motivated us to further investigate the therapeutic applications of EB. The aims of the present study are to investigate the antibacterial activity of EB against Gram-positive clinical pathogens, including MRSA and VRE *in vitro*, to identify antibacterial mechanism of action, to analyze the ability of EB to clear MRSA intracellular infection, to evaluate antibacterial efficacy in MRSA-infected *Caenorhabditis elegans* whole animal models, to evaluate the effect on mitochondrial biogenesis and toxicity in *C. elegans*, and to assess whether EB is capable of working synergistically with conventional antibiotics against MRSA in *in vitro* and in infected cell cultures. This study provided valuable insights into potential therapeutic applications of EB for use as antimicrobial agents for the treatment of multidrug-resistant Gram-positive infections.

2.4.2 Materials and Methods

Bacterial strains and reagents

Bacterial strains employed in this study are presented in Table 1. Mannitol salt agar (MSA) was purchased from Hardy Diagnostics (Santa Maria, CA). Muller-Hinton broth

(MHB) was purchased from Sigma-Aldrich (St. Louis, MO). Trypticase soy broth (TSB) and Trypticase soy agar (TSA) were purchased from Becton, Dickinson (Cockeysville, MD). EB was purchased from (Adipogen corp, San Diego), vancomycin hydrochloride (Gold Biotechnology, St. Louis, MO), linezolid (Selleck Chemicals, Houston, TX), clindamycin (TCI chemicals, Portland, OR), erythromycin, rifampicin, ampicillin, gentamicin, chloramphenicol and fetal bovine serum (FBS) were purchased from Sigma-Aldrich. DMEM media were purchased from Life technologies and MTS reagent (Promega, Madison, WI, USA).

In vitro antibacterial assays

Minimum inhibitory concentrations (MICs) were evaluated using micro dilution broth as per the standards of Clinical and Laboratory Standards Institute (CLSI) [300] . MICs of drugs were interpreted as the lowest concentration of the drug which inhibits the growth of bacteria after incubating for at least 16-24 h at 37 °C. The minimum bactericidal concentration (MBC) was determined by sub-culturing 10 µl from the wells were no growth was observed onto TSA plates. The plates were incubated for 24 h before the MBCs were determined. The MBC was categorized as the concentration where ⩾99.9 % reduction in bacterial cell count was observed [296] .

Intracellular infection assay

J774A.1 murine macrophage-like cells were seeded at a density of 20,000 cells per well in 96-well tissue culture plates. Cells were infected with MRSA USA300 (NRS 384-0114; ST-8) for 30 min at a 1:100 multiplicity of infection (MOI). Then the cells were

washed three times with DMEM medium containing 10 IU lysostaphin to kill the extracellular bacteria [221]. Drugs (vancomycin, linezolid and EB) were added at a concentration of 1 µg/ml to the DMEM medium supplemented with 10% FBS and 4 IU lysostaphin. After 24 h incubation, the cells were washed three times with phosphate buffered saline (PBS) and lysed with 0.1% Triton X-100. Lysates were diluted and plated on TSA plates and MRSA colony forming units (CFU) were counted.

Toxicity assay

The toxicity assays were performed in cell culture and *C. elegans*. (a) Cell culture:J774A.1 murine macrophage-like cells at a density of 20,000 cells per well were seeded and allowed to adhere in a 96-well tissue culture plate in DMEM media containing 10% FBS overnight. EB at various concentrations ranging from 0 to 256 µg/ml were added to the cells in DMEM media with FBS. After 24 h incubation with the drug, cells were washed with PBS and the MTS assay reagent,3-(4,5-dimethylthiazol-2-yl)-5-(3-carboxymethoxyphenyl)-2-(4-sulfophenyl)-2H tetrazolium) in DMEM medium was added and incubated for 4 h at 37 °C. Absorbance was measured at 490 nm using ELISA microplate reader (Molecular Devices, Sunnyvale, CA, USA). Cell viability after treatment with EB was expressed as a percentage of the control, DMSO. (b) *C. elegans*: Temperature-sensitive *C. elegans* AU37 (sek-1; glp-4) strain (glp-4(bn2) was used for toxicity studies and the worms were synchronized as described before [301]. Synchronized L4-stage worms were re-suspended in buffer containing 50% M9 buffer and 50% TSB. Then 100 µl of the buffer containing approximately 15-20 worms were deposited in each well in 96-well plates and EB (4 and 8 µg/ml) and vancomycin (8 µg/ml) were added. Worms were counted

daily for three days and the percent of live worms was calculated in each group. At least triplicate wells were used for each treatment

Cell-free bacterial and mammalian transcription/translation assay

The cell-free bacterial translation and mammalian translation assays were performed by the commercially available *Escherichia coli* S30 System and Rabbit Reticulocyte Lysate System (Promega), respectively. The assays were performed as described by the manufacturer, in conjunction with appropriate positive control (chloramphenicol) and negative control (ampicillin) antibiotics. In bacterial translation assay, the reaction mixtures were incubated at 37 °C for 1 h. Mammalian translation assay reaction mixtures were incubated at 30 °C for 1 h. Luciferase assay reagent was added to the reaction and the intensity of the luminescence was measured by luminescence microplate reader (FLx800 BioTek Instruments, Inc. Winooski, Vermont) according to the manufacturer's instructions. Average luciferase readout of protein production from two replicates from two independent experiments was calculated.

Mitochondrial biogenesis assay

The mitobiogenesis assay was done using In-Cell ELISA Kit (MitoSciences Inc., Eugene, OR) as per the manufactures instruction [302]. Briefly, J774A.1 cells were seeded (40,000 cells per well) in 96-well plates for overnight. EB and control antimicrobials (chloramphenicol and ampicillin) were added to the cells and the cells were allowed to grow for approximately 3 days with the drugs. Media were removed and cells were washed with PBS, then fixed with 4% paraformaldehyde. After fixing, cells were washed with PBS

and permeabilization and blocking processes were done according to the manufacturer's instructions. Primary antibodies to detect the levels of two proteins (subunit I of Complex IV (COX-I), which is mitochondrial DNA (mtDNA)-encoded, and the 70 kDa subunit of Complex II (SDH-A), which is nuclear DNA (nDNA)-encoded were added and incubated for overnight at 4 °C. After incubation, cells were washed with PBS and secondary antibodies were added and incubated at room temperature for 1 h. The expression of SDH-A and COX-1 were measured after washing and development at 405 nm and 600 nm wavelength, respectively. The ratio between COX-I and SDH-A was calculated and the percent of inhibition of mitochondrial biogenesis was measured.

Efficacy of EB in infected animal model (*C. elegans*)

L4-stage worms of *C. elegans* AU37 (sek-1; glp-4) strain (glp-4(bn2) were used to test the antimicrobial efficacy of EB as described before [301]. Briefly, worms were infected with MRSA USA300 (NRS 384-0114; ST-8) in nematode growth media plate for 8 h at room temperature. After 8 h of infection, worms were collected and washed with M9 buffer four times before incubation with the drugs. Worms were transferred to 96-well plates (20 worms per well) and the drugs (EB and vancomycin) were added to the wells in triplicates to achieve a final concentration of either 4 or 8 μg/ml. After 24 h incubation with the drugs, worms were transferred to 2-ml centrifuge tubes, washed four times with PBS and 100 mg 1.0-mm silicon carbide particles (Biospec Products, Bartlesville, OK) were added to each tube. The tubes were vortexed for one minute at maximum speed to disrupt the worms without affecting bacterial survival [301]. The resulting suspension was diluted and plated onto MSA plates to count the MRSA CFU. The total CFU obtained from each well was

divided by the number of worms in respective wells and the results were expressed as percent of bacterial reduction per worm.

Synergistic activities of EB with conventional antibiotics in vitro and in cell culture

(a) *In vitro synergistic assay:* The synergistic activities of EB with conventional antibiotics were evaluated using the Bliss Independence Model as described before [282]. Briefly, the optical density of the bacteria grown in the presence of antibiotics and EB (f_{AB}), antibiotics alone (f_{A0}), EB alone (f_{0B}) and in the absence of drugs (f_{00}) were measured and a degree of synergy (S) was calculated using the formula: $S = (f_{A0}/f_{00})(f_{0B}/f_{00})-(f_{AB}/f_{00})$. Positive and negative values represent the degree of synergism and antagonism, respectively. *(b) Intracellular synergistic assay in J774A.1 cells:* J774A.1 cells were seeded and infected as described before under intracellular infection assay. EB at concentration of 0.5 µg/ml was added to infected cells alone or in in combination with control antibiotics such as linezolid (4 µg/ml), clindamycin (1 µg/ml), vancomycin (4 µg/ml), chloramphenicol (4 µg/ml), erythromycin (8 µg/ml), rifampicin (0.5 µg/ml) and gentamicin (1 µg/ml). Untreated cells, and cells treated with antibiotics alone were used as a control. After 24 h incubation, the cells were lysed and intracellular MRSA CFU were determined as described above.. Percent bacterial reduction was calculated in relative to the untreated groups. Combination therapy was compared with single antibiotic therapy treatment groups.

Statistical analyses

Statistical analyses were done using Graph Pad Prism 6.0 (GraphPad Software, La Jolla, CA). *P* values were calculated by the one-tailed Student *t* test. *P* values of < 0.05 were considered as significant.

2.4.3 Results and Discussion

In vitro antibacterial assays

In an attempt to repurpose approved drugs as antimicrobial agents, we investigated the antimicrobial activity of EB against various multidrug-resistant clinical isolates of Gram-positive and Gram-negative pathogens (Table 2.5). EB exhibited potent bactericidal activity, in a nanogram range, against all tested Gram-positive strains regardless of their resistance phenotype. EB showed potent activity against clinical isolates of *Enterococcus faecalis* and *Enterococcus faecium* with MIC_{90} of 0.5 µg/ml (see Table 2.5). EB also showed potent activity against vancomycin-resistant strains of *Enterococcus* (VRE). Next, we tested the activity of EB against the clinical isolates of multidrug-resistant *S. aureus*. EB showed more potent activity against methicillin-sensitive *S. aureus,* MRSA, vancomycin-intermediate *S. aureus* (VISA) and vancomycin-resistant *S. aureus* (VRSA) strains than VRE with MIC_{90} of 0.25 µg/ml (see Table 2.5). Finally, EB also showed potent activity against clinical isolates of *Streptococcus pyogenes* and *Streptococcus agalactiae* with MIC of 0.5 µg/ml (see Table 2.5). On the other hand, EB did not show potent antimicrobial activity (MIC $\geq$16 µg/ml) against Gram-negative pathogens, including *Pseudomonas aeruginosa, Escherichia coli, Klebsiella pneumonia, Salmonella Typhimurium, and Acinetobacter baumannii*. The lack of activity of EB against Gram-

negative pathogens might be due to its reduced ability to enter the cells due to outer membrane barrier or the efflux pump rather than lack of target of EB inside Gram-negative bacteria [303-306].

Intracellular infection and cell toxicity

Some extracellular pathogens such as *S. aureus* are also capable of invading and surviving within the mammalian host cells, leading to persistent chronic infections. Moreover, during the *S. aureus* intracellular invasion phase, treatment with antimicrobials is very challenging because most antibiotics do not actively pass through cellular membranes [237-242]. Therefore, clinical failures of drug of choice, such as vancomycin, to cure *S. aureus* pneumonia have exceeded 40% and have been attributed mainly to poor intracellular penetration of the drug and consequently to the failure to kill intracellular MRSA in alveolar macrophages [307]. Hence, finding antimicrobials that possess both extra- and intracellular activity would be an optimum strategy to treat such invasive intracellular *S. aureus* infections. Therefore, we investigated if EB possesses intracellular anti-staphylococcal activity. As shown in Figure 2.22, EB at a concentration of 1 µg/ml significantly reduced the intracellular MRSA by 32%. In contrast, the conventional antimicrobials such as vancomycin and linezolid (drugs of last resort for treatment of Staphylococcal infections) at the same concentration reduced intracellular MRSA by only 16% and 21%, respectively. EB toxicity was assayed against J774A.1 cells at a concentration ranging from 0 to 256 µg/ml for 24 h. The results shown in Figure 2.23 indicate that EB does not show toxicity up to 64 µg/ml. The concentration of the EB that

Table 2.5 The MIC and MBC of EB against Gram-positive and Gram-negative bacteria

Strain ID	Phenotypic Characteristics	MIC/MBC (μg/ml)
E. faecalis ATCC49533	Resistant to streptomycin	0.25/8
E. faecalis ATCC7080	-	0.25/8
E. faecalis ATCC49532	Resistant to gentamicin	0.25/8
E. faecalis ATCC14506	-	0.5/8
E. faecalis ATCC 51229 (VRE)	Resistant to Vancomycin. Sensitive to Teichoplanin	0.5/0.5
E. faecalis SF24397	Resistance to erythromycin (ermB+) and gentamicin	0.125/4
E. faecalis SF24413 (VRE)	Resistant to erythromycin, gentamicin and vancomycin.	0.125/4
E. faecalis SF28073 (VRE)	Resistant to erythromycin, gentamicin and vancomycin	0.0625/8
E. faecalis HH22	Resistance to penicillin, erythromycin, tetracycline and high levels of aminoglycosides	0.125/4
E. faecalis MMH594	Resistance to erythromycin and gentamicin	0.125/4
E. faecalis SV587 (VRE)	Resistance to vancomycin	0.125/8
E. faecium E1162	Resistance to ampicillin.	0.25/16
E. faecium E0120 (VRE)	Resistant to gentamicin and vancomycin	0.5/32
E. faecium ERV102 (VRE)	Resistant to ampicillin and vancomycin, and displays high levels of resistance to streptomycin.	0.5/16
E. faecium ATCC6569	-	1/32
E. faecium ATCC 700221 (VRE)	Resistant to Vancomycin and Teicoplanin	0.5/1
MSSA (NRS 72)	Resistant to penicillin	0.25/0.5
MRSA (NRS 384)	Resistant to erythromycin, methicillin, and tetracycline	0.125/0.125
MRSA (NRS119)	Resistant to linezolid	0.125/0.25
MRSA (NRS 123)	Resistant to methicillin; susceptible to nonbeta-lactam antibiotics	0.25/0.5
MRSA (NRS194)	Resistant to methicillin	0.25/1
MRSA (NRS108)	Resistant to gentamicin	0.25/0.25
MRSA (NRS70)	Resistant to clindamycin, erythromycin and spectinomycin	0.25/0.25
VISA (NRS 1)	Resistant to aminoglycosides and tetracycline (minocycline)	0.125/0.125
VISA (NRS 19)	Glycopeptide-intermediate S. aureus	0.25/0.025
VRSA11a	Resistant to erythromycin and spectinomycin	0.125/0.25

Table 2.5 continued

VRSA11b	Resistant to erythromycin and spectinomycin	0.25/0.25
VRSA12	Resistant to vancomycin	0.25/0. 5
VRSA13	Resistant to vancomycin	0.25/0.25
Streptococcus pyogenes ATCC 12344	Quality control strain	0.5/1
Streptococcus agalactiae MNZ938	Beta-hemolytic, Serogroup: Group B	0.5/0.5
Streptococcus agalactiae MNZ 933	Beta-hemolytic, Serogroup: Group B	0.5/0.5
Streptococcus agalactiae MNZ 929	Beta-hemolytic, Serogroup: Group B	0.5/0.5
Acinetobacter baumannii ATCC BAA1605	Resistant to ceftazidime, gentamicin, ticarcillin, piperacillin, aztreonam, Cefepime, ciprofloxacin, imipenem, and meropemem	16/ND
E. coli O157:H7 ATCC 700728	-	32/ND
Salmonella enterica serovar Typhimurium ATCC 700720	-	32/ND
Klebsiella pneumonia ATCC BAA 2146	Clinical isolate New Delhi Metallo-β-Lactamase (NDM-1) positive	64/ND
Pseudomonas aeruginosa ATCC 9721	-	>256/ND

VRE: vancomycin-resistant Enterococcus; MSSA: methicillin-sensitive *S. aureus;* MRSA: methicillin-resistant *S. aureus;* VISA: vancomycin-intermediate *S. aureus;* VRSA: vancomycin-resistant *S. aureus;* ND: not determined

causes 50% toxicity (half inhibitory concentration: IC_{50}) in J774A.1 cells is 95.68 $\pm$ 4.12 µg/ml. This value is more than 380-fold higher than the concentration required to inhibit inhibit MRSA. Collectively, these results suggest that EB has great potential for treatment of *S. aureus* infections where not only is eradication of extracellular bacteria important, but the killing of intracellular bacteria is also critical [308].

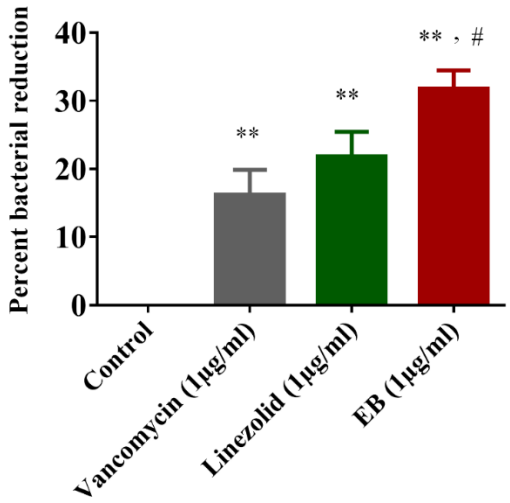

Figure 2.22 Activity of EB, vancomycin and linezolid against intracellular MRSA USA300 in J774A.1 cells. MRSA infected J774A.1 cells were treated with EB and control antibiotics (vancomycin and linezolid) for 24 h and the percent bacterial reduction was calculated compared to untreated control groups. The results are given as means ± SD (n=3). *P* values of (**, # ≤ 0.05) are considered as significant. EB was compared to controls (**) and to antibiotics (#).

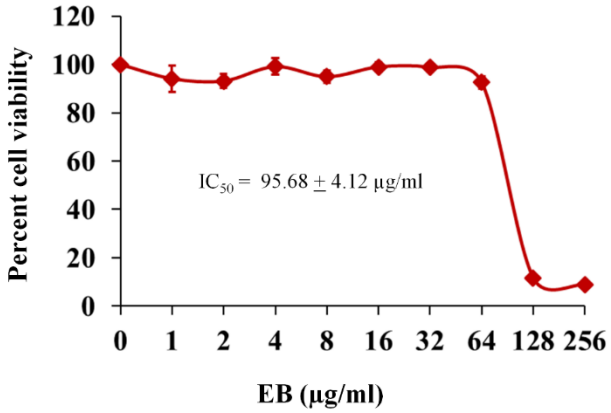

Figure 2.23 Cytotoxicity assay in murine macrophage-like cells (J774A.1) cells**.** J774A.1 cells were treated with different concentration of EB ranging from 0 to 256µg/ml. DMSO was used as a negative control. Cell viability was measured by MTS assay and IC_{50} of EB to cause cytotoxicity in J774A.1 cells was calculated.

Cell-free bacterial transcription/translation assay

Antimicrobials that target microbial protein synthesis such as oxazolidinones and lincomycins are considered excellent choices for the treatment of toxin-mediated bacterial infections caused by *S. aureus*, such as toxic shock syndrome (TSS) and pneumonia [232-235]. In addition to the suppression of *S. aureus* toxins such as Panton-Valentine leucocidin (PVL), α-hemolysin (hla), and toxic shock syndrome toxin–1 (TSST-1), these antimicrobials also reduce excessive host-inflammatory responses associated with these toxins [309,310]. Hence, protein synthesis inhibitors are often preferred in clinical practice for the treatment of toxin-associated staphylococcal infections [232-235]. We tested the effects of EB in our study on bacterial, mammalian and mitochondrial protein-synthesis. For bacterial protein-synthesis inhibition, we used *E. coli* cellular extracts in a transcription and translation assay that monitors protein production via luciferase readout. Unlike the antibiotic ampicillin that inhibits cell wall synthesis, EB strongly inhibited bacterial transcription/translation process similar to chloramphenicol antibiotic that inhibits protein synthesis (Figure 2.24a). EB inhibited bacterial protein synthesis in the cell-free transcription-translation, exhibiting IC_{50} of 0.25±0.10 µg/ml which is comparable to IC_{50} of chloramphenicol antibiotic 0.48 ± 0.10 µg/ml (Figure 2.24b). These results indicate that EB acts by a favorable mechanism of action and inhibits bacterial protein synthesis and, most likely, toxin production. However, inhibition of bacterial protein synthesis does not exclude other possible mechanism of action of EB.

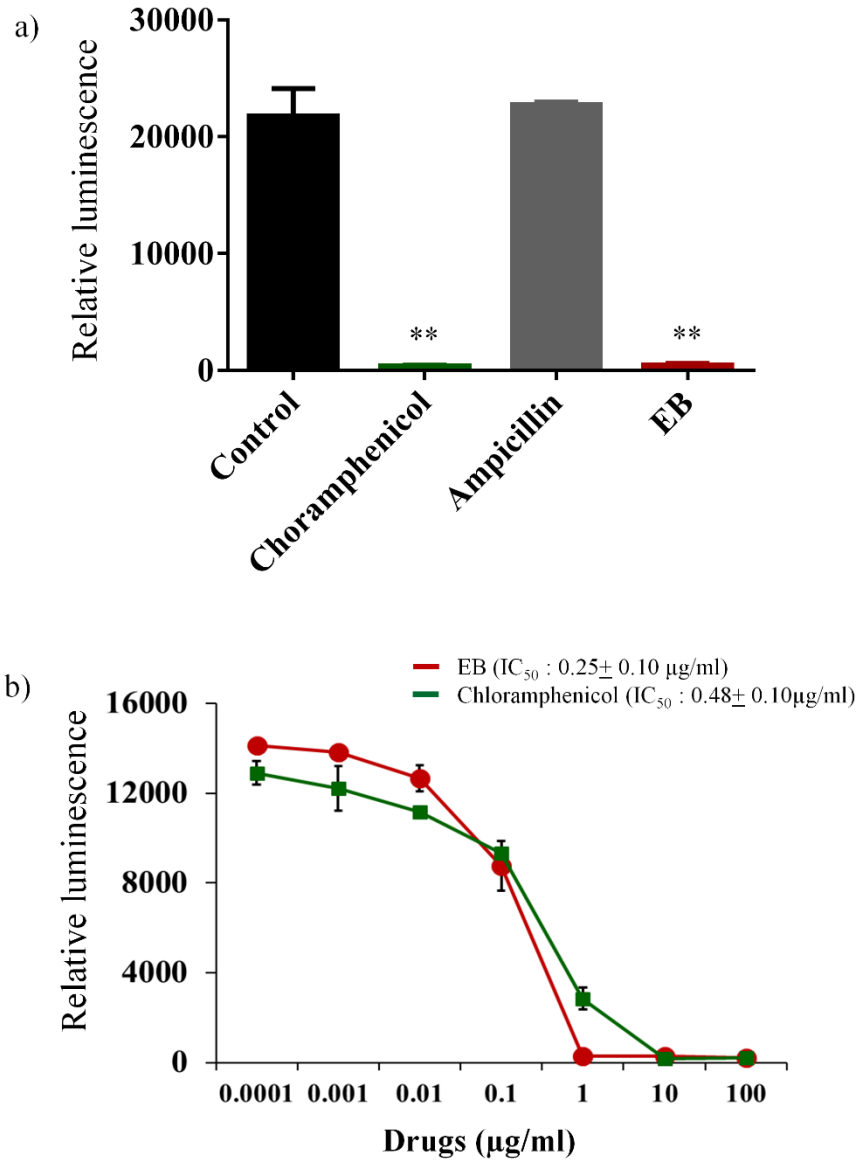

Figure 2.24 Effects of EB on coupled transcription-translation (TT) in S30 extracts from *E. coli*. (a) Average luciferin protein production in the presence of EB, ampicillin and chloramphenicol at the concentration of 2µg/ml were shown. The results are given as means ± SD (n = 3). (b) Concentration dependent TT-inhibition of EB and chloramphenicol were shown. IC_{50} of the drugs required to inhibit 50% TT-activity were determined. *P* values of (** ≤ 0.05) are considered as significant.

Cell-free mammalian transcription/translation assay and mitochondrial biogenesis

Due to concern about the possible mitochondrial toxicities associated with many antibacterial protein synthesis inhibitors such as linezolid and chloramphenicol [311-317], we tested the effect of EB on the inhibition of eukaryotic transcription/translation process using the rabbit reticulocyte lysate system with the cellular components necessary for mammalian protein synthesis [318,319]. As shown in Figure 2.25a, EB showed high safety profile with IC_{50} of mammalian protein synthesis of 166.09 $\pm$ 12.08 μg/ml. This value is more than 660-fold higher than the concentration required to inhibit protein synthesis in bacteria. However, in order to test the effect of EB more specifically on mitochondrial biogenesis and to confirm the above *in vitro* results obtained from rabbit reticulocyte lysate system, we measured the effect of EB on mitochondrial protein synthesis directly within the mammalian cells. In-cell ELISA was performed in J774A.1 cells treated with EB and chloramphenicol for three days to detect the levels of mtDNA-encoded COX-I and nDNA-encoded SDH-A proteins. Results shown in Figure 2.25b indicate that EB had no significant inhibition (less than 10%) of mitobiogenesis, similar to the effect of ampicillin, which does not interfere with mitochondrial protein synthesis process. At the same time, chloramphenicol had more than 60% inhibition of mitochondrial protein synthesis. These results provide valuable information about EB's safety profile and the lack of interference with mammalian protein synthesis and mitobiogenesis.

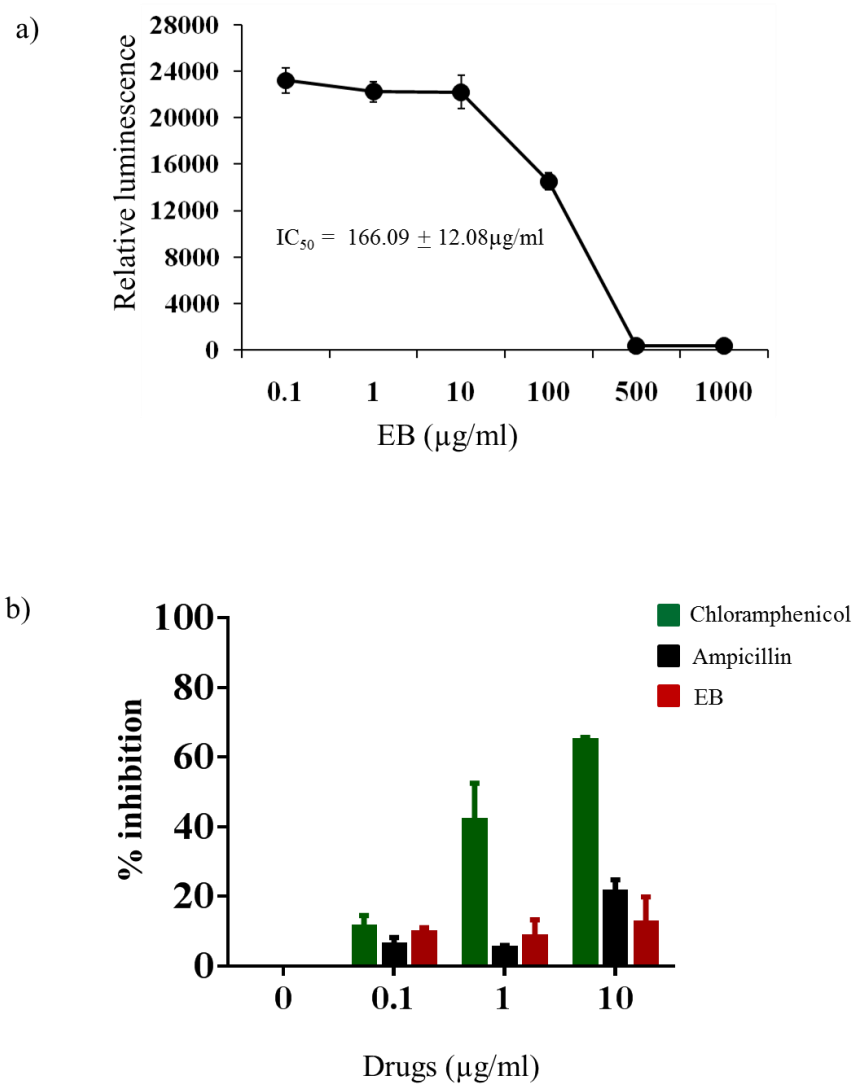

Figure 2.25 Effects of EB on mammalian protein synthesis. (a) Concentration dependent inhibition of protein synthesis were determined using rabbit reticulocyte lysate extract system. IC_{50} of the EB required to inhibit 50% translational activity were determined. (b) Effect of EB, chloramphenicol and ampicillin on mitobiogenesis. J774A.1 cell In cell-ELISA was carried out in the presence and absence of these drugs, and the levels of mitochondrial (mt)-DNA encoded protein (COX-I) and nuclear-DNA encoded protein (SDH-A) were quantified. Ratio of COX-I and SDH-A were calculated and the results were shown as percent inhibition of mitochondrial biogenesis.

Efficacy of EB in infected animal model (*C. elegans*)

To investigate if the potent *in vitro* antimicrobial activity of EB translates to antimicrobial efficacy *in vivo,* we tested antimicrobial efficacy of EB in an infected *C. elegans* whole animal model. A whole animal model, such as *C. elegans*, represents a great platform for drug discovery and enables simultaneous assessment of efficacy and toxicity of the tested drugs. Additionally, using a *C. elegans* model reduces the associated cost of drug discovery and lowers the burden for extensive animal testing [301,320]. Prior to testing the efficacy of treatment with EB in infected *C. elegans,* we tested toxicity of EB in non-infected *C. elegans*. As shown in Figure 2.26a, treatment of *C. elegans* with EB at 4 and 8 µg/ml for three days did not show any significant toxicity, similar to control groups. With no observable toxicity noticed in EB treated groups at a concentration of 4 and 8 µg/ml, we moved forward with an *in vivo* infection model using *C. elegans* infected with MRSA. As seen in Figure 2.26b, treatment with EB had a significant reduction in bacterial load when compared to untreated groups. EB at a concentration of 4 and 8 µg/ml significantly reduced the mean bacterial count by 56% and 85%, respectively. Moreover, treatment with EB at a concentration of 8 µg/ml showed comparable effect to treatment with the drug of last resort vancomycin in reducing MRSA burden in infected *C. elegans*. Taken together, these results show that EB exhibits potent *in vivo* antistapylococcal efficacy in MRSA-infected *C. elegans.*

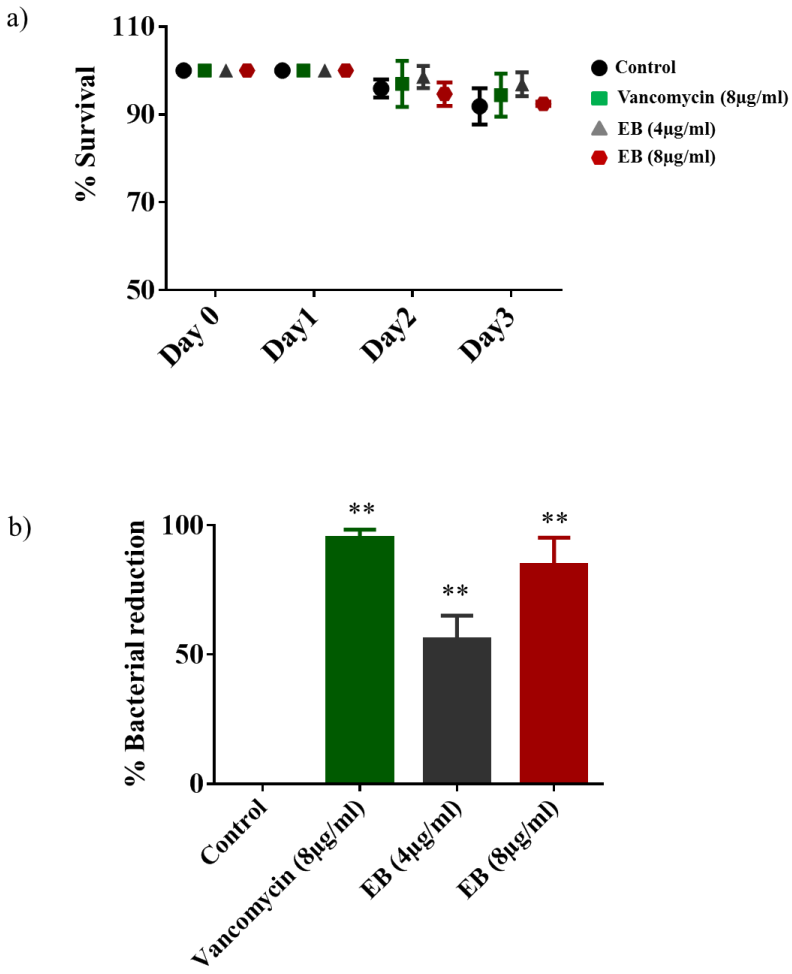

Figure 2.26 Evaluation of toxicity and antimicrobial efficacy of EB in *C. elegans* model. (a) *C. elegans* strain glp-4; sek-1 (L4-stage) were grown for three days in the presence of EB (4µg and 8 µg/ml) and vancomycin (8 µg/ml). Live worms were counted and the results were expressed as percent live worms in relative to the untreated control groups. (b) MRSA USA300 infected L4-stage worms were treated with EB (4µg and 8 µg/ml) and vancomycin (8 µg/ml) for 24 h. Worms were lysed and the CFU were counted and the percent bacterial reduction per worm in treated groups were calculated in relative to the untreated control groups. *P* values of (** ≤ 0.05) are considered as significant.

Synergistic activities of EB with conventional antibiotics in vitro and in cell culture

After confirming that EB has a potential use as an antibacterial agent for the treatment of infections caused by multidrug resistant pathogens, it was important to explore the synergistic relationship of EB with conventional antibiotics *in vitro* and in cell culture. With the rapid emergence of multidrug-resistant strains of *S. aureus*, monotherapy with single antibiotic has become less effective [244,245]. Therefore, alternative strategies such as combinational therapy have been used in the healthcare setting to improve the morbidity associated with MRSA infections and to reduce the likelihood of emergence of resistant strains [244,246,247,296]. To ascertain whether EB has the potential to be combined *in vitro* and in cell culture with conventional antimicrobials such as linezolid, clindamycin, vancomycin, chloramphenicol, erythromycin, rifampicin, and gentamicin against MRSA USA300, we used the *in vitro* Bliss independence model of synergism and infected cell culture assay [282]. *In vitro* results from the Bliss independence model of synergism are presented in Figure 2.27a. EB was found to exhibit a synergistic relationship with all tested conventional antimicrobials *in vitro* against MRSA USA300. Results of synergistic relationship of EB with conventional antimicrobials in infected cell culture against intracellular MRSA USA300 are presented in Figure 2.27b. Conventional antimicrobials (clindamycin, erythromycin, and rifampicin) showed synergistic activity when combined with EB and significantly reduced intracellular MRSA when compared to monotherapy. However, EB did not show synergistic activity with linezolid, vancomycin, chloramphenicol, or gentamicin in clearing intracellular MRSA. Identifying antibiotics that

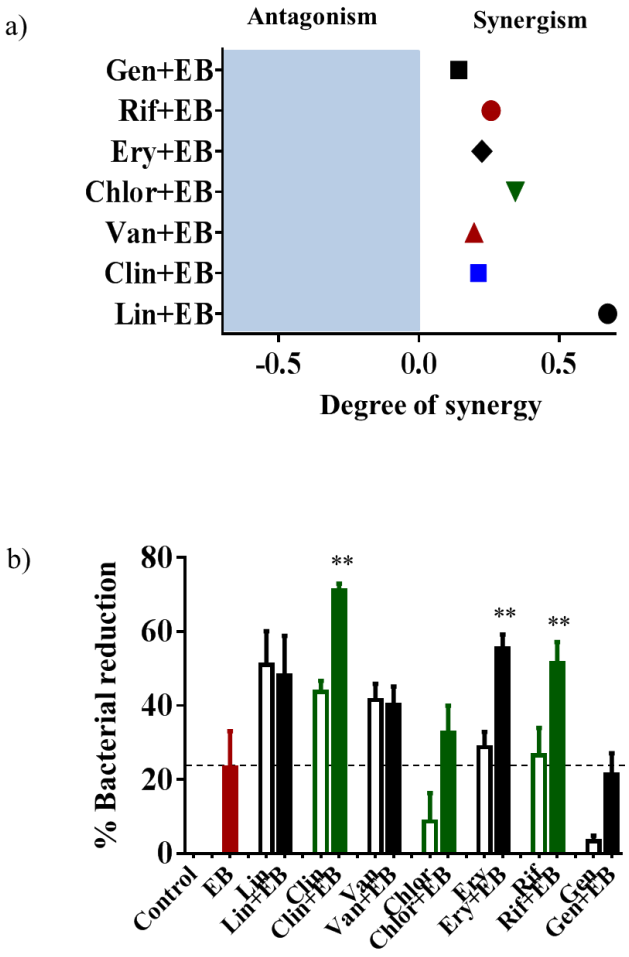

Figure 2.27 Synergistic activities of EB with conventional antibiotics in vitro and in cell culture. (a) The Bliss Model for Synergy confirms the in vitro synergism with conventional antimicrobials (gentamicin, rifampicin, erythromycin, chloramphenicol, vancomycin, clindamycin and linezolid) against MRSA USA300. Degree of synergy was calculated in the presence of EB (0.0312 µg/ml) in combination with sub-inhibitory concentrations of conventional antimicrobials. (b) Synergistic activity of EB with conventional antimicrobials in infected cell culture. Efficacy of EB (0.5µg/ml) in combination with linezolid (4µg/ml), clindamycin (1µg/ml), vancomycin (4µg/ml), chloramphenicol (4µg/ml), erythromycin (8µg/ml), rifampicin (0.5µg/ml) and gentamicin (1µg/ml) in clearing intracellular MRSA USA300 was determined in J774A.1 cells. Percent bacterial reduction was calculated in relative to the untreated groups. The results are given as means ± SD (n=3). Combination therapy was compared to monotherapy and the *P* values of (**, ≤ 0.05) are considered as significant.

can be synergistically paired with EB can potentially prolong the clinical utility of these antibiotics and reduce the likelihood of emergence of resistant strains.

In conclusion, we have successfully explored the potential applications of EB *in vitro*, in cell culture, and *in vivo* to combat multidrug-resistant Gram-positive pathogens, especially MRSA. We demonstrated that EB inhibits the bacterial translation process without affecting mitochondrial biogenesis. Additionally, we demonstrated the efficacy of EB *in vivo* in a *C. elegans* MRSA-infected model. Finally, we identified potential antibiotics that can be synergistically combined with EB to prolong the clinical utility of these antibiotics and reduce the likelihood of the emergence of resistant strains. Taken together, our study results demonstrate that EB, with its potent antimicrobial activity and safety profiles, might be a potential candidate drug for systemic and (or) topical applications to treat multidrug resistant Gram-positive bacterial infections alone or in combination with other antibiotics and should therefore be further clinically evaluated.

2.5 Exploring simvastatin, an antihyperlipidemic drug, as a potential topical antibacterial agent

(Thangamani S, Mohammad H, Abushahba MF, Hamed MI, Sobreira TJ, Hedrick VE, Paul LN, Seleem MN. Exploring simvastatin, an antihyperlipidemic drug, as a potential topical antibacterial agent. *Scientific Reports*. 2015 Nov 10;5:16407)

2.5.1 Introduction

The blockbuster statin drugs have revolutionized the treatment of cardiovascular disease, primarily by reducing low-density lipoprotein cholesterol (LDL-C) levels, leading to a decline in the morbidity and mortality associated with coronary artery diseases [1]. All statins drugs exert their effect by inhibiting the enzyme class I 3-hydroxy-3-methyl-glutaryl- Coenzyme A reductase (HMG-CoA) leading to decreased synthesis of cholesterol and increased removal of low-density lipoprotein (LDL) circulating in the body [2,3]. These drugs possess a good safety profile with limited side effects thus permitting their frequent use in reducing lipid levels in patients with high cholesterol levels [4,5]. In addition to their lipid-lowering effect, statins have been found to have potential use for other applications including influencing the host immune response via the drugs' anti-inflammatory and immune-modulatory properties [6]. Furthermore, multiple reports have investigated the potential role of statins in preventing and treating various infectious diseases and have demonstrated that statins can prevent the establishment of infections (by decreasing host cholesterol synthesis [7-9] limiting certain bacterial species'

ability to invade host cells) and potentially decrease the mortality rate attributed to bacterial infection [10-12]. Interestingly, several studies have shown that certain statins possess antimicrobial activity directly inhibiting growth of *Staphylococcus*, *Streptococcus*, *Enterococcus* and *Moraxella* spp. [13-17]. In addition, simvastatin and atorvastatin are capable of increasing the mycobactericidal effect of rifampicin[18]. However, limited information is available regarding the mechanism by which statins exert their antibacterial effect, statins' antimicrobial effect on Gram-negative pathogens, and potential applications for statins as novel antibacterial agents.

Given the tremendous pressure bacterial resistance to currently available antibiotics has placed on the healthcare system (with certain bacterial strains of *Staphylococcus aureus* and *Pseudomonas aeruginosa* exhibiting resistance to nearly every class of antibiotics), new antimicrobials are urgently needed to counter this significant public health challenge [19]. Repurposing existing drugs (initially approved for treatment of one clinical indication such as lowering cholesterol levels) that also possess antibacterial activity has the potential to expedite the process to discovering new antibacterial agents (given much of the rigorous safety, pharmacokinetic, and pharmacodynamic studies have already been conducted) [20]. Based upon preliminary studies performed to date, statins, in particular simvastatin, have potential to be repurposed as novel antibacterial agents. However additional research is required to understand statins' antibacterial spectrum of activity, their antibacterial mechanism of action, and to elucidate potential clinical applications in the management of bacterial infections. In this study, we aim to lay the foundation for utilizing statins as topical antibacterial agents by investigating the

antibacterial activity of statins and their spectrum of activity on clinically-relevant Gram-positive and Gram-negative pathogens, elucidating the antibacterial mode of action of the most active statin (simvastatin), examining the effect of simvastatin on specific virulence factors (such as bacterial toxins and disruption of staphylococcal biofilms) and finally to validate the therapeutic efficacy of simvastatin in an appropriate animal model of *S. aureus* infection. Our study reveals that simvastatin has considerable promise for use as a therapeutic agent to treat MRSA skin infections and does warrant further investigation as a novel topical antibacterial agent.

2.5.2 Materials and Methods

Bacterial strains and reagents

Bacterial strains used in this study are presented in Table 1 and Table 2. Mueller-Hinton broth (MHB), gentamicin and tetracycline were purchased from Sigma-Aldrich while mupirocin (Applichem), linezolid (Selleck Chemicals), and vancomycin hydrochloride (Gold Biotechnology) were acquired from other commercial vendors. Mannitol salt agar (MSA), Trypticase soy agar (TSA) and Trypticase soy broth (TSB) were purchased from Becton, Dickinson and Company (Cockeysville, MD). All statin drugs used in this study were purchased from Sigma-Aldrich (St. Louis, MO, USA), with the exception of pitavastatin and rosuvastatin which were obtained from Selleckchem (Houston, TX, USA).

Antibacterial assays

The antibacterial activity (MIC) of all test agents was examined using the broth microdilution method as per the guidelines outlined by the Clinical and Laboratory Standards Institute (CLSI)[55].

Gram-negative bacteria outer membrane permeabilization assay

The MIC of simvastatin and control antibiotics, in the presence of a sub-inhibitory concentration of colistin, against Gram-negative bacteria was evaluated as described in the antibacterial assay section above.

Macromolecular synthesis assay

The macromolecular synthesis assay was conducted as described elsewhere [56]. Briefly, *S. aureus* strain ATCC 29213 was grown in TSB, until it reached exponential phase (OD_{600} = 0.2 to 0.3), and then treated with different concentrations of simvastatin and control antibiotics (ciprofloxacin, rifampicin, linezolid, vancomycin and cerulenin). Bacterial cells treated with drugs were incubated at 37 °C for 30 min and the radio labeled precursors for DNA ([3H] thymidine (0.5μCi)), RNA ([3H] uridine (0.5μCi)), protein ([3H] leucine (1.0 μCi)), cell wall ([14C] N-acetylglucosamine (0.4 μCi)) and lipid synthesis ([3H] glycerol (0.5 μCi)) were added for each reaction. The incorporation of radiolabeled precursors was quantified and the results expressed as percent inhibition of each specific pathway examined.

Proteomics assay

An overnight culture of MRSA USA300 was treated with 10 × MIC of simvastatin for one hour at 37 °C. Bacterial cells were centrifuged and sequence grade Lys-C/Trypsin (Promega) was used to enzymatically digest samples. Samples were reduced and alkylated prior to digestion. All trypsin digestions were carried out in a Barocycler NEP2320 (PBI) at 50 °C under 20 kpsi for two hours. After digestion, samples were cleaned using MicroSpin C18 columns (Nest Group, Inc.) and the resulting pellets were re-suspended in 97% H_2O/3% ACN/0.1% FA. A small aliquot (5 µL) of sample was analyzed via nanoLC-MS/MS.

The WIFF files from MS analysis were processed using the MaxQuant computational proteomics platform version 1.5.2.8 (Cox and Mann, 2008). The peak list generated was screened against the *Staphylococcus aureus* (10972 entries reviewed) and *Bos taurus* (41521 entries unreviewed) sequence from UNIPROT retrieved on 04/10/2015, in addition to a common contaminants database. The following settings were used for MaxQuant: initial precursor and fragment mass tolerance set to 0.07 and 0.02 Da respectively, Minimum peptides length of seven amino-acid, data were analyzed with 'Label-free quantification' (LFQ) checked and the 'Match between runs' interval set to one min, the fasta databases were randomized and the protein FDR was set to 1%, enzyme trypsin allowing for two missed cleavages and three modifications per peptide, fixed modifications were carbamidomethyl (C), variable modifications were set to Acetyl (Protein N-term) and Oxidation (M).

The MaxQuant results were used in in-house script, and the average LFQ intensity values for the technical replicates were used for each sample. All the *Bos taurus* and

the common contaminant proteins were removed. All the values were transformed [$\log_2(x)$] and the missing values were inputted using the average values of all samples. The volcano plot and statistical analyses were performed in the R environment (www.cran.r-project.org). A t-test was performed on the LFQ intensity and only proteins with $P \leq 0.05$ were used for further analyses. A function-enrichment analysis of proteins was annotated using the Database for Annotation, Visualization and Integrated Discovery – DAVID [57]

Cell-free bacterial transcription/translation assay

The cell-free bacterial transcription/ translation assay was performed using *Escherichia coli* S30 System (Promega). The assay was carried out as per the manufacturer's instructions. Gentamicin was used as a positive control. Briefly, simvastatin and gentamicin were added at the indicated concentrations to the reaction mixtures and incubated at 37 °C for one hour. The intensity of luminescence was quantified using a standard FLx800 microplate reader (BioTek Instruments, Inc. Winooski, Vermont) after addition of the luciferase assay reagent.

Mitochondrial biogenesis assay

An In-Cell ELISA Kit (MitoSciences Inc., Eugene, OR) was employed to evaluate the effect of simvastatin and control antibiotics (tetracycline and vancomycin) on mitochondrial protein synthesis and the experiment was conducted as described previously [58]. The ratio between COX-I and SDH-A was calculated and the percent inhibition of mitochondrial protein synthesis was determined.

Measuring toxin production by ELISA

The effect of simvastatin and control antibiotics (linezolid and vancomycin) on production of two important *S. aureus* toxins (Hla and PVL) was measured utilizing ELISA as described elsewhere [56,59,60].

Mice infection

The animal care and all experiments were performed in accordance with the guidelines approved by Purdue University Animal Care and Use Committee (PACUC). The murine model of MRSA skin infection utilized in this study has been described previously [56]. Briefly, mice (eight week old female BALB/c mice, five mice per group) were injected intradermally with MRSA USA300 (1.65×10^8 CFU per mouse) and left for 48 h before an open wound formed at the injection site. Each group was subsequently treated with either 1% or 3% simvastatin or 2% mupirocin (using petroleum jelly as the vehicle) once a day for four days. Control group was treated with the vehicle alone. 24 h after the last treatment, the area around the wound was lightly swabbed with 70% ethanol and the wound (1 cm^2) was excised, homogenized, serially diluted, and plated on MSA. Plates were incubated at 37 °C for 18 hours before counting viable bacterial CFU.

Quantifying inflammatory cytokines by ELISA

Skin homogenates obtained from the mice skin infection procedure described above were centrifuged and the supernatants were assayed in order to measure the levels of three cytokines TNF-α, IL-6 and IL-1β by Duo-set ELISA Kits (R&D Systems, Inc.) The

quantification of cytokines and the experiment were carried out as per the manufacturer's instructions [56].

Biofilm assay

The effect of simvastatin and control antibiotics (vancomycin and linezolid) on disrupting established staphylococcal biofilm was evaluated using the microtiter dish biofilm formation assay [56]. Briefly, *S. aureus* (ATCC 6538) and *S. epidermidis* (ATCC 35984) were grown in TSB supplemented with 1% glucose in a 96-well tissue-culture treated plate. Bacteria were incubated at 37 °C for 24 h to permit the formation of an adherent biofilm. The medium was removed and washed with PBS. Drugs at indicated concentration were added and incubated again at 37 °C for 24 h. Plates were washed again and biofilms were stained with 0.1% (wt/vol) crystal violet. Plates were washed, air dried and biofilm mass was dissolved using 95% ethanol. The intensity of crystal violet was measured using a micro plate reader (Bio-Tek Instruments Inc.). Data are presented as the percent biofilm mass reduction in treated groups in relation to untreated wells.

Synergistic assay

Synergism was calculated using the Bliss independence model as described in previous reports [54,56]. Briefly, bacterial strains were incubated with a sub-inhibitory concentration of simvastatin and control antimicrobials for 12 h and the degree of synergy was calculated using the formula: $S = (f_{A0}/f_{00})(f_{0B}/f_{00})-(f_{AB}/f_{00})$, where f_{AB} refers to

bacterial growth rate in the presence of the combined drugs at concentration *A*, for one of the antibiotics, and *B* for the simvastatin; f_{A0} and f_{0B} refer to the bacterial growth rates in the presence of antibiotics (or) simvastatin at a concentration of *A* and *B*, respectively; f_{00} refers to the bacterial growth rate in the absence of drugs. Positive values correlate with synergistic behavior while negative values are indicative of an antagonistic interaction between the drugs.

ATP release assay

In order to determine if simvastatin and control antibiotics were capable of disrupting the MRSA cell membrane, MRSA USA300 cells were treated with 5 × MIC of simvastatin, tetracycline, or lysostaphin for one hour at 37°C. DMSO was used as a negative control. Bacteria were centrifuged and supernatants were analyzed using the Enliten ATP Assay System (Promega) per the manufacturer's instructions. Aliquots (10 µl) of supernatant were mixed with 75 µl of luciferase assay reagent and the intensity of luminescence was recorded using a microplate reader (FLx800 BioTek Instruments, Inc. Winooski, Vermont).

Electron Microscopy

An overnight culture of MRSA USA300 was diluted (OD_{600} = 0.3) and incubated with 5 × MIC of simvastatin before samples were subsequently collected at two time points (0 and 12 hours). Samples were centrifuged and the bacterial pellets were fixed with 2.5% buffered glutaraldehyde for one hour. Cells were next treated with 1% osmium tetroxide and 1% uranyl acetate. Further dehydration was done using ethanol and embedded in white

resin. The samples were stained with 1% uranyl acetate and lead citrate prior to viewing samples under a Philips CM-100 microscope

Statistical analyses

Statistical analyses were assessed using GraphPad Prism 6.0 (Graph Pad Software, La Jolla, CA). *P* values were calculated using the two-tailed Student *t* test. $P < 0.05$ was deemed significant.

2.5.3 Results

In vitro antibacterial assays

The antibacterial activity of eight statin drugs including simvastatin, atorvastatin, fluvastatin, lovastatin, mevastatin, pitavastatin, pravastatin and rosuvastatin were evaluated against two representative Gram-positive and Gram-negative bacterial pathogens (methicillin-resistant *Staphylococcus aureus* (MRSA) ATCC 4330 and *Pseudomonas aeruginosa* ATCC 15442 respectively) (see Table 2.6). Simvastatin was the only drug capable of inhibiting MRSA ATCC 4330 growth with a minimum inhibitory concentration (MIC) value of 32 µg/ml. Interestingly, none of the statin drugs examined possessed antibacterial activity against *P. aeruginosa* ATCC 15442 (MIC>1024 µg/ml), indicating simvastatin's effectiveness as an antibacterial activity may be restricted to Gram-positive pathogens.

Table 2.6 Screening statins for antibacterial activity

Statins/ Molecular formula	Pub Chem ID	M.wt	InChIKey	MRSA ATCC 4330 (µg/ml)	*P. aeruginosa* ATCC 15442 (µg/ml)
Simvastatin $C_{25}H_{38}O_5$	54454	418.56	RYMZZMVNJRMUDDHGQWONQESA-N	32	>1024
Atorvastatin $C_{33}H_{35}FN_2O_5$	60823	558.63	XUKUURHRXDUEBCKAYWLYCHSA-N	>1024	>1024
Fluvastatin $C_{24}H_{26}FNO_4$	446155	411.46	FJLGEFLZQAZZCDMCBHFWOFSA-N	>1024	>1024
Lovastatin $C_{24}H_{36}O_5$	53232	404.53	PCZOHLXUXFIOCFBXMDZJJMSA-N	>1024	>1024
Mevastatin $C_{23}H_{34}O_5$	64715	390.51	AJLFOPYRIVGYMJINTXDZFKSA-N	>1024	>1024
Pitavastatin $C_{25}H_{24}FNO_4$	5282452	421.46	VGYFMXBACGZSILMCBHFWOFSA-N	>1024	>1024
Pravastatin $C_{23}H_{36}O_7$	54687	424.52	TUZYXOIXSAXUGOPZAWKZKUSA-N	>1024	>1024
Rosuvastatin $C_{44}H_{54}CaF_2N_6O_{12}S_2$	5282455	1001.1	LALFOYNTGMUKGGBGRFNVSISA-L	>1024	>1024

Confirmation of simvastatin's antibacterial activity against MRSA ATCC 43300 led us to examine simvastatin's ability to inhibit growth of important multidrug-resistant strains of Gram-positive pathogens (Table 2.7). Simvastatin exhibited bacteriostatic activity against all methicillin-sensitive *S. aureus* (MSSA), MRSA, vancomycin-intermediate *S. aureus* (VISA), vancomycin-resistant *S. aureus* (VRSA), vancomycin-sensitive *Enterococcus*, vancomycin-resistant *Enterococcus* (VRE) and *Listeria monocytogenes* strains, inhibiting 90% of the strains (MIC_{90}) tested at a concentration of 32µg/ml. Simvastatin also inhibited growth of strains of *Streptococcus pneumoniae* and *Bacillus anthracis* with a MIC_{90} of 64 and 16 µg/ml respectively.

Table 2.7 MIC of simvastatin against a panel of Gram-positive bacteria

Bacteria (no. of strains screened)	Simvastatin (μg/ml)	
	MIC_{50}	MIC_{90}
Methicillin-resistant *S. aureus* (18)	32	32
Vancomycin-resistant *S. aureus* (15)	32	32
Methicillin-sensitive *S. aureus* (6)	32	32
Vancomycin-intermediate *S. aureus* (3)	32	32
Vancomycin-sensitive *Enterococcus* (9)	32	32
Vancomycin-resistant *Enterococcus* (7)	32	32
Listeria monocytogenes (6)	32	32
Streptococcus pneumoniae (2)	64	64
Bacillus anthracis (3)	16	16

The antimicrobial activity of simvastatin was next assessed against various Gram-negative pathogens (Table 2.8). Initial investigation indicated that simvastatin did not possess antibacterial activity against Gram-negative bacteria. However, when the outer membrane (OM) permeability in these bacteria was compromised using a sub-inhibitory concentration of colistin, simvastatin displayed antimicrobial activity against all tested strains of Gram-negative pathogens including *Acinetobacter baumannii, Escherichia coli, Salmonella Typhimurium, Klebsiella pneumoniae, and P. aeruginosa* with the MIC ranging from 8-32 μg/ml. The antibacterial activity of simvastatin was further investigated against *E. coli* SM1411Δ *acrAB*, a strain that is deficient in the multidrug-resistant AcrAB efflux pump. Simvastatin alone was not active against *E. coli* SM1411Δ *acrAB* (MIC>256 μg/ml). However simvastatin was able to inhibit growth of this strain when combined with colistin (the MIC was 16 μg/ml).

Table 2.8 MIC of simvastatin against a panel of Gram-negative bacteria

Bacterial strains	MIC of colistin	Sub-inhibitory concentration of colistin used	Simvastatin (μg/ml)		Erythromycin (μg/ml)		Fusidic acid (μg/ml)	
			colistin		colistin		colistin	
			(-)	(+)	(-)	(+)	(-)	(+)
Acinetobacter baumannii ATCC BAA19606	0.25	0.0625	>256	16	64	2	64	0.5
Acinetobacter baumannii ATCC BAA1605	0.25	0.0625	>256	16	64	2	128	1
Acinetobacter baumannii ATCC BAA747	0.25	0.0625	>256	16	64	2	128	1
Escherichia coli O157:H7 ATCC 700728	0.25	0.0625	>256	16	128	1	>256	4
Escherichia coli O157:H7 ATCC 35150	0.125	0.0625	>256	8	128	4	>256	4
Salmonella Typhimurium ATCC 700720	1	0.25	>256	16	256	0.5	>256	0.5
Klebsiella pneumoniae ATCC BAA 2146	0.25	0.125	>256	16	>256	0.125	>256	0.125
Klebsiella pneumoniae ATCC BAA 1705	0.25	0.125	>256	16	>256	8	>256	8
Pseudomonas aeruginosa ATCC 9721	0.5	0.25	>256	16	>256	2	>256	1
Pseudomonas aeruginosa ATCC 9027	0.5	0.25	>256	32	>256	0.5	>256	2
Pseudomonas aeruginosa ATCC 27853	0.5	0.25	>256	16	256	0.5	>256	0.5
Pseudomonas aeruginosa ATCC BAA-1744	0.25	0.125	>256	16	>256	1	>256	2
Pseudomonas aeruginosa ATCC 25619	0.125	0.0625	>256	16	256	2	>256	0.5
Pseudomonas aeruginosa ATCC 35032	0.5	0.25	>256	16	>256	1	>256	1
Pseudomonas aeruginosa ATCC 10145	0.25	0.125	>256	16	256	1	>256	2
Pseudomonas aeruginosa ATCC 15442	0.5	0.25	>256	16	>256	0.5	>256	1
Escherichia coli 1411	0.25	0.0625	>256	16	32	0.03	>256	0.03
Escherichia coli SM1411Δ *acrAB*	0.25	0.0625	>256	16	0.03	<0.03	8	<0.03

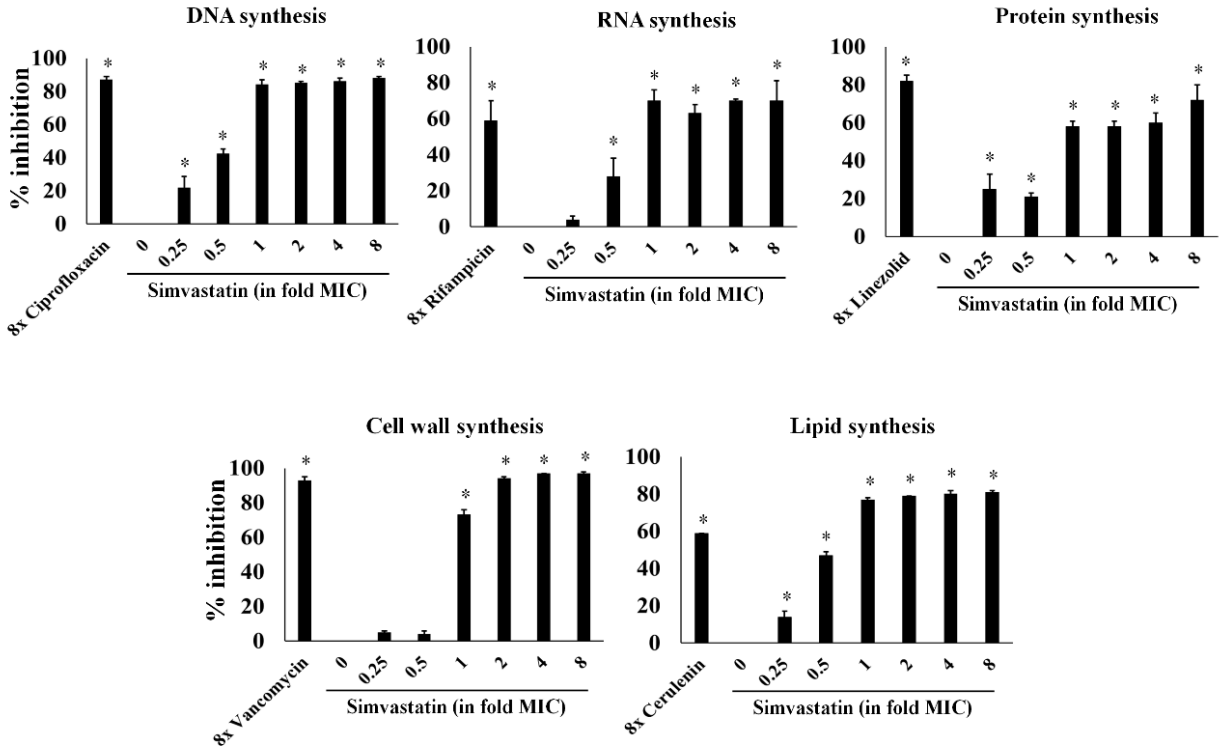

Figure 2.28 Macromolecular synthesis in the presence of simvastatin. Effect of simvastatin and control antimicrobials at indicated concentration (in fold MICs) on incorporation of radiolabeled precursors of DNA, RNA, protein, cell wall and lipid synthesis ([3H] thymidine, [3H] uridine, [3H] leucine, [14C] N-acetylglucosamine and [3H] glycerol, respectively) were quantified in *S. aureus* ATCC 29213. Results are expressed as percent of inhibition calculated based on the incorporation of each radiolabeled precursor. Statistical analyses were done using the two-tailed Student's't' test. *P* values of (* $\leq$ 0.05) are considered as significant.

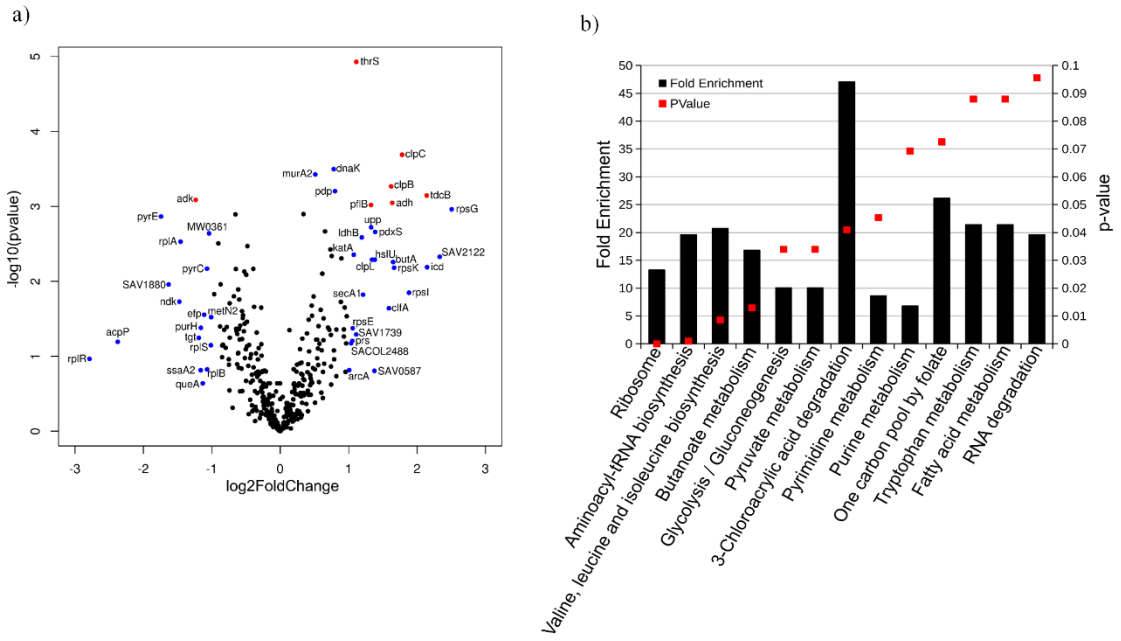

Figure 2.29 Quantitative proteome analysis of *S. aureus* cells treated with simvastatin reveals extensive protein degradation. (a) *S. aureus* treated with simvastatin in biological triplicates was analyzed for changes in the global proteome in relation to untreated controls, as shown in the volcano plot. The volcano plot depicts the *P*-values (-log10) versus gene ratio in the simvastatin- treated group (log2). Genes marked in blue indicate an absolute fold change higher than 1. The genes marked in red represent an adjusted *P*-value lower than 0.05 and an absolute fold change higher than 1.5. (b) Function–enrichment analysis of proteins degraded by simvastatin were annotated using Database for Annotation, Visualization and Integrated Discovery (DAVID). The overrepresented pathways are shown in columns and their *P*-values are represented by the red dots.

Simvastatin inhibits multiple macromolecular synthesis pathways

Simvastatin's antibacterial mechanism of action was investigated using a standard macromolecular synthesis inhibition assay in *S. aureus* ATCC 29213. As shown in Figure 2.28, DNA, protein and lipid synthesis were significantly inhibited at concentrations

below the drug's MIC (0.25×). In addition, simvastatin also significantly inhibited RNA synthesis at 0.5× MIC. Inhibition of cell wall synthesis was observed only at the MIC.

Simvastatin causes extensive protein degradation and disrupts cellular homeostasis

In order to gain additional insight into the different cellular pathways regulated by simvastatin, proteomic profiling was employed to investigate the response of bacteria to simvastatin [21-23]. The alterations in the proteome caused by treatment with simvastatin were compared to an untreated control group. The proteomic analysis identified 521 proteins with 85 proteins that were significantly differentially expressed ($P \leq 0.05$) in the simvastatin treatment group as compared to the control group (Figure 2.29a). The seven proteins marked in red have an adjusted P-value lower than 0.05 and absolute fold change higher than 1.5. An important protein that is regulated is adenylate kinase (adk) which is involved in the interconversion of ADP to AMP and ATP and helps to maintain the adenine nucleotide balance within cells [24]. From the six upregulated proteins, three are ATP-dependent enzymes; clpC (ATP- dependent Clp protease), clpB (chaperone protein ClpB) and thrS (threonine-tRNA ligase). The Clp proteases and chaperon proteins are central components in bacteria necessary to help mount an appropriate stress response to cope with adverse conditions experienced inside the host [25,26].

The function-enrichment analysis found eight pathways showed a significant ($P \leq 0.05$) fold enrichment ranging from 8.6 to 47 (Figure 2.29b). From these pathways, the

proteins involved in pyrimidine metabolism, valine, leucine and isoleucine biosynthesis and aminoacyl- tRNA biosynthesis were significantly downregulated (average $\log_2$ fold change: -1.42, -0.29 and -0.11 respectively). On the other hand, the proteome involved in 3-chloroacrylic acid degradation, butanoate metabolism, glycolysis/gluconeogenesis, pyruvate metabolism and the proteins that bind to one or more ribosomal subunits were significantly upregulated (average $\log_2$ fold change:1.98, 1.26, 1.26, 0.82 and 0.61 respectively). Thus the proteomic analysis suggests that simvastatin treatment leads to an extensive degradation of different proteins involved in various essential cellular pathways resulting in dysregulation of cellular homeostasis and ultimately leading to arrest of bacterial growth.

Simvastatin inhibits bacterial but not mammalian protein synthesis

In order to confirm simvastatin is a potent, selective inhibitor of bacterial protein synthesis, its activity against both bacterial and mammalian mitochondrial protein synthesis was assessed. An *E. coli* S30 coupled transcription and translation assay was performed to determine the concentration of simvastatin required to inhibit 50% of the bacterial translational process (IC_{50}). As presented in Figure 2.30a, the IC_{50} of simvastatin was found to be 18.85 ± 0.95 µg/ml. The effect of simvastatin on mammalian mitochondrial protein synthesis was subsequently evaluated in J774A.1 cells.

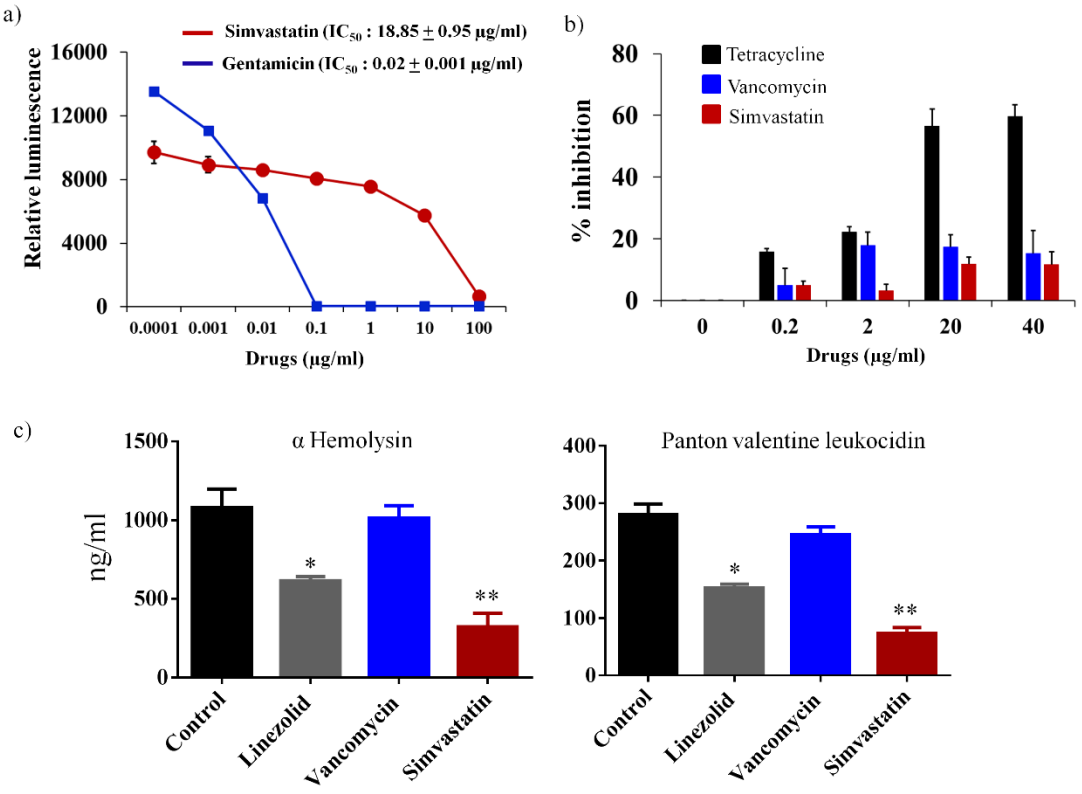

Figure 2.30 Simvastatin inhibits bacterial protein synthesis and toxin production. (a) Transcription- translation (TT) assay was carried out using S30 extracts from *E. coli*. IC_{50} of simvastatin and gentamicin required to inhibit 50% TT-activity in bacteria were determined. (b) Effect of simvastatin, vancomycin and tetracycline on mammalian mitobiogenesis was assessed via In cell- ELISA. J774A.1 cells were treated with indicated concentration of drugs and the levels of mitochondrial (mt)-DNA encoded protein (COX-I) and nuclear-DNA encoded protein (SDH-A) were quantified. The ratio of COX-I and SDH-A was calculated and the results shown are percent inhibition of mitochondrial biogenesis. (c) Effect of simvastatin on *S. aureus* toxin production. MRSA USA300 was treated with drugs for one hour and toxin production (ng/ml) (corrected for organism burden) was measured by ELISA. The results are given as means ± SD (n = 3). *P* values of (* $P \leq 0.05$) (** $P \leq 0.01$) are considered as significant in comparison to control groups.

The change in expression level of subunit I of Complex IV (COX-I), which is mitochondrial DNA (mtDNA)-encoded, and the 70 kDa subunit of Complex II (SDH-A), which is nuclear DNA (nDNA)-encoded proteins, after treatment with simvastatin and control antibiotics (tetracycline and vancomycin) was measured by In-cell ELISA. As presented in Figure 2.30B, simvastatin (40 µg/ml), similar to vancomycin (40 µg/ml), has a very minimal effect (less than 15% inhibition observed) on inhibition of mitochondrial protein synthesis (Figure 6.3b). In contrast, the positive control antibiotic, tetracycline, inhibited more than 50% of mitochondrial protein synthesis, at a concentration of 40 µg/ml (Figure 2.30b).

Simvastatin inhibits *S. aureus* toxin production

In view of results demonstrating the specific effect of simvastatin on bacterial protein synthesis inhibition, its effect on production of *S. aureus* toxins such as Panton-Valentine leucocidin (PVL) and α-hemolysin (Hla) was investigated using ELISA. Simvastatin significantly suppressed two key toxins (PVL and Hla) produced by MRSA USA300 when compared to the control group. This mimics the results obtained with linezolid (an antibiotic that inhibits protein synthesis) which also significantly suppressed production of both PVL and Hla by MRSA USA300 (Figure 2.30c).

Simvastatin effectively reduces pre-formed staphylococcal biofilms

Given the challenge associated with bacterial biofilms and their role in promoting recurring infection in hosts, we next moved to investigate the effect of simvastatin on

disrupting established biofilms caused by *S. aureus* and *S. epidermidis*. Utilizing the microtiter dish biofilm formation assay, simvastatin was found to be capable of significantly reducing the adherent biofilms of both *S. aureus* and *S. epidermidis* when compared to conventional antibiotics (linezolid and vancomycin) (Figure 6.4). Simvastatin, at 2 × MIC and 4 × MIC, significantly reduced *S. aureus* and *S. epidermidis* biofilm mass by approximately 40%. Contrary to simvastatin, the control antibiotics (linezolid and vancomycin) even at 64 × MIC and 128 × MIC were only able to reduce the biofilm mass of both *S. aureus* and *S. epidermidis* by 10% (Figure 2.31).

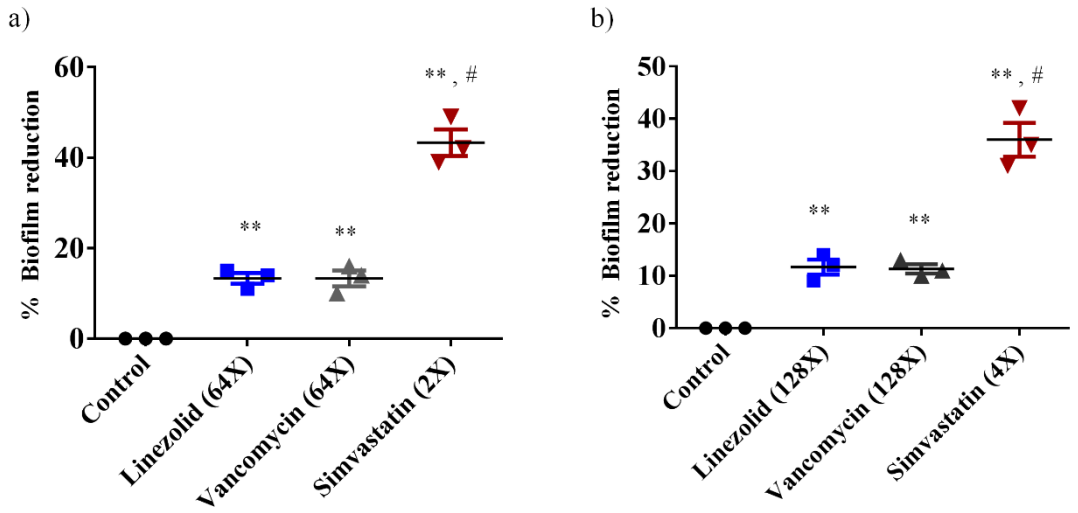

Figure 2.31 The effects of simvastatin and antibiotics (linezolid and vancomycin) on established biofilms of *S. aureus* (a) or *S. epidermidis* (b) were evaluated. The pre-formed biofilms were treated with control antibiotics or simvastatin and then stained with crystal violet. The optical density of the dissolved crystal violet was measured using a spectrophotometer. Values are the mean of triplicate samples with standard deviation bars. *P* values of (*, # $P \leq 0.05$) are considered as significant. (*) indicates simvastatin was compared to control and (#) to control antibiotics.

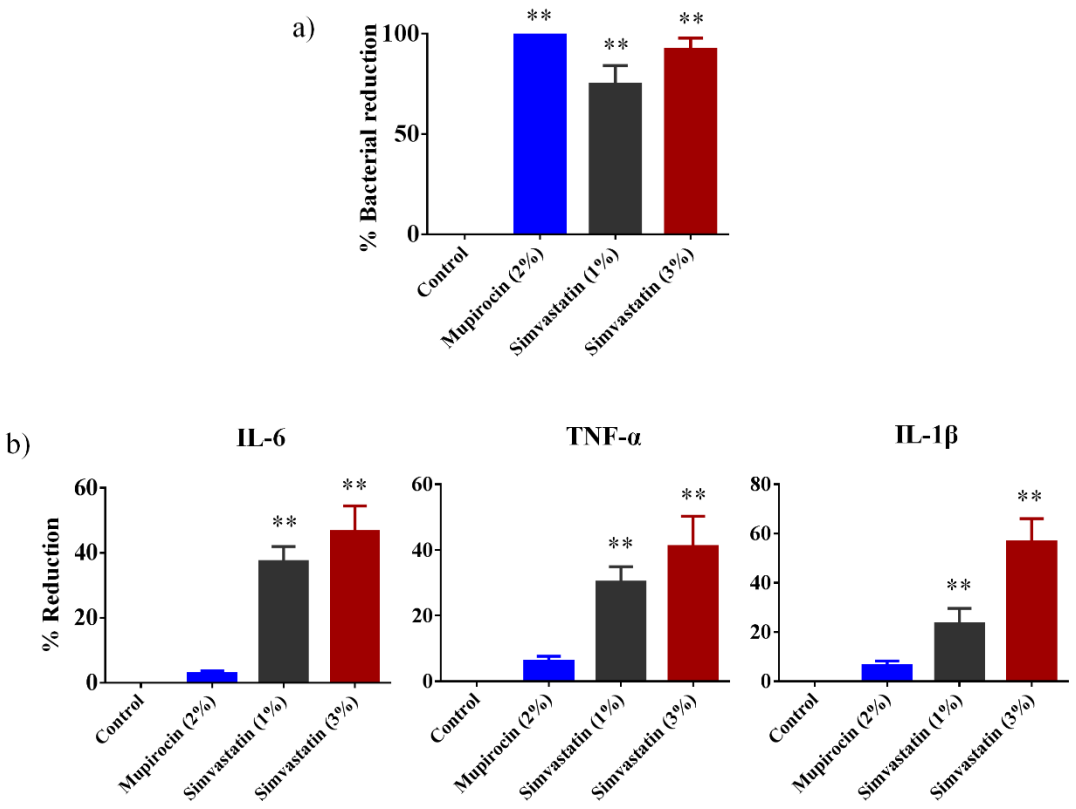

Figure 2.32 Antibacterial and anti-inflammatory activities of simvastatin in a mouse model of MRSA skin infection. (a) Efficacy of treatment of MRSA skin lesions with simvastatin (1 and 3%), mupirocin (2%) and petroleum jelly (negative control) once daily for four days. Percent bacterial reduction was calculated and shown in the figure. Statistical analysis was performed via the two- tailed Student *t* test. *P* values of (** $P \leq 0.01$) are considered as significant. (b) Effect of simvastatin on cytokines production in supernatants from skin homogenates of MRSA skin lesions. Percent reduction in inflammatory cytokines was calculated. Statistical analysis was performed via the two-tailed Student *t* test. *P* values of (** $P \leq 0.01$) are considered as significant.

Simvastatin is effective in reducing bacterial load in a mouse model of MRSA skin infection

Four groups of MRSA-infected mice were treated topically either with simvastatin (1% or 3%), a control antibiotic (2% mupirocin), or the vehicle alone (petroleum jelly) once a day for four days. As shown in Figure 2.32a, all treatment groups significantly reduced the mean bacterial counts compared with the control group ($P \leq 0.01$). Topical treatment with 1 and 3% simvastatin significantly reduced the MRSA load in infected skin wounds by 75 and 90% respectively. Mupirocin (2%) produced a 99% reduction in mean bacterial count as compared to the untreated group.

Simvastatin reduces inflammatory cytokines induced by MRSA skin infection

The immune-modulatory activity of simvastatin against MRSA skin infection was evaluated by measuring levels of pro-inflammatory cytokines produced during infection including tumor necrosis factor-α (TNF-α), interleukin-6 (IL-6) and interleukin-1 beta (IL-1β) in the MRSA infected wounds of mice from the skin infection experiment described above. As shown in Figure 2.32b, topical application of simvastatin (1 and 3%) significantly reduced all tested inflammatory cytokines. Simvastatin-treated (3%) group reduced production of all three cytokines examined (IL-6, TNF-α and IL-1β). Topical application of 1% simvastatin also decreased production of inflammatory cytokines in the MRSA infected wound lesions by 20%. However, mice treated with mupirocin (2%) did not show a significant reduction in the levels of all the tested inflammatory cytokines when compared to the control group.

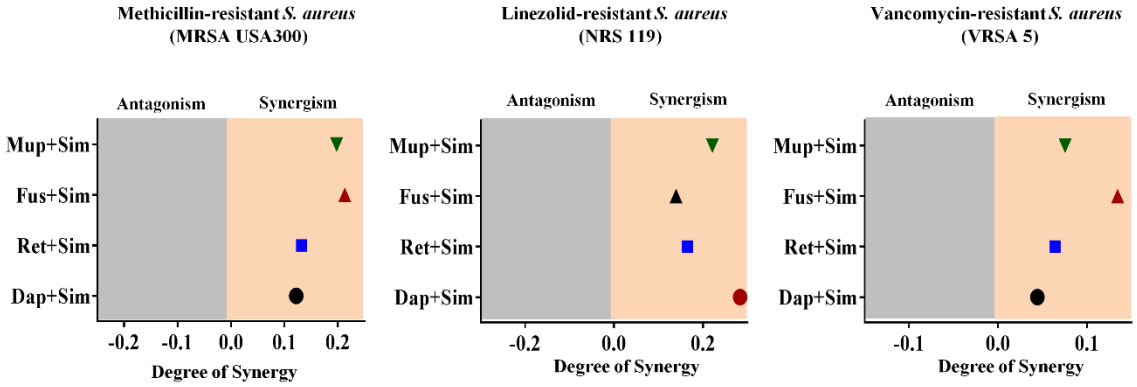

Figure 2.33 Synergistic activity of simvastatin with topical antimicrobials. The Bliss independence model confirms a synergistic relationship between simvastatin and four topical antimicrobials (mupirocin, fusidic acid, retapamulin and daptomycin) against various clinical isolates of multidrug-resistant strains of *S. aureus*. The positive and negative values along the x-axis represent the degree of synergism and antagonism respectively.

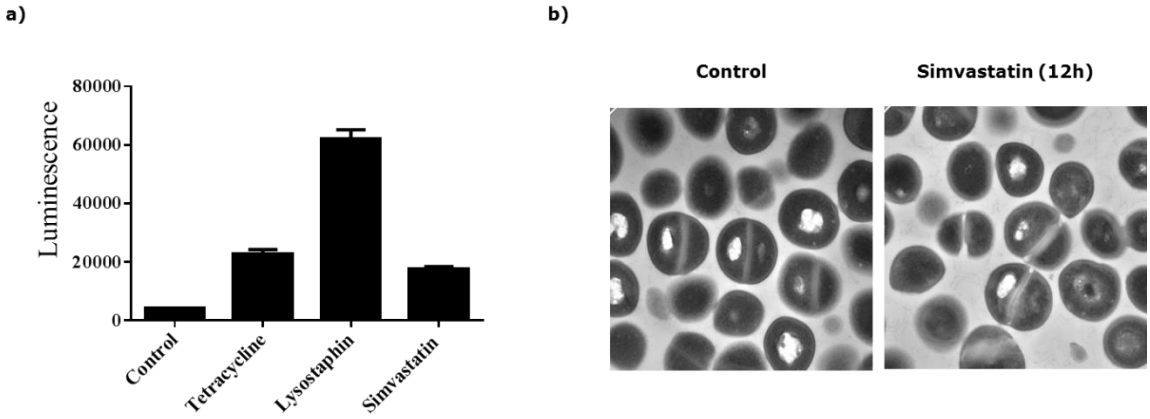

Figure 2.34 Simvastatin does not disrupt the cell membrane of *S. aureus*. (A) MRSA USA300 cells were treated with 5 × MIC of simvastatin, tetracycline or lysostaphin and the level of ATP was measured in the supernatant for each treatment condition . (B) Transmission electron microscopy (TEM) images of untreated and simvastatin (5 × MIC) treated MRSA USA300 cells at the indicated time points, in hours (h), are shown.

Simvastatin exhibits synergistic activity with conventional topical antimicrobials

Combination therapy employing two or more antibiotics together has been utilized for treating skin wounds and infections in the healthcare setting. Given simvastatin exhibited good antibacterial activity against MRSA both *in vitro* and *in vivo*, we examined the possibility of using simvastatin with antimicrobials commonly used to treat skin infections. The antimicrobial activity of simvastatin in combination with four topical antimicrobials (fusidic acid, mupirocin, daptomycin, and retapamulin) was investigated *in vitro* using the Bliss independence model of synergism against three *S. aureus* clinical isolates. As shown in Figure 2.33, simvastatin demonstrated a synergistic relationship with all tested topical antibiotics against *S. aureus* clinical isolates.

2.5.4 Discussion

Antibiotics have long been key allies in the treatment of bacterial infections. However, the emergence of pathogens (in particular MRSA) exhibiting resistance to many antimicrobial classes including to therapeutic agents of last resort, such as vancomycin and linezolid, presents an ominous premonition that our current arsenal of antibiotics will no longer be effective in the near future [27-29]. Thus there is an urgent need to drive research efforts to discover new antimicrobials in order to circumvent this burgeoning health challenge. The conventional strategies used to develop new drugs are highly unlikely to keep pace with acquired resistance by bacterial pathogens and often comes at a significant financial risk to pharmaceutical companies (the success rate of receiving regulatory approval for a new antibiotic varies between 1.5 – 3.5% even after investing nearly one billion dollars in research and development costs)

[30] . Though government regulatory agencies have attempted to provide incentives to encourage pharmaceutical companies to re-enter the arena of antibacterial drug discovery, such as the U.S. Food and Drug Administration's "reboot" pledge, it will take many years for these incentives to translate into the discovery of new antibiotics (using conventional methods of screening compound libraries for lead hits) [31]. An alternative strategy that has promise to expedite the discovery and approval process is repurposing old drugs, such as statins that have already passed rigorous safety assessments, as novel antibacterial agents to combat multidrug-resistant pathogens [32].

Statins, widely used to control hyperlipidemia, are known to exhibit antimicrobial properties [13-17]. We investigated the antibacterial activity of eight statin drugs including simvastatin, atorvastatin, fluvastatin, lovastatin, mevastatin, pitavastatin, pravastatin and rosuvastatin against a representative Gram-positive and Gram-negative bacterial species (methicillin-resistant *S. aureus* ATCC 4330 and *P. aeruginosa* ATCC 15442). Our results correlate with previous reports that have found that only simvastatin exhibits antibacterial activity against Gram-positive bacteria [17]. However its activity against Gram-negative bacteria was previously unknown. Our initial investigation indicated that simvastatin lacks antibacterial activity against the Gram-negative pathogen *P. aeruginosa*. However, further analysis revealed that the outer membrane in Gram-negative bacteria acts as an intrinsic barrier for simvastatin to gain entry into Gram-negative bacteria. When the OM is compromised using a sub-inhibitory concentration of colistin, simvastatin exhibits antibacterial activity against many clinically-pertinent Gram- negative pathogens including *A. baumannii*, *E. coli*, *S.*

Typhimurium, K. pneumoniae, and P. aeruginosa.. The enhanced antimicrobial activity of simvastatin in comparison to other statin drugs may be related to differences in their chemical characteristics, as described previously [14,17]. However, further structure-activity relationship studies need to be performed to confirm the structural elements in simvastatin that contribute to its antimicrobial properties. This will permit rational modifications to be made to the drug's structure in order to potentially enhance its potency against bacterial pathogens and mitigate potential toxicity issues to host tissues.

In view of the broad-spectrum activity of simvastatin, its antibacterial mode of action was investigated. Simvastatin exerts its antihyperlipidemic effect in humans by inhibiting the enzyme class I HMG-CoA reductase present in the mevalonate pathway [2,3]. We hypothesized that the mechanism of action (MOA) of simvastatin in *S. aureus* differs from the MOA in humans due to the absence of the class I HMG-CoA reductase enzyme in *S. aureus* [33]. In order to confirm this hypothesis, we tested the activity of simvastatin on *S. aureus* cultures supplemented with mevalonate. As expected, mevalonate supplementation (0.1 and 1 mM) did not diminish simvastatin's antibacterial activity against *S. aureus* (data not shown). This clearly indicates that the MOA of simvastatin differs between *S. aureus* and humans. In order to further explore the MOA of simvastatin on *S. aureus*, a macromolecular synthesis assay was performed. Treatment of *S. aureus* cells with a subinhibitory concentration of simvastatin resulted in the suppression of multiple biosynthetic pathways including DNA, protein, lipid and RNA synthesis indicating that simvastatin might have a complex mechanism of action involving multiple targets. Additionally, the impact of simvastatin on multiple

biosynthetic pathways might be due to dysregulation in pathways involved in general cellular homeostasis and energy metabolism such as glycolysis, pyruvate metabolism and butanoate metabolism as observed in the proteomic profiling. In order to ascertain whether cell membrane damage is the cause for inhibition of multiple macromolecular synthesis pathways, as noticed in antimicrobial peptides such as lactoferricin B and pleurocidin-derived peptides [34,35], we performed an ATP release assay. Our results strongly suggest that simvastatin does not physically damage the bacterial cell membrane as was validated using transmission electron microscopy (Figure 2.34). Finally, in an attempt to determine the exact molecular target of simvastatin, *S. aureus* was serially passaged for two weeks in the presence of simvastatin. Though *S. aureus* mutants that were resistant to simvastatin were generated, whole genome sequencing indicated that these mutants were not stable. This result provides indirect evidence that multiple targets might be a reason for the inability to form stable mutants resistant to simvastatin (data not shown). Future studies are needed to elucidate the exact molecular target(s) of simvastatin by which it exerts its antibacterial activity.

The macromolecular synthesis assay revealed that simvastatin inhibits bacterial protein synthesis which raises an important question; is this action specific or can simvastatin also inhibit protein synthesis in mammalian cells? Multiple antibacterials that inhibit bacterial protein synthesis (including tetracycline, linezolid and chloramphenicol) are non- selective and result in toxicity to the mitochondria in mammalian cells (given the similarity between the ribosomal subunits involved in protein synthesis in bacterial and human cells) [36,37]. When simvastatin's ability to inhibit protein synthesis was further examined it was found that, unlike tetracycline

which had a profound impact on inhibiting mitochondrial protein synthesis, simvastatin was a selective inhibitor of bacterial protein synthesis. The discovery led us to examine if this effect on protein synthesis inhibition would lead to suppression in the production of key toxins by *S. aureus*. Utilizing ELISA, we found that simvastatin is capable of inhibiting production of both PVL and αHla, two pore-forming cytotoxins that injure host immune cells and promote infection of host tissues [38].

Confirmation of simvastatin's broad spectrum antimicrobial activity *in vitro* led us to proceed forward with an *in vivo* experiment in a mouse model of MRSA infection. However, given simvastatin's high MIC value cannot be achieved systemically, this limits the application of this drug to being used as a topical agent [39]. Due to the fact that *S. aureus* causes the vast majority of skin infections in humans and there is a demand for topical antimicrobial agents to treat these infections (given increasing resistance to first-line agents such as mupirocin), there is great potential for using simvastatin to treat/prevent bacterial infections in wounds [40,41]. Therefore we assessed the effectiveness of simvastatin as a topical antibacterial in a MRSA skin infection mouse model. Simvastatin, both at 1% and 3%, significantly reduced the mean MRSA counts compared with the control group ($P \leq 0.01$), producing a 90% reduction in bacterial burden at the higher concentration. Thus, this skin infection study appears to strongly suggest that simvastatin has potential use as a topical antimicrobial for treatment of MRSA skin infections.

The clinical severity of *S. aureus*-based skin infections is driven in large part by production of excess host pro-inflammatory cytokines more so than by bacterial

burden[42,43]. As simvastatin has known anti-inflammatory properties, it should be superior to traditional antibiotics for treatment of skin infection (as it should hypothetically suppress production of inflammatory cytokines) [44]. To confirm this, we measured the levels of three inflammatory cytokines in the supernatant of homogenized skin tissues obtained from the MRSA murine skin infection experiment described above. As predicted, topical treatment with simvastatin, both at 1 and 3%, significantly reduced production of three inflammatory cytokines (IL-1β, IL-6 and TNF-α); the suppression of these cytokines may contribute to enhanced healing of infected wounds[45,46]. Prolonged inflammation, especially due to the presence of inflammatory cytokines such as TNF-α and IL-6, delays healing in chronic infected wounds [47]. Simvastatin significantly ($P \leq 0.01$) inhibits both cytokines (TNF-α and IL-6), which should provide a favorable outcome in wound healing [47]. Additionally, simvastatin has been shown to play a beneficial role in the healing process of diabetic and infected wounds by enhancing the formation of new blood and lymphatic vessels and increasing the formation of new tissue; these three effects undoubtedly confer an added advantage for using simvastatin to treat bacterial skin infections [48,49] Recurring infection in skin wounds can persist and impair wound healing due to the presence of complex microbial communities called biofilms. Bacterial biofilms, contribute significantly to the treatment failure of staph infections, due to hindering penetration of antibacterial drugs [50]. Simvastatin has been previously reported to exhibit anti-biofilm activity as it inhibited both growing and mature biofilms of *Candida* spp. and

Cryptococcus spp [51,52]. Thus we decided to examine simvastatin's capability to disrupt staphylococcal biofilms given their prevalence in the healthcare setting (in particular on medical implant devices). In addition to its broad-spectrum antibacterial activity, we confirmed that simvastatin is capable of disrupting established bacterial biofilms of two leading cause of hospital-acquired implant-based infections caused (*S. aureus* and *S. epidermidis*)[17]. The ability to disrupt staphylococcal biofilms by simvastatin lends further support to its potential use as a topical agent in the treatment of skin wounds.

The final component of the present study involved examining simvastatin's ability to be used in combination with other topical antimicrobials. Due to the increasing incidence of MRSA strains demonstrating resistance to topical drugs of choice, such as fusidic acid and mupirocin, combination therapies are being explored as a potential mechanism to ward off the emergence of further resistance to these important agents [53]. The Bliss independence model was utilized to investigate if simvastatin has the potential to act synergistically with topical drug of choice against multidrug-resistant *S. aureus* [54]. Simvastatin behaved synergistically with fusidic acid, mupirocin, daptomycin, and retapamulin against *S. aureus* strains resistant to vancomycin, linezolid, and methicillin. This result provides a strong platform to further examine combining simvastatin with topical antimicrobials to treat staphylococcal skin infections (and potentially contribute to reducing the likelihood of strains developing resistance to each agent if used alone).

In conclusion, the present study builds upon previous reports that demonstrate simvastatin possesses antimicrobial activity against important Gram-positive pathogens,

in particular methicillin-resistant *S. aureus*. We confirmed that simvastatin does possess antibacterial activity against Gram-negative pathogens as well, once the barrier imposed by the outer membrane is permeabilized, a finding not previously known. The antibacterial mechanism of action of simvastatin appears to be complex and involve inhibition of multiple biosynthetic pathways and cellular processes, including selective interference with bacterial protein synthesis. This property appears to play an important role in simvastatin's ability to suppress production of key toxins (α-hemolysin and PVL) critical to permit skin wounds infected by *S. aureus* to fully heal. A murine MRSA skin infection experiment revealed simvastatin is capable of significantly reducing the bacterial burden present in infected wounds. Additionally, simvastatin demonstrates the ability to disrupt adherent staphylococcal biofilms and to be used in combination with other topical antimicrobials currently employed to treat MRSA skin infections. Collectively the present study lays the foundation for further investigation of repurposing simvastatin as a topical antibacterial agent to treat skin infections caused by pathogens including MRSA.

2.6 Repurposing celecoxib as a topical antimicrobial agent for staphylococcal skin infections

(Thangamani S, Younis W, Seleem MN. Repurposing celecoxib as a topical antimicrobial agent. *Frontiers in Microbiology*. 2015 Jul 28;6:750)

2.6.1 Introduction

Bacterial infections caused by multi-resistant pathogens have emerged as a major global crisis during the past few decades [109]. In 2013, the U.S. Centers for Disease Control and Prevention indicated that at least two million individuals per year in the United States become infected with multidrug-resistant pathogens, including methicillin-resistant *Staphylococcus aureus* (MRSA), multidrug-resistant *Pseudomonas aeruginosa*, carbapenem-resistant *Klebsiella pneumoniae*, and vancomycin-resistant *Enterococcus faecium* [1]. More importantly, the emergence and spread of multidrug-resistant *S. aureus* clones such as MRSA USA300 are highly virulent and cause skin and soft tissue infections that lead to morbidity and mortality in infected patients [288]. Furthermore, the exo-proteins and toxins secreted by these MRSA strains trigger excess host inflammatory responses and further complicate the situation, especially in the management of wound infections [107,310,321,322]. In addition, virulence factors secreted by MRSA strains hinders wound healing and often contagious staphylococcal skin infections lead to invasive infections resulting in septicemia [257,258,323]. These observations speak to the specific need for topical antibacterial agents with novel mechanism of action combined with anti-inflammatory and wound

healing property that can address the issue of skin infections cause by multidrug-resistant staphylococcal strains.

The number of conventional antimicrobials available to treat MRSA skin infections is highly limited and those that are available are becoming less effective [324,325]. Though topical antimicrobials such as tedizolid and dalbavancin to treat Gram-positive pathogens including MRSA has been recently approved by FDA, still there is an unmet need exist for novel topical drugs to combat these pathogens [261,262]. The development of new antimicrobials capable of being used to treat multidrug-resistant pathogens is very slow and has not been able to keep pace with the emergence of bacterial resistance [109]. Hence, novel drugs and treatment strategies are urgently needed to combat these bacterial pathogens. Repurposing of approved drugs is a promising alternative strategy that can accelerate the process of antimicrobial research and development [276,326]. Unlike conventional drug discovery, finding new uses for existing drugs is a proven shortcut from bench to bedside, that reduces the cost and time associated with antibiotic development [276-278,326].

Celecoxib (Celebrex) is a nonsteroidal anti-inflammatory drug widely used for the treatment of pain, fever, and inflammation [327,328]. It specifically inhibits the enzyme cyclooxygenase-2 (COX2), thereby reducing the synthesis of proinflammatory prostaglandins [329]. Beyond its anti-inflammatory activity, celecoxib has been shown to possess antimicrobial activity against several microbial pathogens. In a study by Pereira et al, celecoxib was found to reduce the total fungal load in *Histoplasma capsulatum* infected mice [330]. Further, celecoxib treatment also increased the survival rate of the mice infected with lethal dose of *H. capsulatum* [330]. Another study by Chiu et al, found that celecoxib

inhibited the growth of *Francisella tularensis* and *F. novicida* [331]. In addition, celecoxib also exhibited antibacterial activity against *S. aureus* and *S. epidermidis* [80]. Apart from antimicrobial activity, celecoxib inhibits multidrug efflux pumps in *Mycobacterium smegmatis* and *S. aureus*, and increases the sensitivity of bacteria to various antibiotics, including ampicillin, kanamycin, ciprofloxacin and chloramphenicol [332,333]. However, the antibacterial mechanism of action of celecoxib and its potential clinical application remain underexplored.

In this study, we investigated the antibacterial activity of celecoxib, as well as the spectrum of its activity against various clinical isolates of multidrug-resistant Gram-positive and Gram-negative pathogens. We also investigated its mechanism of action and validated its *in vivo* antimicrobial efficacy in two different animal models, including *C. elegans* and mouse models of MRSA infection. Finally, we tested the activity of celecoxib in combination with various antimicrobial agents to investigate the potential for synergistic activities.

2.6.2 Materials and Methods

Bacterial strains and reagents

The bacterial strains used in this study are presented in Tables 1-3. Mueller-Hinton broth was purchased from Sigma-Aldrich. Trypticase soy broth (TSB), Trypticase soy agar (TSA), and Mannitol salt agar (MSA) were purchased from Becton, Dickinson (Cockeysville, MD). Celecoxib was purchased from TSZ chemicals. Vancomycin hydrochloride was obtained from Gold Biotechnology; linezolid from Selleck Chemicals,

mupirocin from Aapplichem, NE, clindamycin from TCI Chemicals, and fusidic acid and rifampicin from Sigma-Aldrich.

Antibacterial assays

Minimum inhibitory concentrations **(**MICs) were determined in triplicate, in Mueller-Hinton broth, using the broth micro dilution method described by the Clinical and Laboratory Standards Institute (CLSI) [216]. The MIC was interpreted as the lowest concentration of the drug able to completely inhibit the visible growth of bacteria after incubating plates for at least 16 h at 37°C. The highest MIC value taken from two independent experiments was reported.

Determining antibacterial activity in Gram-negative bacteria: (i) Outer membrane permeability assay

The MIC of celecoxib in the presence of colistin was measured as described in the antibacterial assays section, above. Sub-inhibitory concentration of colistin was added to the media to increase outer membrane permeability and facilitate the entrance of celecoxib. The following sub-inhibitory concentration of colistin was used for the strains used in this study. *Pseudomonas aeruginosa* ATCC15442 and *Salmonella Typhimurium* (0.25 µg/ml), *P. aeruginosa* ATCC BAA-1744 and *Klebsiella pneumoniae* (0.125 µg/ml), *Escherichia coli* O157:H7ATCC 700728 and *Acinetobacter baumannii* (0.0625 µg/ml). (ii) Inactivation of efflux pumps: Role of efflux pumps in contributing resistance to celecoxib in Gram-negative bacteria was investigated by using an efflux pump inhibitor (reserpine) and an efflux pump deletion mutant strain of *E.coli*. The MIC of celecoxib was examined in the

presence of sub-inhibitory concentration of reserpine (32 µg/ml) against all the strains of Gram-negative bacteria used in this study. Efflux pump deletion mutant strain of *E. coli* SM1411 Δ *acrAB* was employed to determine if *acrAB* efflux pump plays a role in contributing intrinsic resistance to celecoxib in *E. coli* as described [217].

Time kill assay

The time kill assay was performed as described before [216]. Briefly, MRSA USA300 was diluted to 1×10^6 CFU/mL and treated with 4X MIC of control antimicrobials (vancomycin or linezolid), 4X and 8X MIC of celecoxib (in triplicates) in MHB. Samples were incubated at 37°C and collected at indicated time points to count MRSA colony forming units (CFU).

Macromolecular synthesis assay

S. aureus strain ATCC 29213 was grown overnight on TSA plates and the isolated colonies cultured in 15ml of MHB to an early exponential phase (OD_{600} = 0.2 to 0.3) was used for the macromolecular synthesis assay. Aliquots (100 µl) of the culture were added to triplicate wells of a 96-well microtiter plate. Antibiotics with known mechanisms of action (ciprofloxacin, rifampicin, linezolid, vancomycin, and cerulenin) and auranofin were added to the plate as controls. DMSO was added to the control groups. After 30 min of incubation at 37°C, radiolabeled precursors such as [3H] thymidine (0.5µCi), [3H] uridine (0.5µCi), [3H] leucine (1.0 µCi), [14C] N-acetylglucosamine (0.4 µCi), and [3H] glycerol (0.5 µCi) were added to quantify the amount of for DNA, RNA, protein, cell wall and lipid synthesis respectively. Reactions measuring the inhibition of DNA and RNA

synthesis were stopped after 15 min by the addition of 5% trichloroacetic acid (TCA). Then, the tubes were chilled on ice for 30 min. The TCA-precipitated materials were collected on a 25 mm GF/1.2 μM PES 96-well filter plate. Filters were washed five times with 5% TCA, dried, and then counted using a Packard Top Count microplate scintillation counter. Reaction wells measuring the inhibition of protein synthesis were stopped after 40 min, precipitated, and counted in a manner similar to that used for the DNA and RNA synthesis inhibition assays. Reaction wells measuring the inhibition of cell wall synthesis were stopped after 40 min by the addition of 8% SDS and then heated for 30 min at 95°C. After cooling, the material were spotted onto nitrocellulose membrane filters (0.8 μM) and washed three times with 0.1% SDS. Filters were dried and counted using a Beckman LS3801 liquid scintillation counter. Reactions measuring the inhibition of lipid synthesis were stopped after 40 min by the addition of chloroform/methanol (1:2) and centrifuged at 13,000 rpm for 10 min. Then, the organic phase was carefully transferred to a scintillation vial, dried, and counted using liquid scintillation counting. Incorporation of radiolabeled DNA, RNA, protein, cell wall, and lipid precursors was quantified using the scintillation data and inhibition was calculated. Results were presented as the percent inhibition of each macromolecular synthesis pathway.

Toxicity assay in *C. elegans*

C. elegans AU37 (sek-1; glp-4) strain glp-4(bn2) were used for the toxicity studies. L4-stage worms were synchronized as described previously [301]. Synchronized worms (approximately 20 worms) in 50% M9 buffer and 50% TSB were added to each well of a 96-well plate. Drugs (celecoxib and linezolid) at indicated concentrations (16 or 32 μg/ml)

were added to the wells and the plates were incubated for 4 days at room temperature. Worms were assessed every day; the percentage of worms remaining alive in each group was calculated.

Efficacy of celecoxib in MRSA-infected *C. elegans*

C. elegans AU37 (sek-1; glp-4) strain glp-4(bn2) was used to test the *in vivo* antimicrobial efficacy of celecoxib as described previously [301]. *S. aureus* strain MRSA USA300 was used for infection and the MIC of control antibiotic (linezolid) and celecoxib against MRSA USA300 were 2 and 32 µg/ml. Briefly, L4-stage worms were infected with MRSA USA300 for 8 h at room temperature. The worms were washed with M9 buffer, and then drugs (celecoxib and linezolid) at indicated concentrations were added to the 96-well plates containing approximately 20 worms per well. After 24 h, the worms were washed four times with PBS and 100 mg of sterile, 1.0-mm silicon carbide particles (Biospec Products, Bartlesville, OK) were added to each tube. Worms were disrupted by vortexing the tubes at maximum speed for one minute. The final suspension containing MRSA was plated onto MSA plates to count the bacteria. The total CFU count in each well was divided by the number of worms present in the respective well. The results shown are the percent reduction in CFU per worm, compared with an untreated control.

Efficacy of celecoxib in MRSA-infected *Mice*

Eight-week-old female BALB/c mice (Harlan Laboratories, Indianapolis, IN) were used in this study. All animal procedures were approved by the Purdue University Animal Care and Use Committee (PACUC). The mouse model of MRSA skin infection was

performed as described previously [334-336]. Briefly, mice were infected intradermally with 1.65×10^8 CFU MRSA300. After 48 h of infection, open wounds formed and the mice were divided into five groups of 5 mice each. Two groups were treated topically with 20 mg of either 1%, or 2% celecoxib in petroleum jelly. One group received the vehicles alone (20 mg petroleum jelly). Another group was treated topically with 20 mg of 2% fusidic acid in petroleum jelly and the last group was treated orally with clindamycin (25 mg/kg). All groups were treated twice a day for 5 days. 24 h after the last treatment, the skin area around the wound was swabbed with 70% ethanol and the wound (around 1 cm^2) was precisely excised and homogenized. Bacteria in the homogenate were counted using MSA plates.

Determination of Cytokine levels

Skin homogenates obtained from infected mice were centrifuged at 4000 rpm for 10 min and the supernatants were used for the detection of cytokine levels. Tumor necrosis factor-α (TNF-α), interleukin-6 (IL-6), interleukin-1 beta (IL-1β), and monocyte chemo attractant protein-1 (MCP-1) ELISA kits (R&D Systems, Inc.) were used to determine the levels of these cytokines according to the manufacture's instruction [281].

Synergy assay

Synergy between celecoxib and conventional antimicrobials (gentamicin, clindamycin, vancomycin, linezolid, daptomycin, retapamulin, fusidic acid and mupirocin) in the treatment of four clinical isolates of *S. aureus* (MRSA300, NRS107, NRS119 and VRSA5) was evaluated using the Bliss Independence Model, as described previously [282]. Synergy (S) was calculated using the formula: $S = (f_{A0}/f_{00})(f_{0B}/f_{00})-(f_{AB}/f_{00})$. The parameter f_{AB} refers

to the optical density of the bacteria grown in the presence of celecoxib and antibiotics; parameters f_{A0} and f_{0B} refer to the bacterial growth rate in the presence of antibiotics alone and celecoxib alone, respectively; the parameter f_{00} refers to the bacterial growth in the absence of drugs. Degree of synergy (S) values corresponds to the following cut-offs.: Zero indicates neutral, values above zero (positive value) represents synergism and values below zero (negative values) correspond to antagonism. Drug combinations with higher positive value represents high degree of synergism.

Statistical analyses

Statistical analyses were performed using Graph Pad Prism 6.0 software (Graph Pad Software, La Jolla, CA). *P* values were calculated by using two-tailed unpaired Student *t* tests. *P* values < 0.05 were considered significant.

2.6.3 Results

Antibacterial activity

The antibacterial activity of celecoxib was tested using various important multidrug-resistant strains of Gram-positive (Table 2.9) and Gram-negative (Table 7.2) pathogens. Celecoxib showed activity against most of the Gram-positive bacteria tested, including methicillin- and vancomycin-resistant *S. aureus, Streptococcus pneumonia, Listeria monocytogenes, Bacillus anthracis, Bacillus subtilis,* and *Mycobacterium smegmatis*, with MICs ranging from 16 to 64 µg/ml (Table 2.9).

Table 2.9 MIC of celecoxib against Gram-positive bacteria

Bacteria	Description	Celecoxib (μg/ml)
Methicillin-resistant *S. aureus* ATCC 4330	Clinical isolate resistant to methicillin and oxacillin	32
Vancomycin-resistant *S. aureus* (VRSA10)	Resistant to ciprofloxacin, clindamycin, erythromycin and gentamicin	32
Streptococcus pneumoniae ATCC 49619	Isolated from sputum of 75-year-old male, Phoenix, AZ, USA	64
Bacillus anthracis	Stern vaccine strain	16
B. anthracis UM23	Weybridge strain which contains the toxigenic pXO1 plasmid and lacks the pXO2 capsule plasmid	16
B. anthracis AMES35	Isolated from 14-month-old heifer that died in Texas in 1981. It is a derivative of *B. anthracis*, strain Ames that was treated with novobiocin to cure it of the pXO2 plasmid.	16
Bacillus subtilis CU 1065	-	16
Listeria monocytogenes	F4244 CDC. Clinical isolate from patient cerebrospinal fluid (CSF)	32
Mycobacterium smegmatis ATCC 14468	Reference strain	16

In contrast, celecoxib alone did not show antibacterial activity against Gram-negative bacteria. However, when the outer membranes of Gram-negative bacteria were compromised with a sub-inhibitory concentration of colistin, celecoxib showed antimicrobial activity against all Gram-negative pathogens tested, including *P. aeruginosa, Escherichia coli, K. pneumonia, Salmonella Typhimurium, Acinetobacter baumannii*, with MICs ranging from 8 to 32 μg/ml (Table 2.10).

Next, the activity of celecoxib was investigated in the presence of sub-inhibitory concentration of an efflux pump inhibitor reserpine. Celecoxib did not exhibited antibacterial activity against all tested strains of Gram-negative bacteria in the presence of

reserpine (Table 2.10). However, celecoxib showed activity against *E. coli* SM1411Δ *acrAB* which is deficient for acrAB efflux pump at a concentration of 64 µg/ml (Table 2.10).

Table 2.10 MIC of celecoxib against Gram-negative bacteria

Bacteria	Description	MIC of celecoxib (µg/ml)		
		(-)	(+)colistin	(+)reserpine
Pseudomonas aeruginosa ATCC15442	Isolated from animal room water bottle	>256	16	>256
Pseudomonas aeruginosa ATCC BAA-1744	Clinical isolate and VITEK 2 GN identification card quality control organism	>256	16	>256
Escherichia coli O157:H7ATCC 700728	Nontoxigenic and quality control strain	>256	16	>256
Acinetobacter baumannii ATCC BAA1605	MDR strain isolated from the sputum of a Canadian soldier	>256	8	>256
Acinetobacter baumannii ATCC BAA747	Human clinical specimen - ear pus	>256	16	>256
Salmonella Typhimurium ATCC 700720	Wild type strain isolated from a natural source	>256	32	>256
Klebsiella pneumoniae ATCC BAA 2146	Clinical isolate New Delhi Metallo-β-Lactamase (NDM-1)	>256	8	>256
Klebsiella pneumoniae ATCC BAA 1705	Clinical isolate with Carbapenemase (KPC) resistant to carbapenem	>256	16	>256
Escherichia coli 1411	Wild type strain	>256	ND	ND
Escherichia coli SM1411 Δ *acrAB*	Mutant for *acrAB* efflux pump	64	ND	ND

The antibacterial activity of celecoxib was also assessed using a series of multidrug-resistant *S. aureus* clinical isolates (Table 2.11). The MIC of celecoxib required to inhibit 90% (MIC_{90}) of the MRSA and vancomycin-intermediate *S. aureus* (VISA) clinical isolates was found to be 32 µg/ml. However, the MIC_{90} of celecoxib against vancomycin-resistant *S. aureus* (VRSA) clinical isolates tested was 128 µg/ml.

Table 2.11 MIC of celecoxib against clinical isolates of *Staphylococcus aureus* strains

Strain type	Strain ID	Phenotypic properties	Celecoxib (μg/ml)
Methicillin resistant *S.*	USA100	Resistant to ciprofloxacin, clindamycin,	32
aureus (MRSA)		erythromycin	
	USA200	Resistant to clindamycin, methicillin	32
		erythromycin, gentamicin,	
	USA300	Resistant to erythromycin, methicillin, tetracycline	32
	USA400	Resistant to methicillin, tetracycline	16
	USA500	Resistant to ciprofloxacin, clindamycin,	32
		erythromycin, gentamicin,	
		methicillin, tetracycline, trimethoprim	
	USA700	Resistant to erythromycin, methicillin	32
	USA800	Resistant to methicillin	32
	USA1000	Resistant to erythromycin, methicillin	32
	USA1100	Resistant to methicillin	32
	NRS194	Resistant to methicillin	32
	NRS108	Resistant to gentamicin	32
	NRS119 (Lin^r)	Resistant to linezolid	16
	ATCC 43300	Resistant to methicillin	32
	ATCC BAA-44	Multidrug-resistant strain	32
	NRS70	Resistant to erythromycin, clindamycin, spectinomycin	32
	NRS71	Resistant to tetracycline, methicillin	32
	NRS100	Resistant to tetracycline, methicillin	32
	NRS107	Resistant to methicillin, mupirocin	32
Vancomycin-intermediate	NRS1	Resistant to aminoglycosides and	32
S. aureus (VISA)		tetracycline; glycopeptide- intermediate *S. aureus*	
	NRS19	Glycopeptide-intermediate *S. aureus*	32
	NRS37	Glycopeptide-intermediate *S. aureus*	32
Vancomycin-resistant *S.*	VRS1	Resistant to vancomycin	128
aureus (VRSA)	VRS2	Resistant to vancomycin, erythromycin, spectinomycin	128
	VRS3a	Resistant to vancomycin	32
	VRS3b	Resistant to vancomycin	32
	VRS4	Resistant to vancomycin, erythromycin, spectinomycin	128
	VRS5	Resistant to vancomycin	16
	VRS6	Resistant to vancomycin	16
	VRS7	Resistant to vancomycin, β-lactams	128
	VRS8	Resistant to vancomycin	32
	VRS9	Resistant to vancomycin	64
	VRS11a	Resistant to vancomycin	32
	VRS11b	Resistant to vancomycin	32
	VRS12	Resistant to vancomycin	32
	VRS13	Resistant to vancomycin	32

Killing kinetics of *S. aureus* by celecoxib

Celecoxib with broad-spectrum activity, we determined to investigate the rate of bacterial killing. As seen in Figure 2.35, MRSA USA300 treated with 4X and 8X MIC of celecoxib exhibits a typical biphasic killing pattern. Treatment with celecoxib consist of an initial rapid bactericidal phase (2.49±0.23 $\log_{10}$ and 3.01±0.26 $\log_{10}$ CFU reduction at 4 h with 4X and 8X MIC) followed by a predominant regrowth. In comparison, vancomycin had a bactericidal activity after 24 h, while linezolid treatment results in single log reduction after 24 h incubation exhibiting a bacteriostatic activity.

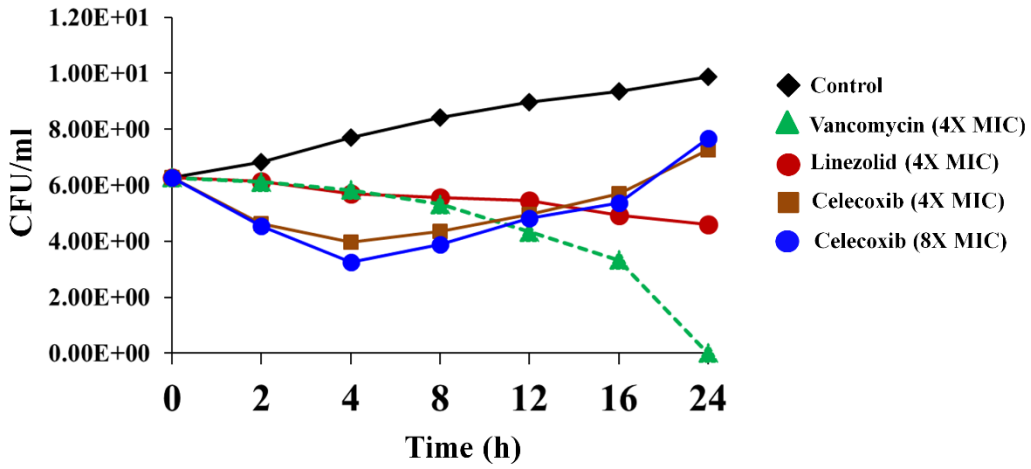

Figure 2.35 Time-kill assay for celecoxib tested against *S. aureus*. Killing kinetics of celecoxib (4X and 8X MIC), vancomycin (4X MIC), and linezolid (4X MIC), against MRSA USA300 in MHB are shown. The results are presented as means ± SD (n = 3). Data without error bars indicate that the SD is too small to be seen.

Mechanism of action

In view of the results demonstrating broad-spectrum antibacterial activity, we used macromolecular synthesis assays in *S. aureus* ATCC 29213 to investigate the antibacterial mode of action of celecoxib. As shown in Figure 2.36, RNA, DNA and protein synthesis inhibition were detected at concentrations significantly below the MIC (0.25X).

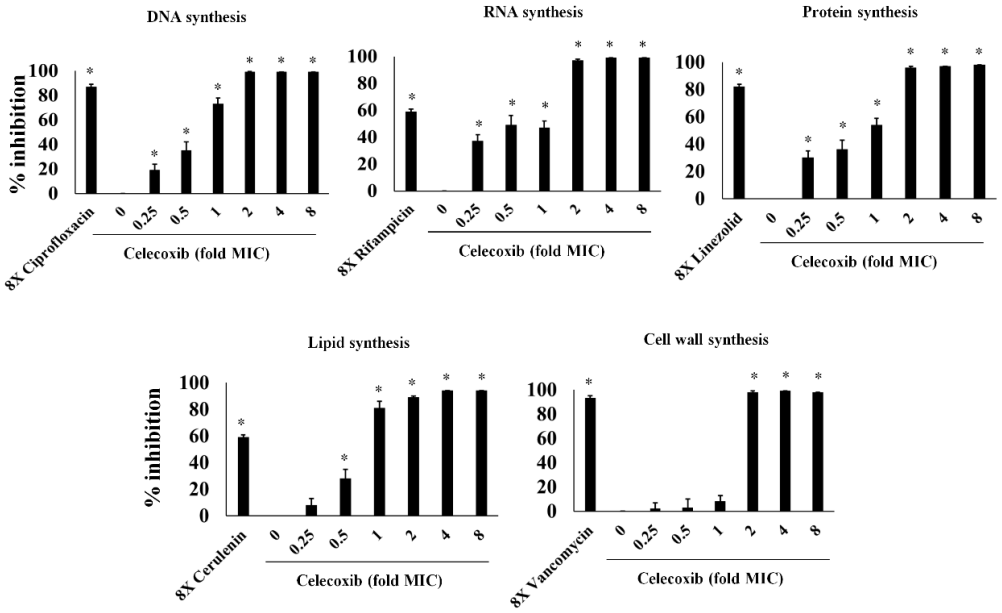

Figure 2.36 Macromolecular synthesis assay in the presence of celecoxib and control antibiotics. Incorporation of radiolabeled precursors such as [3H] thymidine, [3H] uridine, [3H] leucine, [14C] N-acetylglucosamine and [3H] glycerol for DNA, RNA, protein, cell wall and lipid synthesis respectively were quantified in *S. aureus* ATCC 29213. Based on the incorporation of radiolabeled precursors, percent of inhibition by celecoxib at concentration dependent manner was examined. Control antibiotics including ciprofloxacin (DNA), rifampicin (RNA), linezolid (protein), cerulenin (lipid synthesis) and vancomycin (cell wall synthesis) at 8X MIC were used. Triplicate samples were used for each group and the statistical analysis was calculated by the two-tailed Student *t* test. All treatment groups were compared to untreated control group. *P* value of ($*P \leq 0.05$) is considered as significant.

However, a secondary effect was also observed at higher concentration, with a clear dose-dependent disruption of [3H] glycerol incorporation indicating decreased lipid synthesis. Cell wall synthesis inhibition was evident only at a concentration above the MIC (2X).

Toxicity in *C. elegans*

The safety of celecoxib was evaluated in a *C. elegans* whole-animal model. As shown in Figure 2.37, *C. elegans* treated with 16 or 32 µg/ml of celecoxib for four days did not show any significant toxicity. These results are similar to those seen in the linezolid (16µg/ml) and untreated control groups

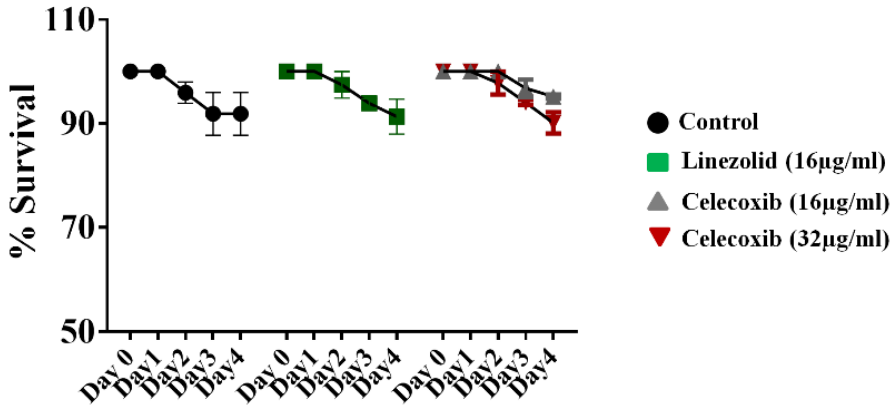

Figure 2.37 Evaluation of toxicity in *C. elegans* model. *C. elegans* strain glp-4; sek-1 (L4-stage) were grown for four days in the presence of celecoxib (16 and 32 µg/ml) and linezolid (16µg/ml). Worms were monitored daily and the live worms were counted. Results were expressed as percent live worms in relative to the untreated control groups. Triplicate wells were used for each group and the results were means ± SD (n = 3).

Efficacy in animal models

Having demonstrated a comfortable safety profile, the antibacterial efficacy of celecoxib was tested in a *C. elegans*, whole-animal MRSA infection model. As seen in Figure 2.38A, celecoxib treatment significantly reduced the mean bacterial count, compared with the untreated control. Treatment with celecoxib at 16 and 32 µg/ml significantly decreased the bacterial CFU of 0.56±0.33 $\log_{10}$ and 0.94±0.43 $\log_{10}$ respectively. For comparison, linezolid at 16 µg/ml also had significant reduction in bacterial CFU (0.99±0.17 $\log_{10}$), compared with the untreated control.

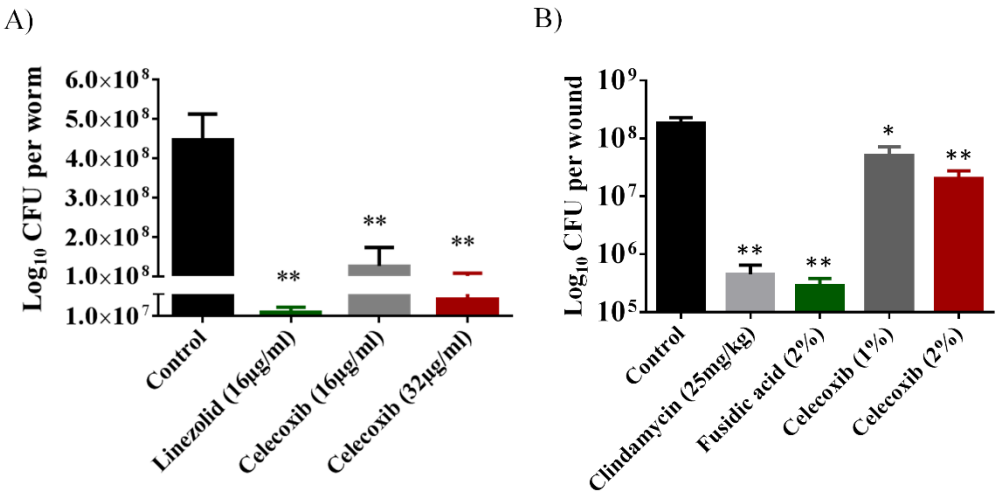

Figure 2.38 Efficacy of celecoxib in MRSA-infected animal models (a) L4-stage worms infected with MRSA USA300 were treated with celecoxib (16 and 32 µg/ml) and linezolid (16µg/ml) for 24 h. At this point, the worms were disrupted and the amount of MRSA in the lysate (CFU) was determined. CFU per worm in treated groups relative to the untreated control groups were shown. Triplicate wells were used for each group and the results were means ± SD (n = 3). (b) Efficacy of treatment of MRSA-infected mouse skin lesions with celecoxib 1 and 2%, clindamycin (25 mg/kg), fusidic acid 2% and petroleum jelly (negative control) twice daily for five days were evaluated. Five mice per group was used and the results were means ± SD of five mice. CFU per wound was calculated and presented. . *$P \leq 0.05$ and *$P \leq 0.01$ were considered as significant.

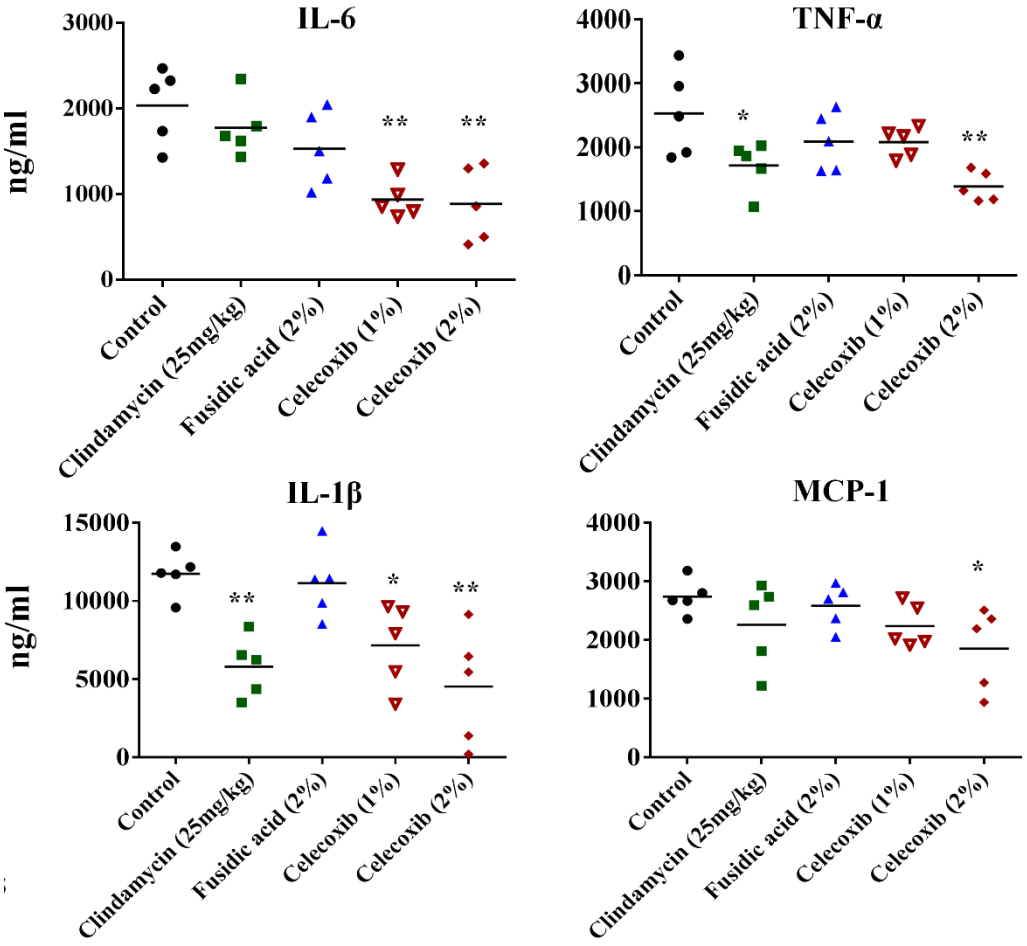

Figure 2.39 Effect of celecoxib on IL-6, TNF-α, IL-1β and MCP-1 production in MRSA infected skin lesions. Supernatants from skin homogenates were used for cytokine detection by ELISA. Each point represents single mice and each group has five mice. Statistical analysis was calculated by the two-tailed Student *t* test. *P* values of ($*P \leq 0.05$) ($**P \leq 0.01$) are considered as significant.

Next we tested the *in vivo* antibacterial efficacy of celecoxib in a mouse model of MRSA skin infection. As shown in Figure 2.38B, all treatment groups (1 or 2% celecoxib, 2% fusidic acid, or clindamycin oral treatment) significantly reduced the mean bacterial counts, compared with the control group ($P \leq 0.05$). Groups treated topically with 1% and 2% celecoxib had a reduction in MRSA CFU of 0.66±0.19 $\log_{10}$and 1.02±0.27 $\log_{10}$ respectively. Topical treatment with 2% fusidic acid and oral clindamycin (25 mg/kg) treatment reduced the bacterial load of 2.90±0.23 $\log_{10}$ and 2.40±0.32 $\log_{10}$ CFU respectively.

Effect of celecoxib on inflammatory cytokine levels induced by MRSA skin infection

We investigated the immune-modulatory activity of celecoxib in MRSA skin infection by measuring the levels of the inflammatory cytokines IL-6, TNF-α, IL-1β and MCP-1 using ELISA. As shown in Figure 2.39, treatment with 2% celecoxib significantly reduced the levels of all tested inflammatory cytokines, compared with an untreated control. Treatment with 1% celecoxib significantly reduced the levels of IL-6 and IL-1β. Clindamycin treatment also reduced levels of TNF-α and IL-1β.

Synergism with topical and systemic antimicrobials

The antimicrobial activities of combinations of celecoxib with topical and systemic antimicrobials were investigated *in vitro,* using the Bliss independence model, with clinical isolates of multidrug-resistant *S. aureus*. Celecoxib acted synergistically with all tested antimicrobials (with the exception of linezolid) against all strains of multi-drug resistant *S.*

aureus tested, including MRSA300, VRSA5, linezolid-resistant *S. aureus* (NRS119) and mupirocin-resistant *S. aureus* (NRS107). However, celecoxib showed slight antagonism when combined with linezolid against VRSA5 (Figure 2.40).

2.6.4 Discussion

The emergence of bacterial resistance is not a new phenomenon. However, because only a few antibiotics have been developed over the past few decades, the continuous evolution and spread of multidrug-resistant bacterial strains is a serious threat to the public health [1]. The pharmaceutical companies' lack of interest in antimicrobial research and development has also become a major concern [276]. The World Health Organization has already warned that we are heading toward a "post-antibiotic era" and suggested that urgent measures need to be taken [337]. Therefore, recent research had been directed toward finding new antimicrobials and novel strategies to combat multidrug-resistant bacterial pathogens. One promising approach gaining increased attention is the repurposing of existing approved drugs as antimicrobials.

In an attempt to repurpose approved drugs, we and others [80,330,331] have found that celecoxib exhibits broad-spectrum antimicrobial activity against Gram-positive and Gram-negative bacterial pathogens. Celecoxib, a classical NSAID drug and inhibitor of the enzyme cyclooxygenase-2 (COX2), has been widely used as an anti-inflammatory drug for *tularensis* and *S. aureus* [80,331].

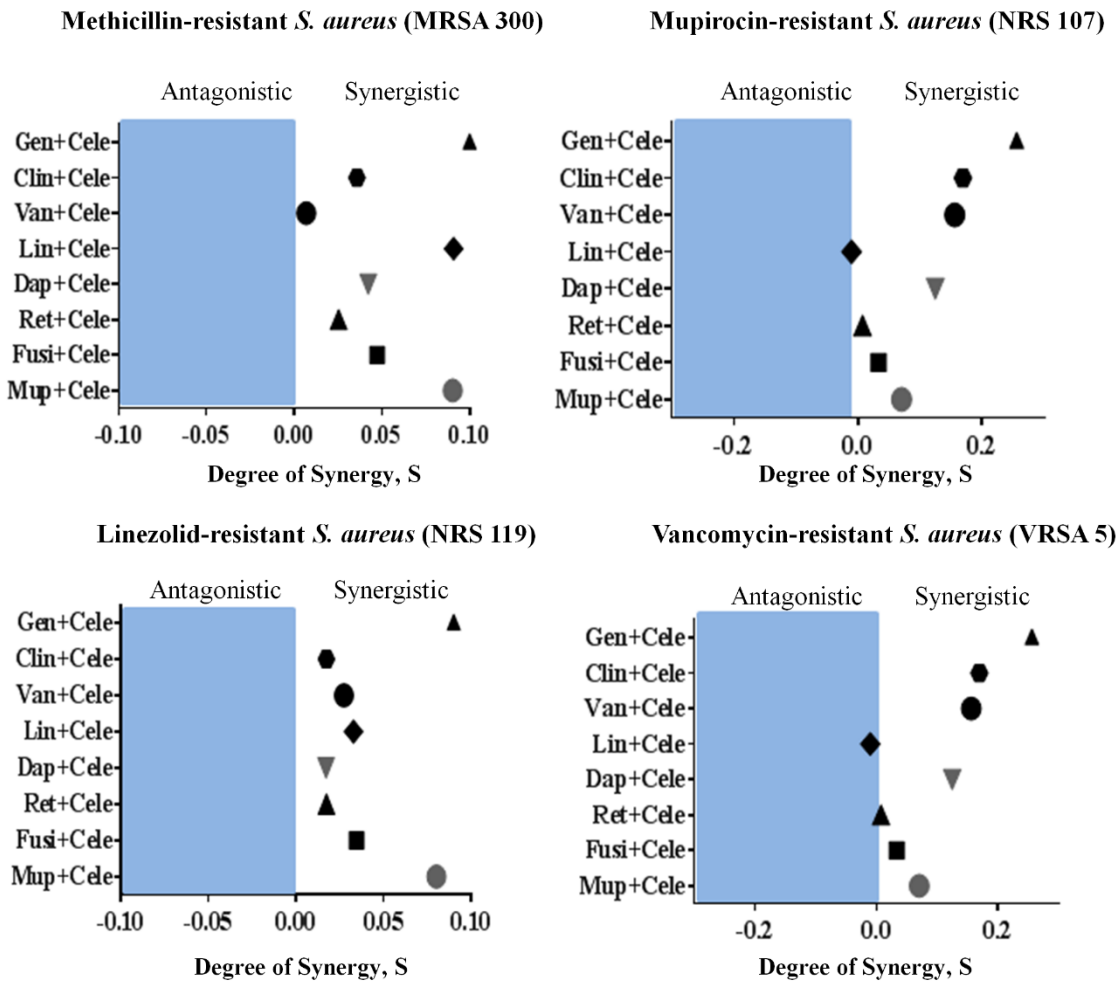

Figure 2.40 **Synergistic activity of celecoxib with topical and systemic antimicrobials.** The Bliss Independence Model confirms a synergistic effect between celecoxib and conventional antimicrobials against various drug-resistant strains of *S. aureus* (MRSA300, NRS119, NRS107 and VRSA5). The degree of synergy was quantified after 12 h of treatment with celecoxib (8µg/ml) in combination with sub-inhibitory concentrations of topical (mupirocin, fusidic acid, daptomycin and retapamulin) and systemic antimicrobials (gentamicin, clindamycin, vancomycin and linezolid).

Celecoxib also reduces *H. capsulatum* burden by enhancing phagocytosis of alveolar macrophages and decreasing levels of inflammatory cells and cytokines, thereby exhibiting a protective role in pathogenesis of *H. capsulatum* [330]. Our study demonstrated that celecoxib possesses activity against various multidrug-resistant Gram-positive pathogens, including *S. aureus*, *S. pneumonia*, *L. monocytogenes*, *B. anthracis*, *B. subtilis*, and *M. smegmatis*. However, we noticed that Gram-negative pathogens are not susceptible to celecoxib, and the lack of activity was found to be due to the permeability barrier conferred by the outer membrane. This was further confirmed by the fact that the antimicrobial activity of celecoxib against Gram-negative bacteria was restored when the integrity of the outer membrane was compromised using a sub-inhibitory concentration of colistin [338-340]. In addition, celecoxib also showed activity when an efflux pump such as *acrAB* was deleted in *E. coli*. AcrAB has been known to contribute for resistant phenotype for various antibiotics including ampicillin, chloramphenicol and rifampicin [228].. However, celecoxib did not restore its activity in the presence of efflux pump inhibitor reserpine in any of the Gram-negative bacteria tested in this study. This might be due to the variation in the efflux systems in different bacterial strains. Taken together, in addition to the intrinsic physical barrier outer membrane, celecoxib entry into Gram-negative bacteria is also influenced by efflux pumps such as AcrAB. Our results indicate that the target of celecoxib is present in both Gram-positive and Gram-negative bacteria and that celecoxib can be combined with other approved drugs that cause leakage in the outer membrane, such as colistin, to sensitize Gram-negative pathogens. Next, we investigated the activity of celecoxib against clinical isolates of multidrug-resistant *S. aureus*. Celecoxib inhibited the growth of all tested clinical isolates of MRSA, VISA, VRSA, linezolid-resistant *S. aureus* (NRS119)

and mupirocin-resistant *S. aureus* (NRS107). MIC values determined in our study for celecoxib against MRSA correlates with MIC values reported for celecoxib against *F. tularensis* and *S. aureus* in previous published studies [80,331].

Time kill kinetics of celecoxib against *S. aureus* revealed a unique biphasic killing pattern. The bactericidal effect of celecoxib lasted for only a short time, after which gradual regrowth of bacteria was noticed. This pattern was reported for azlocillin and tobramycin against *Pseudomonas aeruginosa* [341,342]. The bactericidal activity and the extent of regrowth in *P. aeruginosa* after incubation with azlocillin and tobramycin was concentration dependent manner [341,342]. However, the bactericidal activity (at 4 h) of celecoxib at 8X MIC was found to be slightly higher than 4X MIC but the regrowth was found to be similar at both the concentration after 24 h of incubation.

The mechanism of celecoxib's broad-spectrum antibacterial activity remains unidentified. In our study, we found that celecoxib inhibited the synthesis of DNA, RNA, and protein at concentrations significantly below the MIC . Additionally, the disruption of lipid synthesis was evident at higher MIC concentration, whereas no significant effect was observed on the cell wall synthesis. These results indicate that perturbation of the lipid synthesis by celecoxib might be a secondary effect due to RNA and protein synthesis inhibition. The effect of celecoxib on multiple macromolecular synthesis pathways might likely due to the disruption in general cellular energy metabolism or membrane perturbation. Antimicrobial peptides such as pleurocidin-derived peptides at sub-lethal concentration cause cell membrane damage leading to the inhibition of multiple

macromolecular synthesis pathways [343]. Lactoferricin B, a cationic peptide which also cause membrane permeabilization is believed to have effect on general energy metabolism which results in inhibition of multiple pathways [344,345]. Celecoxib with initial rapid bactericidal property (biphasic killing pattern) might possibly also lead to the disruption of various macromolecular pathways. However, the cause for inhibition on multiple pathways is not yet clear. Further, we also attempted to generate a *S. aureus* that is resistant to celecoxib. No colonies resistant to celecoxib at three-, five-, or tenfold the MIC were detected. In addition, serial passage of *S. aureus* with sub-inhibitory concentration of celecoxib for twelve days did not resulted in colonies that were resistant to celecoxib. Therefore, future studies are warranted to identify the precise molecular target of celecoxib.

In view of the broad spectrum antibacterial activity exhibited by celecoxib *in vitro*, we decided to investigate the *in vivo* antibacterial activity of celecoxib in animal models of MRSA infection. First we tested the efficacy in MRSA infected *C. elegans.* Whole animal model including *C. elegans,* provides a great platform for validating the *in vivo* efficacy of novel compounds [301,320]. Our results indicates that celecoxib at 16 and 32 µg/ml, which are concentrations without considerable toxicity to the host, significantly reduced the mean bacterial load (by 71% and 85% respectively) when compared with a control group ($P \leq 0.05$). Celecoxib at 32 µg/ml had an effect on the mean bacterial count that was comparable to that of linezolid (16 µg/ml). Next, we moved forward to validate celecoxib's efficacy in a mouse model of MRSA infection. However, a high MIC that cannot be achieved systemically is a major impediment to the potential use of celecoxib as an antimicrobial agent. While the use of celecoxib to treat systemic bacterial infections is not currently

possible, local application of celecoxib for treating/preventing bacterial infections in wounds is a novel application for this drug that holds considerable promise. Therefore we decided to test the activity of celecoxib in a topical MRSA skin infection model. Celecoxib 1% and 2% significantly reduced the bacterial load in the wounds (by 72% and 87%, respectively) when compared with a control group ($P \leq 0.05$).

However, staphylococcal skin infections often induce excess host inflammatory cytokines, which in turn aggravate the pathogenesis [256,293]Drugs with anti-inflammatory properties, especially those that inhibit pro-inflammatory cytokines such as IL-6 and TNF-α, would accelerate the healing of chronic wounds. [107,293,328,346,347]. Celecoxib, which is known to have anti-inflammatory activity, would potentially be able to limit the inflammatory process induced by MRSA infection. Therefore, we measured the inflammatory cytokines in MRSA lesions treated with celecoxib. Topical treatment with celecoxib 1% significantly ($P \leq 0.05$) reduced levels of TNF-α and IL-1β, while celecoxib 2% significantly ($P \leq 0.05$) reduced the levels of all the inflammatory cytokines measured (IL-6, TNF-α, IL-1β and MCP-1). This ability of celecoxib to dampen the inflammatory response might aid the healing of chronic wounds [102-107]. Celecoxib's recognized beneficial role in the wound healing process, reducing scar formation without disrupting reepithelization, is an added advantage for the treatment of bacterial skin infections [348].

With increased emergence of resistant strains of *S. aureus* to topical drugs of choice, such as mupirocin and fusidic acid, combination therapies have recently been gaining attention [204,259,260,268,269,349]. We, therefore, investigated whether celecoxib has potential to

be combined with antibiotics against multidrug-resistant *S. aureus* strains by using the Bliss independence model [282]. Celecoxib was found to exhibit a synergistic relationship with topical (mupirocin, fusidic acid, daptomycin and retapamulin) and systemic antimicrobials (gentamicin, clindamycin, vancomycin and linezolid), against most of the tested multidrug-resistant staphylococcal strains, including MRSA300, NRS119, NRS107 and VRSA5. This finding provides a potential basis for the combination of celecoxib with conventional antimicrobial drugs for the treatment staphylococcal skin infections and reducing the likelihood of strains developing resistance to monotherapy.

Taken together, our results show that celecoxib exhibits several beneficial properties, including broad spectrum antimicrobial activity against various multidrug resistant Gram-positive and Gram-negative pathogens, synergistic action with conventional antimicrobials, and anti-inflammatory activity that reduces excess host inflammation during infection. Celecoxib may, therefore, be a good candidate for repurposing for the treatment of topical bacterial infections. This emerging approach might form a novel alternative strategy in search of new antimicrobials.

CHAPTER 3. DRUG REPURPOSING FOR FUNGAL INFECTIONS

3.1 Repurposing approach identifies auranofin with broad spectrum antifungal activity that targets Mia40-Erv1 pathway

(S. Thangamani, M. Maland, H. Mohammad, P. Pascuzzi, L. Avramova, C. Koehler, T. R. Hazbun and M. N. Seleem. Repurposing approach identifies auranofin with broad spectrum antifungal activity that targets Mia40-Erv1 pathway, "*Frontiers in Cellular and Infection Microbiology*"-Under Review.)

3.1.1 Introduction

Invasive fungal infections, particularly those caused by *Candida* and *Cryptococcus*, afflict millions of patients annually resulting in more than 1,350,000 deaths despite the introduction of new antifungal agent [350-354]. Unfortunately, current antifungal therapies have limited effectiveness in treating invasive fungal infections and suffer from restrictions in route of administration, spectrum of activity, and bioavailability in target tissues such as the brain [354,355]. Further compounding this problem, the development of new antifungal is currently unable to keep pace with the urgent demand for safe and effective new drugs. Hence, there is a pressing and urgent need for novel, inexpensive, and safe antifungal drugs to combat these dangerous pathogens.

The concept of drug repositioning has recently gained momentum and emerged as a viable approach to expedite anti-infective drug development [210,356]. For example, several reports have demonstrated that auranofin, an orally bioavailable FDA-approved drug for treatment of rheumatoid arthritis, exhibits potent antibacterial and antiparasitic activities [58,212,215,249,263,357,358]. This discovery led to the FDA granting auranofin Orphan Drug status for treatment of amebiasis. Recent studies by Fuchs *et al*.[359] and Stylianou *et al*.[360] reported that auranofin also possesses antifungal activity. However, the antifungal mechanism of action and *in vivo* antifungal efficacy of auranofin remain unclear with several possible targets reported. Thus, the objectives of our study were to determine the antifungal activity of auranofin against clinical isolates of different fungal pathogens, to investigate the drug's antibiofilm activity, to deduce auranofin's antifungal mechanism of action using an unbiased chemogenomic approach, and to validate the drug's *in vivo* antifungal efficacy in a *C. neoformans*-infected *Caenorhabditis elegans* whole animal model.

3.1.2 Materials and Methods

Fungal strains and reagents

Fungal strains used in this study are presented in Table 1. Yeast peptone dextrose agar (YPD) was purchased from BD Biosciences (San Jose, CA). Auranofin (Enzo Life Sciences, Farmingdale, NY), fluconazole (Acros Organics, New Jersey), and flucytosine (TCI chemicals, Tokyo, Japan) were purchased from commercial vendors. XTT-sodium salt, menadione, RPMI powder, and MOPS were purchased from Sigma-Aldrich (St. Louis,

MO). Concanavalin A–conjugated with FITC 488 dye was acquired from Thermo Fisher Scientific Inc. (Waltham, MA).

Antifungal susceptibility testing

Antifungal susceptibility testing was carried out as per the National Committee for Clinical Laboratory Standards M-27A3 (NCCLS) guidelines [361]. Briefly, the inocula were prepared from 24 h old cultures of *Candida* spp. or 48 h old cultures of *Cryptococcus* spp. in YPD plates. Five colonies were then transferred to 5 mL of sterile 0.9% saline (PBS). The suspensions were adjusted to McFarland standard 0.5 and then diluted 1:2000 in RPMI 1640 buffered to pH 7.0 with 0.165 M MOPS (RPMI-MOPS) to yield an inoculum of 5.0 × 10^2 to 2.5 × 10^3 CFU/mL. An aliquot (100 μL) of the resulting suspension was incubated with serially diluted fluconazole, flucytosine, and auranofin for 24 h for *Candida* spp and 72 h for *Cryptococcus* spp. The minimum inhibitory concentration (MIC) of fluconazole and flucytosine were determined as the prominent decrease (approximately 50%) in visible growth compared to untreated controls, as per NCCLS guidelines. Similarly the MIC of auranofin was determined as the lowest concentration resulting in 50% reduction in visible growth. All experiments were carried out in triplicate wells.

Time kill assay

Fungal cultures of *Candida albicans* and *Cryptococcus neoformans* were diluted approximately to 5 × 10^5 CFU/mL and treated with 5 × and 10 × MICs of auranofin and fluconazole (in triplicate) in RPMI-MOPS, at 35°C. Samples were collected at indicated time points and serially diluted in PBS and plated onto YPD plates. Plates were incubated

at 35°C for 24-48 h prior to counting fungal colony forming units (CFU), as described elsewhere [362].

XTT-reduction assay

C. albicans ATCC 10231 was grown in YPD broth at 35°C for 24 h. Cells were washed with PBS and resuspended in RPMI-MOPS at 10^6 cells/mL [363,364]. An aliquot (100 µL) of cell suspension was transferred to wells in a 96-well tissue culture plate. After 48 h incubation (at 37°C), wells were washed with PBS and drugs (auranofin, fluconazole, and flucytosine) were added at indicated concentrations. After 24 h of incubation, the supernatant was removed and 100 µL of XTT/menadione solution was added to each well. The plates were covered with aluminum foil and incubated at 37°C for 1 hour. Aliquots (75 µL) were taken from each well and the absorbance (OD_{495}) was measured using a spectrophotometer. The antifungal activity of each drug was expressed as a percentage of metabolic activity of treatment groups relative to the DMSO-treated control groups. The experiment was performed using triplicate samples for each treatment regimen.

Confocal imaging of fungal biofilms

C. albicans ATCC 10231 was seeded on FBS-coated glass cover slips in 6-well tissue-culture plates and grown in RPMI-MOPS medium with 0.2% glucose at 37°C [365]. After 48 h, wells were washed with PBS and drugs (auranofin, fluconazole, and flucytosine) were added at indicated concentrations. After 24 h of treatment, wells were washed with PBS and stained with concanavalin A– conjugated with FITC 488 dye (25 µg/mL in PBS) for 45 minutes at 37°C. After incubation, the coverslips were washed three times with PBS

and mounted on glass slides. Stained biofilms were observed using Leica confocal laser scanning microscopy. Images were reconstructed using IMARIS software.

Chemogenomics profiling of *Saccharomyces cerevisiae*

Initial testing of *Saccharomyces cerevisiae* sensitivity to auranofin was performed with the wild-type BY4743 diploid strain, the isogenic parent to the heterozygous diploid deletion collection. BY4743 was grown in YPD in 96-well plates with 1% DMSO or auranofin in concentrations ranging from 10 to 200 μM to determine a suitable level of growth inhibition. Auranofin (75 μM) was used for haploinsufficiency profiling because it delayed growth by 30% compared to the no drug control half-maximal optical density (OD). All experiments were performed at 30°C and cultures were shaken at 300 rpm. The heterozygous deletion set was purchased in a pooled format (Thermo Fisher Scientific, Waltham, MA). A frozen aliquot (200 μL) was thawed and used to inoculate 2 mL of YPD and grown for 9 h to reach an OD_{600} of 4.0. The culture was diluted to an OD_{600} of 0.13 and either 1% DMSO or 75 μM auranofin was added (three replicates each, 1 mL) and grown for 7 h. The cultures were grown again by diluting to an OD of 0.13 in 1 mL YPD with DMSO or 60 μM auranofin and grown for 8 h. Cultures were harvested and genomic DNA extracted using the YeaStar Genomic DNA kit (Zymo Research, Irvine, CA). The UPTAGs were amplified by PCR with Phusion Hot Start II High-Fidelity DNA polymerase at 0.02 U/μL (Thermo Fisher Scientific, Waltham, MA) using 0.5 ng/μL genomic DNA. Primers are listed (Table S1). The PCR reactions were electrophoresed on an agarose gel and the 267 bp product extracted using a QIAquick Gel Extraction Kit (Qiagen, Valencia, CA). Purified DNA was measured using a Qubit instrument and samples were normalized

and mixed together to a final concentration of 10 nM. Strains were grown and maintained on media according to standard practices [366].

The pooled PCR products were sequenced using standard Illumina sequencing in a HiSeq 2500 instrument. The reads were separated based on a 5 base multiplex tag unique for each experiment and an average of 5 million reads per replicate was obtained. The UPTAG barcodes in each experimental sample were separated based on a reference database of recharacterized barcode sequences [367].

The resulting strain counts were imported into R and analyzed with edgeR [368]. Sequencing library sizes were normalized using the default parameters. Only strains with one or more counts in three or more samples were analyzed further. Differential representation of strains was determined using the quantile-adjusted conditional maximum likelihood (qCML) method. False discovery rates were determined to control for multiple testing.

Saccharomyces deletion strain haploinsufficiency validation

Overnight grown yeast cells were diluted ($O.D_{600}$ ~ 0.03) and grown in the presence and absence of auranofin, at indicated concentrations. Growth was monitored using a spectrophotometer (OD_{600}) at indicated time points and the results were expressed as percent growth rate for each strain compared to the untreated control group. To assess growth on solid medium, 5 µL of ten-fold diluted yeast cells were spotted onto YPD agar containing DMSO or auranofin (6.25 µg/mL). Growth of yeast strains was monitored after incubating the plates for 48 h, as described elsewhere [369].

Oxygen consumption and membrane potential measurements

Mitochondria were purified from yeast cells grown on YPEG as described previously [370]. Oxygen consumption measurements with isolated mitochondria were performed using an oxygen electrode (Hansatec) as described previously [371]. Membrane potential measurements of purified mitochondria were performed with fluorescent 3, 3'-dipropylthiadicarbocyanine iodide dye *[*DiSC3(5)]. 1% DMSO, carbonyl cyanide *m*-chlorophenyl hydrazone (CCCP), MB-6, or MB-7 was added to mitochondria in import buffer (0.6 M sorbitol, 2 mM KH_2PO_4, 60 mM KCl, 50 mM HEPES-KOH, 5 mM $MgCl_2$, 2.5 mM EDTA,5 mM L-methionine, pH 7.1) for 10 min. Subsequently 0.2 μM DiSC3(5) in import buffer was added, incubated for 5 min, and fluorescence was measured at excitation and emission length of 620 nm and 670 nm, respectively.

Purification of mitochondria

Mitochondria were purified from wild-type yeast or yeast overexpressing Erv1 with a hexahistidine tag ([a2up] Erv1) grown in YPEG as described previously [372,373]. Yeast cultures were kept at 25°C with vigorous shaking during growth. Mitochondria concentration was measured by BCA assay and stored at 25 mg/mL at -80°C. Mitochondria with increased levels of Erv1 were purified from a strain in which Erv1 was overexpressed from a 2-micron plasmid (Dabir et al., 2007).

Import of radiolabeled proteins into yeast mitochondria

Prior to import into purified mitochondria, [^{35}S]-methionine and cysteine labeled proteins were generated with TNT Quick Coupled Transcription/Translation kits (Promega) and

plasmids carrying the genes of interest. Transcription of genes was driven by either a T7 or SP6 promoter. Import reactions were conducted as previously described [370,371]. After frozen mitochondria aliquots were thawed and added to the import buffer at a final concentration of 100 µg/mL, 1% DMSO or the small molecule was added as indicated. A final concentration of 1% DMSO was used in all experiments. Following incubation at 25°C for 15 min, import reactions were initiated by the addition of 5-10 µl of translation mix. Aliquots were removed at intervals during the reaction time course and import was terminated with addition either of cold buffer or 25 µg/mL trypsin, or the combination. If trypsin was added to digest non-imported precursor protein, soybean trypsin inhibitor was subsequently added in excess after 15 min incubation on ice. After a final recovery of by centrifugation (12,000 x *g*, 6 min), mitochondria were disrupted in Laemmli sample buffer. Samples from import reaction time points were resolved by SDS-PAGE and visualized by autoradiography. For experiments to investigate the Cmc1-Mia40 intermediate, nonreducing conditions were used. The import reactions were stopped in the presence of 20 mM iodoacetamide and mitochondria disrupted in Laemmli sample buffer lacking β-mercaptoethanol. The imported products were separated by nonreducing SDS-PAGE.

Caenorhabditis elegans (*C. elegans*) infection study

L4-stage worms of *C. elegans* AU37 (sek-1; glp-4) strain (glp-4(bn2) were used to examine the antifungal efficacy of auranofin as described elsewhere [226,374]. Briefly, L4-stage worms were infected with *Cryptococcus neoformans* NR-41292 for two hours at room temperature. After infection, worms were washed with M9 buffer and treated either with DMSO or drugs (auranofin, fluconazole, and flucytosine), at a concentration of 8 µg/mL. After 24 h, worms

were washed with PBS and disrupted using silicon carbide particles [226]. The final suspensions were plated onto YPD agar plates containing ampicillin (100 μg/mL), streptomycin (100 μg/mL) and kanamycin (45 μg/mL) to determine the colony forming unit (CFU) per worm [66].

Statistical analyses

Statistical analyses were done using GraphPad Prism 6.0 (GraphPad Software, La Jolla, CA). *P* values were calculated via the Student *t* test and *P* values of ≤ 0.05 were deemed significant.

3.1.3 Results and Discussion

Antifungal activity and killing kinetics of auranofin

Auranofin has a well-established pharmacological and toxicological profile that has permitted it to be used for the treatment of rheumatoid arthritis for more than 30 years [47,48]. Independent of its antirheumatic effect, several studies have reported the anti-infective properties of this drug against important parasitic and bacterial pathogens including *Schistosoma mansoni*, *Trypanosoma brucei*, *Plasmodium falciparum*, *Entamoeba histolytica*, *Staphylococcus aureus* and *Streptococcus pneumoniae* [58,212,215,249,263,357,358]. In this study, the antifungal activity of auranofin was tested against various clinical isolates of *Candida* and *Cryptococcus*. Auranofin retains efficacy against clinically relevant drug-resistant fungal strains including fluconazole-resistant *C. albicans*, *C. glabrata*, *C. tropicalis* and *C. parapsilosis* with the minimum inhibitory concentration (MIC) ranging

Table 3.1 MIC of auranofin and control antifungal drugs against Candida and Cryptococcus strains

Strains	Description	Auranofin (µg/ml)	Fluconazole (µg/ml)	Flucytosine (µg/ml)
C. albicans NR 29434	Bloodstream isolate from a person with a bloodstream infection collected in Winnipeg, Manitoba, Canada, in 2000	8	4	0.125
C. albicans ATCC 10231	Isolated from a man with bronchomycosis	2	2	0.25
C. albicans NR 29449	Is a vaginal isolate from a person with vaginitis collected in Ann Arbor, Michigan, USA, between 1990 and 1992	8	2	4
C. albicans NR 29435	Is a bloodstream isolate from a person with a bloodstream infection collected in Iowa City, Iowa, USA, in 2000.	1	4	0.0625
C. albicans NR 29448	Is an isolate from a person with a bloodstream infection, collected in Arizona, USA.	4	>64	0.0625
C. albicans NR 29437	Is a bloodstream isolate from a person with a bloodstream infection collected in Brussels, Belgium in 2000	4	2	0.0625
C. albicans NR 29446	Is a bloodstream isolate from a person with a bloodstream infection collected in Utah, USA.	16	>64	0.25
C. albicans NR 29453	Is an oral isolate from an HIV+ person collected in Pretoria, South Africa	8	2	0.0625
C. albicans NR 29438	Is a bloodstream isolate from a person with a bloodstream infection, collected in Tel-Hashomer, Israel, in 2000.	16	2	0.0625
C. albicans ATCC 26790	Pulmonary candidiasis	8	2	0.0625
C. albicans ATCC 24433	Nail infection	8	4	1
C. albicans ATCC 14053	Human blood, Bethesda, MD	8	4	0.125
C. albicans ATCC 90028	Blood, Iowa	16	4	1
C. albicans NR 29366	Human isolate collected in China	16	>64	0.0625
C. albicans NR 29367	Human isolate collected in China.	16	>64	0.0625
C. glabrata ATCC MYA-2950	-	8	4	0.0625
C. glabrata ATCC 66032	-	8	2	0.0625
C. tropicalis ATCC 13803	-	16	2	0.125
C. tropicalis ATCC 1369	-	4	1	0.25
C. parapsilosis ATCC 22019	Case of sprue, Puerto Rico	4	1	0.25

Table 3.1 continued

C. neoformans NR-41291	Obtained from human cerebrospinal fluid in China in July 2011.	4	1	0.5
C. neoformans NR-41292	Obtained from human cerebrospinal fluid in China in February 2012.	0.5	1	0.5
C. neoformans NR-41296	Obtained from human cerebrospinal fluid in China in February 2012.	1	2	0.5
C. neoformans NR-41295	Obtained from human cerebrospinal fluid in China in February 2012.	4	2	0.5
C. neoformans NR-41294	Obtained from human cerebrospinal fluid in China in June 2011.	0.5	4	2
C. neoformans NR-41297	Obtained from human cerebrospinal fluid in China in February 2012.	1	8	4
C. neoformans NR-41298	Obtained from human cerebrospinal fluid in China in February 2012.	1	4	2
C. neoformans NR-41299	Obtained from human cerebrospinal fluid in China in August 2009.	4	4	2
C. neoformans NR-41291	Obtained from human cerebrospinal fluid in China in July 2011.	1	4	1
Cryptococcus gattii - CBS1930	Isolated from a goat in Aruba prior to the outbreak in Vancouver, British Columbia, Canada.	0.5	2	2
Cryptococcus gattii - R265	Isolated from a human on Vancouver Island, Canada during the outbreak that began in the late 1990's	1	1	1
Cryptococcus gattii - Alg40	Progeny of a genotypic cross between *C. gattii* strains R265 and CBS1930.	0.5	2	0.5
Cryptococcus gattii - Alg75	Progeny of a genotypic cross between *C. gattii* strains R265 and Alg40.	8	8	8
Cryptococcus gattii - Alg81	Progeny of a genotypic cross between *C. gattii* strains R265 and Alg75.	4	8	4
Cryptococcus gattii - Alg99	Progeny of a genotypic cross between *C. gattii* strains R265 and Alg81.	4	8	4
Cryptococcus gattii - Alg114	Progeny of a genotypic cross between *C. gattii* strains R265 and Alg99.	8	8	4
Cryptococcus gattii - Alg115	Progeny of a genotypic cross between *C. gattii* strains R265 and Alg114.	8	8	4
Cryptococcus gattii - Alg127	Progeny of a genotypic cross between *C. gattii* strains R265 and Alg115.	4	4	4

from 1 to 16 µg/mL (Table 3.1). Auranofin also displayed potent activity against both *C. neoformans* and *Cryptococcus gattii* inhibiting growth of these fungal species at concentrations ranging from 0.5 to 8 µg/mL (Table 3.1).

A time-kill assay was employed to investigate the killing kinetics of auranofin against both *C. albicans* and *C. neoformans*. Similar to fluconazole, auranofin (at 5 × MIC) exhibited

fungistatic activity against *C. albicans* and *C. neoformans* (Figure 3.1). However, at 10 × MIC, auranofin (unlike fluconazole) completely kills *C. neoformans* after 48 h of incubation (Figure 3.1).

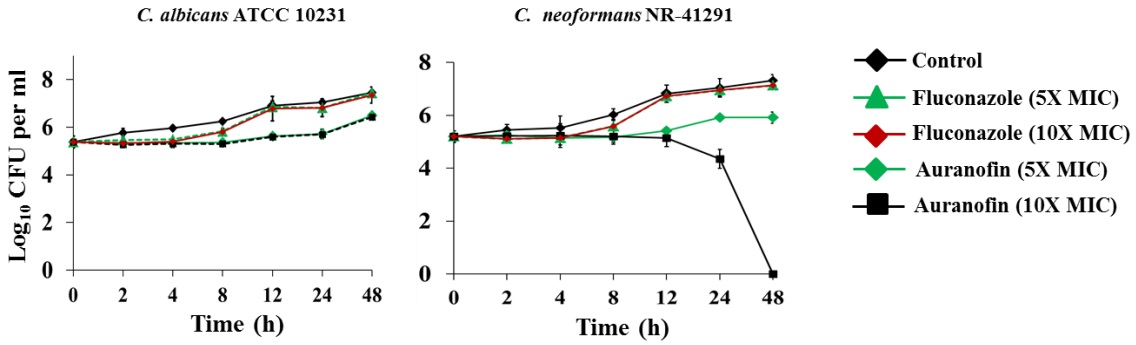

Figure 3.1Killing kinetics of auranofin. An overnight culture of *C. albicans* ATCC 10231 and *C. neoformans* NR-41291 were treated with 5 × and 10 × MIC of auranofin and fluconazole (in triplicate) in RPMI-MOPS and incubated at 35°C. Samples were collected at indicated time points and plated onto YPD plates. Plates were incubated for 24-48 h prior to counting the colony forming units (CFU).

Antibiofilm activity of auranofin

In addition to planktonic growth, fungi especially, *Candida* spp., are known to form biofilms that are recalcitrant to treatment with antifungal agents. Fungal cells encased within the biofilm are resistant to most clinically used antifungals, including azole drugs, ultimately resulting in treatment failure [375-377].

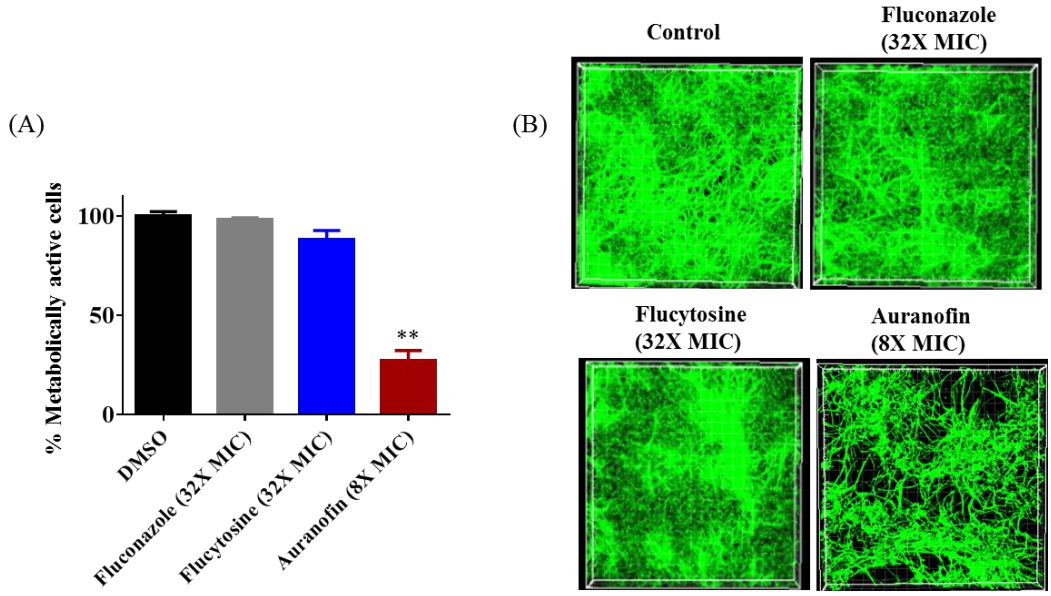

Figure 3.2 Effect of auranofin on *Candida* biofilms. (A) *C. albicans* ATCC 10231 biofilm was treated with indicated concentrations of auranofin, fluconazole, and flucytosine for 24 h. The percent metabolic activity of fungal cells in biofilms, after treatment, was determined using the XTT reduction assay. Results are presented as means ± SD (n = 3). Statistical analysis was calculated using the two-tailed Student's *t* test. *P* values of (** $P \leq 0.01$) are considered as significant. Auranofin was compared both to controls and antifungal drugs (**). (B) *C. albicans* ATCC 10231 biofilm was formed on FBS-coated glass cover slips and treated with indicated drugs for 24 h and stained with concanavalin A– conjugated with FITC dye and imaged by Leica confocal laser scanning microscopy.

Therefore, the antibiofilm activity of auranofin, against *C. albicans*, was evaluated using the XTT reduction assay in order to measure the metabolic activity of fungal cells post-treatment. The metabolic activity of *C. albicans* was reduced by more than 70% with the treatment of auranofin (Figure 3.2A). Fluconazole and flucytosine, were ineffective (less than 10% reduction observed) at reducing the metabolic activity of *C. albicans* biofilm, even at a concertation equivalent to 32 × MIC (Figure 3.2A).

The effect of auranofin on reducing fungal biofilm density was further evaluated using confocal microscopy. Fungal cells stained with ConA-conjugated with FITC revealed that auranofin (8 × MIC) eradicates a considerable portion of *Candida* cells in comparison to the control group (Figure 3.2B). However, treatment with fluconazole and flucytosine, even at 32 × MIC, appear similar to control group (Figure 2B). These findings illustrate that auranofin is a potential candidate for use in treatment of biofilm-related fungal infections.

Chemogenomic profiling identifies Mia40 as a potential target of auranofin

After verifying auranofin's antifungal activity, we proceeded to investigate the antifungal mechanism of auranofin. Chemogenomic profiling was employed given it is a highly-specific technique to investigate the target of unknown compounds [378-380]. This technique uses drug-induced haploinsufficiency, where it causes a strain-specific fitness defect after treatment with compounds, and thereby aids in identifying the drug target [378-383]. Haploinsufficiency profiling (HIP) allows for the simultaneous assessment of the sensitivity of the pooled genome-wide set of heterozygous deletion strains because each strain is uniquely identified with a synthetic DNA barcode. The method is an unbiased approach to survey the genome-wide strain set in order to identify the strains with the most sensitivity to auranofin. We first identified the concentration that reduced wild-type growth by 30% and used 75 μM to profile the pooled heterozygous strains in biological samples. PCR was used to amplify the unique UPTAG DNA barcodes located at the gene deletion site and we tracked the barcode abundance with Illumina sequencing. The resulting counts were normalized and visualized using EdgeR (Figure 3.3A). We identified 85

heterozygous deletion strains that were under-represented based on an FDR less than 0.1 when comparing auranofin treatment to DMSO. These 85 strains were analyzed to identify associated gene ontology cellular component annotations and found to be enriched in several categories including the mitochondrial intermembrane space and chromatin components. Five heterozygous deletion strains within these categories (*mia40Δ*, *acn9Δ*, *coa4Δ*, *rad18Δ* and *nsi1Δ*) were selected to validate sensitivity to auranofin using a variety of growth assays (Figure 3.3A).

Growth of these five heterozygous deletion strains and the wild-type (BY4743) strain were monitored in the presence of different concentrations of auranofin (6.25, 12.5 and 25 µg/mL) in a liquid growth assay. The result indicated that only three heterozygous deletion strains (*mia40Δ*, *acn9Δ*, and *coa4Δ*) exhibited drug-induced haploinsufficiency under these conditions. The growth of these deletion strains was suppressed, even in the presence of low concentrations of auranofin (6.25 µg/mL) (Figure 3B). However, auranofin does not induce haploinsufficiency in the other two deletion strains (*rad18Δ* and *nsi1Δ*) as growth of these strains, in the presence of auranofin, mimics the pattern observed with the wild-type strain (Figure 3.3B). These two deletion strains were not affected possibly because of the concentration used in our validation studies or because they may be false positives.

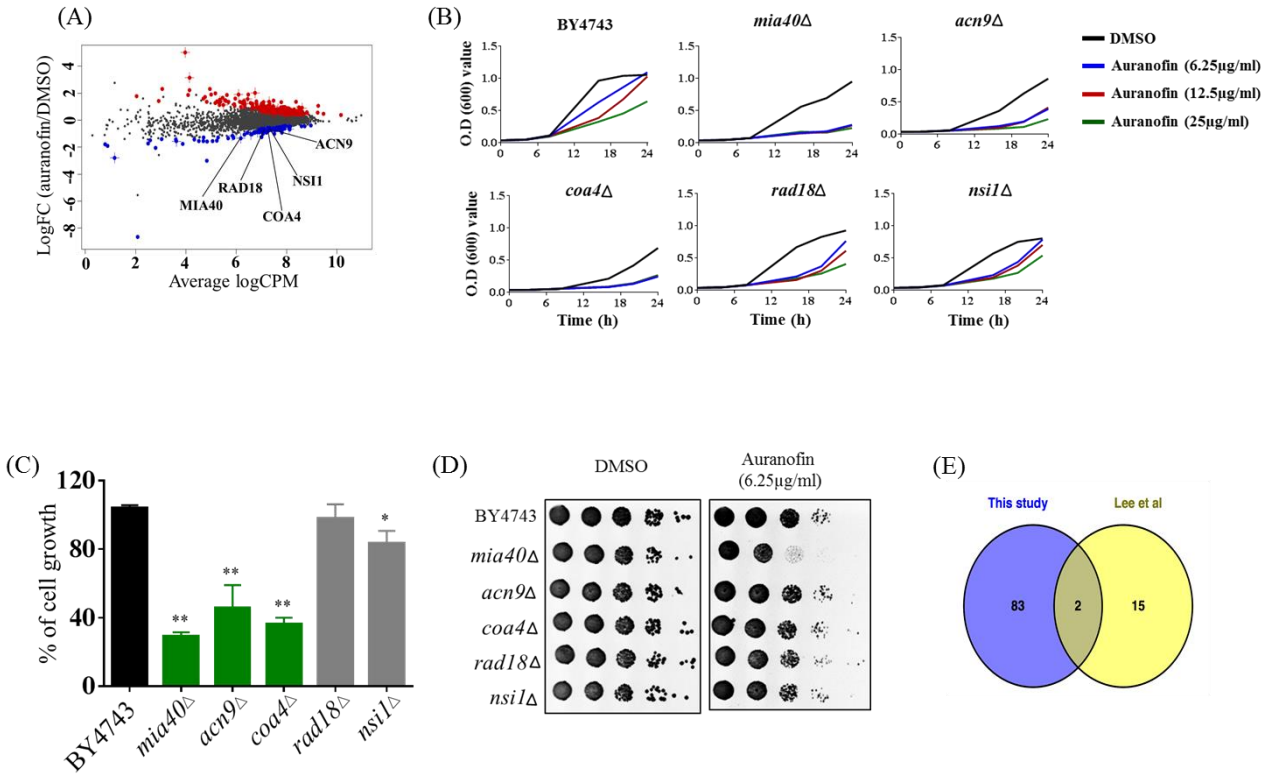

Figure 3.3 Auranofin targets mitochondrial protein(s). (A) Chemogenomic profiling of *S. cerevisiae* with treatment of auranofin. The strain abundance were normalized using EdgeR and shown. (B) Growth curve of wild type (BY4743) and heterozygous deletion strains (*mia40Δ*, *acn9Δ*, *coa4Δ*, *rad18Δ* and *nsi1Δ*) in the presence of indicated concentration of auranofin in YPD broth were determined. (C) The percent growth of yeast cells (OD_{600} after 24 h) incubated with auranofin (6.25 µg/mL) in YPD broth was determined in relation to the DMSO treatment. The results are presented as means ± SD (n = 3). Statistical analysis was calculated using the two-tailed Student's *t* test. *P* values of (* $P \leq 0.05$) (** $P \leq 0.01$) are considered as significant. (D) Yeast cells grown in YPD broth overnight were serially diluted and spotted on solid YPD agar containing auranofin (6.25 µg/mL) or DMSO and the CFU were shown. (E) Comparison of Lee *et al.*'s HIP results with our 85 strains are shown as a Venn diagram.

For each strain, the growth of cells (OD_{600} after 24 h) incubated with auranofin (6.25 µg/mL) was determined in relation to DMSO treatment. The growth of three heterozygous deletion strains (*mia40Δ*, *acn9Δ* and *coa4Δ*) was drastically suppressed by more than 50% in the presence of auranofin (6.25 µg/mL). However, the remaining two deletion strains (*rad18Δ* and *nsi1Δ*) had a modest reduction in growth of approximately 10% compared to the wild-type strain (Figure 3.3C).

The growth of these five deletion strains was further confirmed by spotting serial dilutions of cultures on solid agar. As shown in Figure 3.3D, growth of the wild-type and five heterozygous deletion strains was normal in agar containing DMSO. However, the heterozygous deletion strain, *mia40Δ,* exhibited a nearly two-fold reduction in colony forming units when spotted onto YPD agar containing auranofin (6.25 µg/mL).

A study conducted by Lee *et al.* [384] previously analyzed a heterozygous deletion pool representing essential genes using haploinsufficiency profiling and identified 17 strains as possibly sensitive to auranofin. Comparison of Lee *et al*.'s results with our 85 strains showed that two strains, *rho1Δ* and *mia40Δ*, overlapped in the data sets (Figure 3E). An additional study by Gamberi *et al.* [369] specifically assessed sensitivity of haploid deletion strains involved in mitochondrial function and found them to be differentially sensitive to auranofin. Based on studies by Gamberi *et al.* [369] and Lee *et al.* [384], we next moved to examine sensitivity of the corresponding heterozygous deletion strains involved in mitochondrial function and redox homeostasis that are possibly sensitive to auranofin.

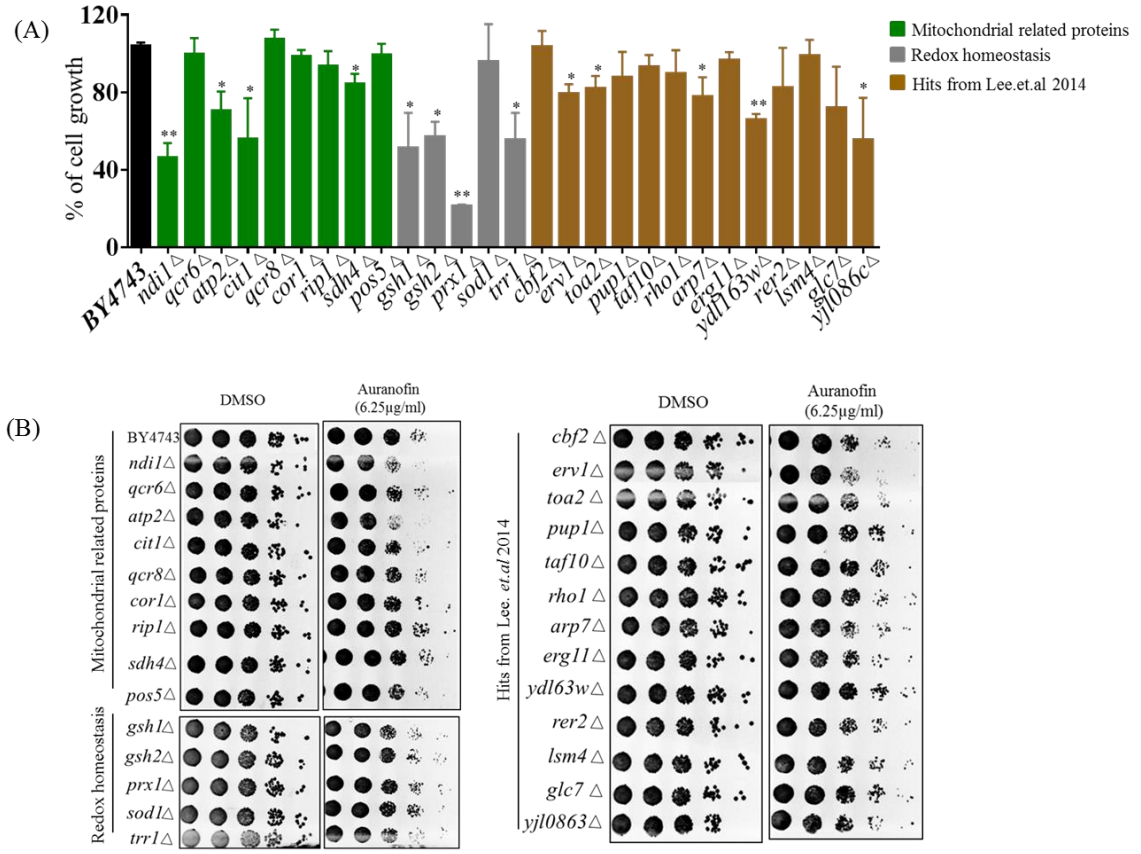

Figure 3.4 Effect of auranofin on deletion strains related to ROS production and mitochondrial function. (A) The percent growth of wild type and heterozygous deletion strains incubated with auranofin (6.25 µg/mL) in YPD broth (OD_{600} after 24 h) was determined in relation to the DMSO treatment. The results are presented as means ± SD (n = 3). Statistical analysis was calculated using the two-tailed Student's *t* test. *P* values of (* $P \leq 0.05$) (** $P \leq 0.01$) are considered as significant. (B) Yeast cells grown in YPD broth overnight were spotted on solid YPD agar containing auranofin (6.25 µg/mL) or DMSO. The colony forming units are shown.

Heterozygous deletion strains including *ndilΔ, atp2Δ, citlΔ, sdh4Δ, gsh1Δ, gsh2Δ, prx1Δ, trr1Δ, erv1Δ, toa2Δ, arp7Δ, ydl63wΔ and yjl086cΔ* experienced a significant growth reduction when treated with auranofin (6.25µg/mL) relative to DMSO-treated cells (Figure 3.4A). These results are in agreement with Gamberi *et al.*'s [369] and Lee *et al.*'s [384] reports. It should be noted that Gamberi *et al.* used haploid deletion strains which generally do not inform on direct targets of a compound as opposed to the heterozygous deletion strains used in our study. These results were confirmed using the YPD agar spotting assay. Interestingly, heterozygous deletion strains involved in ROS response and redox homeostasis (*sdh4Δ, gsh1Δ, gsh2Δ* and *prx1Δ*) which had significant growth reduction in liquid medium did not demonstrate considerable reduction in growth when spotted onto YPD agar containing auranofin (6.25 µg/mL) (Figure 3.4B). Gamberi *et.al*. through various experiments also demonstrated that auranofin does not elicit the production of ROS [369] but some haploid deletion strains associated with ROS were sensitive suggesting they are selectively important for resistance to auranofin. Taken together it appears that the ROS response enzymes are not direct targets of auranofin but several of these enzymes do mediate resistance to the inhibitory activity of auranofin.

As noted earlier, heterozygous deletion strains that encode genes required for mitochondrial function (including *ndilΔ, atp2Δ, citlΔ* and *erv1Δ*), showed a considerable decrease in colony count (almost one-fold log reduction) when spotted onto YPD agar containing auranofin (6.25µg/mL) (Figure 3.4B). More notably, the *pos5Δ* strain does not demonstrate any sensitivity to auranofin (Figure 4B). *POS5* encodes a mitochondrial NADH kinase required to respond to oxidative stress. This is in contrast to the haploid

deletion version, which was demonstrated to have slight resistance to auranofin [369]. Chemogenomic profiling by Lee *et al.* [369] also did not identify the *pos5Δ* heterozygous deletion strain as sensitive to auranofin. Interestingly, a deletion strain (*erv1Δ*), which forms a complex with Mia40, also showed considerable sensitivity to auranofin, which coincides with Lee *et al.*'s findings [385] (Figure 3.4B). Taken altogether, our findings support the notion that Mia40 is the probable antifungal target of auranofin.

The Mia40 (mitochondrial intermembrane space import and assembly protein 40) –Erv1 pathway is mainly involved in oxidation of several cysteine rich proteins that enter the mitochondria from the cytoplasm [385,386]. These proteins, present in the inner mitochondrial space, are essential for cell viability and are functionally linked to the respiratory chain [385,387]. In addition, an *erv1* mutant strain was shown to be deficient in respiration [388] consistent with the metabolic shift from respiration to fermentation observed in auranofin treated cells [369].

To further confirm the specific inhibition of the Mia40-Erv1 pathway by auranofin we employed several biochemical experiments using purified yeast mitochondria similar to a previous study that investigated the effect of several small molecule inhibitors of redox-regulated protein import into mitochondria [371]. A possible indirect mechanism of inhibition of mitochondrial function and the Mia40-Erv1 pathway is by the disruption of membrane potential or diminished oxidative phosphorylation. Maintenance of membrane potential was determined by mitochondrial uptake of DiSC3 (5) dye and subsequent quenching in the presence of membrane potential. Auranofin had no effect on the membrane potential

compared to DMSO whereas the uncoupling agent, CCCP, caused a 4-fold increase in fluorescence indicating uncoupled mitochondria (Figure 3.5A). The effect on mitochondrial respiration was determined by measuring dissolved oxygen in a chamber with purified mitochondria and respiration was initiated with NADH resulting in an oxygen consumption rate (-0.45 O_2 nmol/s) consistent with well-coupled mitochondria. The addition of DMSO did not increase respiration rate and auranofin at a concentration of 34µg/mL only slightly increased the respiration rate (-0.64 O_2 nmol/s) (Figure 3.5B). As a control, the addition of CCCP resulted in a severe increase in consumption rate (-1.15 O_2 nmol/s) suggestive of uncoupled mitochondria (Figure 3.5B). Overall, auranofin does not have a generalized mode of action resulting in the disruption of membrane potential or respiration and mitochondrial integrity is maintained in the presence of the compound.

To confirm that auranofin targets the Erv1/Mia40 pathway we measured the effect of compound on the import of mitochondrial protein substrates compared to control compounds previously identified as Erv1 inhibitors [371]. Radiolabeled precursor proteins were incubated with mitochondria in the presence of small molecules or DMSO and the reaction was terminated with protease and subsequently analyzed by gel electrophoresis. Protein substrates from different import pathways were assessed including the Tim23 substrate, Su9-DHFR, and the Mia40 substrate, Cmc1. Auranofin at a lower concentration of 6.8 µg/mL inhibits import of Su-DHFR to a 60% level and Cmc1 to a 25% level compared to untreated samples (Figure 3.5C and 3.5D). These results indicate the preferential activity of auranofin towards inhibiting Cmc1 import compared to Su9-DHFR, which is expected because Cmc1 is directly imported by Mia40/Erv1.

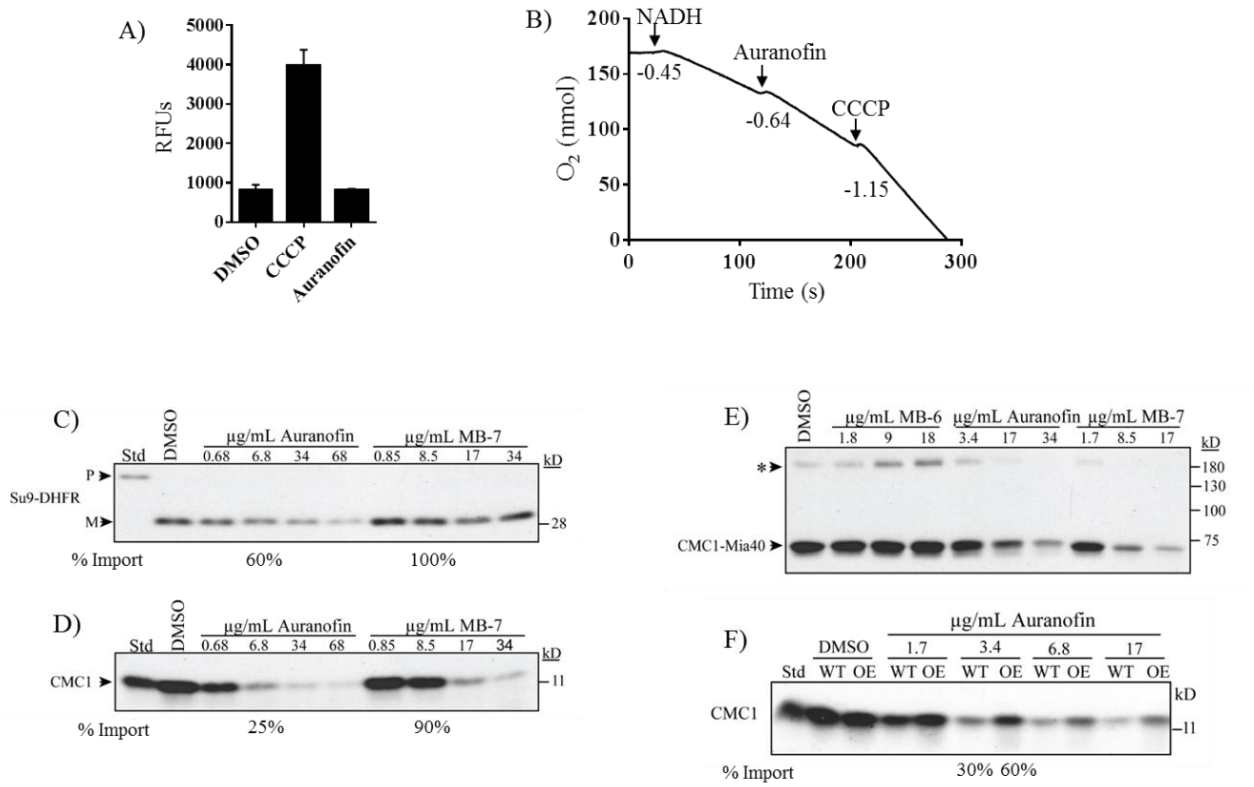

Figure 3.5 Auranofin does not impair general mitochondrial function but inhibits the import of substrates of the Mia40 pathway. (A) Mitochondrial uptake and quenching of DiSC3(5) dye when membrane potential is present. Dye fluorescence was measured as relative fluorescence units (RFUs) in the presence of DMSO, auranofin and CCCP. (B) Respiration of mitochondria was initiated by NADH followed by the addition of auranofin and CCCP. Respiration levels measurements were performed using an oxygen electrode and rates represent the consumption of O_2 nmol/s. (C, D) Radiolabeled proteins Su9-DHFR and Cmc1 were imported into mitochondria in the presence of varying concentrations of auranofin and MB-7. (E) Non-reducing gel demonstrating the formation of the Cmc1-Mia40 intermediate in the presence of auranofin, MB-6 and MB-7. (F) Auranofin inhibition of protein import is dependent on *in organello* mitochondrial Erv1 expression level. Wild-type (WT) and Erv1 overexpressed (OE) mitochondria were treated with varying concentrations of auranofin and the level of radiolabeled Cmc1 was detected. The asterisk represents a large complex of unknown composition that is observed in most Mia40 precursor studies. Representative gels have been shown (n = 3).

Strikingly, auranofin exhibits more potent activity than control compound, MB-7 with a drastic difference in import efficiency observed between the compounds at 10 μM (6.8μg/mL for auranofin and 8.5μg/mL for MB-7; Figure 3.5D). Although auranofin does inhibit Su9-DHFR import at high concentrations, these results demonstrate the compound has specificity towards the Mia40 pathway and increased potency compared to previously identified inhibitors from a large-scale chemical library screen [371]. It is not surprising that the import of Su9-DHFR is mildly inhibited because mitochondrial import pathways are interconnected. Mia40 has previously been demonstrated to form an intermediate with Cmc1 as part of the import process [389,390]. The effect of compounds on the formation of a disulfide intermediate between Mia40 and Cmc1 was monitored *in organello*. Auranofin inhibits radiolabeled Cmc1 from interacting with Mia40 in a similar dose dependent manner to MB-7 (Figure 3.5E). The addition of another control, MB-6, causes the accumulation of the intermediate. In sum, auranofin inhibits the heterodimer formation of the Mia40-Cmc1 intermediate and is a potent inhibitor of the Mia40 import pathway.

To further validate the Mia40 pathway as a target of auranofin, import of Cmc1 was performed with mitochondria from WT and Erv1 overexpressing yeast. Erv1 overexpression is expected to maintain the Mia40 pool in an oxidized state, which is required for the interaction with substrate proteins [373,391] and hence should be more resistant to auranofin inhibition. As predicted, the Erv1 overexpressing mitochondria were resistant to auranofin (3.4 μg/mL) treatment as evidenced by the increased level of Cmc1 (60%) import compared to WT (30%) mitochondria providing further confirmation of Mia40 as a target (Figure 3.5F).

It should also be taken into account the affinity of auranofin to human Mia40 protein. The central part of the human homolog of Mia40 shares high sequence identity with most of its eukaryotic analogues. However, Mia40 in yeast differs from its human homolog in one major respect – yeast Mia40 lacks the N-terminal extension including a transmembrane region [386]. Future studies are needed to examine the affinity and binding of auranofin to Mia40 and *in vivo* studies will determine if Mia40 function is affected. It may be possible that a therapeutic window exists because human Mia40 is not accessible or affected by auranofin at the concentrations needed for antifungal activity.

Previous studies in bacteria and parasites proposed thioredoxin reductase (TrxR) to be the target of auranofin [263,264]. However, a recent crystallographic study conducted by Parsonage *et al.* [392] revealed that auranofin most likely does not bind to the cysteine residues in TrxR of *Entamoeba histolytica.* As it pertains to yeast, Gamberi *et al*. used homozygous deletion strains and demonstrated that deletion of the mitochondrial thioredoxin reductase (*TRR2*) or glutathione reductase (*GLR1*) genes in *S. cerevisiae* do not display resistance to auranofin [369]. However, the effect of auranofin on the cytoplasmic thioredoxin reductase (*TRR1*) gene was not explored in their study [369]. Results from our investigation indicate that the heterozygous deletion strain (*trr1Δ*) behaves similar to the wild-type (Figure 4b). We therefore conclude that auranofin does not primarily target the thioredoxin reductase in yeast or fungi, which is in agreement with a previous study [369].

In vivo efficacy of auranofin in *C. neoformans* infected *C. elegans* model

To investigate if the *in vitro* antifungal activity of auranofin translates *in vivo*, the antifungal efficacy of auranofin was examined in a *C. neoformans*-infected *C. elegans* animal model. As shown in Figure 3.6, treatment of infected *C. elegans* with fluconazole, flucytosine and auranofin, at 8 µg/mL, produced a significant reduction ($P \leq 0.01$) in mean fungal load when compared to the untreated control groups.

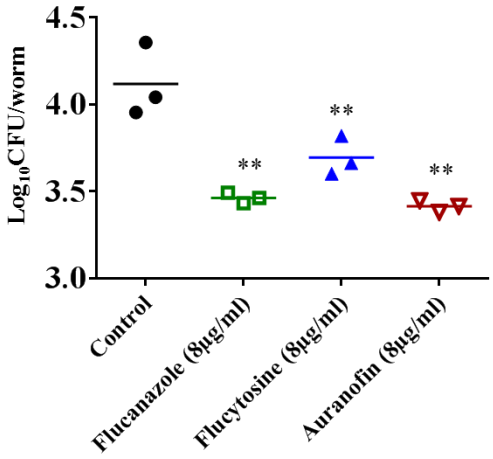

Figure 3.6 Efficacy of auranofin in *C. neoformans*-infected *C. elegans*. L4-stage worms were infected with *C. neoformans* and treated with auranofin, fluconazole, and flucytosine, at a concentration of 8 µg/mL. After 24 h, worms were lysed and plated onto YPD plates to determine the CFU per worm. Each dot represents average fungal load in each worm per well. The results are presented as means ± SD (n = 3). Statistical analysis was calculated using the two-tailed Student's *t* test. *P* value of (** $P \leq 0.01$) are considered as significant.

Strikingly, *C. elegans* treated with auranofin (8 µg/mL) generated the largest reduction in *C. neoformans* CFU (0.87±0.03 $\log_{10}$), followed by fluconazole (8 µg/mL) (0.82±0.03 $\log_{10}$) and flucytosine (8 µg/mL) (0.58±0.11 $\log_{10}$) (Figure 3.6). Altogether, results from

our study suggest that auranofin, with its unique mechanism of action and potent *in vivo* antifungal activity, warrants further investigation as an antifungal agent to combat drug-resistant fungal infections.

3.2 Ebselen exerts antifungal activity by regulating glutathione (GSH) and reactive oxygen species (ROS) production in fungal cells

(S. Thangamani, H. E. Eldesouky, H. Mohammad, P. Pascuzzi, L. Avramova, T. R. Hazbun and M. N. Seleem. Ebselen exerts antifungal activity by regulating glutathione (GSH) and reactive oxygen species (ROS) production in fungal cells. "*BBA- General Subjects*"-Under Review.)

3.2.1 Introduction

Ebselen (2-phenyl-1,2-benzisoselenazol-3(2H)-one) is an organoselenium compound that is known to possess anti-atherosclerotic, anti-inflammatory, antioxidative, cytoprotective, anti-mutagenic and anti-lipoperoxidative properties [59-62]. Several studies have demonstrated that ebselen, due to its highly electrophilic nature, interacts with cysteine rich proteins (such as thioredoxin) and non-proteins (thiols) [60,393-399]. Ebselen specifically interacts with free thiols such as glutathione (GSH) to form ebselen selenenyl sulfide; this intermediate catalyzes reactive oxygen species (ROS) formation. Interestingly, ebselen selenenyl sulfide can be reduced by GSH to form ebselen selenol. This particular intermediate functions as a ROS scavenger, and thereby protects the cell from free radical damage [60,394,395]. As a clinically safe molecule, ebselen has been investigated for the

treatment of various ailments such as arthritis, stroke, cardiovascular disease and cancer [60,63-66].

In addition to the beneficial properties of ebselen in mammalian cells, ebselen has also been investigated for its antimicrobial activity against multidrug-resistant *Staphylococcus aureus* and *Enterococcus* [67,68,211,226,400,401]. Recently, we demonstrated that ebselen exerts its antibacterial activity through the inhibition of protein synthesis in bacteria [211,226]. Ebselen has also been shown to possess potent antifungal activity, though different molecular targets have been proposed [69,402,403]. Studies by Billack et.al and Chan et.al demonstrated that ebselen inhibits the plasma membrane H(+)-ATPase pump (Pma1p) in yeast [69,403]. Azad et.al proposed that ebselen inhibits glutamate dehydrogenase (GDH3) and induces ROS production in yeast [404]. A follow-up study by their research group also proposed that ebselen activates the DNA damage response and alters nuclear proteins in yeast [405]. The studies above highlight that the antifungal mechanism of action of ebselen is challenging to elucidate and currently remains unresolved.

Given the tremendous pressure imposed by the emergence of resistance to antifungal agents currently utilized in the clinic, identifying new classes of antifungal drugs remains an unmet challenge [355,356,406,407]. However, the traditional pathway for drug discovery is an arduous process that yields few approved new antimicrobials annually. An alternative approach steadily gaining support is utilizing drug repurposing to identify promising new anti-infective agents and expedite their regulatory approval [210,356].

Based upon the preliminary data presented in literature, ebselen is a promising drug to repurpose as a novel antifungal agent. However, additional research is necessary to

elucidate ebselen's antifungal mechanism of action. Thus, the objectives of our study were to examine ebselen's spectrum of activity against an array of fungal clinical isolates, to deduce ebselen's antifungal mechanism of action, and to confirm the drug's *in vivo* efficacy in two *Caenorhabditis elegans* animal models of fungal infection.

3.2.2 Materials and Methods

Fungal strains and reagents

Candida and *Cryptococcus* strains used in this study are presented in Table 1. RPMI powder, MOPS and L-reduced glutathione were purchased from Sigma-Aldrich (St. Louis, MO). Yeast peptone dextrose agar (YPD) **(**BD Biosciences, San Jose, CA), fluconazole (Acros Organics, New Jersey), flucytosine and ebselen (TCI chemicals, Tokyo, Japan) were purchased from commercial vendors.

Antifungal susceptibility testing

Antifungal susceptibility testing was done as per the National Committee for Clinical Laboratory Standards M-27A3 (NCCLS) guidelines [361]. Briefly, five colonies from 24-hour old cultures of *Candida* spp. or 48-hour old cultures of *Cryptococcus* were transferred to 5 ml of sterile 0.9% saline (PBS). After adjusting to reach a McFarland standard 0.5, fungal suspensions were diluted 1:2000 in RPMI 1640 buffered to pH 7.0 with 0.165 M MOPS (RPMI-MOPS). The drugs (ebselen, ebselen, fluconazole, flucytosine and amphotericin) were serially diluted and the minimum inhibitory concentration (MIC) was determined as follows: (i) For fluconazole and flucytosine, the MIC was classified as a significant decrease (approximately 50%) in visible growth compared to untreated controls;

(ii) For ebselen and amphotericin B, the MIC was categorized as the lowest concentration that produced no visible fungal growth. All experiments were carried out in triplicate wells.

Time kill assay

Cultures of *Candida albicans* and *Cryptococcus neoformans* at a dilution of 5×10^5 CFU/ml were treated with 5 × MICs of ebselen, fluconazole, flucytosine and amphotericin B (in triplicate) in RPMI-MOPS, at 35°C. At specific time points, aliquots were collected, serially diluted in PBS, and plated onto YPD agar plates. After incubation at 35°C for 24-48 hours the fungal colony forming units (CFU) were obtained, as described elsewhere [362].

Chemogenomics profiling of *Saccharomyces cerevisiae*

The initial testing of *Saccharomyces cerevisiae* response to ebselen was performed with the wild type BY4743 diploid strain, the isogenic parent to the heterozygous diploid deletion collection. BY4743 was grown in YPD in 96-well plates with 1% DMSO or ebselen in concentrations ranging from 10 to 200 μM to determine a suitable level of growth inhibition. Ebselen (25 μM) was used for haploinsufficiency profiling because it delayed growth by 30% compared to the no drug control half-maximal optical density (OD). All experiments were performed at 30°C and cultures were shaken at 300 rpm. A frozen aliquot (200 μL) of the heterozygous deletion pool (Thermo Fisher Scientific, Waltham, MA) was thawed and used to inoculate 2 mL of YPD and grown for 9 hours to reach an OD_{600} of 4.0. The culture was diluted to an OD_{600} of 0.13 and either 1% DMSO or 25 μM ebselen was added (three replicates each) and grown for 7 hours. The cultures were grown again by diluting to an OD_{600} of 0.13 in 1 mL YPD with DMSO or 25 μM ebselen and

grown for 8 hours, harvested and genomic DNA extracted using the YeaStar Genomic DNA kit (Zymo Research, Irvine, CA). The UPTAGs were amplified by PCR with Phusion Hot Start II High-Fidelity DNA polymerase at 0.02 U/µL (Thermo Fisher Scientific, Waltham, MA) using 0.5 ng/µL genomic DNA. The 267 bp PCR product was electrophoresed on an agarose gel and the DNA extracted using a QIAquick Gel Extraction Kit (Qiagen, Valencia, CA). Purified DNA was measured using a Qubit instrument and samples were normalized and mixed to a final concentration of 10 nM. Strains were grown and maintained on media using standard practices [366].

The pooled PCR products were sequenced using standard Illumina sequencing in a HiSeq 2500 instrument. The reads were separated based on a 5 base multiplex tag unique for each experiment and an average of 5 million reads per replicate was obtained. The UPTAG barcodes in each experimental sample were separated based on a reference database of recharacterized barcode sequences [367].

The resulting strain counts were imported into R and analyzed with edgeR [368]. Sequencing library sizes were normalized using default parameters. Only strains with one or more counts in three or more samples were analyzed further. Differential representation of strains was determined using the quantile-adjusted conditional maximum likelihood (qCML) method. False discovery rates were determined to control for multiple testing.

Saccharomyces deletion strain haploinsufficiency validation

Overnight grown saturated cultures of yeast cells were diluted to 1 to 10 and further to 1 to 5000 before treating with indicated concentration of ebselen. After 24 hours of incubation,

yeast growth was monitored using a spectrophotometer (OD_{600}) and the results were expressed as percent growth rate for each strain compared to the untreated control group, as described elsewhere [369].

Determining fungal growth with L-reduced glutathione supplementation

In experiments with L-reduced glutathione supplementation, indicated concentration of glutathione was added to the fungal cultures (with or without ebselen) and the percent growth rate or MIC was determined as described above.

Glutathione assay

The assay was conducted as per the manufacturer's instructions (Glutathione assay kit from Cayman chemicals, Michigan, USA). Briefly, saturated cultures of wild type and deletion strains of *S. cerevisiae* cells were diluted to 1:5 in YPD broth and treated with ebselen (20 µg/ml) for 2.5 hours. After treatment, tubes were centrifuged. The cells were subsequently washed once with cold water and followed by 1 × GSH MES buffer (supplied by the manufacturer). After washing, cells were re-suspended in 250 µL of 1 × GSH MES buffer and sonicated for 45 seconds. Tubes were centrifuged and the supernatant was collected for the assay. An aliquot (50 µL) of cell supernatant was added to each well in a 96-well plate and then 150 µL of the assay cocktail, prepared per the manufacturer's guidelines, was added. After two minutes of incubation, the intensity of yellow color produced was measured using a spectrophotometer (OD_{410}). The results are expressed either as absorbance per ml or percent glutathione production relative to untreated control groups.

Measuring ROS production in yeast cells

The Image-iT™ LIVE Green Reactive Oxygen Species (ROS) detection kit (Molecular Probes, Inc. Eugene, OR) was utilized and the ROS production was measured as per the manufacturer's instructions. Briefly, saturated cultures of wild type and deletion strains of *S. cerevisiae* cells were diluted to 1:5 in YPD broth and treated with ebselen (20 μg/ml) for 2.5 hours. Then 10mM of 5-(and-6)-carboxy-2',7'-dichlorodihydrofluorescein diacetate (carboxy-H_2DCFDA) dye was added at a dilution of 1:500. After 2 hours of incubation, the cells were washed once with PBS and the intensity of fluorescence produced was measured using spectrophotometer or imaged by Leica confocal laser scanning microscopy.

Caenorhabditis elegans (*C. elegans*) infection study

C. elegans AU37 (sek-1; glp-4) strain (glp-4(bn2) was used to investigate the antifungal efficacy of ebselen, as described elsewhere [226,374]. Briefly, L4-stage worms were infected either with *Cryptococcus neoformans* NR-41292 or *Candida albicans* ATCC 10232 for two-three hours at room temperature. After infection, worms were washed with M9 buffer and treated for 24 hours either with DMSO or drugs (ebselen, amphotericin B, fluconazole, and flucytosine), at indicated concentrations. Post-treatment, worms were washed, disrupted using silicon carbide particles [226], and the resulting suspensions were serially diluted and transferred to YPD agar plates containing ampicillin (100 μg/ml), streptomycin (100 μg/ml) and kanamycin (45 μg/ml). Plates were incubated for 24-48 hours at 35°C before the colony forming unit (CFU) per worm was determined [66].

Statistical analyses

Statistical analyses were done using GraphPad Prism 6.0 (GraphPad Software, La Jolla, CA). *P* values were calculated using the Student *t* test. *P* values ≤ 0.05 were deemed significant.

3.2.3 Results

Antifungal activity and killing kinetics of ebselen

Ebselen's antifungal activity was examined against numerous clinical isolates of *Candida* and *Cryptococcus*. Ebselen inhibited isolates of *Candida albicans, C. glabrata, C. tropicalis* and *C. parapsilosis* at concentrations ranging from 0.5 to 2 µg/ml (Table 3.2). Ebselen retained its potent antifungal activity against *Cryptococcus neoformans* and *Cryptococcus gattii*, as the drug inhibited growth of these fungal species at concentrations ranging from 0.5 to 1 µg/ml (Table 3.2).

In order to investigate the killing kinetics of ebselen against both *C. albicans* and *C. neoformans*, a time-kill assay was conducted. Unlike fluconazole and flucytosine, ebselen (at 5 × MIC) completely eradicated *C. albicans* ATCC 10231 and *C. neoformans* NR-41291 within two hours of treatment (Figure 3.7). Ebselen's fungicidal activity was superior to amphotericin which required at least four hours to completely eliminate fungal cells (Figure 3.7).

Table 3.2. MIC of ebselen and control antifungal drugs against *Candida* and *Cryptococcus* strains

Strains	Fluconazole (µg/ml)	Flucytosine (µg/ml)	Amphotericin (µg/ml)	Ebselen (µg/ml)
C. albicans NR 29434	4	0.125	1	1
C. albicans ATCC 10231	2	0.25	0.5	2
C. albicans NR 29449	2	4	1	2
C. albicans NR 29435	4	0.0625	0.5	2
C. albicans NR 29448	>64	0.0625	1	2
C. albicans NR 29437	2	0.0625	1	2
C. albicans NR 29446	>64	0.25	0.5	1
C. albicans NR 29453	2	0.0625	0.5	2
C. albicans NR 29438	2	0.0625	1	2
C. albicans ATCC 26790	2	0.0625	1	2
C. albicans ATCC 24433	4	1	1	2
C. albicans ATCC 14053	4	0.125	1	2
C. albicans ATCC 90028	4	1	1	2
C. albicans NR 29366	>64	0.0625	1	4
C. albicans NR 29367	>64	0.0625	1	2
C. glabrata ATCC MYA-2950	4	0.0625	1	0.5
C. glabrata ATCC 66032	2	0.0625	2	0.5
C. tropicalis ATCC 13803	2	0.125	1	2
C. tropicalis ATCC 1369	1	0.25	1	2
C. parapsilosis ATCC 22019	1	0.25	1	1
C. neoformans NR-41291	1	0.5	1	1
C. neoformans NR-41292	1	0.5	0.5	0.25
C. neoformans NR-41296	2	0.5	0.5	0.5
C. neoformans NR-41295	2	0.5	0.5	0.5
C. neoformans NR-41294	4	2	0.5	0.5
C. neoformans NR-41297	8	4	0.5	1
C. neoformans NR-41298	4	2	0.5	1
C. neoformans NR-41299	4	2	1	1
Cryptococcus gattii - CBS1930	2	2	0.5	0.5
Cryptococcus gattii - R265	1	1	0.5	0.5
Cryptococcus gattii - Alg40	2	0.5	0.5	0.5
Cryptococcus gattii - Alg75	8	8	0.5	2
Cryptococcus gattii - Alg81	8	4	0.5	2
Cryptococcus gattii - Alg99	8	4	1	2
Cryptococcus gattii - Alg114	8	4	1	2
Cryptococcus gattii - Alg115	8	4	1	2
Cryptococcus gattii - Alg127	4	4	1	2

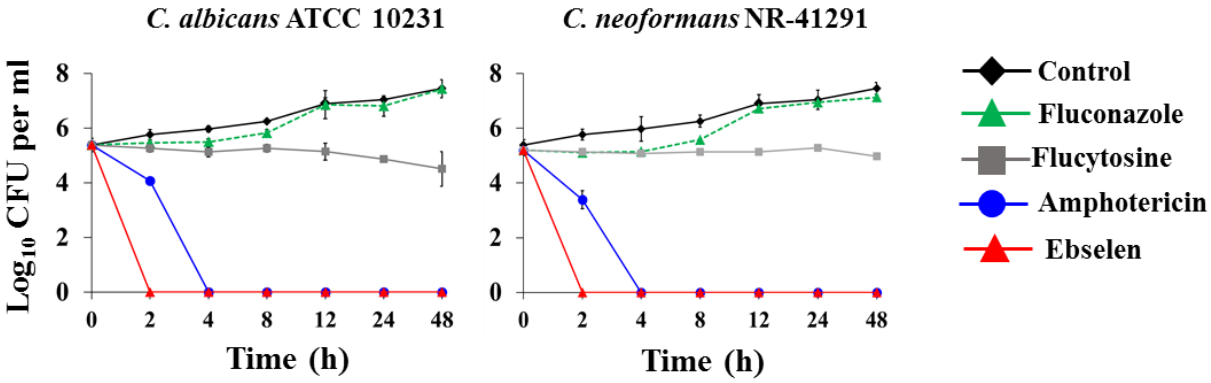

Figure 3.7 Killing kinetics of ebselen. An overnight culture of *C. albicans* ATCC 10231 and *C. neoformans* NR-41291 were treated with 5 × of ebselen, fluconazole, flucytosine and amphotericin (in triplicate) in RPMI-MOPS and incubated at 35°C. Samples were collected at indicated time points and plated onto YPD plates. Plates were incubated for 24-48 h prior to counting the colony forming units (CFU).

Glutathione as a potential target of ebselen

After verifying ebselen's potent antifungal activity, we proceeded to investigate the antifungal mechanism of ebselen. Chemogenomic profiling, using drug-induced haploinsufficiency, was utilized due to its nature as a highly-specific technique to deduce the molecular mechanism of unknown compounds [378-380]. Haploinsufficiency profiling (HIP) allows for the simultaneous assessment of the sensitivity of the pooled genome-wide set of heterozygous deletion strains due to the fact that each strain possesses a unique synthetic DNA barcode. The method is an unbiased approach to find strains exhibiting the most sensitivity to ebselen. After determining the concentration that reduced wild-type growth by 30%, we used 25 μM of drug to profile the pooled heterozygous strains in the biological samples. PCR was used to amplify the unique UPTAG DNA barcodes located

at the gene deletion site and the barcode abundance was tracked using Illumina sequencing. The resulting counts were normalized and visualized using EdgeR.

We identified 33 heterozygous deletion strains that were under-represented based on a FDR less than 0.01, when comparing ebselen treatment to DMSO. These strains were enriched for glutathione metabolic process (p-value = 0.0026). In addition, we also included additional heterozygous deletion strains based on previous chemogenomic profiling using heterozygous and homozygous diploid strains. *pma1Δ* which was the fourth ranked strain from a heterozygous screen [384]*; glrΔ, gsh1Δ, gsh2Δ* hits from a homozygous screen [384]; *ubx4Δ, gsh1Δ, trp2Δ, brp1Δ, ecm38Δ, ylr287cΔ, cts1Δ, cda2Δ, imh1Δ* from a homozygous screen [380]; and *rad4Δ* from a heterozygous screen [380].

The heterozygous strains including *gsh1Δ*, *gsh2Δ*, *glr1Δ*, *trr1Δ*, *trr2Δ, fks1Δ, ylr287cΔ, ylr282cΔ, guf1Δ, yle296wΔ, est2Δ, rrf1Δ* and *ycr006cΔ* experienced a significant reduction in growth when exposed to ebselen (Figure 3.8A). Importantly, two heterozygous deletion strains (*gsh1Δ* and *gsh2Δ*) encoding genes involved in glutathione (GSH) synthesis were the most sensitive to ebselen. A haploid set of these two deletion strains (*gsh1Δ* and *gsh2Δ*) was also tested. These haploid deletion strains (*gsh1Δ* and *gsh2Δ*) were not resistant to ebselen and exhibited increased sensitivity to ebselen when compared to the diploid strains (Figure 3.8B). The results indicate that ebselen most likely does not directly target the proteins (Gsh1 and Gsh2) involved in glutathione synthesis but somehow

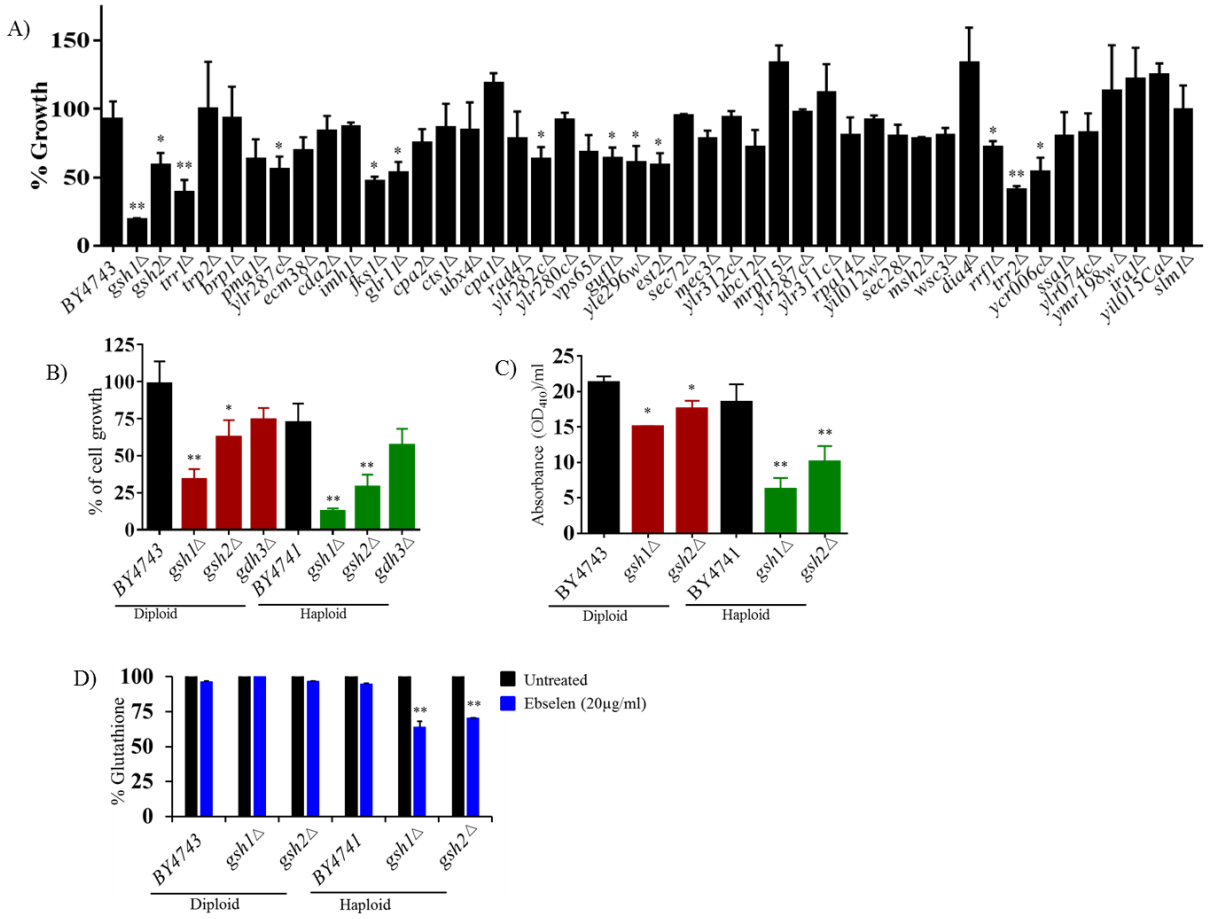

Figure 3.8 Glutathione as a potential target of ebselen. (A and B) The percent growth of yeast cells (OD_{600} after 24 h) incubated with ebselen (2µg/ml) in YPD broth was determined in relation to the DMSO treatment. The results are presented as means ± SD (n = 3). (C) Saturated cultures of yeast cells were diluted to 1:5 and grown for 2.5 h. The cells were sonicated and amount of glutathione was determined using glutathione assay kit. The absorbance measured using spectrophotometer indicates the glutathione production in each strain. (D) Yeast cells were treated with ebselen (20µg/ml) for 2.5 h and the glutathione concentration was measured as indicated above. The results are expressed as percent glutathione production relative to untreated control groups. Statistical analysis was calculated using the two-tailed Student's *t* test. *P* values of (* $P \leq 0.05$) (** $P \leq 0.01$) are considered as significant.

directly target the proteins (Gsh1 and Gsh2) involved in glutathione synthesis Based on the fact that ebselen binds directly to GSH and depletes GSH levels, leading to apoptosis in mammalian cells [398,408], we hypothesized ebselen exhibits a similar mode of action in yeast. Glutathione levels in wild type (BY4743 and BY4741), heterozygous and homozygous deletion strains (*gsh1Δ* and *gsh2Δ*) were quantified using a glutathione assay kit. Results indicate that all deletion strains experienced a significant reduction in GSH levels compared to their respective wild-type strains (Figure 3.8C). Homozygous deletion strains have a very low presence of GSH compared to their heterozygous strain counterpart (Figure 3.8C). However, treatment of homozygous deletion strains with ebselen further reduced GSH levels (approximately by 40%) compared to untreated control groups. On the other hand, the wild type and heterozygous deletion strains (*gsh1Δ* and *gsh2Δ*) showed no considerable decrease in GSH levels when treated with ebselen at this concentration (Figure 3.8D). These results suggest that ebselen depletes intracellular glutathione levels in yeast cells.

Depletion of glutathione by ebselen leads to increased ROS production

Glutathione plays a central role in maintaining redox-homeostasis in yeast [409,410]. Significant decreases in GSH levels might lead to dysregulation of redox homeostasis and in turn increase ROS production [398,408-410]. Given that ebselen was shown to deplete GSH levels in yeast cells, we investigated the effect of ebselen on ROS production. Basal level of ROS production in wild-type and GSH deletion strains were quantified. As expected, homozygous deletion strains (*gsh1Δ* and *gsh2Δ*) displayed a considerable increase in ROS levels compared to both the wild-type and heterozygous deletion strains (Figure 3.9A).

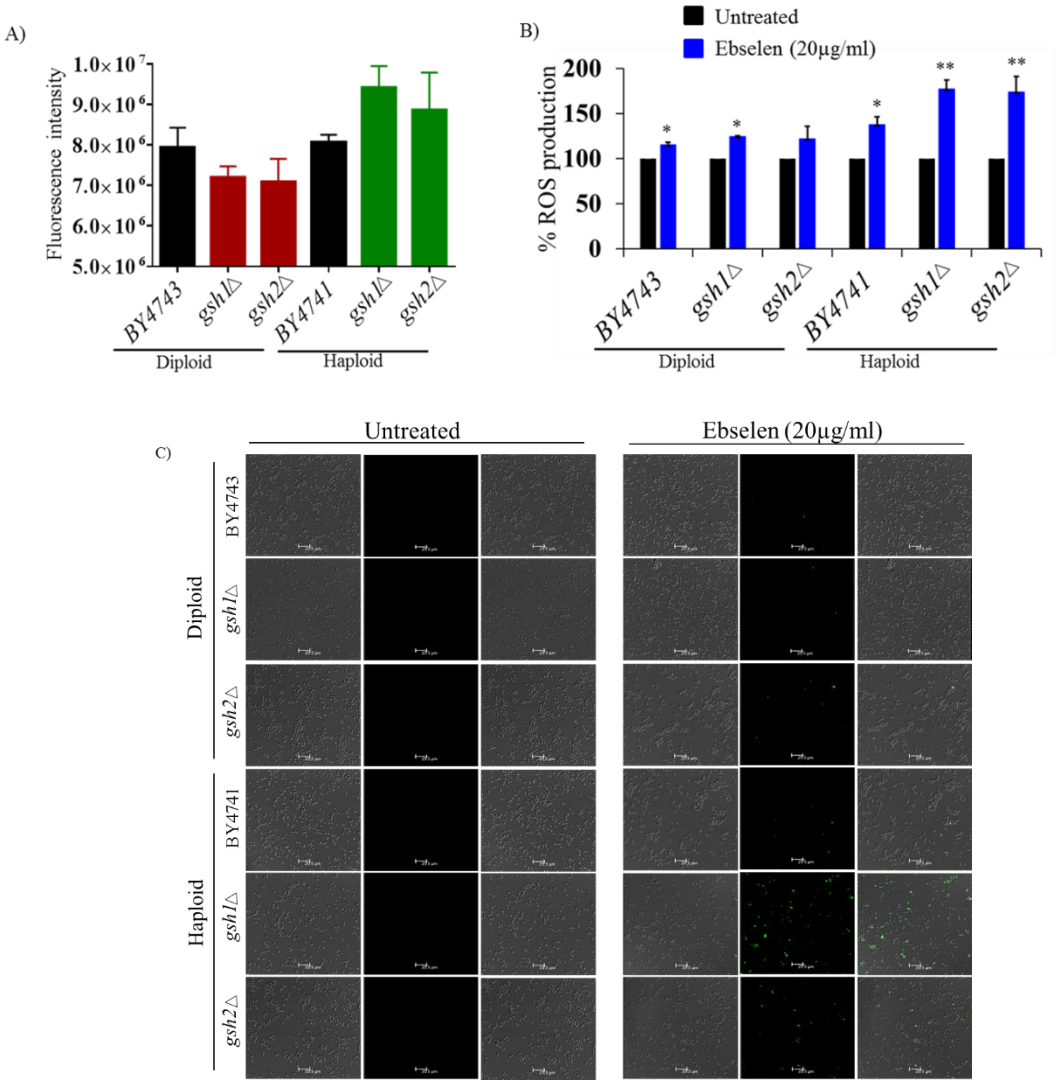

Figure 3.9 Depletion of glutathione by ebselen leads to ROS production in yeast cells. (A)Wild type and deletion strains of *S. cerevisiae* cells were grown in the presence of carboxy-H_2DCFDA dye and the intensity of fluorescence produced was measured using spectrophotometer. (B and C) Yeast cells were grown in the presence of ebselen (20µg/ml) for 2.5 h and incubated with carboxy-H_2DCFDA dye to determine the glutathione production by spectrophotometer or Leica confocal laser scanning microscopy. The results are expressed as percent glutathione in ebselen treated cells in relative to untreated control groups (B). Green fluorescence indicates the ROS production in yeast cells (C). Statistical analysis was calculated using the two-tailed Student's *t* test. *P* values of (* $P \leq 0.05$) (** $P \leq 0.01$) are considered as significant.

However, when exposed to ebselen treatment, all strains (except the *gsh2Δ* heterozygous deletion strain) experienced a significant increase in ROS production (Figure 3.9B). As expected, *gsh1Δ* and *gsh2Δ* homozygous deletion strains exhibited the largest increase in ROS production (almost two-fold increase) compared to untreated control groups (Figure 3.9B). These results were confirmed using confocal microscopy. As presented in Figure 3C, ROS production was prominently noticed only in the *gsh1Δ* and *gsh2Δ* homozygous deletion strains. Collectively, the results support the notion that ebselen exerts its antifungal activity by causing a sharp decrease in GSH levels that subsequently leads to increased ROS production in yeast cells.

Supplementation of L-reduced GSH restored the cell growth

Based upon the above result, we hypothesized that GSH supplementation would reverse the inhibitory effect in yeast caused by ebselen. As expected, supplementation with L-reduced glutathione restored cell growth and reversed the inhibition caused by ebselen, in a concentration-dependent manner (Figure 3.10). GSH, at 25 µg/ml, completely restored the cell growth (Figure 3.10). In addition, the effect of GSH supplementation on susceptibility of *Candida* and *Cryptococcus* strains to ebselen were also examined. Interestingly, with GSH supplementation (0.25 mg/ml), all tested fungal strains including *C. albicans, C. glabrata, C. tropicalis, C. parapsilosis, C. neoformans* and *C. gattii* become resistant to ebselen (MIC >128 µg/ml) (Table 3.3). On the other hand, the MIC of control antifungal drugs (fluconazole and flucytosine amphotericin) was not altered with GSH supplementation (Table 3.3). These results suggest a mode of action of ebselen that is specifically reversed by elevated GSH levels.

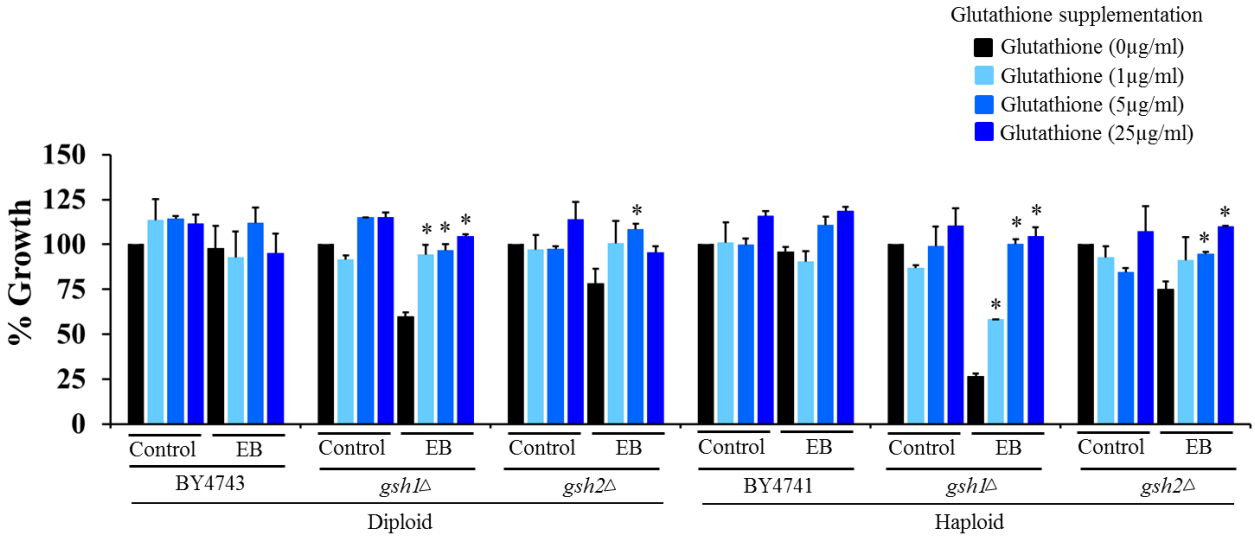

Figure 3.10 Supplementation of L-reduced glutathione restored the cell growth. Wild type and deletion strains of *S. cerevisiae* cells were grown in the absence (or) presence of indicated concentration of ebselen and glutathione and the percent growth rate (OD_{600} after 24 h) was determined by using spectrophotometer. Statistical analysis was calculated using the two-tailed Student's *t* test. *P* values of (* $P \leq 0.05$) (** $P \leq 0.01$) are considered as significant.

Table 3.3 MIC of ebselen and control antifungal drugs against *Candida* and *Cryptococcus* strains with L-reduced glutathione supplementation

Strains	Fluconazole (µg/ml)		Flucytosine (µg/ml)		Amphotericin (µg/ml)		Ebselen (µg/ml)	
	GSH (-)	GSH (+)	GSH (-)	GSH (+)	GSH (-)	GSH (+)	GSH (-)	GSH (+)
C. albicans ATCC 10231	2	2	0.25	0.25	0.5	0.5	2	>128
C. albicans - 18E	2	1	0.0625	0.0625	1	1	1	>128
C. tropicalis ATCC 1369	1	1	0.25	0.25	1	1	2	>128
C. tropicalis ATCC 13803	2	2	0.125	0.125	1	1	2	>128
C. parapsilosis ATCC 22019	1	1	0.25	0.25	1	1	1	>128
C. glabrata ATCC MYA-2950	4	4	0.0625	0.0625	1	1	0.5	>128
C. glabrata LRA 85.10.75	0.5	0.5	0.0625	0.0625	2	2	1	>128
C. gattii - R265	1	1	1	1	0.5	0.5	0.5	>128
C. gattii - CBS1930	2	2	2	2	0.5	0.5	0.5	>128
C. neoformans NR-41297	8	8	4	4	0.5	0.5	1	>128
C. neoformans NR-41299	4	4	1	2	1	1	1	>128

(-) indicates no supplementation and (+) indicates supplementation of L-reduced GSH (0.25mg/ml) to the growth medium.

In vivo efficacy of ebselen in infected *C. elegans* model

To investigate if the *in vitro* antifungal activity of ebselen translates *in vivo*, the antifungal efficacy of ebselen was tested in a *C. albicans* and *C. neoformans*-infected *C. elegans* animal model. As shown in Figure 3.11, treatment of infected *C. elegans* with amphotericin, fluconazole, flucytosine and ebselen at 4 and 8 µg/ml, produced a significant reduction ($P \leq 0.05$) in mean fungal load when compared to the untreated control groups. *C. elegans* treated with ebselen (8 µg/ml) completely eradicated *C. albicans*,. Amphotericin (8 µg/ml) produced a 1.53±0.08 $\log_{10}$ CFU reduction which was nearly identical to ebselen at 4 µg/ml (1.52±0.14 $\log_{10}$). Fluconazole, at 8 µg/ml, reduced the burden of *C. albicans* by 1.36±0.07 $\log_{10}$ followed by amphotericin (4 µg/ml) (1.05±0.16 $\log_{10}$), flucytosine (8 µg/ml) (0.79±0.09 $\log_{10}$), flucytosine (4 µg/ml) (0.62±0.08 $\log_{10}$) and fluconazole (4 µg/ml) (0.55±0.09 $\log_{10}$).

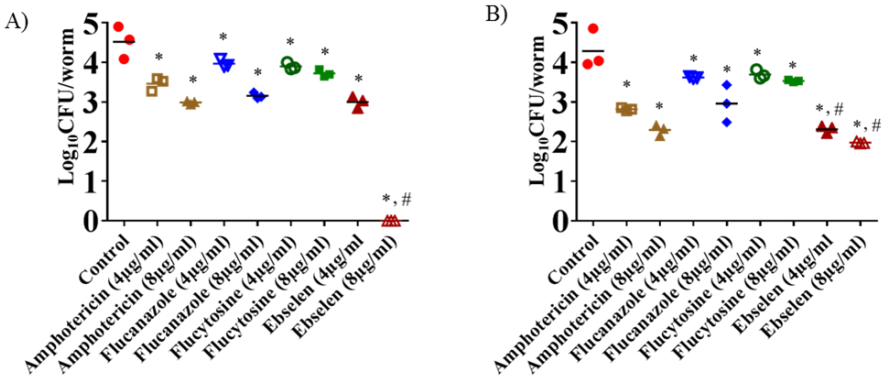

Figure 3.11 Efficacy of ebselen in *C. albicans* (or) *C. neoformans*-infected *C. elegans*. L4-stage worms were infected with *C. albicans* or *C. neoformans* and treated with ebselen, fluconazole, flucytosine and amphotericin at a concentrations of 4 and 8 µg/ml. After 24 h, worms were lysed and plated onto YPD plates to determine the CFU per worm. Each dot represents average fungal load in each worm per well. The results are presented as means ± SD (n = 3). Statistical analysis was calculated using the two-tailed Student's *t* test. *P* value of (** $P \leq 0.01$) are considered as significant.

Treatment of *C. neoformans*-infected *C. elegans* with ebselen (8 µg/ml) also generated the highest reduction in CFU count (2.31±0.02 $\log_{10}$), followed by amphotericin (8 µg/ml) (1.98±0.13 $\log_{10}$), (1.97±0.09 $\log_{10}$), ebselen at 4 µg/ml (1.97±0.09 $\log_{10}$), amphotericin (4 µg/ml) (1.46±0.03 $\log_{10}$), fluconazole (8 µg/ml) (1.32±0.04$\log_{10}$), flucytosine (8 µg/ml) (0.75±0.02 $\log_{10}$), fluconazole (4 µg/ml) (0.66±0.02 $\log_{10}$) and flucytosine (4 µg/ml) (0.58±0.11 $\log_{10}$).

3.2.4 Discussion

Fungal infections are a significant healthcare challenge particularly in immunocompromised individuals, such as HIV patients [411,412]. *Candida albicans* is the fourth leading cause of bloodstream infections in the United States and has been associated with a high mortality rate (50%) [413,414]. In addition to infections caused by *C. albicans*, Cryptococci, particularly *C. gattii*, are a major source of infections in humans. Cryptococcal meningitis is a significant cause of mortality in HIV patients [412]. The immune system in these immunocompromised patients is not capable of eradicating these fungal pathogens. Thus treatment is highly dependent on antifungal drugs successfully resolving the fungal infection [356]. Unfortunately, recent clinical reports indicate current antifungal therapies are not effective in treating invasive fungal infections [355]. Further compounding this problem, the number of antifungal drug classes currently available to clinicians is limited. This issue is exacerbated by the fact that resistance to antifungal agents is increasing and many current antifungal agents exhibit unusual toxicities thus further restricting their use [355,356,406,407]. This highlights the pressing need to identify new antifungal drugs to combat these dangerous pathogens. The traditional route of antifungal

innovation and regulatory approval is a time-consuming, expensive venture. This has led researchers to explore alternative approaches, such as drug repurposing, to expedite anti-infective drug development [210,356].

Ebselen is an organoselenium compound that is currently undergoing clinical trials for the prevention and treatment of cardiovascular disease, arthritis, stroke, atherosclerosis, and cancer [60,63-66]. In an intensive search for non-antifungal drugs exhibiting antifungal activity, we and others [69,402,403] demonstrated that ebselen possesses potent broad-spectrum fungicidal activity against *Candida* and *Cryptococcus spp* with the MIC values ranging from 0.5 to 2 µg/ml. Although, its antifungal activity has been reported before, the antifungal mechanism of action and *in vivo* efficacy of ebselen remains unclear with several potential targets proposed [68,69,402,403]. In the present study, we demonstrated that ebselen reduces GSH concentration in yeast cells leading to dysregulation of redox homeostasis. These results correlate with studies conducted by Yang *et.al* and Shi *et.al* that reported ebselen depletes GSH levels in mammalian cells, ultimately leading to apoptosis [398,408].

Although, ebselen has been shown to have an antioxidant effect and protects cells from free radical damage, it has also been shown to cause apoptosis by reducing thiol levels in mammalian cells [398,408]. The present study indicates that ebselen also exhibits a similar mode of action in yeast cells. Decreased GSH levels subsequently leads to increased ROS production thereby placing cells under oxidative stress. This finding is in agreement with a recent study by Ngo *et. al* that demonstrated ebselen treatment induces ROS in *Candida albicans* [402]. In addition, Azad *et. al* proposed that ebselen increases ROS levels in yeast

by inhibiting the Gdh3 enzyme involved in glutathione synthesis [404]. However, we found that *gdh3Δ* heterozygous and haploid deletion strains were not susceptible to ebselen compared to both the *gsh1Δ* and *gsh2Δ* deletion strains. Studies conducted by Billack *et. al* and Chan *et. al* proposed that the plasma membrane H(+)-ATPase pump (Pma1) is the potential target of ebselen in yeast [69,403]. However, we also confirmed that the *pma1Δ* heterozygous deletion strain does not experience significant growth impairment when exposed to ebselen relative to the *gsh1Δ* and *gsh2Δ* deletion strains. Many of the proposed targets for ebselen have been demonstrated via biochemical based assays in which it is difficult to assess the specificity of ebselen for the protein target compared to other targets especially because of the molecules reactivity to cysteines. Collectively, results from our study demonstrate that ebselen reduces intracellular GSH concentration leading to dysregulation of redox homeostasis and that deficiency in glutathione biosynthesis exacerbates this mode of action.

Glutathione is an essential metabolite required to protect yeast from oxidative stress [409,410,415-418]. *S. cerevisiae* lacking c-glutamyl cysteine synthase (Gsh1), the first enzyme in glutathione biosynthesis leads to glutathione autotrophy in which the cells dependent on exogenous GSH for its growth and survival [419,420]. In the absence of endogenous GSH, yeast has the ability to uptake GSH from an environment through high-affinity glutathione transporters such as Hgt1 [419-421]. In the present study, we also demonstrated that *gsh1Δ* and *gsh2Δ* homozygous deletion strains has relatively low amount of basal GSH when compared to wild type and the counterpart heterozygous deletion strains. The GSH

observed in the *gsh1Δ* and *gsh2Δ* homozygous deletion strains is likely derived from growth medium. The presence of low amount of GSH in these deletion strains was further depleted by ebselen treatment and in turn places cells in oxidative stress. Importance and essentiality of GSH has also been demonstrated in other fungi species including *Candida* [416,421], suggesting that glutathione might form an attractive novel target for the development of new antifungal drugs [422-424]. Future studies are required to delineate the interaction between ebselen and yeast GSH, and also the affinity of ebselen towards mammalian GSH.

Chemogenomic profiling was employed in this study, and it identified 33 heterozygous deletion strains sensitive to ebselen that were under-represented based on an FDR less than 0.01. However, the hits recovered did not include the *GSH1* or *GSH2* genes. It is also interesting to note that these strains were also not identified as hits in other heterozygous chemogenomic profiling screens employed by two other groups [380,384]. Potential hits obtained using this technique greatly depend on (i) the concentration of the drug/compound used to test the deletion pool (ii) Many technical factors such as the PCR quality and number of reads. These factors should be taken into consideration when utilizing chemogenomic profiling to identify the mode of action of unknown compounds.

The final segment of this study investigated the *in vivo* antifungal efficacy of ebselen in a *C. albicans* and *C. neoformans*-infected *C. elegans* animal model. Ebselen, at 8 μg/ml, completely eradicated the *C. albicans* load and produced a more than two- $\log_{10}$ reduction in *C. neoformans* CFU load. Ebselen's antifungal activity was found to be superior to currently approved antifungal drugs including amphotericin, fluconazole and flucytosine

in reducing the fungal load in the *C. elegans* animal model. These results lay a strong foundation for future studies to test the antifungal efficacy of ebselen in appropriate mice models of fungal infection. Ebselen is also known to be capable of crossing the blood brain barrier [66]. This quality provides an added advantage to investigate the potential use of this drug for the treatment of *Cryptococcal* meningitis infections particularly in HIV patients [66,412].

In conclusion, the present study confirms ebselen, with its unique mechanism of action and potent *in vivo* antifungal activity, is a promising clinical molecule that necessitates further investigation for repurposing as a novel antifungal agent.

REFERENCES

REFERENCES

1 CDC. (ed Centers for Disease Control and Prevention) 1-114 (2013).

2 ECDC. (ed European Centre for Disease Prevention and Control) 1-54 (Stockholm, 2009).

3 ECDC. (ed European Centre for Disease Control and Prevention) 1-260 (Stockholm, 2013).

4 Hiramatsu, K. Vancomycin-resistant Staphylococcus aureus: a new model of antibiotic resistance. *Lancet Infect Dis* **1**, 147-155, doi:10.1016/S1473-3099(01)00091-3 (2001).

5 Layer, F., Cuny, C., Strommenger, B. & Witte, W. Linezolid resistance in clinical isolates of Staphylococcus aureus and Staphylococcus epidermidis. *Int J Med Microbiol* **302**, 102-102 (2012).

6 Li, X. *et al.* Ceftriaxone, an FDA-approved cephalosporin antibiotic, suppresses lung cancer growth by targeting Aurora B. *Carcinogenesis* **33**, 2548-2557, doi:DOI 10.1093/carcin/bgs283 (2012).

7 Chong, C. R. & Sullivan, D. J., Jr. New uses for old drugs. *Nature* **448**, 645-646, doi:10.1038/448645a (2007).

8 Cohen, F. J. Macro trends in pharmaceutical innovation. *Nature reviews. Drug discovery* **4**, 78-84, doi:10.1038/nrd1610 (2005).

9 Jin, G. & Wong, S. T. Toward better drug repositioning: prioritizing and integrating existing methods into efficient pipelines. *Drug discovery today* **19**, 637-644, doi:10.1016/j.drudis.2013.11.005 (2014).

10 DiMasi, J. A., Hansen, R. W. & Grabowski, H. G. The price of innovation: new estimates of drug development costs. *Journal of health economics* **22**, 151-185, doi:10.1016/S0167-6296(02)00126-1 (2003).

11 Petsko, G. A. When failure should be the option. *Bmc Biol* **8**, doi:Artn 61 Doi 10.1186/1741-7007-8-61 (2010).

12 Flanders, S. A., Dudas, V., Kerr, K., McCulloch, C. E. & Gonzales, R. Effectiveness of ceftriaxone plus doxycycline in the treatment of patients hospitalized with community-acquired pneumonia. *Journal of hospital medicine : an official publication of the Society of Hospital Medicine* **1**, 7-12, doi:10.1002/jhm.8 (2006).

13 Mandell, L. A. *et al.* Infectious Diseases Society of America/American Thoracic Society consensus guidelines on the management of community-acquired pneumonia in adults. *Clin Infect Dis* **44 Suppl 2**, S27-72, doi:10.1086/511159 (2007).

14 Molyneux, E. *et al.* 5 versus 10 days of treatment with ceftriaxone for bacterial meningitis in children: a double-blind randomised equivalence study. *Lancet* **377**, 1837-1845, doi:10.1016/S0140-6736(11)60580-1 (2011).

15 Whiley, D. M. *et al.* Reduced susceptibility to ceftriaxone in Neisseria gonorrhoeae is associated with mutations G542S, P551S and P551L in the gonococcal penicillin-binding protein 2. *J Antimicrob Chemoth* **65**, 1615-1618, doi:Doi 10.1093/Jac/Dkq187 (2010).

16 Rothstein, J. D. *et al.* Beta-lactam antibiotics offer neuroprotection by increasing glutamate transporter expression. *Nature* **433**, 73-77, doi:10.1038/nature03180 (2005).

17 Cudkowicz, M., Shefner, J. & Consortium, N. STAGE 3 Clinical Trial of Ceftriaxone in Subjects with ALS. *Neurology* **80** (2013).

18 Zhu, S. *et al.* Minocycline inhibits cytochrome c release and delays progression of amyotrophic lateral sclerosis in mice. *Nature* **417**, 74-78, doi:Doi 10.1038/417074a (2002).

19 Shigi, Y. Inhibition of bacterial isoprenoid synthesis by fosmidomycin, a phosphonic acid-containing antibiotic. *The Journal of antimicrobial chemotherapy* **24**, 131-145 (1989).

20 Ruangweerayut, R. *et al.* Assessment of the pharmacokinetics and dynamics of two combination regimens of fosmidomycin-clindamycin in patients with acute uncomplicated falciparum malaria. *Malaria journal* **7**, 225, doi:10.1186/1475-2875-7-225 (2008).

21 Na-Bangchang, K., Ruengweerayut, R., Karbwang, J., Chauemung, A. & Hutchinson, D. Pharmacokinetics and pharmacodynamics of fosmidomycin monotherapy and combination therapy with clindamycin in the treatment of multidrug resistant falciparum malaria. *Malaria journal* **6**, 70, doi:10.1186/1475-2875-6-70 (2007).

22 Teachey, D. T. *et al.* Treatment with sirolimus results in complete responses in patients with autoimmune lymphoproliferative syndrome. *British journal of haematology* **145**, 101-106, doi:10.1111/j.1365-2141.2009.07595.x (2009).

23 Dragana, J. M. *et al.* Rapid Regression of Lymphadenopathy upon Rapamycin Treatment in a Child With Autoimmune Lymphoproliferative Syndrome. *Pediatr Blood Cancer* **53**, 1117-1119, doi:Doi 10.1002/Pbc.22151 (2009).

24 Cai, X. *et al.* Sirolimus Decreases Circulating Lymphangioleiomyomatosis Cells in Patients With Lymphangioleiomyomatosis. *Chest* **145**, 108-+, doi:DOI 10.1378/chest.13-1071 (2014).

25 Debnath, A. *et al.* A high-throughput drug screen for Entamoeba histolytica identifies a new lead and target. *Nature medicine* **18**, 956-960, doi:10.1038/nm.2758 (2012).

26 Smorenburg, C. H. *et al.* Phase II study of miltefosine 6% solution as topical treatment of skin metastases in breast cancer patients. *Anti-cancer drugs* **11**, 825-828 (2000).

27 Dorlo, T. P., Balasegaram, M., Beijnen, J. H. & de Vries, P. J. Miltefosine: a review of its pharmacology and therapeutic efficacy in the treatment of leishmaniasis. *The Journal of antimicrobial chemotherapy* **67**, 2576-2597, doi:10.1093/jac/dks275 (2012).

28 Meyerhoff, A. U.S. Food and Drug Administration approval of AmBisome (liposomal amphotericin B) for treatment of visceral leishmaniasis. *Clinical infectious diseases : an official publication of the Infectious Diseases Society of America* **28**, 42-48; discussion 49-51, doi:10.1086/515085 (1999).

29 Bukirwa, H., Garner, P. & Critchley, J. Chlorproguanil-dapsone for treating uncomplicated malaria. *The Cochrane database of systematic reviews*, CD004387, doi:10.1002/14651858.CD004387.pub2 (2004).

30 Olson, K. B., Thompson, J. F. & Zintheo, C. J., Jr. Treatment of pulmonary tuberculosis with diasone. *American review of tuberculosis* **52**, 474-482 (1945).

31 Robitzek, E. H., Ornstein, G. G. & et al. Diasone in the treatment of pulmonary tuberculosis. *Diseases of the chest* **12**, 185-204 (1946).

32 Abeloff, M. D. *et al.* Phase II trials of alpha-difluoromethylornithine, an inhibitor of polyamine synthesis, in advanced small cell lung cancer and colon cancer. *Cancer treatment reports* **70**, 843-845 (1986).

33 Paulson, Y. J., Gilman, T. M., Heseltine, P. N., Sharma, O. P. & Boylen, C. T. Eflornithine treatment of refractory Pneumocystis carinii pneumonia in patients with acquired immunodeficiency syndrome. *Chest* **101**, 67-74 (1992).

34 Burri, C. & Brun, R. Eflornithine for the treatment of human African trypanosomiasis. *Parasitology research* **90 Supp 1**, S49-52, doi:10.1007/s00436-002-0766-5 (2003).

35 Chappuis, F., Udayraj, N., Stietenroth, K., Meussen, A. & Bovier, P. A. Eflornithine is safer than melarsoprol for the treatment of second-stage Trypanosoma brucei gambiense human African trypanosomiasis. *Clinical infectious diseases : an official publication of the Infectious Diseases Society of America* **41**, 748-751, doi:10.1086/432576 (2005).

36 Robays, J., Raguenaud, M. E., Josenando, T. & Boelaert, M. Eflornithine is a cost-effective alternative to melarsoprol for the treatment of second-stage human West African trypanosomiasis in Caxito, Angola. *Tropical medicine & international health : TM & IH* **13**, 265-271, doi:10.1111/j.1365-3156.2007.01999.x (2008).

37 Tan, K. R. *et al.* Doxycycline for malaria chemoprophylaxis and treatment: report from the CDC expert meeting on malaria chemoprophylaxis. *The American journal of tropical medicine and hygiene* **84**, 517-531, doi:10.4269/ajtmh.2011.10-0285 (2011).

38 Ben Salah, A. *et al.* Topical paromomycin with or without gentamicin for cutaneous leishmaniasis. *The New England journal of medicine* **368**, 524-532, doi:10.1056/NEJMoa1202657 (2013).

39 Monge-Maillo, B. & Lopez-Velez, R. Topical paromomycin and gentamicin for new world cutaneous leishmaniasis in Panama. *The American journal of tropical medicine and hygiene* **90**, 1191, doi:10.4269/ajtmh.14-0040a (2014).

40 Sosa, N. *et al.* Randomized, double-blinded, phase 2 trial of WR 279,396 (paromomycin and gentamicin) for cutaneous leishmaniasis in Panama. *The American journal of tropical medicine and hygiene* **89**, 557-563, doi:10.4269/ajtmh.12-0736 (2013).

41 Robert-Gangneux, F. & Darde, M. L. Epidemiology of and diagnostic strategies for toxoplasmosis. *Clinical microbiology reviews* **25**, 264-296, doi:10.1128/CMR.05013-11 (2012).

42 Baltzan, M., Mehta, S., Kirkham, T. H. & Cosio, M. G. Randomized trial of prolonged chloroquine therapy in advanced pulmonary sarcoidosis. *American journal of respiratory and critical care medicine* **160**, 192-197, doi:10.1164/ajrccm.160.1.9809024 (1999).

43 Cohen, H. G. & Reynolds, T. B. Comparison of metronidazole and chloroquine for the treatment of amoebic liver abscess. A controlled trial. *Gastroenterology* **69**, 35-41 (1975).

44 Montoya, J. G. & Liesenfeld, O. Toxoplasmosis. *Lancet* **363**, 1965-1976, doi:10.1016/S0140-6736(04)16412-X (2004).

45 Baggish, A. L. & Hill, D. R. Antiparasitic agent atovaquone. *Antimicrobial agents and chemotherapy* **46**, 1163-1173 (2002).

46 Araujo, F. G., Huskinson, J. & Remington, J. S. Remarkable in vitro and in vivo activities of the hydroxynaphthoquinone 566C80 against tachyzoites and tissue cysts of Toxoplasma gondii. *Antimicrobial agents and chemotherapy* **35**, 293-299 (1991).

47 Bernhard, G. C. Auranofin Therapy in Rheumatoid-Arthritis. *J Lab Clin Med* **100**, 167-177 (1982).

48 Furst, D. E., Abruzzo, J. L., Katz, W. A., Dahl, S. L. & Ward, J. R. Mechanism of Action, Pharmacology, Clinical Efficacy and Side-Effects of Auranofin - an Orally-Administered Organic Gold Compound for the Treatment of Rheumatoid-Arthritis. *Pharmacotherapy* **3**, 284-298 (1983).

49 Shaw, C. F. Gold-based therapeutic agents. *Chem Rev* **99**, 2589-2600 (1999).

50 Berners-Price, S. J. & Filipovska, A. Gold compounds as therapeutic agents for human diseases. *Metallomics* **3**, 863-873 (2011).

51 Lobanov, A. V., Gromer, S., Salinas, G. & Gladyshev, V. N. Selenium metabolism in Trypanosoma: characterization of selenoproteomes and identification of a Kinetoplastida-specific selenoprotein. *Nucleic acids research* **34**, 4012-4024, doi:10.1093/nar/gkl541 (2006).

52 Kuntz, A. N. *et al.* Thioredoxin glutathione reductase from Schistosoma mansoni: an essential parasite enzyme and a key drug target. *PLoS medicine* **4**, e206, doi:10.1371/journal.pmed.0040206 (2007).

53 Bonilla, M. *et al.* Platyhelminth mitochondrial and cytosolic redox homeostasis is controlled by a single thioredoxin glutathione reductase and dependent on selenium and glutathione. *The Journal of biological chemistry* **283**, 17898-17907, doi:10.1074/jbc.M710609200 (2008).

54 Sannella, A. R. *et al.* New uses for old drugs. Auranofin, a clinically established antiarthritic metallodrug, exhibits potent antimalarial effects in vitro: Mechanistic and pharmacological implications. *FEBS letters* **582**, 844-847, doi:10.1016/j.febslet.2008.02.028 (2008).

55 Ilari, A. *et al.* A gold-containing drug against parasitic polyamine metabolism: the X-ray structure of trypanothione reductase from Leishmania infantum in complex with auranofin reveals a dual mechanism of enzyme inhibition. *Amino acids* **42**, 803-811, doi:10.1007/s00726-011-0997-9 (2012).

56 Gottlieb, N. L. Pharmacology of Auranofin - Overview and Update. *Scand J Rheumatol*, 19-28 (1986).

57 Cassetta, M. I., Marzo, T., Fallani, S., Novelli, A. & Messori, L. Drug repositioning: auranofin as a prospective antimicrobial agent for the treatment of severe staphylococcal infections. *Biometals : an international journal on the role of metal ions in biology, biochemistry, and medicine* **27**, 787-791, doi:10.1007/s10534-014-9743-6 (2014).

58 Hokai, Y. *et al.* Auranofin and related heterometallic gold(I)-thiolates as potent inhibitors of methicillin-resistant Staphylococcus aureus bacterial strains. *Journal of inorganic biochemistry* **138**, 81-88, doi:10.1016/j.jinorgbio.2014.05.008 (2014).

59 Schewe, T. Molecular actions of ebselen--an antiinflammatory antioxidant. *General pharmacology* **26**, 1153-1169 (1995).

60 Azad, G. K. & Tomar, R. S. Ebselen, a promising antioxidant drug: mechanisms of action and targets of biological pathways. *Mol Biol Rep* **41**, 4865-4879, doi:10.1007/s11033-014-3417-x (2014).

61 Muller, A., Cadenas, E., Graf, P. & Sies, H. A novel biologically active seleno-organic compound--I. Glutathione peroxidase-like activity in vitro and antioxidant capacity of PZ 51 (Ebselen). *Biochemical pharmacology* **33**, 3235-3239 (1984).

62 Maiorino, M., Roveri, A. & Ursini, F. Antioxidant effect of Ebselen (PZ 51): peroxidase mimetic activity on phospholipid and cholesterol hydroperoxides vs free radical scavenger activity. *Archives of biochemistry and biophysics* **295**, 404-409 (1992).

63 Handa, Y. *et al.* Effect of an antioxidant, ebselen, on development of chronic cerebral vasospasm after subarachnoid hemorrhage in primates. *Surgical neurology* **53**, 323-329 (2000).

64 Kobayashi, T., Ohta, Y. & Yoshino, J. Preventive effect of ebselen on acute gastric mucosal lesion development in rats treated with compound 48/80. *European journal of pharmacology* **414**, 271-279 (2001).

65 Parnham, M. J. & Sies, H. The early research and development of ebselen. *Biochemical pharmacology* **86**, 1248-1253, doi:10.1016/j.bcp.2013.08.028 (2013).

66 Singh, N. *et al.* A safe lithium mimetic for bipolar disorder. *Nat Commun* **4**, 1332, doi:10.1038/ncomms2320 (2013).

67 Nozawa, R., Yokota, T. & Fujimoto, T. Susceptibility of methicillin-resistant Staphylococcus aureus to the selenium-containing compound 2-phenyl-1,2-benzoisoselenazol-3(2H)-one (PZ51). *Antimicrobial agents and chemotherapy* **33**, 1388-1390 (1989).

68 Lu, J. *et al.* Inhibition of bacterial thioredoxin reductase: an antibiotic mechanism targeting bacteria lacking glutathione. *FASEB J* **27**, 1394-1403, doi:10.1096/fj.12-223305 (2013).

69 Chan, G., Hardej, D., Santoro, M., Lau-Cam, C. & Billack, B. Evaluation of the antimicrobial activity of ebselen: role of the yeast plasma membrane H+-ATPase. *J Biochem Mol Toxicol* **21**, 252-264, doi:10.1002/jbt.20189 (2007).

70 Imai, H., Masayasu, H., Dewar, D., Graham, D. I. & Macrae, I. M. Ebselen protects both gray and white matter in a rodent model of focal cerebral ischemia. *Stroke; a journal of cerebral circulation* **32**, 2149-2154 (2001).

71 Sandrini, M. P., Shannon, O., Clausen, A. R., Bjorck, L. & Piskur, J. Deoxyribonucleoside kinases activate nucleoside antibiotics in severely pathogenic bacteria. *Antimicrobial agents and chemotherapy* **51**, 2726-2732, doi:10.1128/AAC.00081-07 (2007).

72 Hamilton-Miller, J. M. Antimicrobial activity of 21 anti-neoplastic agents. *British journal of cancer* **49**, 367-369 (1984).

73 Jacobs, J. Y., Michel, J. & Sacks, T. Bactericidal effect of combinations of antimicrobial drugs and antineoplastic antibiotics against Staphylococcus aureus. *Antimicrobial agents and chemotherapy* **15**, 580-586 (1979).

74 Phillips, M., Malloy, G., Nedunchezian, D., Lukrec, A. & Howard, R. G. Disulfiram inhibits the in vitro growth of methicillin-resistant staphylococcus aureus. *Antimicrobial agents and chemotherapy* **35**, 785-787 (1991).

75 Dastidar, S. G., Debnath, S., Mazumdar, K., Ganguly, K. & Chakrabarty, A. N. Triflupromazine: a microbicide non-antibiotic compound. *Acta microbiologica et immunologica Hungarica* **51**, 75-83 (2004).

76 Kruszewska, H., Zareba, T. & Tyski, S. Search of antimicrobial activity of selected non-antibiotic drugs. *Acta poloniae pharmaceutica* **59**, 436-439 (2002).

77 Karak, P., Kumar, K. A., Mazumdar, K., Mookerjee, M. & Dastidar, S. G. Antibacterial potential of an antispasmodic drug dicyclomine hydrochloride. *The Indian journal of medical research* **118**, 192-196 (2003).

78 Rani Basu, L., Mazumdar, K., Dutta, N. K., Karak, P. & Dastidar, S. G. Antibacterial property of the antipsychotic agent prochlorperazine, and its synergism with methdilazine. *Microbiological research* **160**, 95-100 (2005).

79 Jerwood, S. & Cohen, J. Unexpected antimicrobial effect of statins. *The Journal of antimicrobial chemotherapy* **61**, 362-364, doi:10.1093/jac/dkm496 (2008).

80 Chiu, H. C. *et al.* Development of novel antibacterial agents against methicillin-resistant Staphylococcus aureus. *Bioorganic & medicinal chemistry* **20**, 4653-4660, doi:10.1016/j.bmc.2012.06.018 (2012).

81 Kruszewska, H., Zareba, T. & Tyski, S. Estimation of antimicrobial activity of selected non-antibiotic products. *Acta poloniae pharmaceutica* **63**, 457-460 (2006).

82 Mandal, A., Sinha, C., Kumar Jena, A., Ghosh, S. & Samanta, A. An Investigation on in vitro and in vivo Antimicrobial Properties of the Antidepressant: Amitriptyline Hydrochloride. *Brazilian journal of microbiology : [publication of the Brazilian Society for Microbiology]* **41**, 635-645, doi:10.1590/S1517-83822010000300014 (2010).

83 El-Nakeeb, M. A., Abou-Shleib, H. M., Khalil, A. M., Omar, H. G. & El-Halfawy, O. M. In vitro antibacterial activity of some antihistaminics belonging to different groups against multi-drug resistant clinical isolates. *Brazilian journal of microbiology : [publication of the Brazilian Society for Microbiology]* **42**, 980-991, doi:10.1590/S1517-838220110003000018 (2011).

84 Kruszewska, H., Zareba, T. & Tyski, S. in *Acta poloniae pharmaceutica* Vol. 59 436-439 (2002).

85 Dutta, N. K. *et al.* Potential management of resistant microbial infections with a novel non-antibiotic: the anti-inflammatory drug diclofenac sodium. *International journal of antimicrobial agents* **30**, 242-249, doi:10.1016/j.ijantimicag.2007.04.018 (2007).

86 Mazumdar, K. *et al.* Antimicrobial potentiality of a new non-antibiotic: the cardiovascular drug oxyfedrine hydrochloride. *Microbiological research* **158**, 259-264, doi:10.1078/0944-5013-00204 (2003).

87 Al-Janabi, A. A. In vitro antibacterial activity of Ibuprofen and acetaminophen. *Journal of global infectious diseases* **2**, 105-108, doi:10.4103/0974-777X.62880 (2010).

88 Kruszewska, H., Zareba, T. & Tyski, S. Examination of antimicrobial activity of selected non-antibiotic products. *Acta poloniae pharmaceutica* **67**, 733-736 (2010).

89 Kruszewska, H., Zareba, T. & Tyski, S. Examination of antibacterial and antifungal activity of selected non-antibiotic products. *Acta poloniae pharmaceutica* **65**, 779-782 (2008).

90 Munoz-Bellido, J. L., Munoz-Criado, S. & Garcia-Rodriguez, J. A. Antimicrobial activity of psychotropic drugs: selective serotonin reuptake inhibitors. *International journal of antimicrobial agents* **14**, 177-180 (2000).

91 Holohan, C., Van Schaeybroeck, S., Longley, D. B. & Johnston, P. G. Cancer drug resistance: an evolving paradigm. *Nature reviews. Cancer* **13**, 714-726, doi:10.1038/nrc3599 (2013).

92 Phillips, T. A., Howell, A., Grieve, R. J. & Welling, P. G. Pharmacokinetics of oral and intravenous fluorouracil in humans. *Journal of pharmaceutical sciences* **69**, 1428-1431 (1980).

93 Bodet, C. A., 3rd, Jorgensen, J. H. & Drutz, D. J. Antibacterial activities of antineoplastic agents. *Antimicrobial agents and chemotherapy* **28**, 437-439 (1985).

94 Barberi-Heyob, M. *et al.* Evaluation of plasma 5-fluorouracil nucleoside levels in patients with metastatic breast cancer: relationships with toxicities. *Cancer chemotherapy and pharmacology* **37**, 110-116 (1995).

95 Roobol, C., De Dobbeleer, G. B. & Bernheim, J. L. 5-fluorouracil and 5-fluoro-2'-deoxyuridine follow different metabolic pathways in the induction of cell lethality in L1210 leukaemia. *British journal of cancer* **49**, 739-744 (1984).

96 Schilcher, R. B., Young, J. D., Ratanatharathorn, V., Karanes, C. & Baker, L. H. Clinical pharmacokinetics of high-dose mitomycin C. *Cancer chemotherapy and pharmacology* **13**, 186-190 (1984).

97 Daum, R. S. Clinical practice. Skin and soft-tissue infections caused by methicillin-resistant Staphylococcus aureus. *The New England journal of medicine* **357**, 380-390, doi:10.1056/NEJMcp070747 (2007).

98 DeLeo, F. R., Otto, M., Kreiswirth, B. N. & Chambers, H. F. Community-associated meticillin-resistant Staphylococcus aureus. *Lancet* **375**, 1557-1568, doi:10.1016/S0140-6736(09)61999-1 (2010).

99 Miller, L. G. & Diep, B. A. Clinical practice: colonization, fomites, and virulence: rethinking the pathogenesis of community-associated methicillin-resistant Staphylococcus aureus infection. *Clinical infectious diseases : an official publication of the Infectious Diseases Society of America* **46**, 752-760, doi:10.1086/526773 (2008).

100 Gallelli, L. *et al.* The effects of nonsteroidal anti-inflammatory drugs on clinical outcomes, synovial fluid cytokine concentration and signal transduction pathways in knee osteoarthritis. A randomized open label trial. *Osteoarthritis and cartilage / OARS, Osteoarthritis Research Society* **21**, 1400-1408, doi:10.1016/j.joca.2013.06.026 (2013).

101 Yan, J., Sun, J., Huang, L., Fu, Q. & Du, G. Simvastatin prevents neuroinflammation by inhibiting N-methyl-D-aspartic acid receptor 1 in 6-hydroxydopamine-treated PC12 cells. *Journal of neuroscience research* **92**, 634-640, doi:10.1002/jnr.23329 (2014).

102 Jialal, I., Miguelino, E., Griffen, S. C. & Devaraj, S. Concomitant reduction of low-density lipoprotein-cholesterol and biomarkers of inflammation with low-dose simvastatin therapy in patients with type 1 diabetes. *The Journal of clinical endocrinology and metabolism* **92**, 3136-3140, doi:10.1210/jc.2007-0453 (2007).

103 Wallace, H. J. & Stacey, M. C. Levels of tumor necrosis factor-alpha (TNF-alpha) and soluble TNF receptors in chronic venous leg ulcers--correlations to healing status. *The Journal of investigative dermatology* **110**, 292-296, doi:10.1046/j.1523-1747.1998.00113.x (1998).

104 Cowin, A. J., Hatzirodos, N., Rigden, J., Fitridge, R. & Belford, D. A. Etanercept decreases tumor necrosis factor-alpha activity in chronic wound fluid. *Wound repair and regeneration : official publication of the Wound Healing Society [and] the European Tissue Repair Society* **14**, 421-426, doi:10.1111/j.1743-6109.2006.00141.x (2006).

105 Donath, M. Y. Targeting inflammation in the treatment of type 2 diabetes: time to start. *Nature reviews. Drug discovery* **13**, 465-476, doi:10.1038/nrd4275 (2014).

106 Khanna, S. *et al.* Macrophage dysfunction impairs resolution of inflammation in the wounds of diabetic mice. *PloS one* **5**, e9539, doi:10.1371/journal.pone.0009539 (2010).

107 Fournier, B. & Philpott, D. J. Recognition of Staphylococcus aureus by the innate immune system. *Clinical microbiology reviews* **18**, 521-540, doi:10.1128/CMR.18.3.521-540.2005 (2005).

108 Bitto, A. *et al.* Simvastatin enhances VEGF production and ameliorates impaired wound healing in experimental diabetes. *Pharmacological research : the official journal of the Italian Pharmacological Society* **57**, 159-169, doi:10.1016/j.phrs.2008.01.005 (2008).

109 Fischbach, M. A. & Walsh, C. T. Antibiotics for emerging pathogens. *Science* **325**, 1089-1093, doi:10.1126/science.1176667 (2009).

110 Cegelski, L., Marshall, G. R., Eldridge, G. R. & Hultgren, S. J. The biology and future prospects of antivirulence therapies. *Nature reviews. Microbiology* **6**, 17-27, doi:10.1038/nrmicro1818 (2008).

111 Lebeis, S. L. & Kalman, D. Aligning antimicrobial drug discovery with complex and redundant host-pathogen interactions. *Cell host & microbe* **5**, 114-122, doi:10.1016/j.chom.2009.01.008 (2009).

112 Khodaverdian, V. *et al.* Discovery of antivirulence agents against methicillin-resistant Staphylococcus aureus. *Antimicrobial agents and chemotherapy* **57**, 3645-3652, doi:10.1128/AAC.00269-13 (2013).

113 Weinandy, F. *et al.* A beta-lactone-based antivirulence drug ameliorates Staphylococcus aureus skin infections in mice. *ChemMedChem* **9**, 710-713, doi:10.1002/cmdc.201300325 (2014).

114 Hilchie, A. L., Wuerth, K. & Hancock, R. E. Immune modulation by multifaceted cationic host defense (antimicrobial) peptides. *Nature chemical biology* **9**, 761-768, doi:10.1038/nchembio.1393 (2013).

115 Ejim, L. *et al.* Combinations of antibiotics and nonantibiotic drugs enhance antimicrobial efficacy. *Nature chemical biology* **7**, 348-350, doi:10.1038/nchembio.559 (2011).

116 Kupferwasser, L. I. *et al.* Salicylic acid attenuates virulence in endovascular infections by targeting global regulatory pathways in Staphylococcus aureus. *The Journal of clinical investigation* **112**, 222-233, doi:10.1172/JCI16876 (2003).

117 Needs, C. J. & Brooks, P. M. Clinical pharmacokinetics of the salicylates. *Clinical pharmacokinetics* **10**, 164-177, doi:10.2165/00003088-198510020-00004 (1985).

118 Siddik, Z. H. Cisplatin: mode of cytotoxic action and molecular basis of resistance. *Oncogene* **22**, 7265-7279, doi:10.1038/sj.onc.1206933 (2003).

119 Moayeri, M., Wiggins, J. F., Lindeman, R. E. & Leppla, S. H. Cisplatin inhibition of anthrax lethal toxin. *Antimicrobial agents and chemotherapy* **50**, 2658-2665, doi:10.1128/AAC.01412-05 (2006).

120 Artenstein, A. W. *et al.* Chloroquine enhances survival in Bacillus anthracis intoxication. *The Journal of infectious diseases* **190**, 1655-1660, doi:10.1086/424853 (2004).

121 Gordon, V. M., Leppla, S. H. & Hewlett, E. L. Inhibitors of receptor-mediated endocytosis block the entry of Bacillus anthracis adenylate cyclase toxin but not that of Bordetella pertussis adenylate cyclase toxin. *Infection and immunity* **56**, 1066-1069 (1988).

122 Sullivan, D. J., Jr., Gluzman, I. Y., Russell, D. G. & Goldberg, D. E. On the molecular mechanism of chloroquine's antimalarial action. *Proceedings of the National Academy of Sciences of the United States of America* **93**, 11865-11870 (1996).

123 Costa, S. S., Viveiros, M., Amaral, L. & Couto, I. Multidrug Efflux Pumps in Staphylococcus aureus: an Update. *The open microbiology journal* **7**, 59-71, doi:10.2174/1874285801307010059 (2013).

124 Poole, K. Efflux pumps as antimicrobial resistance mechanisms. *Annals of medicine* **39**, 162-176, doi:10.1080/07853890701195262 (2007).

125 Davis, J. M. & Casper, R. Antipsychotic drugs: clinical pharmacology and therapeutic use. *Drugs* **14**, 260-282 (1977).
126 Lader, M. Clinical pharmacology of antipsychotic drugs. *The Journal of international medical research* **17**, 1-16 (1989).
127 Kaatz, G. W., Moudgal, V. V., Seo, S. M. & Kristiansen, J. E. Phenothiazines and thioxanthenes inhibit multidrug efflux pump activity in Staphylococcus aureus. *Antimicrobial agents and chemotherapy* **47**, 719-726 (2003).
128 Kristiansen, M. M. *et al.* Thioridazine reduces resistance of methicillin-resistant staphylococcus aureus by inhibiting a reserpine-sensitive efflux pump. *In vivo* **20**, 361-366 (2006).
129 Costa, S. S. *et al.* Exploring the contribution of efflux on the resistance to fluoroquinolones in clinical isolates of Staphylococcus aureus. *BMC microbiology* **11**, 241, doi:10.1186/1471-2180-11-241 (2011).
130 McGoon, M. D., Vlietstra, R. E., Holmes, D. R., Jr. & Osborn, J. E. The clinical use of verapamil. *Mayo Clinic proceedings* **57**, 495-510 (1982).
131 Aeschlimann, J. R., Dresser, L. D., Kaatz, G. W. & Rybak, M. J. Effects of NorA inhibitors on in vitro antibacterial activities and postantibiotic effects of levofloxacin, ciprofloxacin, and norfloxacin in genetically related strains of Staphylococcus aureus. *Antimicrobial agents and chemotherapy* **43**, 335-340 (1999).
132 Foster, T. J. Immune evasion by staphylococci. *Nature reviews. Microbiology* **3**, 948-958, doi:10.1038/nrmicro1289 (2005).
133 Veldkamp, K. E. & van Strijp, J. A. Innate immune evasion by staphylococci. *Advances in experimental medicine and biology* **666**, 19-31 (2009).
134 Hornef, M. W., Wick, M. J., Rhen, M. & Normark, S. Bacterial strategies for overcoming host innate and adaptive immune responses. *Nature immunology* **3**, 1033-1040, doi:10.1038/ni1102-1033 (2002).
135 McCormick, J. K., Yarwood, J. M. & Schlievert, P. M. Toxic shock syndrome and bacterial superantigens: an update. *Annual review of microbiology* **55**, 77-104, doi:10.1146/annurev.micro.55.1.77 (2001).
136 Fraser, J. D. Clarifying the mechanism of superantigen toxicity. *PLoS biology* **9**, e1001145, doi:10.1371/journal.pbio.1001145 (2011).
137 Cavaillon, J. M., Adib-Conquy, M., Fitting, C., Adrie, C. & Payen, D. Cytokine cascade in sepsis. *Scandinavian journal of infectious diseases* **35**, 535-544, doi:10.1080/00365540310015935 (2003).
138 van Hal, S. J. *et al.* Predictors of mortality in Staphylococcus aureus Bacteremia. *Clinical microbiology reviews* **25**, 362-386, doi:10.1128/CMR.05022-11 (2012).
139 Kwiecinski, J. *et al.* Sulfatide attenuates experimental Staphylococcus aureus sepsis through a CD1d-dependent pathway. *Infection and immunity* **81**, 1114-1120, doi:10.1128/IAI.01334-12 (2013).
140 Krakauer, T. Update on staphylococcal superantigen-induced signaling pathways and therapeutic interventions. *Toxins* **5**, 1629-1654, doi:10.3390/toxins5091629 (2013).

141 Watson, A. R., Janik, D. K. & Lee, W. T. Superantigen-induced CD4 memory T cell anergy. I. Staphylococcal enterotoxin B induces Fyn-mediated negative signaling. *Cellular immunology* **276**, 16-25, doi:10.1016/j.cellimm.2012.02.003 (2012).

142 Bowdish, D. M., Davidson, D. J., Scott, M. G. & Hancock, R. E. Immunomodulatory activities of small host defense peptides. *Antimicrobial agents and chemotherapy* **49**, 1727-1732, doi:10.1128/AAC.49.5.1727-1732.2005 (2005).

143 Scott, M. G. *et al.* An anti-infective peptide that selectively modulates the innate immune response. *Nature biotechnology* **25**, 465-472, doi:10.1038/nbt1288 (2007).

144 van der Does, A. M. *et al.* The human lactoferrin-derived peptide hLF1-11 exerts immunomodulatory effects by specific inhibition of myeloperoxidase activity. *Journal of immunology* **188**, 5012-5019, doi:10.4049/jimmunol.1102777 (2012).

145 Cirioni, O. *et al.* IB-367 pre-treatment improves the in vivo efficacy of teicoplanin and daptomycin in an animal model of wounds infected with meticillin-resistant Staphylococcus aureus. *Journal of medical microbiology* **62**, 1552-1558, doi:10.1099/jmm.0.057414-0 (2013).

146 Silva, R. R. *et al.* Short-term therapy with simvastatin reduces inflammatory mediators and heart inflammation during the acute phase of experimental Chagas disease. *Mem Inst Oswaldo Cruz* **107**, 513-521 (2012).

147 Al-Siyabi, K. *et al.* Safety of simvastatin and goal attainment for low-density lipoprotein cholesterol in sultan qaboos university hospital. *Oman Med J* **25**, 264-268, doi:10.5001/omj.2010.79 (2010).

148 Zago, A. C. *et al.* First-in-man study of simvastatin-eluting stent in de novo coronary lesions: the SIMVASTENT study. *Circ J* **76**, 1109-1114 (2012).

149 Gazzerro, P. *et al.* Pharmacological actions of statins: a critical appraisal in the management of cancer. *Pharmacological reviews* **64**, 102-146, doi:10.1124/pr.111.004994 (2012).

150 Bergman, P. *et al.* Studies on the antibacterial effects of statins--in vitro and in vivo. *PLoS One* **6**, e24394, doi:10.1371/journal.pone.0024394 (2011).

151 Masadeh, M., Mhaidat, N., Alzoubi, K., Al-Azzam, S. & Alnasser, Z. Antibacterial activity of statins: a comparative study of atorvastatin, simvastatin, and rosuvastatin. *Ann Clin Microbiol Antimicrob* **11**, 13, doi:10.1186/1476-0711-11-13 (2012).

152 Farmer, A. R. *et al.* Effect of HMG-CoA reductase inhibitors on antimicrobial susceptibilities for gram-negative rods. *J Basic Microbiol* **53**, 336-339, doi:10.1002/jobm.201100614 (2013).

153 Cabral, M. E., Figueroa, L. I. & Fariña, J. I. Synergistic antifungal activity of statin-azole associations as witnessed by Saccharomyces cerevisiae- and Candida utilis-bioassays and ergosterol quantification. *Rev Iberoam Micol* **30**, 31-38, doi:10.1016/j.riam.2012.09.006 (2013).

154 Nalin, D. R. Comment on: unexpected antimicrobial effect of statins. *J Antimicrob Chemother* **61**, 1400, doi:10.1093/jac/dkn089 (2008).

155 Menezes, E. A. *et al.* In vitro synergism of simvastatin and fluconazole against Candida species. *Rev Inst Med Trop Sao Paulo* **54**, 197-199 (2012).

156 den Hollander, W. J. & Kuipers, E. J. Commentary: simvastatin as the key to improving H. pylori eradication rates? *Aliment Pharmacol Ther* **36**, 493; author reply 494, doi:10.1111/j.1365-2036.2012.05195.x (2012).

157 Wu, B. Q. *et al.* Inhibitory effects of simvastatin on staphylococcus aureus lipoteichoic acid-induced inflammation in human alveolar macrophages. *Clin Exp Med*, doi:10.1007/s10238-013-0231-z (2013).

158 Sun, H. Y. & Singh, N. Antimicrobial and immunomodulatory attributes of statins: relevance in solid-organ transplant recipients. *Clinical infectious diseases : an official publication of the Infectious Diseases Society of America* **48**, 745-755, doi:10.1086/597039 (2009).

159 Terblanche, M., Almog, Y., Rosenson, R. S., Smith, T. S. & Hackam, D. G. Statins and sepsis: multiple modifications at multiple levels. *The Lancet. Infectious diseases* **7**, 358-368, doi:10.1016/S1473-3099(07)70111-1 (2007).

160 Wang, H. R., Li, J. J., Huang, C. X. & Jiang, H. Fluvastatin inhibits the expression of tumor necrosis factor-alpha and activation of nuclear factor-kappaB in human endothelial cells stimulated by C-reactive protein. *Clinica chimica acta; international journal of clinical chemistry* **353**, 53-60, doi:10.1016/j.cccn.2004.10.007 (2005).

161 Grip, O., Janciauskiene, S. & Lindgren, S. Atorvastatin activates PPAR-gamma and attenuates the inflammatory response in human monocytes. *Inflammation research : official journal of the European Histamine Research Society ... [et al.]* **51**, 58-62 (2002).

162 Rosenson, R. S., Tangney, C. C. & Casey, L. C. Inhibition of proinflammatory cytokine production by pravastatin. *Lancet* **353**, 983-984, doi:10.1016/S0140-6736(98)05917-0 (1999).

163 Diomede, L. *et al.* In vivo anti-inflammatory effect of statins is mediated by nonsterol mevalonate products. *Arteriosclerosis, thrombosis, and vascular biology* **21**, 1327-1332 (2001).

164 Chang, L. T. *et al.* Impact of simvastatin and losartan on antiinflammatory effect: in vitro study. *Journal of cardiovascular pharmacology* **49**, 20-26, doi:10.1097/FJC.0b013e31802ba4ec (2007).

165 Kanda, H. *et al.* Antiinflammatory effect of simvastatin in patients with rheumatoid arthritis. *The Journal of rheumatology* **29**, 2024-2026 (2002).

166 Devran, O. *et al.* C-reactive protein as a predictor of mortality in patients affected with severe sepsis in intensive care unit. *Multidisciplinary respiratory medicine* **7**, 47, doi:10.1186/2049-6958-7-47 (2012).

167 Lobo, S. M. *et al.* C-reactive protein levels correlate with mortality and organ failure in critically ill patients. *Chest* **123**, 2043-2049 (2003).

168 Chan, K. Y., Boucher, E. S., Gandhi, P. J. & Silva, M. A. HMG-CoA reductase inhibitors for lowering elevated levels of C-reactive protein. *American journal of health-system pharmacy : AJHP : official journal of the American Society of Health-System Pharmacists* **61**, 1676-1681 (2004).

169 Arnaud, C. *et al.* Statins reduce interleukin-6-induced C-reactive protein in human hepatocytes: new evidence for direct antiinflammatory effects of statins. *Arteriosclerosis, thrombosis, and vascular biology* **25**, 1231-1236, doi:10.1161/01.ATV.0000163840.63685.0c (2005).

170 Marz, W., Winkler, K., Nauck, M., Bohm, B. O. & Winkelmann, B. R. Effects of statins on C-reactive protein and interleukin-6 (the Ludwigshafen Risk and Cardiovascular Health study). *The American journal of cardiology* **92**, 305-308 (2003).

171 Pruefer, D., Scalia, R. & Lefer, A. M. Simvastatin inhibits leukocyte-endothelial cell interactions and protects against inflammatory processes in normocholesterolemic rats. *Arteriosclerosis, thrombosis, and vascular biology* **19**, 2894-2900 (1999).

172 Weber, C., Erl, W., Weber, K. S. & Weber, P. C. HMG-CoA reductase inhibitors decrease CD11b expression and CD11b-dependent adhesion of monocytes to endothelium and reduce increased adhesiveness of monocytes isolated from patients with hypercholesterolemia. *Journal of the American College of Cardiology* **30**, 1212-1217 (1997).

173 Yoshida, M. *et al.* Hmg-CoA reductase inhibitor modulates monocyte-endothelial cell interaction under physiological flow conditions in vitro: involvement of Rho GTPase-dependent mechanism. *Arteriosclerosis, thrombosis, and vascular biology* **21**, 1165-1171 (2001).

174 Pruefer, D. *et al.* Simvastatin inhibits inflammatory properties of Staphylococcus aureus alpha-toxin. *Circulation* **106**, 2104-2110 (2002).

175 Liappis, A. P., Kan, V. L., Rochester, C. G. & Simon, G. L. The effect of statins on mortality in patients with bacteremia. *Clinical infectious diseases : an official publication of the Infectious Diseases Society of America* **33**, 1352-1357, doi:10.1086/323334 (2001).

176 Kruger, P., Fitzsimmons, K., Cook, D., Jones, M. & Nimmo, G. Statin therapy is associated with fewer deaths in patients with bacteraemia. *Intensive care medicine* **32**, 75-79, doi:10.1007/s00134-005-2859-y (2006).

177 Niren, N. M. Pharmacologic doses of nicotinamide in the treatment of inflammatory skin conditions: a review. *Cutis* **77**, 11-16 (2006).

178 Ungerstedt, J. S., Blomback, M. & Soderstrom, T. Nicotinamide is a potent inhibitor of proinflammatory cytokines. *Clinical and experimental immunology* **131**, 48-52 (2003).

179 Smith, I. M. & Burmeister, L. F. Biochemically assisted antibiotic treatment of lethal murine Staphylococcus aureus septic shock. *The American journal of clinical nutrition* **30**, 1364-1368 (1977).

180 Kyme, P. *et al.* C/EBPepsilon mediates nicotinamide-enhanced clearance of Staphylococcus aureus in mice. *The Journal of clinical investigation* **122**, 3316-3329, doi:10.1172/JCI62070 (2012).

181 Gombart, A. F. *et al.* Aberrant expression of neutrophil and macrophage-related genes in a murine model for human neutrophil-specific granule deficiency. *Journal of leukocyte biology* **78**, 1153-1165, doi:10.1189/jlb.0504286 (2005).

182 Verbeek, W. *et al.* Myeloid transcription factor C/EBPepsilon is involved in the positive regulation of lactoferrin gene expression in neutrophils. *Blood* **94**, 3141-3150 (1999).
183 Williams, S. C. *et al.* C/EBPepsilon is a myeloid-specific activator of cytokine, chemokine, and macrophage-colony-stimulating factor receptor genes. *The Journal of biological chemistry* **273**, 13493-13501 (1998).
184 LeClaire, R. D., Kell, W., Bavari, S., Smith, T. J. & Hunt, R. E. Protective effects of niacinamide in staphylococcal enterotoxin-B-induced toxicity. *Toxicology* **107**, 69-81 (1996).
185 Krakauer, T. & Buckley, M. Dexamethasone attenuates staphylococcal enterotoxin B-induced hypothermic response and protects mice from superantigen-induced toxic shock. *Antimicrobial agents and chemotherapy* **50**, 391-395, doi:10.1128/AAC.50.1.391-395.2006 (2006).
186 Krakauer, T., Buckley, M. J., Huzella, L. M. & Alves, D. A. Critical timing, location and duration of glucocorticoid administration rescue mice from superantigen-induced shock and attenuate lung injury. *International immunopharmacology* **9**, 1168-1174, doi:10.1016/j.intimp.2009.06.004 (2009).
187 Krakauer, T. Differential inhibitory effects of interleukin-10, interleukin-4, and dexamethasone on staphylococcal enterotoxin-induced cytokine production and T cell activation. *Journal of leukocyte biology* **57**, 450-454 (1995).
188 Krakauer, T. & Buckley, M. Efficacy of two FDA-approved drug combination in a mouse model of staphylococcal enterotoxin B-induced shock. *Military medicine* **178**, 1024-1028, doi:10.7205/MILMED-D-13-00129 (2013).
189 Saunders, R. N., Metcalfe, M. S. & Nicholson, M. L. Rapamycin in transplantation: a review of the evidence. *Kidney international* **59**, 3-16, doi:10.1046/j.1523-1755.2001.00460.x (2001).
190 Krakauer, T., Buckley, M., Issaq, H. J. & Fox, S. D. Rapamycin protects mice from staphylococcal enterotoxin B-induced toxic shock and blocks cytokine release in vitro and in vivo. *Antimicrobial agents and chemotherapy* **54**, 1125-1131, doi:10.1128/AAC.01015-09 (2010).
191 Krakauer, T. & Buckley, M. Intranasal rapamycin rescues mice from staphylococcal enterotoxin B-induced shock. *Toxins* **4**, 718-728, doi:10.3390/toxins4090718 (2012).
192 Krakauer, T. & Stiles, B. G. Pentoxifylline inhibits superantigen-induced toxic shock and cytokine release. *Clinical and diagnostic laboratory immunology* **6**, 594-598 (1999).
193 Huisinga, J. M., Pipinos, II, Stergiou, N. & Johanning, J. M. Treatment with pharmacological agents in peripheral arterial disease patients does not result in biomechanical gait changes. *Journal of applied biomechanics* **26**, 341-348 (2010).
194 Chung, P. Y. & Toh, Y. S. Anti-biofilm agents: recent breakthrough against multi-drug resistant Staphylococcus aureus. *Pathogens and disease* **70**, 231-239, doi:10.1111/2049-632X.12141 (2014).
195 Chen, M., Yu, Q. & Sun, H. Novel strategies for the prevention and treatment of biofilm related infections. *International journal of molecular sciences* **14**, 18488-18501, doi:10.3390/ijms140918488 (2013).

196 Dubreuil, L., Houcke, I., Mouton, Y. & Rossignol, J. F. In vitro evaluation of activities of nitazoxanide and tizoxanide against anaerobes and aerobic organisms. *Antimicrobial agents and chemotherapy* **40**, 2266-2270 (1996).
197 Tchouaffi-Nana, F. *et al.* Nitazoxanide inhibits biofilm formation by Staphylococcus epidermidis by blocking accumulation on surfaces. *Antimicrobial agents and chemotherapy* **54**, 2767-2774, doi:10.1128/AAC.00901-09 (2010).
198 Siles, S. A., Srinivasan, A., Pierce, C. G., Lopez-Ribot, J. L. & Ramasubramanian, A. K. High-throughput screening of a collection of known pharmacologically active small compounds for identification of Candida albicans biofilm inhibitors. *Antimicrobial agents and chemotherapy* **57**, 3681-3687, doi:10.1128/AAC.00680-13 (2013).
199 Shlaes, D. M., Sahm, D., Opiela, C. & Spellbergc, B. The FDA Reboot of Antibiotic Development. *Antimicrobial agents and chemotherapy* **57**, 4605-4607, doi:Doi 10.1128/Aac.01277-13 (2013).
200 FDA. *Silver Spring, MD* (2014).
201 FDA. *Silver Spring, MD* (2014).
202 Cooper, M. A. & Shlaes, D. Fix the antibiotics pipeline. *Nature* **472**, 32-32 (2011).
203 May, M. Drug Development Time for Teamwork. *Nature* **509**, S4-S5 (2014).
204 Mohammad, H., Mayhoub, A. S., Cushman, M. & Seleem, M. N. Anti-biofilm activity and synergism of novel thiazole compounds with glycopeptide antibiotics against multidrug-resistant Staphylococci. *The Journal of antibiotics* **68**, 259-266, doi:10.1038/ja.2014.142 (2015).
205 Gillet, Y. *et al.* Association between Staphylococcus aureus strains carrying gene for Panton-Valentine leukocidin and highly lethal necrotising pneumonia in young immunocompetent patients. *Lancet* **359**, 753-759, doi:Doi 10.1016/S0140-6736(02)07877-7 (2002).
206 David, M. Z. & Daum, R. S. Community-associated methicillin-resistant Staphylococcus aureus: epidemiology and clinical consequences of an emerging epidemic. *Clinical microbiology reviews* **23**, 616-687, doi:10.1128/CMR.00081-09 (2010).
207 Naber, C. K. Staphylococcus aureus bacteremia: epidemiology, pathophysiology, and management strategies. *Clin Infect Dis* **48 Suppl 4**, S231-237, doi:10.1086/598189 (2009).
208 Er, J., Wallis, P., Maloney, S. & Norton, R. Paediatric bacteraemias in tropical Australia. *Journal of paediatrics and child health* **51**, 437-442, doi:10.1111/jpc.12750 (2015).
209 Locke, J. B. *et al.* Elevated Linezolid Resistance in Clinical cfr-Positive Staphylococcus aureus Isolates Is Associated with Co-Occurring Mutations in Ribosomal Protein L3. *Antimicrobial agents and chemotherapy* **54**, 5352-5355, doi:Doi 10.1128/Aac.00714-10 (2010).
210 Thangamani, S., Mohammad, H., Younis, W. & Seleem, M. N. Drug Repurposing for the Treatment of Staphylococcal Infections. *Current pharmaceutical design* **21**, 2089-2100 (2015).

211 Thangamani, S., Younis, W. & Seleem, M. N. Repurposing ebselen for treatment of multidrug-resistant staphylococcal infections. *Scientific reports* **5**, 11596, doi:10.1038/srep11596 (2015).

212 Cassetta, M. I., Marzo, T., Fallani, S., Novelli, A. & Messori, L. Drug repositioning: auranofin as a prospective antimicrobial agent for the treatment of severe staphylococcal infections. *Biometals* **27**, 787-791, doi:DOI 10.1007/s10534-014-9743-6 (2014).

213 Harbut, M. B. *et al.* Auranofin exerts broad-spectrum bactericidal activities by targeting thiol-redox homeostasis. *Proceedings of the National Academy of Sciences of the United States of America* **112**, 4453-4458, doi:10.1073/pnas.1504022112 (2015).

214 Hokai, Y. *et al.* Auranofin and related heterometallic gold(I)-thiolates as potent inhibitors of methicillin-resistant Staphylococcus aureus bacterial strains. *J Inorg Biochem* **138**, 81-88, doi:DOI 10.1016/j.jinorgbio.2014.05.008 (2014).

215 Aguinagalde, L. *et al.* Auranofin efficacy against MDR Streptococcus pneumoniae and Staphylococcus aureus infections. *The Journal of antimicrobial chemotherapy* **70**, 2608-2617, doi:10.1093/jac/dkv163 (2015).

216 Mohamed, M. F., Hamed, M. I., Panitch, A. & Seleem, M. N. Targeting Methicillin-Resistant Staphylococcus aureus with Short Salt-Resistant Synthetic Peptides. *Antimicrobial agents and chemotherapy* **58**, 4113-4122, doi:10.1128/AAC.02578-14 (2014).

217 Randall, C. P., Mariner, K. R., Chopra, I. & O'Neill, A. J. The target of daptomycin is absent from Escherichia coli and other gram-negative pathogens. *Antimicrobial agents and chemotherapy* **57**, 637-639, doi:10.1128/AAC.02005-12 (2013).

218 Viljanen, P. & Vaara, M. Susceptibility of gram-negative bacteria to polymyxin B nonapeptide. *Antimicrobial agents and chemotherapy* **25**, 701-705 (1984).

219 Andrews, G. L., Simons, B. L., Young, J. B., Hawkridge, A. M. & Muddiman, D. C. Performance characteristics of a new hybrid quadrupole time-of-flight tandem mass spectrometer (TripleTOF 5600). *Analytical chemistry* **83**, 5442-5446, doi:10.1021/ac200812d (2011).

220 Cox, J. & Mann, M. MaxQuant enables high peptide identification rates, individualized p.p.b.-range mass accuracies and proteome-wide protein quantification. *Nature biotechnology* **26**, 1367-1372, doi:10.1038/nbt.1511 (2008).

221 Seral, C., Van Bambeke, F. & Tulkens, P. M. Quantitative analysis of gentamicin, azithromycin, telithromycin, ciprofloxacin, moxifloxacin, and oritavancin (LY333328) activities against intracellular Staphylococcus aureus in mouse J774 macrophages. *Antimicrob Agents Chemother* **47**, 2283-2292 (2003).

222 Younis, W., Thangamani, S. & Seleem, M. N. Repurposing Non-Antimicrobial Drugs and Clinical Molecules to Treat Bacterial Infections. *Current pharmaceutical design* **21**, 4106-4111 (2015).

223 Meletiadis, J., Pournaras, S., Roilides, E. & Walsh, T. J. Defining fractional inhibitory concentration index cutoffs for additive interactions based on self-drug additive combinations, Monte Carlo simulation analysis, and in vitro-in vivo correlation data for antifungal drug combinations against Aspergillus fumigatus. *Antimicrobial agents and chemotherapy* **54**, 602-609, doi:10.1128/AAC.00999-09 (2010).

224 King, A. M. *et al.* Aspergillomarasmine A overcomes metallo-beta-lactamase antibiotic resistance. *Nature* **510**, 503-506, doi:10.1038/nature13445 (2014).

225 Wu, Y. S., Koch, K. R., Abratt, V. R. & Klump, H. H. Intercalation into the DNA double helix and in vivo biological activity of water-soluble planar [Pt(diimine)(N,N-dihydroxyethyl-N'-benzoylthioureato)]+Cl- complexes: a study of their thermal stability, their CD spectra and their gel mobility. *Archives of biochemistry and biophysics* **440**, 28-37, doi:10.1016/j.abb.2005.05.022 (2005).

226 Thangamani, S., Younis, W. & Seleem, M. N. Repurposing Clinical Molecule Ebselen to Combat Drug Resistant Pathogens. *PloS one* **10**, e0133877, doi:10.1371/journal.pone.0133877 (2015).

227 Haste, N. M. *et al.* Activity of the thiopeptide antibiotic nosiheptide against contemporary strains of methicillin-resistant Staphylococcus aureus. *J Antibiot* **65**, 593-598, doi:DOI 10.1038/ja.2012.77 (2012).

228 Okusu, H., Ma, D. & Nikaido, H. AcrAB efflux pump plays a major role in the antibiotic resistance phenotype of Escherichia coli multiple-antibiotic-resistance (Mar) mutants. *J Bacteriol* **178**, 306-308 (1996).

229 Lok, C. N. *et al.* Proteomic analysis of the mode of antibacterial action of silver nanoparticles. *Journal of proteome research* **5**, 916-924, doi:10.1021/pr0504079 (2006).

230 Bandow, J. E., Brotz, H., Leichert, L. I., Labischinski, H. & Hecker, M. Proteomic approach to understanding antibiotic action. *Antimicrobial agents and chemotherapy* **47**, 948-955 (2003).

231 Wenzel, M. *et al.* Proteomic signature of fatty acid biosynthesis inhibition available for in vivo mechanism-of-action studies. *Antimicrobial agents and chemotherapy* **55**, 2590-2596, doi:10.1128/AAC.00078-11 (2011).

232 Stevens, D. L. *et al.* Impact of antibiotics on expression of virulence-associated exotoxin genes in methicillin-sensitive and methicillin-resistant Staphylococcus aureus. *J Infect Dis* **195**, 202-211, doi:Doi 10.1086/510396 (2007).

233 Diep, B. A. *et al.* Effects of Linezolid on Suppressing In Vivo Production of Staphylococcal Toxins and Improving Survival Outcomes in a Rabbit Model of Methicillin-Resistant Staphylococcus aureus Necrotizing Pneumonia. *J Infect Dis* **208**, 75-82, doi:DOI 10.1093/infdis/jit129 (2013).

234 Otto, M. P. *et al.* Effects of subinhibitory concentrations of antibiotics on virulence factor expression by community-acquired methicillin-resistant Staphylococcus aureus. *J Antimicrob Chemoth* **68**, 1524-1532, doi:Doi 10.1093/Jac/Dkt073 (2013).

235 Karau, M. J. *et al.* Linezolid Is Superior to Vancomycin in Experimental Pneumonia Caused by Superantigen-Producing Staphylococcus aureus in HLA Class II Transgenic Mice. *Antimicrobial agents and chemotherapy* **56**, 5401-5405, doi:Doi 10.1128/Aac.01080-12 (2012).

236 Lemaire, S. *et al.* Restoration of susceptibility of intracellular methicillin-resistant Staphylococcus aureus to beta-lactams: comparison of strains, cells, and antibiotics. *Antimicrobial agents and chemotherapy* **52**, 2797-2805, doi:10.1128/AAC.00123-08 (2008).

237 Tenover, F. C. & Goering, R. V. Methicillin-resistant Staphylococcus aureus strain USA300: origin and epidemiology. *The Journal of antimicrobial chemotherapy* **64**, 441-446, doi:10.1093/jac/dkp241 (2009).

238 Garzoni, C. & Kelley, W. L. Staphylococcus aureus: new evidence for intracellular persistence. *Trends in microbiology* **17**, 59-65, doi:10.1016/j.tim.2008.11.005 (2009).

239 Ellington, J. K. *et al.* Intracellular Staphylococcus aureus. A mechanism for the indolence of osteomyelitis. *The Journal of bone and joint surgery. British volume* **85**, 918-921 (2003).

240 Fowler, V. G., Jr. *et al.* Staphylococcus aureus endocarditis: a consequence of medical progress. *Jama* **293**, 3012-3021, doi:10.1001/jama.293.24.3012 (2005).

241 Ellington, J. K. *et al.* Intracellular Staphylococcus aureus and antibiotic resistance: implications for treatment of staphylococcal osteomyelitis. *Journal of orthopaedic research : official publication of the Orthopaedic Research Society* **24**, 87-93, doi:10.1002/jor.20003 (2006).

242 Seleem, M. N. *et al.* Targeting Brucella melitensis with polymeric nanoparticles containing streptomycin and doxycycline. *FEMS microbiology letters* **294**, 24-31, doi:10.1111/j.1574-6968.2009.01530.x (2009).

243 Rubinstein, E., Kollef, M. H. & Nathwani, D. Pneumonia caused by methicillin-resistant Staphylococcus aureus. *Clinical infectious diseases : an official publication of the Infectious Diseases Society of America* **46 Suppl 5**, S378-385, doi:10.1086/533594 (2008).

244 Deresinski, S. Vancomycin in combination with other antibiotics for the treatment of serious methicillin-resistant Staphylococcus aureus infections. *Clinical infectious diseases : an official publication of the Infectious Diseases Society of America* **49**, 1072-1079, doi:10.1086/605572 (2009).

245 Appelbaum, P. C. Microbiology of antibiotic resistance in Staphylococcus aureus. *Clinical infectious diseases : an official publication of the Infectious Diseases Society of America* **45 Suppl 3**, S165-170, doi:10.1086/519474 (2007).

246 Huang, V. & Rybak, M. J. Pharmacodynamics of cefepime alone and in combination with various antimicrobials against methicillin-resistant Staphylococcus aureus in an in vitro pharmacodynamic infection model. *Antimicrobial agents and chemotherapy* **49**, 302-308, doi:10.1128/AAC.49.1.302-308.2005 (2005).

247 Drago, L., De Vecchi, E., Nicola, L. & Gismondo, M. R. In vitro evaluation of antibiotics' combinations for empirical therapy of suspected methicillin resistant Staphylococcus aureus severe respiratory infections. *BMC infectious diseases* **7**, 111, doi:10.1186/1471-2334-7-111 (2007).

248 Seras-Franzoso, J. *et al.* Disulfide bond formation and activation of Escherichia coli beta-galactosidase under oxidizing conditions. *Applied and environmental microbiology* **78**, 2376-2385, doi:10.1128/AEM.06923-11 (2012).

249 Jackson-Rosario, S. *et al.* Auranofin disrupts selenium metabolism in Clostridium difficile by forming a stable Au-Se adduct. *Journal of biological inorganic chemistry : JBIC : a publication of the Society of Biological Inorganic Chemistry* **14**, 507-519, doi:10.1007/s00775-009-0466-z (2009).

250 Jackson-Rosario, S. & Self, W. T. Inhibition of selenium metabolism in the oral pathogen Treponema denticola. *Journal of bacteriology* **191**, 4035-4040, doi:10.1128/JB.00164-09 (2009).

251 Kryukov, G. V. & Gladyshev, V. N. The prokaryotic selenoproteome. *EMBO reports* **5**, 538-543, doi:10.1038/sj.embor.7400126 (2004).

252 O'Neill, A. J., Cove, J. H. & Chopra, I. Mutation frequencies for resistance to fusidic acid and rifampicin in Staphylococcus aureus. *The Journal of antimicrobial chemotherapy* **47**, 647-650 (2001).

253 Ling, L. L. *et al.* A new antibiotic kills pathogens without detectable resistance. *Nature* **517**, 455-459, doi:10.1038/nature14098 (2015).

254 Surewaard, B. G. *et al.* Staphylococcal alpha-phenol soluble modulins contribute to neutrophil lysis after phagocytosis. *Cellular microbiology* **15**, 1427-1437, doi:10.1111/cmi.12130 (2013).

255 Stryjewski, M. E. & Chambers, H. F. Skin and soft-tissue infections caused by community-acquired methicillin-resistant Staphylococcus aureus. *Clinical infectious diseases : an official publication of the Infectious Diseases Society of America* **46 Suppl 5**, S368-377, doi:10.1086/533593 (2008).

256 Montgomery, C. P. *et al.* Local inflammation exacerbates the severity of Staphylococcus aureus skin infection. *PloS one* **8**, e69508, doi:10.1371/journal.pone.0069508 (2013).

257 del Rio, A., Cervera, C., Moreno, A., Moreillon, P. & Miro, J. M. Patients at risk of complications of Staphylococcus aureus bloodstream infection. *Clinical infectious diseases : an official publication of the Infectious Diseases Society of America* **48 Suppl 4**, S246-253, doi:10.1086/598187 (2009).

258 Keynan, Y. & Rubinstein, E. Staphylococcus aureus bacteremia, risk factors, complications, and management. *Critical care clinics* **29**, 547-562, doi:10.1016/j.ccc.2013.03.008 (2013).

259 McNeil, J. C., Hulten, K. G., Kaplan, S. L. & Mason, E. O. Mupirocin resistance in Staphylococcus aureus causing recurrent skin and soft tissue infections in children. *Antimicrobial agents and chemotherapy* **55**, 2431-2433, doi:10.1128/AAC.01587-10 (2011).

260 Farrell, D. J., Castanheira, M. & Chopra, I. Characterization of global patterns and the genetics of fusidic acid resistance. *Clinical infectious diseases : an official publication of the Infectious Diseases Society of America* **52 Suppl 7**, S487-492, doi:10.1093/cid/cir164 (2011).

261 Corey, G. R., Jiang, H. & Moeck, G. Dalbavancin or oritavancin for skin infections. *The New England journal of medicine* **371**, 1162-1163 (2014).

262 Shorr, A. F. *et al.* Analysis of the phase 3 ESTABLISH trials of tedizolid versus linezolid in acute bacterial skin and skin structure infections. *Antimicrobial agents and chemotherapy* **59**, 864-871, doi:10.1128/AAC.03688-14 (2015).

263 Debnath, A. *et al.* A high-throughput drug screen for Entamoeba histolytica identifies a new lead and target. *Nat Med* **18**, 956-+, doi:Doi 10.1038/Nm.2758 (2012).

264 Harbut, M. B. *et al.* Auranofin exerts broad-spectrum bactericidal activities by targeting thiol-redox homeostasis. *Proceedings of the National Academy of Sciences of the United States of America* **112**, 4453-4458, doi:DOI 10.1073/pnas.1504022112 (2015).

265 Aguinagalde, L. *et al.* Auranofin efficacy against MDR Streptococcus pneumoniae and Staphylococcus aureus infections. *The Journal of antimicrobial chemotherapy*, doi:10.1093/jac/dkv163 (2015).

266 Mohamed, M. F. & Seleem, M. N. Efficacy of short novel antimicrobial and anti-inflammatory peptides in a mouse model of methicillin-resistant Staphylococcus aureus (MRSA) skin infection. *Drug design, development and therapy* **8**, 1979-1983, doi:10.2147/DDDT.S72129 (2014).

267 Conlon, B. P. *et al.* Activated ClpP kills persisters and eradicates a chronic biofilm infection. *Nature* **503**, 365-370, doi:10.1038/nature12790 (2013).

268 Hu, Y. & Coates, A. R. Enhancement by novel anti-methicillin-resistant Staphylococcus aureus compound HT61 of the activity of neomycin, gentamicin, mupirocin and chlorhexidine: in vitro and in vivo studies. *The Journal of antimicrobial chemotherapy* **68**, 374-384, doi:10.1093/jac/dks384 (2013).

269 Huang, L., Dai, T., Xuan, Y., Tegos, G. P. & Hamblin, M. R. Synergistic combination of chitosan acetate with nanoparticle silver as a topical antimicrobial: efficacy against bacterial burn infections. *Antimicrobial agents and chemotherapy* **55**, 3432-3438, doi:10.1128/AAC.01803-10 (2011).

270 Mah, T. F. & O'Toole, G. A. Mechanisms of biofilm resistance to antimicrobial agents. *Trends in microbiology* **9**, 34-39 (2001).

271 Egsmose, C. *et al.* Patients with rheumatoid arthritis benefit from early 2nd line therapy: 5 year followup of a prospective double blind placebo controlled study. *The Journal of rheumatology* **22**, 2208-2213 (1995).

272 Forcade, N. A. *et al.* Prevalence, severity, and treatment of community-acquired methicillin-resistant Staphylococcus aureus (CA-MRSA) skin and soft tissue infections in 10 medical clinics in Texas: a South Texas Ambulatory Research Network (STARNet) study. *Journal of the American Board of Family Medicine : JABFM* **24**, 543-550, doi:10.3122/jabfm.2011.05.110073 (2011).

273 Odell, C. A. Community-associated methicillin-resistant Staphylococcus aureus (CA-MRSA) skin infections. *Current opinion in pediatrics* **22**, 273-277, doi:10.1097/MOP.0b013e328339421b (2010).

274 Skiest, D. J. & Cooper, T. W. High recurrence rate of CA-MRSA skin and soft tissue infections. *Archives of internal medicine* **167**, 2527author reply 2527, doi:10.1001/archinte.167.22.2527-a (2007).

275 Austin, C. P., Brady, L. S., Insel, T. R. & Collins, F. S. NIH Molecular Libraries Initiative. *Science* **306**, 1138-1139, doi:10.1126/science.1105511 (2004).

276 Thangamani, S., Mohammad, H., Younis, W. & Seleem, M. N. Drug Repurposing for the Treatment of Staphylococcal Infections. *Current pharmaceutical design* (2015).

277 Chong, C. R. & Sullivan, D. J. New uses for old drugs. *Nature* **448**, 645-646 (2007).
278 Ashburn, T. T. & Thor, K. B. Drug repositioning: identifying and developing new uses for existing drugs. *Nat Rev Drug Discov* **3**, 673-683, doi:10.1038/nrd1468 (2004).
279 Stevens, D. L., Maier, K. A. & Mitten, J. E. Effect of antibiotics on toxin production and viability of Clostridium perfringens. *Antimicrobial agents and chemotherapy* **31**, 213-218 (1987).
280 Stevens, D. L. *et al.* Impact of antibiotics on expression of virulence-associated exotoxin genes in methicillin-sensitive and methicillin-resistant Staphylococcus aureus. *The Journal of infectious diseases* **195**, 202-211, doi:10.1086/510396 (2007).
281 Rioja, I., Bush, K. A., Buckton, J. B., Dickson, M. C. & Life, P. F. Joint cytokine quantification in two rodent arthritis models: kinetics of expression, correlation of mRNA and protein levels and response to prednisolone treatment. *Clinical and experimental immunology* **137**, 65-73, doi:10.1111/j.1365-2249.2004.02499.x (2004).
282 Morones-Ramirez, J. R., Winkler, J. A., Spina, C. S. & Collins, J. J. Silver enhances antibiotic activity against gram-negative bacteria. *Science translational medicine* **5**, 190ra181, doi:10.1126/scitranslmed.3006276 (2013).
283 Bassani, A. S. P., Banov, D. M. & Lehman, P. A. M. Evaluation of the Percutaneous Absorption of Promethazine Hydrochloride, In Vitro, Using the Human Ex Vivo Skin Model. *International journal of pharmaceutical compounding* **12**, 270-273 (2008).
284 Berk, D. R. & Bayliss, S. J. MRSA, staphylococcal scalded skin syndrome, and other cutaneous bacterial emergencies. *Pediatric annals* **39**, 627-633, doi:10.3928/00904481-20100922-02 (2010).
285 Antonelou, M., Knowles, J., Siddiqi, S. & Sharma, P. Recurrent cutaneous abscesses caused by PVL-MRSA. *BMJ case reports* **2011**, doi:10.1136/bcr.01.2011.3680 (2011).
286 Payne, D. J., Gwynn, M. N., Holmes, D. J. & Pompliano, D. L. Drugs for bad bugs: confronting the challenges of antibacterial discovery. *Nature reviews. Drug discovery* **6**, 29-40, doi:10.1038/nrd2201 (2007).
287 Lubick, N. Tools for tracking antibiotic resistance. *Environmental health perspectives* **119**, A214-217, doi:10.1289/ehp.119-a214 (2011).
288 King, M. D. *et al.* Emergence of community-acquired methicillin-resistant Staphylococcus aureus USA 300 clone as the predominant cause of skin and soft-tissue infections. *Annals of internal medicine* **144**, 309-317 (2006).
289 Diep, B. A. *et al.* Effects of linezolid on suppressing in vivo production of staphylococcal toxins and improving survival outcomes in a rabbit model of methicillin-resistant Staphylococcus aureus necrotizing pneumonia. *The Journal of infectious diseases* **208**, 75-82, doi:10.1093/infdis/jit129 (2013).
290 Otto, M. P. *et al.* Effects of subinhibitory concentrations of antibiotics on virulence factor expression by community-acquired methicillin-resistant Staphylococcus aureus. *The Journal of antimicrobial chemotherapy* **68**, 1524-1532, doi:10.1093/jac/dkt073 (2013).

291 Karau, M. J. *et al.* Linezolid is superior to vancomycin in experimental pneumonia caused by Superantigen-Producing staphylococcus aureus in HLA class II transgenic mice. *Antimicrobial agents and chemotherapy* **56**, 5401-5405, doi:10.1128/AAC.01080-12 (2012).

292 Molina-Manso, D. *et al.* In vitro susceptibility to antibiotics of staphylococci in biofilms isolated from orthopaedic infections. *International journal of antimicrobial agents* **41**, 521-523, doi:10.1016/j.ijantimicag.2013.02.018 (2013).

293 Sharma-Kuinkel, B. K., Zhang, Y., Yan, Q., Ahn, S. H. & Fowler, V. G., Jr. Host gene expression profiling and in vivo cytokine studies to characterize the role of linezolid and vancomycin in methicillin-resistant Staphylococcus aureus (MRSA) murine sepsis model. *PloS one* **8**, e60463, doi:10.1371/journal.pone.0060463 (2013).

294 Kuhl, P., Borbe, H. O., Romer, A., Fischer, H. & Parnham, M. J. Selective inhibition of leukotriene B4 formation by Ebselen: a novel approach to antiinflammatory therapy. *Agents and actions* **17**, 366-367 (1986).

295 Jacqueline, C. *et al.* Linezolid Dampens Neutrophil-Mediated Inflammation in Methicillin-Resistant Staphylococcus aureus-Induced Pneumonia and Protects the Lung of Associated Damages. *The Journal of infectious diseases*, doi:10.1093/infdis/jiu145 (2014).

296 Mohammad, H., Mayhoub, A. S., Cushman, M. & Seleem, M. N. Anti-biofilm activity and synergism of novel thiazole compounds with glycopeptide antibiotics against multidrug-resistant Staphylococci. *The Journal of antibiotics*, doi:10.1038/ja.2014.142 (2014).

297 Younis, W., Thangamani, S. & Seleem, M. N. Repurposing Non-antimicrobial Drugs and Clinical Molecules to Treat Bacterial Infections. *Current pharmaceutical design* (2015).

298 Favrot, L. *et al.* Mechanism of inhibition of Mycobacterium tuberculosis antigen 85 by ebselen. *Nature communications* **4**, 2748, doi:10.1038/ncomms3748 (2013).

299 Younis, W. T., S.; and Seleem, M.N. Repurposing non-antimicrobial drugs and clinical molecules to treat bacterial infections. *Current pharmaceutical design* (2015).

300 **CLSI**. Methods for dilution antimicrobial susceptibility tests for bacteria that grow aerobically; approved standard M7-A7. CLSI, Wayne, PA. (2007).

301 Alajlouni, R. A. & Seleem, M. N. Targeting listeria monocytogenes rpoA and rpoD genes using peptide nucleic acids. *Nucleic acid therapeutics* **23**, 363-367, doi:10.1089/nat.2013.0426 (2013).

302 Cohen, D. J. *et al.* Postoperative intraperitoneal 5-fluoro-2'-deoxyuridine added to chemoradiation in patients curatively resected (R0) for locally advanced gastric and gastroesophageal junction adenocarcinoma. *Annals of surgical oncology* **19**, 478-485, doi:10.1245/s10434-011-1940-8 (2012).

303 Delcour, A. H. Outer membrane permeability and antibiotic resistance. *Biochimica et biophysica acta* **1794**, 808-816, doi:10.1016/j.bbapap.2008.11.005 (2009).

304 Nakae, T. The problems in the outer membrane permeability and the antibiotic resistance of Pseudomonas aeruginosa. *The Kitasato archives of experimental medicine* **64**, 115-121 (1991).

305 Li, X. Z., Plesiat, P. & Nikaido, H. The challenge of efflux-mediated antibiotic resistance in Gram-negative bacteria. *Clinical microbiology reviews* **28**, 337-418, doi:10.1128/CMR.00117-14 (2015).

306 Aeschlimann, J. R. The role of multidrug efflux pumps in the antibiotic resistance of Pseudomonas aeruginosa and other gram-negative bacteria. Insights from the Society of Infectious Diseases Pharmacists. *Pharmacotherapy* **23**, 916-924 (2003).

307 Cruciani, M. *et al.* Penetration of vancomycin into human lung tissue. *J Antimicrob Chemoth* **38**, 865-869 (1996).

308 Peltola, H., Paakkonen, M., Kallio, P. & Kallio, M. J. T. Bad Bugs, No Drugs: No ESCAPE Revisited Reply. *Clinical Infectious Diseases* **49**, 993-993 (2009).

309 Nau, R. & Eiffert, H. Modulation of release of proinflammatory bacterial compounds by antibacterials: potential impact on course of inflammation and outcome in sepsis and meningitis. *Clinical microbiology reviews* **15**, 95-110 (2002).

310 Diep, B. A., Equils, O., Huang, D. B. & Gladue, R. Linezolid effects on bacterial toxin production and host immune response: review of the evidence. *Current therapeutic research, clinical and experimental* **73**, 86-102, doi:10.1016/j.curtheres.2012.04.002 (2012).

311 McKee, E. E., Ferguson, M., Bentley, A. T. & Marks, T. A. Inhibition of mammalian mitochondrial protein synthesis by oxazolidinones. *Antimicrobial agents and chemotherapy* **50**, 2042-2049 (2006).

312 Gerson, S. L. *et al.* Hematologic effects of linezolid: Summary of clinical experience. *Antimicrobial agents and chemotherapy* **46**, 2723-2726 (2002).

313 Kuter, D. J. & Tillotson, G. S. Hematologic effects of antimicrobials: Focus on the oxazolidinone linezolid. *Pharmacotherapy* **21**, 1010-1013 (2001).

314 McKee, E. E., Ferguson, M., Bentley, A. T. & Marks, T. A. Inhibition of mammalian mitochondrial protein synthesis by oxazolidinones. *Antimicrobial agents and chemotherapy* **50**, 2042-2049, doi:10.1128/AAC.01411-05 (2006).

315 Manyan, D. R., Arimura, G. K. & Yunis, A. A. Chloramphenicol-induced erythroid suppression and bone marrow ferrochelatase activity in dogs. *The Journal of laboratory and clinical medicine* **79**, 137-144 (1972).

316 Parashar, S., Rao, R., Tikare, S. K. & Tikare, S. S. Chloramphenicol induced reversible bone marrow suppression. A case report. *Journal of postgraduate medicine* **18**, 90-92 (1972).

317 Yunis, A. A. Chloramphenicol-induced bone marrow suppression. *Seminars in hematology* **10**, 225-234 (1973).

318 Skripkin, E. *et al.* R chi-01, a new family of oxazolidinones that overcome ribosome-based linezolid resistance. *Antimicrobial agents and chemotherapy* **52**, 3550-3557 (2008).

319 Yan, K. *et al.* Biochemical characterization of the interactions of the novel pleuromutilin derivative retapamulin with bacterial ribosomes. *Antimicrobial agents and chemotherapy* **50**, 3875-3881 (2006).

320 Rajamuthiah, R. *et al.* Repurposing Salicylanilide Anthelmintic Drugs to Combat Drug Resistant Staphylococcus aureus. *PloS one* **10**, e0124595, doi:10.1371/journal.pone.0124595 (2015).

321 Diep, B. A., Carleton, H. A., Chang, R. F., Sensabaugh, G. F. & Perdreau-Remington, F. Roles of 34 virulence genes in the evolution of hospital- and community-associated strains of methicillin-resistant Staphylococcus aureus. *The Journal of infectious diseases* **193**, 1495-1503, doi:10.1086/503777 (2006).

322 Gordon, R. J. & Lowy, F. D. Pathogenesis of methicillin-resistant Staphylococcus aureus infection. *Clinical infectious diseases : an official publication of the Infectious Diseases Society of America* **46 Suppl 5**, S350-359, doi:10.1086/533591 (2008).

323 Guo, S. & Dipietro, L. A. Factors affecting wound healing. *Journal of dental research* **89**, 219-229, doi:10.1177/0022034509359125 (2010).

324 McNeil, J. C., Hulten, K. G., Kaplan, S. L. & Mason, E. O. Decreased susceptibilities to Retapamulin, Mupirocin, and Chlorhexidine among Staphylococcus aureus isolates causing skin and soft tissue infections in otherwise healthy children. *Antimicrobial agents and chemotherapy* **58**, 2878-2883, doi:10.1128/AAC.02707-13 (2014).

325 Ellington, M. J. *et al.* Emergent and evolving antimicrobial resistance cassettes in community-associated fusidic acid and meticillin-resistant Staphylococcus aureus. *International journal of antimicrobial agents*, doi:10.1016/j.ijantimicag.2015.01.009 (2015).

326 Rangel-Vega, A., Bernstein, L. R., Mandujano-Tinoco, E. A., Garcia-Contreras, S. J. & Garcia-Contreras, R. Drug repurposing as an alternative for the treatment of recalcitrant bacterial infections. *Frontiers in microbiology* **6**, 282, doi:10.3389/fmicb.2015.00282 (2015).

327 Frampton, J. E. & Keating, G. M. Celecoxib: a review of its use in the management of arthritis and acute pain. *Drugs* **67**, 2433-2472 (2007).

328 McCormack, P. L. Celecoxib: a review of its use for symptomatic relief in the treatment of osteoarthritis, rheumatoid arthritis and ankylosing spondylitis. *Drugs* **71**, 2457-2489, doi:10.2165/11208240-000000000-00000 (2011).

329 Bensen, W. G. Antiinflammatory and analgesic efficacy of COX-2 specific inhibition: from investigational trials to clinical experience. *The Journal of rheumatology. Supplement* **60**, 17-24 (2000).

330 Pereira, P. A. *et al.* Celecoxib improves host defense through prostaglandin inhibition during Histoplasma capsulatum infection. *Mediators of inflammation* **2013**, 950981, doi:10.1155/2013/950981 (2013).

331 Chiu, H. C. *et al.* Pharmacological exploitation of an off-target antibacterial effect of the cyclooxygenase-2 inhibitor celecoxib against Francisella tularensis. *Antimicrobial agents and chemotherapy* **53**, 2998-3002, doi:10.1128/AAC.00048-09 (2009).

332 Kalle, A. M. & Rizvi, A. Inhibition of bacterial multidrug resistance by celecoxib, a cyclooxygenase-2 inhibitor. *Antimicrobial agents and chemotherapy* **55**, 439-442, doi:10.1128/AAC.00735-10 (2011).

333 Annamanedi, M. & Kalle, A. M. Celecoxib sensitizes Staphylococcus aureus to antibiotics in macrophages by modulating SIRT1. *PloS one* **9**, e99285, doi:10.1371/journal.pone.0099285 (2014).

334 Cho, J. S. *et al.* Noninvasive in vivo imaging to evaluate immune responses and antimicrobial therapy against Staphylococcus aureus and USA300 MRSA skin infections. *The Journal of investigative dermatology* **131**, 907-915, doi:10.1038/jid.2010.417 (2011).

335 Cho, J. S. *et al.* IL-17 is essential for host defense against cutaneous Staphylococcus aureus infection in mice. *The Journal of clinical investigation* **120**, 1762-1773, doi:10.1172/JCI40891 (2010).

336 Mohamed, M. F. & Seleem, M. N. Efficacy of short novel antimicrobial and anti-inflammatory peptides in a mouse model of methicillin-resistant Staphylococcus aureus (MRSA) skin infection. *Drug Des Dev Ther* **8**, 1979-1983, doi:Doi 10.2147/Dddt.S72129 (2014).

337 Aryee, A. & Price, N. Antimicrobial stewardship - can we afford to do without it? *British journal of clinical pharmacology* **79**, 173-181, doi:10.1111/bcp.12417 (2015).

338 Vaara, M. Polymyxins and their novel derivatives. *Curr Opin Microbiol* **13**, 574-581, doi:10.1016/j.mib.2010.09.002 (2010).

339 Vaara, M. *et al.* A novel polymyxin derivative that lacks the fatty acid tail and carries only three positive charges has strong synergism with agents excluded by the intact outer membrane. *Antimicrob Agents Chemother* **54**, 3341-3346, doi:10.1128/AAC.01439-09 (2010).

340 Velkov, T. *et al.* Surface changes and polymyxin interactions with a resistant strain of Klebsiella pneumoniae. *Innate Immun*, doi:10.1177/1753425913493337 (2013).

341 McFarland, M. M., Scott, E. M. & Li Wan Po, A. Time-survival studies for quantifying effects of azlocillin and tobramycin on Pseudomonas aeruginosa. *Antimicrobial agents and chemotherapy* **38**, 1271-1276 (1994).

342 White, A. R., Comber, K. R. & Sutherland, R. Comparative bactericidal effects of azlocillin and ticarcillin against Pseudomonas aeruginosa. *Antimicrobial agents and chemotherapy* **18**, 182-189 (1980).

343 Patrzykat, A., Friedrich, C. L., Zhang, L., Mendoza, V. & Hancock, R. E. Sublethal concentrations of pleurocidin-derived antimicrobial peptides inhibit macromolecular synthesis in Escherichia coli. *Antimicrobial agents and chemotherapy* **46**, 605-614 (2002).

344 Ulvatne, H., Samuelsen, O., Haukland, H. H., Kramer, M. & Vorland, L. H. Lactoferricin B inhibits bacterial macromolecular synthesis in Escherichia coli and Bacillus subtilis. *FEMS microbiology letters* **237**, 377-384, doi:10.1016/j.femsle.2004.07.001 (2004).

345 Freer, E. *et al.* Brucella-Salmonella lipopolysaccharide chimeras are less permeable to hydrophobic probes and more sensitive to cationic peptides and EDTA than are their native Brucella sp. counterparts. *Journal of bacteriology* **178**, 5867-5876 (1996).

346 Tindall, E. Celecoxib for the treatment of pain and inflammation: the preclinical and clinical results. *The Journal of the American Osteopathic Association* **99**, S13-17 (1999).

347 Kumar, V., Kaur, K., Gupta, G. K., Gupta, A. K. & Kumar, S. Developments in synthesis of the anti-inflammatory drug, celecoxib: a review. *Recent patents on inflammation & allergy drug discovery* **7**, 124-134 (2013).

348 Wilgus, T. A., Vodovotz, Y., Vittadini, E., Clubbs, E. A. & Oberyszyn, T. M. Reduction of scar formation in full-thickness wounds with topical celecoxib treatment. *Wound repair and regeneration : official publication of the Wound Healing Society [and] the European Tissue Repair Society* **11**, 25-34 (2003).

349 Brynildsen, M. P., Winkler, J. A., Spina, C. S., MacDonald, I. C. & Collins, J. J. Potentiating antibacterial activity by predictably enhancing endogenous microbial ROS production. *Nature biotechnology* **31**, 160-165, doi:10.1038/nbt.2458 (2013).

350 Perlin, D. S. Mechanisms of echinocandin antifungal drug resistance. *Annals of the New York Academy of Sciences* **1354**, 1-11, doi:10.1111/nyas.12831 (2015).

351 Perlin, D. S., Shor, E. & Zhao, Y. Update on Antifungal Drug Resistance. *Current clinical microbiology reports* **2**, 84-95, doi:10.1007/s40588-015-0015-1 (2015).

352 Pfaller, M. A. Antifungal drug resistance: mechanisms, epidemiology, and consequences for treatment. *The American journal of medicine* **125**, S3-13, doi:10.1016/j.amjmed.2011.11.001 (2012).

353 Sanguinetti, M., Posteraro, B. & Lass-Florl, C. Antifungal drug resistance among Candida species: mechanisms and clinical impact. *Mycoses* **58 Suppl 2**, 2-13, doi:10.1111/myc.12330 (2015).

354 Brown, G. D. *et al.* Hidden killers: human fungal infections. *Sci Transl Med* **4**, 165rv113, doi:10.1126/scitranslmed.3004404 (2012).

355 Vandeputte, P., Ferrari, S. & Coste, A. T. Antifungal resistance and new strategies to control fungal infections. *Int J Microbiol* **2012**, 713687, doi:10.1155/2012/713687 (2012).

356 Butts, A. & Krysan, D. J. Antifungal drug discovery: something old and something new. *PLoS Pathog* **8**, e1002870, doi:10.1371/journal.ppat.1002870 (2012).

357 Thangamani, S. *et al.* Antibacterial activity and mechanism of action of auranofin against multi-drug resistant bacterial pathogens. *Scientific reports* **6**, 22571, doi:10.1038/srep22571 (2016).

358 Thangamani, S., Mohammad, H., Abushahba, M. F., Sobreira, T. J. & Seleem, M. N. Repurposing auranofin for the treatment of cutaneous staphylococcal infections. *International journal of antimicrobial agents* **47**, 195-201, doi:10.1016/j.ijantimicag.2015.12.016 (2016).

359 Fuchs, B. B. *et al.* Inhibition of bacterial and fungal pathogens by the orphaned drug auranofin. *Future medicinal chemistry* **8**, 117-132, doi:10.4155/fmc.15.182 (2016).

360 Stylianou, M. *et al.* Antifungal application of nonantifungal drugs. *Antimicrobial agents and chemotherapy* **58**, 1055-1062, doi:10.1128/AAC.01087-13 (2014).

361 da Silva, A. R. *et al.* Berberine Antifungal Activity in Fluconazole-resistant Pathogenic Yeasts: Action Mechanism Evaluated by Flow Cytometry and Biofilm Growth Inhibition in Candida spp. *Antimicrobial agents and chemotherapy*, doi:10.1128/AAC.01846-15 (2016).

362 Canton, E., Peman, J., Gobernado, M., Viudes, A. & Espinel-Ingroff, A. Patterns of amphotericin B killing kinetics against seven Candida species. *Antimicrobial agents and chemotherapy* **48**, 2477-2482, doi:10.1128/AAC.48.7.2477-2482.2004 (2004).

363 Rane, H. S., Bernardo, S. M., Walraven, C. J. & Lee, S. A. In vitro analyses of ethanol activity against Candida albicans biofilms. *Antimicrobial agents and chemotherapy* **56**, 4487-4489, doi:10.1128/AAC.00263-12 (2012).

364 Pierce, C. G. *et al.* A simple and reproducible 96-well plate-based method for the formation of fungal biofilms and its application to antifungal susceptibility testing. *Nature protocols* **3**, 1494-1500, doi:10.1038/nport.2008.141 (2008).

365 Dongari-Bagtzoglou, A., Kashleva, H., Dwivedi, P., Diaz, P. & Vasilakos, J. Characterization of mucosal Candida albicans biofilms. *PloS one* **4**, e7967, doi:10.1371/journal.pone.0007967 (2009).

366 Amberg, D. C., D. Burke, and J. N. Strathern. Methods in Yeast Genetics. A Cold Spring Harbor Laboratory Course Manual *Cold Spring Harbor Laboratory Press* (2005).

367 Smith, A. M. *et al.* Quantitative phenotyping via deep barcode sequencing. *Genome research* **19**, 1836-1842, doi:10.1101/gr.093955.109 (2009).

368 Robinson, M. D., McCarthy, D. J. & Smyth, G. K. edgeR: a Bioconductor package for differential expression analysis of digital gene expression data. *Bioinformatics* **26**, 139-140, doi:10.1093/bioinformatics/btp616 (2010).

369 Gamberi, T. *et al.* Evidence that the antiproliferative effects of auranofin in Saccharomyces cerevisiae arise from inhibition of mitochondrial respiration. *The international journal of biochemistry & cell biology* **65**, 61-71, doi:10.1016/j.biocel.2015.05.016 (2015).

370 Hasson, S. A. *et al.* Substrate specificity of the TIM22 mitochondrial import pathway revealed with small molecule inhibitor of protein translocation. *Proc Natl Acad Sci U S A* **107**, 9578-9583, doi:10.1073/pnas.0914387107 (2010).

371 Dabir, D. V. *et al.* A small molecule inhibitor of redox-regulated protein translocation into mitochondria. *Developmental cell* **25**, 81-92, doi:10.1016/j.devcel.2013.03.006 (2013).

372 Glick, B. S. & Pon, L. A. Isolation of highly purified mitochondria from Saccharomyces cerevisiae. *Methods Enzymol* **260**, 213-223 (1995).

373 Dabir, D. V. *et al.* A role for cytochrome c and cytochrome c peroxidase in electron shuttling from Erv1. *The EMBO journal* **26**, 4801-4811, doi:10.1038/sj.emboj.7601909 (2007).

374 Mylonakis, E., Ausubel, F. M., Perfect, J. R., Heitman, J. & Calderwood, S. B. Killing of Caenorhabditis elegans by Cryptococcus neoformans as a model of yeast pathogenesis. *Proceedings of the National Academy of Sciences of the United States of America* **99**, 15675-15680, doi:10.1073/pnas.232568599 (2002).

375 Chandra, J. *et al.* Biofilm formation by the fungal pathogen Candida albicans: development, architecture, and drug resistance. *Journal of bacteriology* **183**, 5385-5394 (2001).

376 Chandra, J. & Mukherjee, P. K. Candida Biofilms: Development, Architecture, and Resistance. *Microbiology spectrum* **3**, doi:10.1128/microbiolspec.MB-0020-2015 (2015).
377 Mathe, L. & Van Dijck, P. Recent insights into Candida albicans biofilm resistance mechanisms. *Current genetics* **59**, 251-264, doi:10.1007/s00294-013-0400-3 (2013).
378 Giaever, G. *et al.* Chemogenomic profiling: identifying the functional interactions of small molecules in yeast. *Proceedings of the National Academy of Sciences of the United States of America* **101**, 793-798, doi:10.1073/pnas.0307490100 (2004).
379 Roemer, T., Davies, J., Giaever, G. & Nislow, C. Bugs, drugs and chemical genomics. *Nature chemical biology* **8**, 46-56, doi:10.1038/nchembio.744 (2012).
380 Hoepfner, D. *et al.* High-resolution chemical dissection of a model eukaryote reveals targets, pathways and gene functions. *Microbiological research* **169**, 107-120, doi:10.1016/j.micres.2013.11.004 (2014).
381 Hillenmeyer, M. E. *et al.* The chemical genomic portrait of yeast: uncovering a phenotype for all genes. *Science* **320**, 362-365, doi:10.1126/science.1150021 (2008).
382 Giaever, G. *et al.* Genomic profiling of drug sensitivities via induced haploinsufficiency. *Nature genetics* **21**, 278-283, doi:10.1038/6791 (1999).
383 Nijman, S. M. Functional genomics to uncover drug mechanism of action. *Nature chemical biology* **11**, 942-948, doi:10.1038/nchembio.1963 (2015).
384 Lee, A. Y. *et al.* Mapping the cellular response to small molecules using chemogenomic fitness signatures. *Science* **344**, 208-211, doi:10.1126/science.1250217 (2014).
385 Rissler, M. *et al.* The essential mitochondrial protein Erv1 cooperates with Mia40 in biogenesis of intermembrane space proteins. *Journal of molecular biology* **353**, 485-492, doi:10.1016/j.jmb.2005.08.051 (2005).
386 Banci, L. *et al.* MIA40 is an oxidoreductase that catalyzes oxidative protein folding in mitochondria. *Nature structural & molecular biology* **16**, 198-206, doi:10.1038/nsmb.1553 (2009).
387 Bihlmaier, K. *et al.* The disulfide relay system of mitochondria is connected to the respiratory chain. *The Journal of cell biology* **179**, 389-395, doi:10.1083/jcb.200707123 (2007).
388 Lisowsky, T. Dual function of a new nuclear gene for oxidative phosphorylation and vegetative growth in yeast. *Molecular & general genetics : MGG* **232**, 58-64 (1992).
389 Neal, S. E. *et al.* Mia40 Protein Serves as an Electron Sink in the Mia40-Erv1 Import Pathway. *The Journal of biological chemistry* **290**, 20804-20814, doi:10.1074/jbc.M115.669440 (2015).
390 Bourens, M. *et al.* Role of twin Cys-Xaa9-Cys motif cysteines in mitochondrial import of the cytochrome C oxidase biogenesis factor Cmc1. *The Journal of biological chemistry* **287**, 31258-31269, doi:10.1074/jbc.M112.383562 (2012).
391 Mesecke, N. *et al.* A disulfide relay system in the intermembrane space of mitochondria that mediates protein import. *Cell* **121**, 1059-1069, doi:10.1016/j.cell.2005.04.011 (2005).

392 Parsonage, D. *et al.* X-ray structures of thioredoxin and thioredoxin reductase from Entamoeba histolytica and prevailing hypothesis of the mechanism of Auranofin action. *Journal of structural biology* **194**, 180-190, doi:10.1016/j.jsb.2016.02.015 (2016).

393 Ullrich, V., Weber, P., Meisch, F. & von Appen, F. Ebselen-binding equilibria between plasma and target proteins. *Biochem Pharmacol* **52**, 15-19 (1996).

394 Haenen, G. R., De Rooij, B. M., Vermeulen, N. P. & Bast, A. Mechanism of the reaction of ebselen with endogenous thiols: dihydrolipoate is a better cofactor than glutathione in the peroxidase activity of ebselen. *Mol Pharmacol* **37**, 412-422 (1990).

395 Cotgreave, I. A., Morgenstern, R., Engman, L. & Ahokas, J. Characterisation and quantitation of a selenol intermediate in the reaction of ebselen with thiols. *Chem Biol Interact* **84**, 69-76 (1992).

396 Hattori, R. *et al.* Effect of ebselen on bovine and rat nitric oxide synthase activity is modified by thiols. *Jpn J Pharmacol* **72**, 191-193 (1996).

397 Kade, I. J., Balogun, B. D. & Rocha, J. B. In vitro glutathione peroxidase mimicry of ebselen is linked to its oxidation of critical thiols on key cerebral suphydryl proteins - A novel component of its GPx-mimic antioxidant mechanism emerging from its thiol-modulated toxicology and pharmacology. *Chem Biol Interact* **206**, 27-36, doi:10.1016/j.cbi.2013.07.014 (2013).

398 Yang, C. F., Shen, H. M. & Ong, C. N. Ebselen induces apoptosis in HepG(2) cells through rapid depletion of intracellular thiols. *Arch Biochem Biophys* **374**, 142-152, doi:10.1006/abbi.1999.1574 (2000).

399 Zembowicz, A., Hatchett, R. J., Radziszewski, W. & Gryglewski, R. J. Inhibition of endothelial nitric oxide synthase by ebselen. Prevention by thiols suggests the inactivation by ebselen of a critical thiol essential for the catalytic activity of nitric oxide synthase. *J Pharmacol Exp Ther* **267**, 1112-1118 (1993).

400 Cai, W., Wu, J., Xi, C., Ashe, A. J., 3rd & Meyerhoff, M. E. Carboxyl-ebselen-based layer-by-layer films as potential antithrombotic and antimicrobial coatings. *Biomaterials* **32**, 7774-7784, doi:10.1016/j.biomaterials.2011.06.075 (2011).

401 Wojtowicz, H. *et al.* Azaanalogues of ebselen as antimicrobial and antiviral agents: synthesis and properties. *Farmaco* **59**, 863-868, doi:10.1016/j.farmac.2004.07.003 (2004).

402 Ngo, H. X., Shrestha, S. K. & Garneau-Tsodikova, S. Identification of Ebsulfur Analogues with Broad-Spectrum Antifungal Activity. *ChemMedChem*, doi:10.1002/cmdc.201600236 (2016).

403 Billack, B. *et al.* Evaluation of the antifungal and plasma membrane H+-ATPase inhibitory action of ebselen and two ebselen analogs in S. cerevisiae cultures. *J Enzyme Inhib Med Chem* **25**, 312-317, doi:10.3109/14756360903179419 (2010).

404 Azad, G. K. *et al.* Ebselen induces reactive oxygen species (ROS)-mediated cytotoxicity in Saccharomyces cerevisiae with inhibition of glutamate dehydrogenase being a target. *FEBS Open Bio* **4**, 77-89, doi:10.1016/j.fob.2014.01.002 (2014).

405 Azad, G. K., Balkrishna, S. J., Sathish, N., Kumar, S. & Tomar, R. S. Multifunctional Ebselen drug functions through the activation of DNA damage response and alterations in nuclear proteins. *Biochem Pharmacol* **83**, 296-303, doi:10.1016/j.bcp.2011.10.011 (2012).

406 Odds, F. C., Brown, A. J. & Gow, N. A. Antifungal agents: mechanisms of action. *Trends Microbiol* **11**, 272-279 (2003).

407 Lewis, R. E. Current concepts in antifungal pharmacology. *Mayo Clin Proc* **86**, 805-817, doi:10.4065/mcp.2011.0247 (2011).

408 Shi, H., Liu, S., Miyake, M. & Liu, K. J. Ebselen induced C6 glioma cell death in oxygen and glucose deprivation. *Chem Res Toxicol* **19**, 655-660, doi:10.1021/tx0502544 (2006).

409 Grant, C. M. & Dawes, I. W. Synthesis and role of glutathione in protection against oxidative stress in yeast. *Redox Rep* **2**, 223-229, doi:10.1080/13510002.1996.11747054 (1996).

410 Grant, C. M., MacIver, F. H. & Dawes, I. W. Glutathione is an essential metabolite required for resistance to oxidative stress in the yeast Saccharomyces cerevisiae. *Curr Genet* **29**, 511-515 (1996).

411 Low, C. Y. & Rotstein, C. Emerging fungal infections in immunocompromised patients. *F1000 Med Rep* **3**, 14, doi:10.3410/M3-14 (2011).

412 Jarvis, J. N. & Harrison, T. S. HIV-associated cryptococcal meningitis. *Aids* **21**, 2119-2129, doi:10.1097/QAD.0b013e3282a4a64d (2007).

413 Wisplinghoff, H. *et al.* Nosocomial bloodstream infections in US hospitals: analysis of 24,179 cases from a prospective nationwide surveillance study. *Clin Infect Dis* **39**, 309-317, doi:10.1086/421946 (2004).

414 Gudlaugsson, O. *et al.* Attributable mortality of nosocomial candidemia, revisited. *Clin Infect Dis* **37**, 1172-1177, doi:10.1086/378745 (2003).

415 Spector, D., Labarre, J. & Toledano, M. B. A genetic investigation of the essential role of glutathione: mutations in the proline biosynthesis pathway are the only suppressors of glutathione auxotrophy in yeast. *J Biol Chem* **276**, 7011-7016, doi:10.1074/jbc.M009814200 (2001).

416 Yadav, A. K. *et al.* Glutathione biosynthesis in the yeast pathogens Candida glabrata and Candida albicans: essential in C. glabrata, and essential for virulence in C. albicans. *Microbiology* **157**, 484-495, doi:10.1099/mic.0.045054-0 (2011).

417 Gostimskaya, I. & Grant, C. M. Yeast mitochondrial glutathione is an essential antioxidant with mitochondrial thioredoxin providing a back-up system. *Free Radic Biol Med* **94**, 55-65, doi:10.1016/j.freeradbiomed.2016.02.015 (2016).

418 Lee, J. C. *et al.* The essential and ancillary role of glutathione in Saccharomyces cerevisiae analysed using a grande gsh1 disruptant strain. *FEMS Yeast Res* **1**, 57-65 (2001).

419 Bourbouloux, A., Shahi, P., Chakladar, A., Delrot, S. & Bachhawat, A. K. Hgt1p, a high affinity glutathione transporter from the yeast Saccharomyces cerevisiae. *J Biol Chem* **275**, 13259-13265 (2000).

420 Thakur, A., Kaur, J. & Bachhawat, A. K. Pgt1, a glutathione transporter from the fission yeast Schizosaccharomyces pombe. *FEMS Yeast Res* **8**, 916-929, doi:10.1111/j.1567-1364.2008.00423.x (2008).

421 Desai, P. R. *et al.* Glutathione utilization by Candida albicans requires a functional glutathione degradation (DUG) pathway and OPT7, an unusual member of the oligopeptide transporter family. *J Biol Chem* **286**, 41183-41194, doi:10.1074/jbc.M111.272377 (2011).

422 Bertoti, R. *et al.* Glutathione protects Candida albicans against horseradish volatile oil. *J Basic Microbiol*, doi:10.1002/jobm.201600082 (2016).

423 Maras, B. *et al.* Glutathione metabolism in Candida albicans resistant strains to fluconazole and micafungin. *PLoS One* **9**, e98387, doi:10.1371/journal.pone.0098387 (2014).

424 Lemar, K. M. *et al.* Diallyl disulphide depletes glutathione in Candida albicans: oxidative stress-mediated cell death studied by two-photon microscopy. *Yeast* **24**, 695-706, doi:10.1002/yea.1503 (2007).

VITA

VITA

Shankar Thangamani

Education

2010-Present	PhD	Microbiology and Immunology Graduate Program, College of Veterinary Medicine, Purdue University.
2005-2009	D.V.M	Madras Veterinary College, Tamilnadu Veterinary and Animal Sciences University, India.

Post Graduate Employment

2013-2016	Teaching Assistant	Animal Disease Diagnostic Laboratory (ADDL), College of Veterinary Medicine, Purdue University
2010-2012	Research Assistant	Laboratory of Immunology and Hematopoiesis, College of Veterinary Medicine, Purdue University

Awards/Honors

- First place in poster presentation at "The 29th Annual Phi Zeta Research Day", Purdue University, West Lafayette, IN, April 11, 2016.
- First place in poster presentation at Indiana Branch of American Association for Microbiologist (IBASM) conference, Fort Wayne, IN, April 2, 2016.
- American *Association of Veterinary Laboratory Diagnosticians* (AAVLD) travel grant to attend and present poster in AAVLD conference at Kansas city, MO, Oct 16-22, 2014.

- Third Place in oral presentation for "Clinical investigation of a case with recurrent regurgitation" at Phi Zeta research conference, Madras Veterinary College, Chennai, India. April 26, 2008.

Presentations

1. W.Yonis, **S. Thangamani**, M. Hostetler, López-Pérez, C. Steussy, M.Lipton, C. Stauffacher, M. Wael Abd Al-Azeem & M.N.Seleem(2016) Class II HMG-CoA Reductase Inhibitors targeting gram positive pathogens. The 29th Annual Phi Zeta Research Day , West Lafayette, IN, USA. April 11, 2016.

2. **S. Thangamani**, Haroon Mohammad, **Mostafa F.N. Abushahba,** Paschoal Sobreira Tiago Jose, Lake Paul, Hedrick Victoria and Mohamed N. Seleem. Repurposing auranofin, an FDA approved antirheumatic drug, for the treatment of staphylococcal infections The 29th Annual Phi Zeta Research Day, West Lafayette, IN, USA. April 11, 2016.

3. W.Yonis, **S. Thangamani,** M. Hostetler, López-Pérez, C. Steussy, M.Lipton, C. Stauffacher, M. Wael Abd Al-Azeem & M.N.Seleem, Class II HMG-CoA Reductase Inhibitors targeting gram positive pathogens. Indiana Branch of American Society for Microbiology, Fort Wayne, IN. April 1-2, 2016.

4. **S. Thangamani**, Haroon Mohammad, **Mostafa F.N. Abushahba,** Paschoal Sobreira Tiago Jose, Lake Paul, Hedrick Victoria and Mohamed N. Seleem. Repurposing auranofin, an FDA approved antirheumatic drug, for the treatment of staphylococcal infections. Indiana Branch of American Society for Microbiology, Fort Wayne, IN. April 1-2, 2016.

5. Waleed Younis, **S. Thangamani**, Ahmed A. Hassan and Mohamed N. Seleem. Repurposing FDA- approved drugs to combat drug-resistant bacteria, Health and Disease Symposium, Purdue University, West Lafayette, IN, USA. March 28, 2016.

6. **S. Thangamani**, Haroon Mohammad, **Mostafa F.N. Abushahba,** Paschoal Sobreira Tiago Jose, Lake Paul, Hedrick Victoria and Mohamed N. Seleem. An FDA approved antirheumatic drug to target MRSA infections. Health and Disease Symposium, Purdue University, West Lafayette, IN, USA. March 28, 2016.

7. Waleed Younis, **S. Thangamani**, Ahmed A. Hassan and Mohamed N. Seleem. Repurposing non-antimicrobial drugs to combat multidrug-resistant bacteria, ISS Research symposium, Purdue University. March 8, 2016.

8. W.Yonis, **S. Thangamani**, M. Hostetler, López-Pérez, C. Steussy, M.Lipton, C. Stauffacher, M. Wael Abd Al-Azeem & M.N.Seleem, Class II HMG-CoA Reductase Inhibitors targeting gram positive bacteria, Sigma Xi Graduate Student Research Poster Award Competition, West Lafayette, IN, USA. March 2, 2016.

9. **S. Thangamani**, Haroon Mohammad, **Mostafa F.N. Abushahba,** Paschoal Sobreira Tiago Jose and Mohamed N. Seleem. Repurposing auranofin for the treatment of cutaneous staphylococcal infections. Sigma Xi Graduate Student Research Poster Award Competition, West Lafayette, IN, USA. March 2, 2016.

10. W.Younis, **S. Thangamani** & M. N. Seleem. Teaching an Old drug a new trick. Sigma Xi Graduate Student Research Poster Award Competition, West Lafayette, IN, USA. February 18, 2015.

11. W.Younis, **S. Thangamani** & M. N. Seleem. Repurposing non-antimicrobial drugs and clinical molecules to treat bacterial infections. The 28th Annual Phi Zeta Research Day, West Lafayette, IN. USA April 13, 2015.

12. W.Yonis, **S. Thangamani**, M. Hostetler, López-Pérez, C. Steussy, M.Lipton, C. Stauffacher , M. Wael Abd Al-Azeem & M.N.Seleem. Class II HMG-CoA Reductase Inhibitors targeting multi-drug resistant *Staphylococcus aureus.* Health and Disease, West Lafayette, IN, USA. March 5th, 2015.

13. **S. Thangamani**, Waleed Younis and Mohamed Seleem.“ Drug Repurposing: Ebselen to target MRSA.” Phi-zeta research conference, Purdue University. April 13, 2015.

14. **S. Thangamani**, Waleed Younis and Mohamed Seleem. “Ebselen: a novel topical antibacterial agent for Staphylococcal infections”. Health and Disease Symposium, Purdue University. March 5, 2015.

15. **S. Thangamani**, Waleed Younis and Mohamed Seleem. “Repurposing ebselen for treatment of multidrug-resistant staphylococcal infections”. Office of Interdisciplinary Graduate Program-Spring Reception”, Purdue University. April 1, 2015.

16. **S. Thangamani,** Waleed Younis and Mohamed Seleem. “Ebselen as a novel antibacterial agent against methicillin-resistant *Staphylococcus aureus*”. Sigma Xi Graduate research competition, Purdue University, Feb 18, 2015.

17. **S. Thangamani**, Paulo Gomes and Kenitra Hammac. Prevalence and antibiotic susceptibility dynamics of bacterial isolates from canine skin infections at a Purdue veterinary teaching hospital (2004–2013). Kansas city, MO, Oct 16-22, 2014.

18. M. Nepal, **S. Thangamani**, M.N. Seleem, J. Chmielewski. Coupling Antimicrobial Action of a Novel Unnatural Cationic Amphiphilic Polyproline Helix with its Cell Penetrating Ability to Target Intracellular Bacteria. 2014 H.C. Brown Lectures, West Lafayette, IN, April 9, 2014.

19. M. Nepal, **S. Thangamani**, M.N. Seleem, J. Chmielewski. Coupling Antimicrobial Action of a Novel Unnatural Cationic Amphiphilic Polyproline Helix with its Cell Penetrating Ability to Target Intracellular Bacteria. The 28th Annual Symposium of The Protein Society, San Diego, July 27-30, 2014.

20. Mostafa F.N. Abushahba, **S. Thangamani**, H. Mohammad , Asmaa A.A Hussein and Mohamed N. Seleem. "Novel antisense therapeutics for treatment of intracellular pathogens" Phi-zeta research conference, Purdue University. April 14, 2014.

21. **S. Thangamani**, **Mostafa F.N. Abushahba** and Mohamed Seleem. "Repurposing non-antibiotics FDA approved drugs to treat Staphylococcal infections" Phi-zeta research conference, Purdue University. April 14, 2014.

22. **S. Thangamani**, **Mostafa F.N. Abushahba** Maha I Hamed and Mohamed Seleem. "Beating Bad bugs with old drugs"., Health and Disease Symposium, Purdue University. March 31, 2014.

23. **S. Thangamani**, **Mostafa F.N. Abushahba** Maha I Hamed and Mohamed Seleem. "Old drug up to new trick in fighting resistant bacteria". Office of Interdisciplinary Graduate Program-Spring Reception", Purdue University. April 2, 2014.

24. **S. Thangamani**, Maha I Hamed and Mohamed Seleem. "Old drug for Bad bugs". Sigma Xi Graduate research competition, Purdue University, Feb 12, 2014.

25. **S. Thangamani**, Maha I Hamed and Mohamed Seleem. "Teaching an old drug a new trick". Next Generation Scholars, Purdue University. Nov 19, 2013.

26. Ashley, **S. Thangamani**, M.H.Kim and C.H.Kim, "Deep tissue Imaging of intestine by Multiphoton Microscopy", Phi zeta day, Purdue University, Purdue University. April, 2012.

27. Kimberley Jen, M.H.Kim, **S. Thangamani**, and C.H.Kim. "Intravital Imaging of intestine by Two-Photon Microscopy". Phi zeta day, Purdue University. Phi-zeta research conference, Purdue University. April, 2011.

28. **S. Thangamani** and Parimol Roy. "Antimicrobial activity of *Jatropha curcas* against *Bacillus anthracis".* National conference on current trends in medicinal plants research and herbal technology, Chennai, India, July 10, 2008.

29. **S. Thangamani** and L.Nagarajan."Clinical investigation of a case with Recurrent Regurgitation". Phi-zeta Research Day, Madras Veterinary College, Chennai, India. April 26, 2008.

30. **S. Thangamani** and Pugazhendhi. "Antibiotic Residues in Milk". National conference on safety assessment and Consumer protection with reference to dairy and food industry, Chennai, India, Oct 21, 2007.

Adhoc reviewer

1. International Journal of Nanomedicine
2. Scientific reports
3. Current Pharmaceutical Design
4. PLoS ONE
5. Asian Pacific Journal of Tropical Disease
6. Journal of Bacteriology & Parasitology
7. Clinical, Cosmetic and Investigational Dentistry

PUBLICATIONS

PUBLICATIONS

1. **Thangamani S**, Mohammad H, Abushahba MF, Hamed MI, Sobreira TJ, Hedrick VE, Paul LN, Seleem MN. Antibacterial activity and mechanism of action of auranofin against multi-drug resistant bacterial pathogens. ***Scientific Reports.*** 2016 Mar 3;6:22571.
   (Impact Factor: 5.5)

2. **Thangamani S**, Mohammad H, Abushahba MF, Hamed MI, Sobreira TJ, Hedrick VE, Paul LN, Seleem MN. Repurposing auranofin for the treatment of cutaneous staphylococcal infections. ***International journal of antimicrobial agents and chemotherapy.*** 2016 Jan 23; S0924-8579(16)00012-1 (Impact Factor: 4.2)

3. Abushahba MF, Mohammad H, **Thangamani S**, Hussein AA, Seleem MN. Impact of different cell penetrating peptides on the efficacy of antisense therapeutics for targeting intracellular pathogens. ***Scientific Reports.*** 2016 Feb 10;6:20832. (Impact Factor: 5.5)

4. **Thangamani S**, Mohammad H, Abushahba MF, Hamed MI, Sobreira TJ, Hedrick VE, Paul LN, Seleem MN. Exploring simvastatin, an antihyperlipidemic drug, as a potential topical antibacterial agent. ***Scientific Reports.*** 2015 Nov 10;5:16407. (Impact Factor: 5.5)

5. **Thangamani S**, Nepal M, Chmielewski J, Seleem MN. Antibacterial activity and therapeutic efficacy of Fl-P(R)P(R)P(L)-5, a cationic amphiphilic polyproline helix, in a mouse model of staphylococcal skin infection. ***Drug Des Devel Ther***. 2015 Oct 22;9:5749-54. (Impact Factor: 3.5)

6. **Thangamani S**, Younis W, Seleem MN. Repurposing celecoxib as a topical antimicrobial agent. ***Frontiers in Microbiology.*** 2015 Jul 28;6:750 (Impact Factor: 4.0)

7. **Thangamani S**, Younis W, Seleem MN. Repurposing Clinical Molecule Ebselen to Combat Drug Resistant Pathogens. ***PLoS One***. 2015 Jul 29;10(7):e0133877 (Impact Factor: 3.2)

8. **Thangamani S**, Younis W, Seleem MN. Repurposing ebselen for treatment of multidrug-resistant staphylococcal infections. ***Scientific Reports*.** 2015, Jun 26;5:11596 (Impact Factor: 5.5)

9. Younis W, **Thangamani S**, Seleem MN. Repurposing Non-antimicrobial Drugs and Clinical Molecules to Treat Bacterial Infections. ***Current Pharmaceutical Design***. 2015, May 6. (Impact Factor: 3.5)

10. Nepal M, **Thangamani S**, Seleem MN, Chmielewski J. Targeting intracellular bacteria with an extended cationic amphiphilic polyproline helix. ***Organic and Biomolecular Chemistry***. 2015, Apr 30. (Impact Factor: 3.3)

11. Mohammad H, **Thangamani S**, Seleem MN. Antimicrobial peptides and peptidomimetics - potent therapeutic allies for staphylococcal infections. ***Current Pharmaceutical Design***. 2015;21(16):2073-88. (Impact Factor: 3.5)

12. **Thangamani S**, Mohammad H, Younis W, Seleem MN. Drug repurposing for the treatment of staphylococcal infections. ***Current Pharmaceutical Design***. 2015;21(16):2089-100. (Impact Factor: 3.5)

13. **Thangamani S***, Kim M*, Son Y, Huang X, Kim H, Lee JH, Cho J, Ulrich B, Broxmeyer HE, Kim CH. Cutting edge: progesterone directly up regulates vitamin d receptor gene expression for efficient regulation of T cells by calcitriol. ***Journal of Immunology***. 2015 Feb 1;194(3):883-6. (* Co-first authors) (Impact Factor: 5.5)

14. Wang C*, **Thangamani S***, Kim M, Gu BH, Lee JH, Taparowsky EJ, Kim CH. BATF is required for normal expression of gut-homing receptors by T helper cells in response to retinoic acid. ***Journal of Experimental Medicine***. 2013 Mar 11;210(3):475-89.
(* Co-first authors) (Impact Factor: 14.3)

15. Chang J, **Thangamani S**, Kim MH, Ulrich B, Morris SM Jr, Kim CH. Retinoic acid promotes the development of Arg1-expressing dendritic cells for the regulation of T-cell differentiation. ***European Journal of Immunology***. 2013 Apr;43(4):967-78 (Impact Factor: 4.5)

16. **Thangamani S**, M. Maland, H. Mohammad, P. Pascuzzi, L. Avramova, C. Koehler, T. R. Hazbun and M. N. Seleem. Repurposing approach identifies auranofin with broad spectrum antifungal activity that targets Mia40-Erv1 pathway, "***Frontiers in Cellular and Infection Microbiology***"-Under Review

17. **Thangamani S**, H. E. Eldesouky, H. Mohammad, P. Pascuzzi, L. Avramova, T. R. Hazbun and M. N. Seleem. Ebselen exerts antifungal activity by regulating glutathione (GSH) and reactive oxygen species (ROS) production in fungal cells. "***BBA- General Subjects***"-Under Review